

DISSERTATION ZUR ERLANGUNG DES DOKTORGRADES  
DER FAKULTÄT FÜR BIOLOGIE  
DER LUDWIG-MAXIMILIANS-UNIVERSITÄT MÜNCHEN

**CHROMATIN REMODELING IN EPSTEIN-BARR  
VIRUS AFTER INDUCTION OF THE LYTIC PHASE:  
MOLECULAR CHARACTERIZATION OF THE ROLE  
OF BZLF1 AND ITS INTERACTIONS**



**MARISA SCHÄFFNER**

**Dissertation eingereicht am 30. April 2015**

Erstgutachter: Prof. Dr. Dirk Eick

Zweitgutachter: Prof. Dr. Heinrich Leonhardt

**Tag der mündlichen Prüfung: 26.11.2015**

# ERKLÄRUNG

Hiermit erkläre ich, dass die vorliegende Arbeit mit dem Titel

„CHROMATIN REMODELING IN EPSTEIN-BARR VIRUS AFTER INDUCTION OF THE LYTIC PHASE: MOLECULAR CHARACTERIZATION OF THE ROLE OF BZLF1 AND ITS INTERACTIONS“

von mir selbstständig und ohne unerlaubte Hilfsmittel angefertigt wurde, und ich mich dabei nur der ausdrücklich bezeichneten Quellen und Hilfsmittel bedient habe. Die Arbeit wurde weder in der jetzigen noch in einer abgewandelten Form einer anderen Prüfungskommission vorgelegt.

München, 30. April 2015

Marisa Schöffner

# CONTENT

<b>1. Introduction.....</b>	<b>7</b>
1.1 The architecture of chromatin.....	7
1.1.1 Nucleosomes are histone octamers .....	7
1.1.1.1 Nucleosome components.....	7
1.1.1.2 Histone modifications and histone variants.....	8
1.1.1.3 Nucleosome positioning.....	10
1.1.2 Enhancer-promoter contacts.....	12
1.2 Chromatin regulators and their way of functions.....	14
1.2.1 Chromatin remodelers.....	14
1.2.2 Pioneer factors.....	20
1.3 Epigenetic regulation in EBV .....	22
1.3.1 EBV and its life cycle.....	22
1.3.2 EBV and its lytic switch transactivator BZLF1 .....	24
1.3.3 Epigenetic regulation mechanisms upon lytic reactivation.....	26
1.3.4 Interactions of BZLF1 with viral and host cell proteins .....	28
1.4 Scope of my thesis work.....	30
<b>2. Material.....</b>	<b>31</b>
2.1 Oligonucleotides .....	31
2.2 Plasmids .....	31
2.3 Antibodies.....	32
2.4 Bacterial strains.....	32
2.5 Eukaryotic cell lines.....	33



2.6 Cell culture media and additives .....	33
2.6.1 Media for the cultivation of bacteria.....	33
2.6.2 Media for the cultivation of eukaryotic cells .....	33
2.7 Chemicals and enzymes.....	34
2.8 Buffers and solutions .....	35
2.9 Commercial kits .....	36
2.10 Software .....	37
2.11 Devices and consumables .....	37
<b>3. Methods.....</b>	<b>38</b>
3.1 Bacterial culture .....	38
3.1.1 Growth and storage of bacterial cultures .....	38
3.1.2 Transformation of bacteria.....	38
3.2 Eukaryotic cell culture .....	39
3.2.1 Cell culture conditions .....	39
3.2.2 Storage of eukaryotic cells.....	39
3.2.3 Transient transfection of HEK293 cells.....	39
3.2.4 Electroporation of eukaryotic cells .....	40
3.2.5 Establishment of stable cell lines .....	40
3.2.6 Flow cytometry .....	40
3.3 Nucleic acid techniques .....	41
3.3.1 DNA purification from <i>E.coli</i> .....	41
3.3.2 DNA purification from eukaryotic cells .....	41
3.3.3 Purification of DNA from PCR products and agarose gels .....	41
3.3.4 Electroelution of DNA from native gels.....	42
3.3.5 Dephosphorylation and ligation .....	42
3.3.6 Polymerase chain reaction (PCR) .....	42
3.3.7 Quantitative real time PCR (qPCR).....	42
3.3.8 Mutagenesis PCR.....	43
3.3.9 Isolation of RNA from cells.....	43
3.3.10 Reverse transcription of RNA.....	44
3.4 Protein analysis techniques .....	44
3.4.1 Preparation of whole cell extracts.....	44
3.4.2 Preparation of nuclear cell extracts.....	44
3.4.3 Purification of Strep-tag fusion proteins.....	45
3.4.4 Electromobility shift assay (EMSA) for detecting protein-DNA interactions .....	45
3.4.5 Determination of the equilibrium dissociation constant ( $K_d$ value) .....	46
3.4.6 Sodium dodecyl sulfate polyacrylamide gel electrophoresis (SDS-PAGE) .....	47
3.4.7 Western blot.....	47
3.4.8 Silver staining .....	47

3.5 Chromatin Immunoprecipitation (ChIP).....	48
3.5.1 Chromatin preparation .....	48
3.5.2 Chromatin immunoprecipitation and purification of ChIP DNA .....	48
3.5.3 Quantitation of ChIP DNA by qPCR.....	49
3.6 Sequential ChIP (ReChIP) .....	49
3.6.1 Chromatin preparation for BZLF1-directed ChIP .....	49
3.6.2 ReChIP starting with a BLZF1-directed antibody .....	50
3.6.3 ReChIP starting with an H3K4me1-directed antibody .....	52
3.7 Co-Immunoprecipitation (CoIP).....	53
3.7.1 CoIPs of GFP-tagged bait proteins .....	53
3.7.2 CoIPs of Strep-tagged bait proteins .....	53
3.8 <i>In vitro</i> reconstitution of chromatin .....	54
3.8.1 Histone octamer preparation from <i>Drosophila</i> embryos .....	54
3.8.2 Purification of 156 bp DNA fragments.....	54
3.8.3 Preparation of chromatin via salt gradient dialysis.....	56
3.9 Mass spectrometry analysis .....	56
<b>4. Results .....</b>	<b>57</b>
4.1 BZLF1 changes the epigenetic landscape in viral chromatin .....	57
4.2 BZLF1's molecular role in chromatin remodeling <i>in vitro</i> and <i>in vivo</i> .....	64
4.3 BZLF1 interacts with chromatin regulatory proteins <i>in vivo</i> .....	78
<b>5. Discussion .....</b>	<b>85</b>
5.1 Scope and aim of my thesis work .....	85
5.2 Novel findings of BZLF1 and the regulation of meZREs .....	87
5.2.1 BZLF1 shows characteristics of a pioneer factor .....	87
5.2.2 BZLF1 might read epigenetic modifications in silenced chromatin .....	91
5.2.3 BZLF1's binding to meZREs in silenced chromatin .....	92
5.2.4 BZLF1 and its interactions with chromatin regulatory proteins .....	94
<b>6. Summary.....</b>	<b>96</b>
<b>7. Abbreviations .....</b>	<b>98</b>
<b>8. Literature.....</b>	<b>102</b>
<b>9. Appendix.....</b>	<b>119</b>
9.1 Oligonucleotides .....	119
9.1.1 RT-PCR primer.....	119
9.1.2 qPCR primer .....	119
9.1.3 EMSA DNA template primer .....	120
9.2 Sequences of EMSA DNA templates (156 bps long).....	120
9.3 (Re)ChIP qPCR triplicates.....	122
9.4 Mass spectrometry analysis (data tables).....	128

# 1. INTRODUCTION

## 1.1 The architecture of chromatin

When chromatin components compact and organize genomic DNA, almost all DNA-related metabolic processes including transcription, recombination, DNA repair, replication, kinetochore and centromere formation are affected. The major structural components of chromatin are nucleosomes, composed of histone octamers, but insulators, chromatin domains and enhancer-promoter contacts determine the three-dimensional architecture of chromatin.

### 1.1.1 Nucleosomes are histone octamers

#### 1.1.1.1 Nucleosome components

The condensation of two meters of DNA into a nucleus of a human cell is mediated by the packaging function of nucleosomes (Fig. 1.1). Typically, nucleosomes consist of two copies of the four canonical histone proteins (H2A, H2B, H3 and H4), the so-called histone octamer (Kornberg, 1977). 147 base pairs (bps) of DNA are wrapped 1.65 turns around the histone octamer. Every 10.4 bps histones and the phosphate backbone make connections, which are mediated by the charged residues of the histone proteins. This nucleosomal structure provides 14 histone-DNA contacts and establishes positional stability (Luger *et al.*, 1997). In higher eukaryotes, a linker histone (most commonly an H1 or H5 subtype) packages often regions of chromosomes in a dense manner forming the chromatosome (Kornberg, 1974). Depending on the organism and cell type, the typical distance between nucleosomes varies between seven

and 100 bps. Within one cell the linker region can vary up to 40 bps compassing active and repressed genes (Grigoryev, 2012).

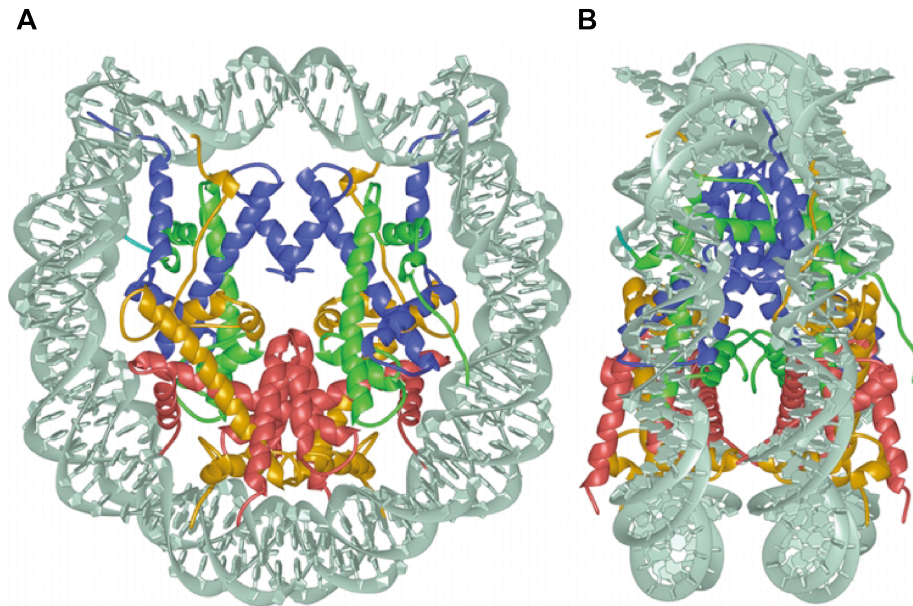


**Fig. 1.1 The crystal structure of the nucleosome in two different orientations demonstrates the compaction of DNA wrapped around the histone octamer (adopted from Luger, 2001)**

The  $\alpha$ -helices of the histone proteins are shown as spirals. H3 is colored blue, H4 green, H2A yellow and H2B red. The DNA is shown in grey.

(A) The nucleosome core particle viewed down the superhelical axis.

(B) The same structure is rotated  $90^\circ$  around the y-axis to emphasize the disc-like shape of the particle.

The nucleosome is not a simple static but a highly dynamic entity regulated by additional proteins complexes. Nucleosomes vary also in the composition of their histone protein components. Nucleosome specialization is based on the incorporation of posttranslational modifications of histone amino acid side chains and histone variants (see chapter 1.1.1.2). Nucleosomes often occupy important regulatory regions in the DNA, and their occupancy competes with other transcription factors. Architectural chromatin proteins, nucleosome-binding proteins, histone chaperones, and ATP-dependent chromatin remodelers play important roles in the regulation of the chromatin structure and gene expression at all levels.

### 1.1.1.2 Histone modifications and histone variants

Modifications of nucleosomes are frequent and highly dynamic. Their impact on transcriptional regulation is well established. More than 60 different amino acid residues of both histone tails and globular domains can carry posttranslational modifications (Kouzarides, 2007). The modifications include the addition of a small chemical residue or the incorporation of large and bulky peptides: methylation (me) of arginine (R) residues, methylation, acetylation (ac), ubiquitination, ADP-ribosylation, and sumolation of lysines (K), and

phosphorylation of serines (S) and threonines (T). The amino acids in the histone tail can be singly, doubly, or triply modified depending on the amino acid. With four core histone proteins, at least eight modes of modifications and the possibility of different modifications of single residues, the diversity of combinations is very high reflecting a plethora of possible chromatin states. Modifications like acetylation of histone 3 (H3) or histone 4 (H4) and di- or trimethylation (me2 or me3) of H3K4 are associated with active transcription (euchromatin). In contrast, modifications like H3K9me and H3K27me are associated with transcriptional repression (heterochromatin). An overview of histone modifications is listed below (Tab.1.1).

**Tab. 1.1 A selection of possible histone modifications and their putative functions**

Histone modification	Putative functions
H3K4me1	Mark of regulatory elements associated with enhancers and other distal elements, but also enriched downstream of transcription start sites (TSS)
H3K4me2	Mark of regulatory elements associated with promoters and enhancers
H3K4me3	Mark of regulatory elements primarily associated with promoters/TSS
H3K9ac	Mark of active regulatory elements with preference for promoters
H3K9me1	Preference for the 5' end of genes
H3K9me3	Repressive mark associated with constitutive heterochromatin and repetitive elements
H3K27ac	Mark of active regulatory elements; may distinguish active enhancers and promoters from their inactive counterparts
H3K27me3	Repressive mark established by polycomb complex activity associated with repressive domains and silent developmental genes
H3K36me3	Elongation mark associated with transcribed portions of genes, with preference for 3' regions after intron 1
H3K79me2	Transcription-associated mark, with preference for 5' end of genes
H4K20me1	Preference for 5' end of genes

(table modified from Consortium TEP, 2012)

Histone-modifying enzymes add and remove posttranslational modifications. The enzymes are recruited through diverse mechanisms including site-specific DNA-binding factors (Eissenberg and Shilatifard, 2010), co-activators and repressors (Brownell *et al.*, 1996), RNA polymerase II (Krogan *et al.*, 2003), or preceding histone modifications (Zippo *et al.*, 2009). A variety of histone acetyltransferase complexes (HATs) carry out histone acetylation at multiple lysine residues (Brown *et al.* 2000). Histone acetylation of numerous lysine residues might have a cumulative effect. In contrast, histone methylation, phosphorylation, ubiquitination, etc. are often carried out by a specific enzyme at a specific amino acid residue resulting in unique functions. Histone modifications can lead to (i) the disruption of DNA-histone contacts due to the change in the net charge of nucleosomes, which can provoke loosening of inter- or intranucleosomal interactions. Histone modifications can (ii) encourage or discourage other chromatin modifying proteins to bind. Specific domains mediate the recruitment of proteins to specific histone modifications. Chromatin organization modifier

(chromo)-like domains of the Royal family (chromo, tudor, MBT) and nonrelated plant homeodomain (PHD) domains, bromodomains, and a domain within 14-3-3 proteins recognize methylation, acetylation and phosphorylation, respectively (Bannister and Kouzarides, 2011). Certain histone modifications (iii) affect contacts between different histones in adjacent nucleosomes or the interactions of histones with the DNA. For instance, H4K16ac can directly influence higher-order chromatin structure by inhibiting the compaction into 30 nm fibers (Shogren-Knaak *et al.*, 2006).

In addition to the four canonical histone proteins, all eukaryotes contain histone variant proteins, which are able to positively or negatively regulate gene transcription (Kamakaka and Biggins, 2005; Bernstein and Hake, 2006). Histone variants are expressed independently of the cell cycle and its S phase. They can be incorporated into nucleosomes independent of DNA replication and assembly of canonical histones. Most histone variants have been identified for histone H2A and H3. They are highly conserved between different species and fulfill important functions that cannot be accomplished by their canonical counterparts. At active genes, histones H3 and H2A are replaced by the histone variants H3.3 and H2A.Z, respectively (Kamakaka and Biggins, 2005; Sarma and Reinberg, 2005). Certain histone H3 variants localize to the centromeres, where their unique N-terminal tails likely play roles in establishing the kinetochore. H2A variants like H2A.Z differ from canonical H2A at several specific residues near the C-terminus and are integral components of nucleosomes, which flank the TSS (Clapier and Cairns, 2009). The incorporation of H2A.Z into a nucleosome can be mediated by the SWR1 chromatin remodeler family (Mizuguchi *et al.*, 2004) or by the histone chaperone Nap1 (Park *et al.*, 2005). The INO80 (inositol requiring 80) chromatin remodeler family catalyses the reversal exchange of H2A.Z/H2B dimers with free H2A/H2B (Papamichos-Chronakis *et al.*, 2011).

### 1.1.1.3 Nucleosome positioning

The mapping of nucleosome position over entire genomes to near base pair precision is possible with high-resolution sequencing techniques (Jiang and Pugh, 2009). Across all eukaryotic species, promoters and other regulatory sequences tend to be more nucleosome-depleted, whereas transcribed regions are generally occupied with well-positioned, high-density nucleosomal arrays (Bai and Morozov, 2010). Several factors are known to control nucleosome positions: DNA sequence preferences, DNA methylation, histone variants and posttranslational modifications, higher order chromatin structure, and the actions of transcription factors, chromatin remodelers and other DNA-binding proteins.

*DNA sequence preferences:*

DNA sequence preferences are not caused by the few base-specific contacts between histone and DNA but by the characteristics of the DNA flexibility (Widom, 2001; Morozov *et al.*, 2009). The DNA sequence contains particular dinucleotides (AA, TT and TA), which occur at ten bp intervals (Ioshikhes *et al.*, 2006; Segal *et al.*, 2006). This arrangement provides a rotational setting of the DNA on the histone surface because AA or TT dinucleotides tend to expand the major groove of DNA. When the particular dinucleotides are placed in phase with the helical twist of DNA, they facilitate the sharp bending of DNA around the histone octamer. In contrast, GC dinucleotides tend to contract the major groove stiffening the DNA strand so that DNA-wrapping around the histone octamer is avoided (Jiang and Pugh, 2009). Also, many pentamers in the linker regions are disfavored by nucleosomes, for example AAAAA, pentamers composed exclusively of A/T nucleotides, and CGCGC (Field *et al.*, 2008).

*DNA methylation:*

In higher eukaryotes, cytosine methylation at CpG dinucleotides might decrease the ability of DNA to bend into the major groove and can thereby directly influence nucleosome positioning (Nathan and Crothers, 2002; Pennings *et al.*, 2005). The regulation mechanism, which is so far poorly understood, needs further investigation.

*Histone variants and posttranslational modifications:*

Histone variants and posttranslational modifications influence the binding of DNA-binding proteins and govern nucleosome positioning. Hyperacetylation and the presence of the core histone tails increase the accessibility and stability of nucleosomal DNA (Polach *et al.*, 2000; Widlund *et al.*, 2000; Anderson *et al.*, 2001). The core histone tails can also contribute to sequence-dependent nucleosome positioning (Yang *et al.*, 2007). Nucleosomes containing histone variants show also a different nucleosome position pattern because of altered histone-DNA interactions. Additionally, the nucleosomes with altered histone compositions show DNA sequence preferences, which differ from nucleosomes with canonical histones. The presence or absence of the linker histone H1 or its variants can also influence the DNA sequence preferences of the nucleosome (McArthur and Thomas, 1996).

*Higher order chromatin structure:*

Nucleosomes are present in long and dense one-dimensional arrays (10 nm fibre) resulting in a five-fold compaction of DNA. The next level of compaction is the three-dimensional organization of the nucleosome arrays in a 30 nm fibre. Higher order chromatin structure can influence nucleosome positioning in four ways. First, the density of nucleosomes along the DNA imposes a trade-off between occupancy and sequence specificity in nucleosome positioning (Kornberg and Stryer, 1988). The positioning of loosely scattered nucleosomes depends more on sequence specificity, whereas dense nucleosomes will be positioned often despite contradictory sequence specificity. Second, neighboring nucleosomes influence each other through repulsive and attractive interactions dictating the tolerated linker lengths (Widom, 1992). Third, there is emerging evidence that a periodicity of strong nucleosome positioning sites may encode regularly spaced chromatin (Davey *et al.*, 1995). Fourth, nucleosome positioning might also depend on the role of the linker histone H1 in DNA packing of nucleosomes, because H1 facilitates the folding of chromatin into 30 nm fibres (Thoma *et al.*, 1979; Yao *et al.*, 1991).

*Transcription factors, chromatin remodelers and other DNA-binding proteins:*

Transcription factors, chromatin remodelers and other DNA-binding proteins (e.g. pioneer factors) can directly or indirectly influence nucleosome positioning by competing with nucleosomes for access to DNA (see chapter 1.2). The outcome of this competition depends on the relative affinities of the nucleosomes and the above-mentioned factors to the underlying DNA and on their concentrations (Segal and Widom, 2009).

**1.1.2 Enhancer-promoter contacts**

Nuclear organization is not only maintained by nucleosomal structures, but also by enhancer-promoter contacts. Studies of long-range interactions revealed that gene regulation is often decoupled from the promoter-proximal region and distributed among distal sequence elements, termed enhancers. Enhancers can be located far from the TSS and their activity is associated with activation of transcription regardless of the location or orientation relative to the promoter. Promoters and enhancers show distinct characteristic chromatin signatures that distinguish them. Promoters and enhancers share certain features such as nucleosome depletion and enrichment of histone acetylation, but they also show characteristic chromatin signatures that can be used to identify and locate both regulatory elements in the human genome. The H3K4 methylation signature is the most studied one. Promoters are located at



the 5' ends of genes in close vicinity of the TSS. Promoters are the point of assembly of the transcriptional machinery and initiation of transcription (Smale and Kadonaga, 2003). Conserved across species, active promoters are marked by acetylation of various residues of histones H3 and H4 and methylation of H3K4. They show high level of H3K4me3 and low level of H3K4me1 at TSS. Nucleosome depletion in active promoters is also a general characteristic in yeast and flies, but is still an open issue in mammalian systems. Enhancers contribute to the activation of their target genes from positions upstream, downstream or within the introns of the genes they regulate or even within the introns of neighboring genes (Blackwood and Kadonaga, 1998; Bulger and Groudine, 1999). Enhancers show no H3K4me3 signature but are marked by H3K4me1 (Barski *et al.*, 2007; Birney *et al.*, 2007; Heintzman *et al.*, 2007; Koch *et al.*, 2007; Wang *et al.*, 2008). Often HATs e.g. p300, which acetylates H3K27, are present at enhancers (Blow *et al.*, 2010; Ghisletti *et al.*, 2010). H3K27ac in combination with H3K4me1 correlates with enhancers near active genes. In the absence of H3K27ac, the H3K4me1 marked enhancer is considered to be inactive or “poised” (Creyghton *et al.*, 2010; Rada-Iglesias *et al.*, 2010). Hypersensitive sites have been also correlated with enhancer elements carrying the H3K4 methylation signature (Xi *et al.*, 2007).

The broadly accepted mechanism of linking enhancers and promoters is termed looping. Looping out the intervening DNA permits the direct interaction of promoter and enhancer (Blackwood and Kadonaga, 1998; Bulger and Groudine, 1999; de Laat *et al.*, 2008). Special transcription factors can bring distal gene loci into proximity with each other regulating gene expression. The CCCTC-binding factor (CTCF) is able to bind to insulator elements and forms chromatin loops (Phillips and Corces, 2009; Hou *et al.*, 2010). CTCF co-operates with cohesins (protein complexes that physically connect sister chromatids during mitosis and meiosis) to partition the genome in looped chromatin domains. Depending on the location of the anchor points of these looped domains, enhancers are either separated from the corresponding promoter or brought in close proximity to the corresponding promoter resulting in transcriptional repression and activation, respectively (Rubio *et al.*, 2008; Wendt *et al.*, 2008).

## 1.2 Chromatin regulators and their way of functions

Transcription factors sequence-specifically bind regulatory regions (so-called DNA binding sites) in the context of free DNA and target the assembly of the transcriptional machinery, which controls gene expression (Hahn, 2004). In eukaryotic cells, the majority of potential DNA-binding sites is not accessible because they are compacted by nucleosomes (nucleosomal DNA) and occupied by higher-order chromatin structures and repressor complexes. The recruitment of transcription factors to their cognate binding sites depends on the chromatin landscape i.e. the nucleosomal distribution, epigenetic modifications, and the three-dimensional structure of the chromatin (Magnani *et al.*, 2011). How transcription factors can bind to their motifs to activate gene expression is enigmatic because the majority of the DNA-binding sites is inaccessible. Most of the studied transcription factors are not capable of binding nucleosomal DNA, only their cooperative and simultaneous binding supports the successful interaction with nucleosomes (Adams and Workman, 1995; Zaret and Carroll, 2011). Two classes of chromatin regulators find directly access to nucleosomal DNA using two distinct strategies: chromatin remodelers and pioneer factors.

### 1.2.1 Chromatin remodelers

Chromatin remodeling complexes (remodelers) play an important role in chromatin regulation. They carry out various functions and alter the accessibility of DNA to transcription factors by packaging or unpackaging the genome (Clapier and Cairns, 2009). All remodelers show high affinity for nucleosomes. Chromatin remodelers utilize the energy of ATP hydrolysis to alter histone-DNA contacts by moving, destabilizing, ejecting, or restructuring nucleosomes. The presence of 53 different chromatin remodelers in the human cell suggests specialized functions of these enzymes and the associated complexes (Manelyte and Längst, 2013).

The catalytic subunit of chromatin remodelers consists of a conserved ATPase domain and unique flanking regions (Fig. 1.2). The ATPase domain consists of two tandem RecA-like folds (DExx and HELICc), containing seven conserved helicase-related sequence motifs that classify the enzymes as part of the Superfamily 2 group of helicase-like proteins (Eisen *et al.*, 1995; Flaus *et al.*, 2006). Chromatin remodelers do not separate nucleic acid strands like typical helicases, but they use the energy of ATP hydrolysis to reposition nucleosomes like

DNA translocases. The association of the catalytic subunit with unique subunits ensures the specialization of a given remodeler complex. It can recognize covalent histone modifications, regulate the catalytic subunit, and interact with other chromatin or transcription factors (Clapier and Cairns, 2009).

Individual families are conserved from yeast to human, although there is a certain variation in their species-specific complex composition. The division of chromatin remodelers into classes is based on different protein compositions and functions. There are four major remodeler families: SWI/SNF, ISWI, INO80 and CHD (Clapier and Cairns, 2009). In the following I will concentrate on discussing chromatin remodelers in human cells.

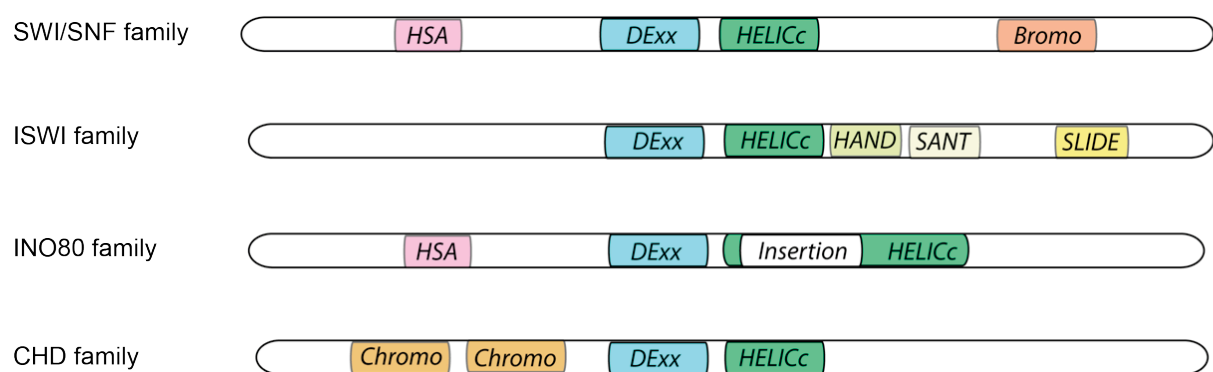


**Fig. 1.2 Classical organization of remodeler families defined by their catalytic domain (modified from Manelyte and Längst, 2013).**

All remodeling enzymes consist of a shared ATPase domain and unique flanking domains. DExx and HELICc are responsible for nucleic acid binding and ATP hydrolysis. Bromo recognizes acetylated lysines in histone tails. Chromo binds methylated lysines in histone tails. HAND, SANT and SLIDE recognize nucleosomes and internucleosomal DNA. HSA binds actin-related proteins.

#### *SWI/SNF family remodelers:*

The SWI/SNF (switching defective/sucrose nonfermenting) family remodelers are composed of large, multi-subunit complexes containing eight to 14 proteins. They are conserved in eukaryotes and all contain a DNA-dependent ATPase as their catalytic subunit. The catalytic ATPase (Fig. 1.2) includes a N-terminal helicase-SANT (HSA) domain and a C-terminal bromodomain, which recruit actin/actin-related proteins and bind to acetylated lysines of histones, respectively (Clapier and Cairns, 2009). Each organism builds a slightly different set of SWI/SNF-related complexes, using both conserved proteins and also unique attendant subunits to help specialize each complex. Members of this family have many activities. They slide and eject nucleosomes at many loci and participate in diverse processes of chromatin remodeling but lack roles in chromatin assembly (Clapier and Cairns, 2009). Remodelers like SWI/SNF are targeted to particular nucleosomes either through histone modifications or

through a “pioneering” DNA-binding protein. The human SWI/SNF remodeler complexes BAF and PBAF utilize BRM or BRG1 as catalytic subunits, share nine identical subunits (BAF45, BAF57, BAF53, BAF57, BAF60, BAF155, BAF170, SNF5 and  $\beta$ -actin), but differ with respect to several unique subunits (BAF250 for BAF and BAF180, BAF200 and BRD7 for PBAF) (Wilson and Roberts, 2011). Variant subunits contribute to targeting, assembly and regulation of lineage-specific functions of the remodeler complexes. An overview of all subunits of selected SWI/SNF family remodelers is listed below (Tab.1.2).

**Tab. 1.2 Selected SWI/SNF family remodelers and their composition**

Complex	Catalytic subunit	Attendant subunits
BAF	BRM or BRG1	BAF250, BAF155, BAF170, BAF60 (A, B or C), SNF5, BAF57, BAF53 (A or B), $\beta$ -actin, BAF45 (A, B, C or D)
PBAF	BRG1	BAF180, BAF200, BRD7, BAF155, BAF45 (A, B, C or D), BAF170, BAF60 (A, B or C), SNF5, BAF57, BAF53 (A or B), $\beta$ -actin

(table modified from Manelyte and Längst, 2013)

#### *ISWI family remodelers:*

The ISWI (imitation switch) family comprises highly conserved protein complexes that utilize the energy of ATP hydrolysis to slide nucleosomes along DNA and/or replace histones within nucleosomes. The ISWI family remodelers contain two to four subunits. Most eukaryotes form multiple ISWI family complexes using one or two different catalytic subunits with specialized attendant proteins. The most intensively studied members of this group are ACF (ATP utilizing chromatin assembly and remodeling factor), NURF (nucleosome remodeling factor), and CHRAC (chromatin accessibility complex). All these complexes contain a nucleosome-dependent ATPase (SNF2L or SNF2H), which is homologous with the ATPase of the SWI/SNF remodeler family (Vignali *et al.*, 2000). The ISWI family ATPase contains the conserved catalytic ATPase domain and a helicase domain (Fig. 1.2), but the C-terminus additionally harbors a characteristic set of domains, known as HAND, SANT, and SLIDE (Clapier and Cairns, 2009). The SANT domain binds unmodified histone tails, the SLIDE domain binds nucleosomal DNA near the dyad axis, and the HAND domain is implicated in both histone and DNA binding/recognition. The mammalian homologues SNF2L and SNF2H can act on their own or in presence of one or more attendant subunits forming different remodeling complexes with different properties (Manelyte and Längst, 2013). SNF2L interacts with CECR2 and BPTF to form CERF and NURF complexes, respectively (Manelyte and Längst, 2013). SNF2H interacts with ACF1, Tip5, Rsf1, Wstf, and WCRF180 proteins to form ACF1 or CHRAC, NoRC, RSF, WICH, and WCRF complexes, respectively. Specialized attendant proteins contain many chromatin binding domains,

including histone fold motifs (in CHRAC), PHDs (in Tip5), bromodomains (in BPTF, ACF1, Tip5), and additional DNA-binding motifs (HMGI(Y) in NURF; AT hooks in Tip5). ACF, CHRAC, and NoRC complexes have established roles in chromatin assembly and in the formation of nucleosome arrays with well-ordered, optimized spacing, which might help to promote repression (Cairns, 2005). Instead, NURF randomizes spacing, which can assist RNA polymerase II activation (Clapier and Cairns, 2009). An overview of all subunits of selected ISWI family remodelers is listed below (Tab. 1.3).

**Tab. 1.3 Selected ISWI family remodelers and their composition**

Complex	Catalytic subunit	Attendant subunits
CERF	SNF2L	CECR2
NURF		BPTF, RbAp46 or RbAp48
ACF		ACF1
CHRAC		ACF1, CHRAC17, CHRAC15
NoRC	SNF2H	Tip5
RSF		Rsfl
WICH		Wstf
CRF		WCRF180

(table modified from Manelyte and Längst, 2013)

#### *INO80 family remodelers:*

The INO80 (inositol requiring 80) family remodelers are complexes composed of more than ten subunits (Clapier and Cairns, 2009). They are part of ATP-dependent chromatin-remodeling complexes, which interact with nucleosomes and remodel chromatin by either sliding nucleosomes along the DNA or exchanging histones within nucleosomes. INO80 catalyzes the exchange of H2A.Z/H2B dimers with free H2A/H2B (Papamichos-Chronakis *et al.*, 2011). In yeast, the reverse reaction, the incorporation of H2A.Z is catalyzed by the related SWR1 complex (Mizuguchi *et al.*, 2004), and both complexes regulate the global distribution of H2A.Z with emerging implications in genomic stability, cancer development, and embryonic stem cell differentiation (Billon and Cote, 2012; Li *et al.*, 2012). Both INO80 and SWR1 remodeling complexes can slide nucleosomes and evict histones from DNA (Shen *et al.*, 2003; Tsukuda *et al.*, 2005; van Attikum *et al.*, 2007). INO80 family remodelers have been reported to alter the chromatin structure during transcription (Shen *et al.*, 2000), in recombination and DNA replication (Papamichos-Chronakis and Peterson, 2008; Bao and Shen, 2011), cell division, and DNA repair (Downs *et al.*, 2004; Morrison *et al.*, 2004; van Attikum *et al.*, 2004). Unique is the core ATPase with a split ATPase domain (Fig. 1.2), as well as Rvb proteins, which share limited homology to bacterial RuvB, the Holliday junction DNA helicases (West, 1997). Unlike remodelers of other families, the INO80 remodelers exhibit DNA helicase activity and binds to specialized DNA structures resembling Holliday

junctions and replication forks consistent with the function of the complex in homologous recombination and DNA replication (Shen *et al.*, 2000; Wu *et al.*, 2007). The interactions between the remodeling complexes and nucleosomes likely involve actin and the Arp subunits, which associate with the conserved HSA domain of the core ATPase in each complex. Examples for human orthologs are the core ATPases hINO80 and Domino/p400, which contains also HAT activity. An overview of all subunits of two selected INO80 family remodelers is listed below (Tab. 1.4).

**Tab. 1.4 Selected INO80 family remodelers and their composition**

Complex	Catalytic subunit	Attendant subunits
INO80	hIno80	INO80D, INO80E, Amida, Uch37, NFRKB, MCRS1, Arp4, Arp8, YY1, Arp5, Ies2, Ies6, Tip49a, Tip49b
TIP60	Domino/p400	TRRAP, Rvb1 (RuVB-like), Rvb2, Bdf6, Act1 (actin), Baf53, Gas41, Dmap1, Mrg1, Mrgbp, Epc1, Ing3, Tip60

(table modified from van Attikum and Gasser, 2005 and Chen *et al.*, 2013)

#### *CHD family remodelers:*

The CHD (chromodomain helicase DNA-binding) remodeler family is defined by the presence of two tandem chromodomains, which are N-terminally located of the ATPase domain (Fig. 1.2). Additional structural motifs are used to further divide the CHD family into the subfamilies CHD1, Mi-2 and CHD7 (Flaus *et al.*, 2006; Sims and Wade, 2011). Members of the CHD1 subfamily (CHD1 and CHD2 proteins in higher eukaryotes) contain a C-terminal DNA-binding domain with a SANT-SLIDE like fold that preferentially binds to AT-rich DNA (Delmas *et al.*, 1993; Stokes and Perry, 1995). The Mi-2 subfamily members (CHD3 and CHD4 proteins in humans) contain a pair of PHD domains in their N-terminal part and have been implicated in nucleosome binding (Watson *et al.*, 2012). The CHD7 subfamily members have additional C-terminal domains, like the SANT or BRK domains. An overview of the CHD family remodelers is listed below (Tab. 1.5).

**Tab. 1.5 Selected CHD family remodelers and their composition**

Complex	Catalytic subunit	Attendant subunits
CHD1	CHD1	
CHD2	CHD2	
Mi-2/NuRD	CHD3/CHD4	MBD2/3, MTA1/2/3, HDAC1/2, RbAp46/48, p66a/b, DOC-1
	CHD5	Unknown
	CHD7	PARP1, PBAF complex

(table modified from Manelyte and Längst, 2013)

The Mi-2/NuRD remodelers couple a chromatin remodeling ATPase and the histone deacetylases 1 and 2 (HDAC1/HDAC2) (Tong *et al.*, 1998; Wade *et al.*, 1998; Xue *et al.*, 1998; Zhang *et al.*, 1999). This complex is unique because it links two independent,

chromatin-directed enzymatic functions for gene regulation. This family is broadly distributed in cells and tissues. The subunit composition of the enzyme appears to vary with cell type and in response to physiologic signals within a tissue (Denslow and Wade, 2007). The catalytic helicase-like ATPase subunits are the two Mi-2 a and b proteins, also known as CHD3 and CHD4, respectively (Eisen *et al.*, 1995), which are widely conserved throughout the animal and plant kingdoms, but absent in yeast (Denslow and Wade, 2007). The ATPases contain conserved PHD fingers, implicated in nucleosome binding, N-terminally tandem chromodomains, and a putative C-terminally DNA-binding domain (Woodage *et al.*, 1997). The catalytic deacetylase subunits HDAC1 and HDAC2 of Mi-2/NuRD are highly conserved and present in all eukaryotes. Additionally, the Mi-2/NuRD complex contains several additional proteins of importance. The smallest subunit is a member of the methyl CpG-binding domain (MBD) family of proteins, MBD2 or MBD3 (Wade *et al.*, 1999; Zhang *et al.*, 1999) selectively recognizing methylated DNA. The retinoblastoma associated proteins 46 and 48 (RbAp46 and RbAp48), termed RBBP7 and RBBP4, respectively, are additional subunits of the Mi-2/NuRD complex. Presumably, these two proteins are structural subunits because they contain a number of WD repeats, a sequence motif that forms a propeller structure providing a protein interaction surface (Marhold *et al.*, 2004). Interestingly, RBBP4 and RBBP7 have been shown to be components of several other multi-protein chromatin modification complexes in which they interact directly with core histones (Loyola and Almouzni, 2004). Certain versions of the Mi-2/NuRD complex contain additional structural and/or regulatory subunits. The proteins p66a or p66b, also known as GATAD2A and GATAD2B (Wade *et al.*, 1999; Brackertz *et al.*, 2002; Feng *et al.*, 2002), have the capacity to interact directly with core histones (Brackertz *et al.*, 2006). Another characterized subunit of the Mi-2/NuRD complex consists of the metastasis associated (MTA) protein family (Bowen *et al.*, 2004; Manavathi and Kumar, 2007), but the functional role of MTA1, MTA2, and MTA3 proteins in the Mi-2/NuRD complex remains unknown. The Mi-2/NuRD complex catalyses the conversion of an active, hyperacetylated promoter to that of an inactive, hypoacetylated promoter with densely packed nucleosomes. The Mi-2 ATPase facilitates nucleosome mobility through a sliding mechanism (Brehm *et al.*, 2000; Guschin *et al.*, 2000) and the enzymes HDAC1/2 perform histone deacetylation.

### 1.2.2 Pioneer factors

Pioneer factors are considered as a specific class of transcription factors that autonomously can establish competence for gene expression (Zaret and Carroll, 2011). They find access to their DNA binding sites in condensed chromatin prior to other factors binding and prior to the time of transcriptional activation. They often play crucial roles in development and differentiation by promoting cell type-specific transcriptional programs (Magnani *et al.*, 2011). Pioneer factors are defined as nucleosome-binding proteins that precede and enable the subsequent binding of other transcription factors, chromatin modifiers, and nucleosome remodelers involved in chromatin remodeling. Alternatively, certain pioneer factors can actively open local chromatin themselves (Zaret and Carroll, 2011). Conversely, there is also emerging evidence that pioneer factors might establish stably silenced chromatin domains by recruiting corepressor complexes (Sekiya and Zaret, 2007). Epigenetic modifications provide signals for pioneer factors indicating that they can read and interpret epigenetic modifications. Also, the insulator protein CTCF can influence the binding of pioneer factors to the chromatin (Magnani *et al.*, 2011). The regulation of pioneer factors and their impact on the chromatin structure still remain to be further investigated. There are several known pioneer factors with various peculiar characteristics.

#### *FoxA:*

In liver cells, the fork head-like transcription factor FoxA binds the *albumin* enhancer region, which harbors an array of precisely positioned nucleosomes. FoxA binding results in the expression of the *albumin* gene. In non-liver tissues nucleosomes are randomly positioned over the enhancer in the absence of FoxA promoting a silent state of the *albumin* gene (McPherson *et al.*, 1996; Cirillo *et al.*, 2002). The pioneer factor binds to nucleosomal DNA as well as or even better than to naked DNA (Cirillo *et al.*, 1998). The co-occupancy of FoxA with nucleosomes can serve as a structural recruiting signal for gene regulatory complexes (Chaya *et al.*, 2001). The C-terminus of FoxA contains a core histone motif and binds the histones H3, H4, and weakly H2B (Cirillo *et al.*, 2002). The N-terminus and DNA-binding domain (DBD) do not bind core histones, but the DBD is important for targeting the C-terminus to specific genomic regions. FoxA has a winged helix DBD with a helix-turn-helix (HTH) motif, which makes base-specific DNA contacts, and two flanking loops (wings) of a polypeptide chain that contact the phosphodiester backbone of DNA. FoxA's HTH motif is



highly homologous with that of histone H1 (Cirillo *et al.*, 1998). In that way the DBD of FoxA structurally resembles the linker Histone H1 and disrupts internucleosomal interactions (Cirillo *et al.*, 2002; Sekiya *et al.*, 2009). The recruitment of FoxA to enhancers is dependent on epigenetic changes of enhancer hallmarks (Serandour *et al.*, 2011). The histone binding is facilitated by H3K4me2 (Cirillo and Zaret, 1999; Lupien *et al.*, 2008).

#### *PBX1:*

The pre-B cell leukemia homeobox 1 (PBX1) is a member of the three amino acid loop extension (TALE)-class homeodomain family and is required for hematopoiesis, skeleton patterning, pancreas and urogenital systems organogenesis (Magnani *et al.*, 2011). PBX1 is essential for the estrogen receptor alpha (ER $\alpha$ ) mediated transcriptional response driving aggressive tumors in breast cancer (Holmes *et al.*, 2011). PBX1 occupies chromatin prior to transcription factor recruitment, mediates nucleosome depletion, and recruits other factors involved in transcriptional regulation. The pioneer factor has the capacity to read specific epigenetic signatures like H3K4me2 and can open chromatin at specific chromatin locations (Magnani *et al.*, 2011).

#### *PU.1:*

The transcription factor PU.1 plays an important role at early stages of B cell differentiation and development by binding the enhancer of the *paired box protein Pax-5* gene in multipotent hematopoietic progenitors prior to the time of *Pax5* activation (Zaret and Carroll, 2011). As a pioneer factor, it expands the linker region between nucleosomes and promotes local histone modifications. PU.1 binding initiates nucleosome repositioning and chromatin opening followed by H3K4me1 deposition at enhancers in the course of macrophage and B cell differentiation (Ghisletti *et al.*, 2010; Heinz *et al.*, 2010). H3K4me1 deposition is followed by the recruitment of transcription factors guiding the cell-type specific transcriptional program that promotes B cell or macrophage differentiation (Magnani *et al.*, 2011).

## 1.3 Epigenetic regulation in EBV

### 1.3.1 EBV and its life cycle

EBV is characterized by three phases of its life cycle: the pre-latent phase, the latent phase, and the lytic phase (Fig 1.3).

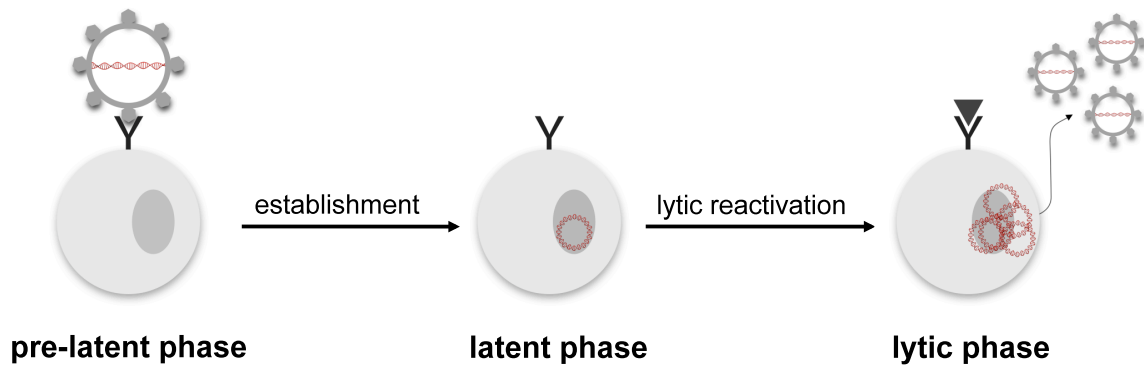


**Fig. 1.3** EBV's life cycle in human B cells

Upon infection of human B lymphocytes, the main target cells of EBV, the pre-latent phase is initiated. The linear viral DNA genome reaches the host cell nucleus and forms a circular plasmid. The viral DNA is first completely naïve, i.e. it is free of histones and devoid of methylated CpG dinucleotides (Kintner and Sugden, 1981; Fernandez *et al.*, 2009; Kalla *et al.*, 2010). Subsequently, proteins of the host cell machinery compact the viral DNA into nucleosomal arrays, modify the N-terminal histone tails and extensively methylate the majority of the many viral CpG sites (Kalla *et al.*, 2010). Two distinct sets of viral genes are expressed during the pre-latent phase: the classical latent set of genes and a restricted number of genes, which are characteristic of the set of lytic genes. The expression of latent genes (Epstein-Barr nuclear antigens (EBNAs), latent membrane proteins (LMPs)), and viral non-coding RNAs and microRNAs activates the quiescent B lymphocytes, which become lymphoblasts and begin to proliferate. Activated B lymphocytes have to be protected from endogenous stress, immediate activation-induced apoptosis (Altmann and Hammerschmidt, 2005) and the consequences of DNA damage response signals (Nikitin *et al.*, 2010). Latent as well as a restricted number of lytic genes encompassing transcription factors and cytokines ensure the survival of the infected primary B lymphocytes. The pre-latent phase lasts about

one to two weeks and progeny virus is not synthesized in this period (Kalla and Hammerschmidt, 2011).

In the consecutive strictly latent phase, characterized by a stable virus-host relationship, the viral DNA is maintained in the nucleus of the proliferating B cells. Only EBNA and LMPs, the viral latent genes, as well as non-coding RNAs are expressed and support cellular proliferation of lymphoblastoid cell lines (LCLs). The expression of EBNA genes is governed by different promoters, indicating a change in viral gene regulation from the pre-latent to the latent phase (Woisetschlaeger *et al.*, 1990; Altmann and Hammerschmidt, 2005). This promoter switch is caused by the gradual epigenetic modifications of viral DNA, which results in a global transcriptional repression and a high degree of CpG methylation of the viral genome (Kalla *et al.*, 2010). In the latent phase, all lytic genes are efficiently repressed but latent viral genes are spared from epigenetic silencing. Latent gene products mimic central cellular functions and contribute to B cell activation, survival and proliferation.

Exogenous signals such as antigen-encounter or artificial cross-linking of the B cell receptor (Tovey *et al.*, 1978; Takada, 1984) initiate a cellular signaling cascade in the latently EBV-infected cells resulting in the transcriptional activation of the viral immediate-early gene *BZLF1*. It encodes the transcription factor BZLF1, which is responsible for the molecular switch from the latent to the lytic phase (Countryman and Miller, 1985; Chevallier-Greco *et al.*, 1986; Takada *et al.*, 1986; Countryman *et al.*, 1987). Upon lytic induction, viral *de novo* synthesis starts and infected cells release viral progeny within 48 hours (Countryman and Miller, 1985; Takada *et al.*, 1986). BZLF1 binds viral and cellular promoters sequence-specifically and induces their gene expression. Upon *BZLF1*'s induced expression, a cascade of three classes of viral lytic genes starts: the immediate-early, early, and late viral genes. The immediate-early gene products encompass the two transcription factors BZLF1 and BRLF1. Early and late lytic genes encode viral proteins important for lytic viral DNA replication and viral structural components, respectively. The released viral progeny contains again a completely naïve viral genome free of histones and unmethylated CpG sites (Kalla *et al.*, 2010).

During the latent phase, EBV genomes persist as multicopy DNA episomes in the nucleus of human B lymphocytes (Lieberman, 2006; Lindner and Sugden, 2007). The establishment of a latent EBV infection efficiently transforms these cells into LCLs *in vitro*, and is implicated in the etiology of infectious mononucleosis, Burkitt's lymphoma, Hodgkin's disease, nasopharyngeal carcinoma and lymphoproliferative diseases in immunocompromised individuals (Young and Rickinson, 2004). In healthy individuals, resting memory B cells are

the reservoir of EBV's latent infection (Babcock *et al.*, 1998). During latency, the EBV genome can adopt one of four different gene expression patterns that are generally referred to as latency programs (termed latency 0, I, II and III) and are classified on the basis of EBNA and LMP protein expression. Type 0 latency is defined as latency with no viral gene expression and is found in non-dividing B cells (Miyashita *et al.*, 1995, Thorley-Lawson *et al.*, 1996; Miyashita *et al.*, 1997;). In cells of Burkitt's lymphoma, only EBNA1 is expressed (latency I) (Thorley-Lawson *et al.*, 1996). In Hodgkin's disease, nasopharyngeal carcinoma and T cell lymphomas, EBNA1 and variable combinations of the three members of the LMP family (LMP1, LMP2A and LMP2B) are expressed (latency II) (Thorley-Lawson *et al.*, 1996). During acute infectious mononucleosis, in lymphoproliferative syndromes in immunocompromised individuals and in LCLs, all six nuclear antigens (EBNA1-6) required for B cell proliferation and survival, and all three LMPs are expressed (latency III) (Hudson *et al.*, 1985; Bodescot *et al.*, 1987).

### 1.3.2 EBV and its lytic switch transactivator BZLF1

The viral transcription factor BZLF1 is an immediate-early gene product that triggers the switch from the latent to the lytic phase (Countryman and Miller, 1985; Chevallier-Greco *et al.*, 1986; Takada *et al.*, 1986; Countryman *et al.*, 1987). EBV encodes BZLF1 from the *BZLF1* gene (Baer *et al.*, 1984). BZLF1 binds to target sites termed BZLF1 Responsive Elements (ZREs) in the promoter regions of early lytic genes and induces their expression (Miller, 1989; Speck *et al.*, 1997; Schwarzmans *et al.*, 1998). BZLF1 binds sequence-specifically to two different classes of ZREs. Class I ZREs includes classical AP1-like recognition elements, while class II ZREs harbor a CpG motif. BZLF1 binds preferentially to class II ZRE sites, only, if they contain 5'-methylated cytosine residues (meZREs) (Bhende *et al.*, 2004; Karlsson *et al.*, 2008; Dickerson *et al.*, 2009; Kalla *et al.*, 2010). meZREs predominate in the early lytic promoters (Bergbauer *et al.*, 2010) and their CpG methylation is essential for the expression of lytic genes (Kalla *et al.*, 2012) and in turn indispensable for viral progeny synthesis (Bergbauer *et al.*, 2010; Kalla *et al.*, 2010). Therefore, DNA methylation is no hindrance but a must for lytic reactivation mediated by BZLF1 (Woellmer *et al.*, 2012). Due to its essential role in the viral life cycle, the structure and function of BZLF1 (Fig 1.4) has been extensively reviewed (Miller, 1989; Sinclair and Farrell, 1992; Speck *et al.*, 1997; Schwarzmans *et al.*, 1998; Petosa *et al.*, 2006).

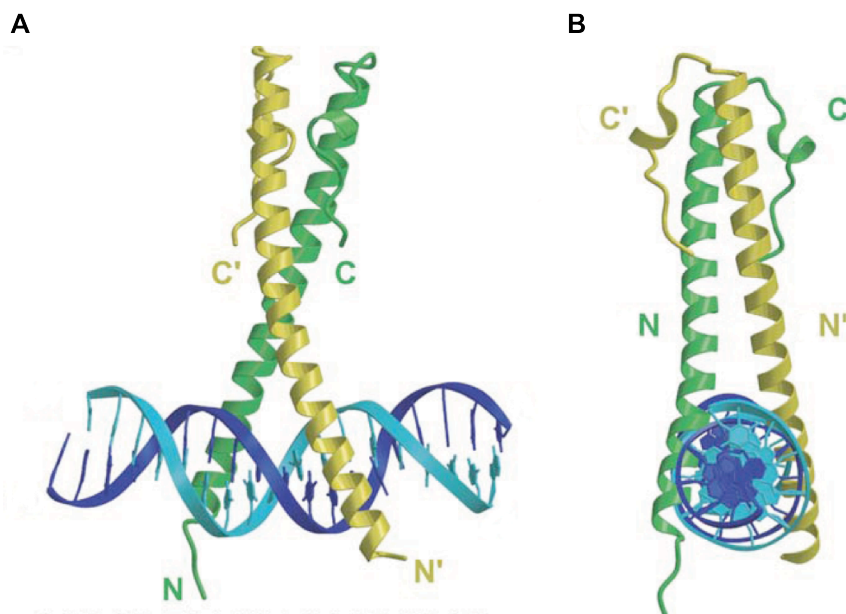


**Fig. 1.4 Crystal structure of the BZLF1-DNA complex (modified from Petosa *et al.*, 2006)**

The  $\alpha$ -helices of the BZLF1 homodimer are shown as spirals in green and yellow. The DNA double helix is shown in light and dark blue. N- and C-terminus are indicated.

(A) The BZLF1-DNA bound structure.

(B) The same structure is rotated by  $90^\circ$  around the x-axis.

BZLF1 is a 245 residue long protein that belongs to the basic leucine-zipper (bZIP) family of transcription factors (Farrell *et al.*, 1989; Chang *et al.*, 1990; Lieberman and Berk, 1990). The bZIP transcription factors, including c-Jun, c-Fos, ATF/CREB, and the C/EBP family of proteins, form homo- and heterodimers through a coiled-coil domain, also called a leucine zipper and bind DNA through a 60 residues long region rich in basic amino acids located adjacent to the dimerization domain. BZLF1 is modular in structure and consists of a N-terminal transactivation domain (TAD) (aa1-174), a bZIP domain (aa175-220), and a C-terminal domain (aa221-245). BZLF1's bZIP domain lacks the otherwise usual heptad repeat of leucine residues, which normally mediates dimerization (Farrell *et al.*, 1989; Chang *et al.*, 1990; Flemington and Speck, 1990; Kouzarides *et al.*, 1991). Like other bZIP proteins, the BZLF1 homodimer binds the DNA via its two long bZIP helices (Morand *et al.*, 2006; Petosa *et al.*, 2006). The basic region of each helix contacts the major groove and the zipper region forms a coiled-coil. The C-terminal tail forms an additional structured motif, which stabilizes the coiled-coil through numerous interactions and greatly enlarges the dimer interface explaining the dimer's stability despite the missing heptad repeat of leucine residues.

BZLF1 fails to heterodimerize with the cellular bZIP proteins c-Fos, c-Jun, C/EBP $\alpha$ , and CREB (Chang *et al.*, 1990; Kouzarides *et al.*, 1991; Wu *et al.*, 2004). Four amino acids, R183, A185, C189, and R190 in the basic domain of BZLF1 have been described to specifically contact DNA with BZLF1 recognition elements, since alanine or valine

substitutions at these positions drastically weakened or abrogated DNA binding (Heston *et al.*, 2006).

In order to maintain infected cells in the latent phase and prevent unwanted activation of the lytic phase, the expression of BZLF1 is tightly regulated at different levels. The transcription of BZLF1 is regulated by epigenetic modifications of its promoter. Repressive histone marks like H3K27me3, H3K9me2/me3, and H4K20me3 negatively regulate *BZLF1* and prevent transcriptional activation maintaining the latent phase (Murata *et al.*, 2012). In addition, heterochromatin protein 1 (HP1) and H2A ubiquitination are associated with the latent phase (Murata and Tsurumi, 2013). The induction of active histone marks such as histone acetylation and H3K4me3 results in transcriptional activation of the *BZLF1* gene and reactivation from latency (Jenkins *et al.*, 2000; Miller *et al.*, 2007; Countryman *et al.*, 2008; Murata *et al.*, 2012). The cellular zinc finger E-box binding factor 1 and 2 (ZEB1 and ZEB2) can repress the *BZLF1* gene expression by directly binding its promoter (Yu *et al.*, 2007; Ellis *et al.*, 2010; Zhao *et al.*, 2011). A silencing element in the *BZLF1* promoter region, termed ZIIR, plays a key role in establishment and maintenance of EBV latency by inhibiting *BZLF1* promoter activation through the proteinase kinase C (PKC) signal transduction pathway (Yu *et al.*, 2011). BZLF1's silencing element is associated with the Jun dimerization protein 2 (JDP2), which suppresses also the promoter activity of *BZLF1*. Additionally, a correlation with HDAC3 association and reduced levels of histone acetylation has been reported (Murata *et al.*, 2011). The promoter region of *BZLF1* contains weak ZREs but no meZREs indicating that its regulation is independent of the methylation status of DNA. The regulation of *BZLF1* itself relies on positive feedback loops (Speck *et al.*, 1997; Binne *et al.*, 2002). Further, reversible posttranslational modifications are in play, which dynamically regulate BZLF1's protein activity. The conjugation of BZLF1 with the small ubiquitin-related modifier (SUMO) negatively modulates its transcriptional activity (Murata *et al.*, 2010). This transcriptional repression by SUMO correlates with the association of repressor complexes, including HDAC3. Additional protein-protein interactions between BZLF1 and cellular proteins have been described to have an impact on the regulation of EBV's life cycle (see chapter 1.3.3).

### 1.3.3 Epigenetic regulation mechanisms upon lytic reactivation

Mechanisms of epigenetic regulation control the different phases of EBV's life cycle. CpG methylation, nucleosome occupancy, histone modifications, and cellular regulatory proteins contribute to the transcriptional regulation of viral latent and lytic promoters.

The repression of early lytic promoters in the latent phase correlates with extensive DNA

methylation, high nucleosome occupancy, and Polycomb silencing with characteristic H3K27me3 histone marks (Woellmer *et al.*, 2012). The repressive histone mark H3K9me3 seems to be important to maintain the compaction of the viral chromatin in certain cell lines (Ramasubramanyan *et al.*, 2011; Woellmer *et al.*, 2012).

Upon lytic reactivation the silenced state of early lytic promoters is reverted. Initially, nucleosomal occupancy drastically diminishes followed by the removal of the repressive histone mark H3K27me3 and the establishment of the active histone marks like H3K4me3. As a consequence the promoters open locally and the transcription machinery is recruited. Since BZLF1 binds its meZRE motifs only if methylated, DNA methylation is the prerequisite for the activation of early lytic promoters (Bergbauer *et al.*, 2010; Kalla *et al.*, 2010; Woellmer *et al.*, 2012). Therefore, the transition to the lytic phase does not alter the level of CpG methylation of viral DNA. The modification of the histone variant H2AX by phosphorylation has been associated with lytic regulatory regions during lytic phase (Ramasubramanyan *et al.*, 2011). Phosphorylation of H2AX is associated with the DNA damage response pathway (Lukas *et al.*, 2006).

The expression and action of the transcription factor BZLF1 correlates with the loss of nucleosomes upon lytic phase induction (Woellmer *et al.*, 2012). The TAD of BZLF1 is required only for the nucleosomal eviction of a subset of early lytic promoters (BMLF1p, BRLF1p and BMRF1p). A truncated BZLF1 version without TAD is capable of evicting histones at many more BZLF1-regulated promoters, suggesting that either the bZIP domain or the C-terminus of BZLF1 play a role for the nucleosomal removal. It has been hypothesized that BZLF1 has pioneering functions because it can reactivate silenced, inactive chromatin and might recruit chromatin remodelers (Adamson and Kenney, 1999; Zerby *et al.*, 1999; Schelcher *et al.*, 2007; McDonald *et al.*, 2009; Woellmer *et al.*, 2012).

The chromatin regulatory factors CTCF and cohesin have been implicated in controlling EBV's latent phase. CTCF binding has been detected at several key regulatory regions and many of these CTCF-binding sites are co-occupied by cohesin (Day *et al.*, 2007; Holdorf *et al.*, 2011; Arvey *et al.*, 2012). A single CTCF binding site controls LMP2A and LMP1 promoter selection, chromatin boundary function, DNA loop formation, and episome copy number control during EBV latency (Chen *et al.*, 2014). The CTCF binding site is required for cohesin binding and for DNA loop formation between LMP1/LMP2A and OriP (Arvey *et al.*, 2012). The loss of CTCF results in the switch from euchromatic to heterochromatic epigenetic marks at the LMP2A and LMP1 promoter regions. Strong binding of CTCF have been also detected immediately upstream of the latent promoters Cp and Qp, and the EBER

TSS (Day *et al.*, 2007; Takacs *et al.*, 2010). CTCF binding at these regions could provide several functions, including insulating neighboring viral lytic promoters from activation during latent infection, and the regulation of enhancer-promoter interactions.

### 1.3.4 Interactions of BZLF1 with viral and host cell proteins

The viral transcription factor BZLF1 has been reported to interact with a large number of viral and cellular host cell proteins influencing both latency and lytic reactivation of the virus.

#### *Viral interactors:*

BZLF1 protein is not only essential as a transactivating factor for early lytic gene expression, but also for lytic viral DNA replication. BZLF1 interrupts viral latency by interacting with the components of EBV's replication machinery. It binds to the helicase-primase complex consisting of BBLF4 (helicase; Gao *et al.*, 1998; Liao *et al.*, 2001), BSLF1 (primase; Gao *et al.*, 1998), and BBLF2/3 (primase-associated factor; Gao *et al.*, 1998). Also BALF5 (DNA polymerase; Baumann *et al.*, 1999) and BMRF1 (polymerase processivity factor; Zhang *et al.*, 1996; Baumann *et al.*, 1999) interact with BZLF1. BZLF1 also binds to a number of classical ZRE motifs in the lytic origin of viral DNA replication and tethers the replication machinery to the origin for its initial activation. In addition, BZLF1 protein binding was shown with BFRF3, a component of the viral capsid antigen complex (Katz *et al.*, 1992; Serio *et al.*, 1996) and BGLF4, the viral kinase and virion tegument protein regulating BZLF1's TAD (Asai *et al.*, 2006; Asai *et al.*, 2009).

#### *Cellular interactors:*

The many reported interactions and regulatory loops of the viral transcription factor BZLF1 with cellular proteins is of great complexity and might have an important influence on the control of EBV's life cycle.

Various interactions of BZLF1 and cellular proteins have been described to inhibit the lytic reactivation process in latently infected cells. BZLF1 may influence cellular regulatory pathways by protein-protein interactions between the basic domain of BZLF1 and key cell cycle control proteins involved in cell cycle arrest. BZLF1's interaction with the tumor suppressor protein p53 may inhibit the transcriptional function of p53 and the ability of BZLF1 to disrupt viral latency (Mauser *et al.*, 2002; Zhang *et al.*, 1994). Interestingly, opposing effects of BZLF1 on p53 function have also been observed, where BZLF1 expression activates p53-dependent transcription (Dreyfus *et al.*, 2000), and BZLF1 induces a



cell cycle arrest and enhances the expression of p53 (Cayrol and Flemington, 1996). BZLF1 causes also cell cycle arrest through induction of the cyclin-dependent kinase inhibitors p21 and p27 (Cayrol and Flemington, 1996; Rodriguez *et al.*, 1999). BZLF1 has also been described to interact with the cellular CCAAT/enhancer binding protein  $\alpha$  (C/EBP $\alpha$ ), which is essential for the induction of p21 and BZLF1-induced G1 arrest during EBV lytic cycle (Wu *et al.*, 2003). The interaction with the p65 component of NF- $\kappa$ B inhibits transactivation of several EBV promoters (Gutsch *et al.*, 1994). Also, the retinoic acid receptors RAR and RXR have been shown to interact with BZLF1 and negatively regulate its transactivation of early lytic promoters (Pfitzner *et al.*, 1995; Sista *et al.*, 1993; Sista *et al.*, 1995). Furthermore, the B cell transcription factor Oct-2 interacts with BZLF1 inhibiting its function as an immediate early protein and preventing lytic viral reactivation (Robinson *et al.*, 2012). Ubinuclein, an ubiquitously expressed nuclear protein, binds to the basic domain of BZLF1, might prevent its DNA binding, and acts as a chaperone for bZIP factors (Aho *et al.*, 2000).

Other cellular interactions with BZLF1 have been described that support reactivation of the productive cycle in latently infected cells. BZLF1 is involved in the activation of transcription by stabilizing the TFIIA-TFIID complex (Lieberman and Berk, 1991; Chi and Carey, 1993; Lieberman and Berk, 1994; Chi *et al.*, 1995; Chi and Carey, 1996; Lieberman *et al.*, 1997; Deng *et al.*, 2001) and interacts also with the TATA-binding protein (TBP) (Mikaelian *et al.*, 1993). BZLF1 also recruits the CREB-binding protein (CBP), which stimulates transcription through histone acetylation (Adamson and Kenney, 1999; Zerby *et al.*, 1999; Chen *et al.*, 2001). The receptor of activated C-kinase, RACK1, was identified as an interaction partner of BZLF1 via its transactivation domain (Baumann *et al.*, 2000). RACK1 is involved in targeting activated PKCs (protein kinase C) that phosphorylate BZLF1 and increase its activity. BZLF1 has been also reported to form a complex with the transducer of regulated CREB activity 2 (TORC2) (Murata *et al.*, 2009). The recruitment of this complex to BZLF1's own promoter induces lytic reactivation of viral latency. Further, the viral latent phase in EBV-infected B cells is negatively influenced by the interaction of BZLF1 and the B cell specific transcription factor Pax5. The interaction may promote lytic replication in B cells by inhibiting Pax5 function (Adamson *et al.*, 2005). The interaction of BZLF1 with the cellular promyelocytic leukemia protein (PML) alters its localization from nuclear dots to a diffuse nuclear pattern (Bowling and Adamson, 2006). Since PML is part of the cell's response to viral invasion, the re-localization of PML by BZLF1 may enhance EBV lytic replication.

## 1.4 Scope of my thesis work

Genome-wide studies during the last years have revealed that the vast majority of transcription factor binding sites in the genome are inaccessible *in vivo* because repressive chromatin structures occlude their binding to DNA. Only cooperative binding of several factors or the concomitant recruitment of chromatin remodelers allow a single transcription factor to access its target sequence and induce transcription. In contrast to the majority of transcription factors, pioneer factors of transcription do bind to repressed and compacted target sequences without the help of chromatin remodeler or the use of ATP. Only very few examples of this type of factors have been identified so far, among them FoxA, PBX1, and PU.1. They are the first proteins engaged at specific sites to open up chromatin and facilitate transcriptional activation at previously repressed loci. Pioneer factors are therefore defined as a specific subclass of transcription factors that are required and sufficient to trigger competency of transcriptional regulatory sites (Magnani *et al.*, 2011; Zaret and Carroll, 2011).

The central hypothesis whether the viral transcription factor BZLF1 might have characteristics of a pioneer factor that acts during the process of lytic gene activation was the starting point of my PhD work. The previous findings of Woellmer *et al.* (2012) let us speculate that BZLF1 might overcome the silenced, repressed state of viral chromatin by binding and positioning nucleosomes that occupy the promoter regions of early lytic genes. In order to provide a better understanding of the epigenetic alterations that occur during the switch from the latent to the lytic phase in EBV, I sought to discover whether BZLF1 is not only required but also sufficient to remodel the chromatin landscape at the proximity of EBV's lytic genes or if cellular chromatin regulatory factors are needed.

## 2. MATERIAL

### 2.1 Oligonucleotides

The synthesis of all oligonucleotides used in my PhD work was performed by the company Metabion (Munich). The sequences of the oligonucleotides are listed in the appendix.

### 2.2 Plasmids

All plasmids listed below were generated (unless noted otherwise) and used in the context of this work. They are part of the plasmid collection of the Research Unit Gene Vectors.

Plasmid	Description
p0509	CMV promoter driven BZLF1 expression vector (Hammerschmidt and Sugden, 1988)
p1925	eGFP-C1 lacking MCS to express GFP (Dagmar Pich)
p3925	FLAG- and tandem Strep-tag II expression plasmid pN-SF-TAP for N-terminal fusion proteins (Marius Ueffing and Johannes Glöckner)
p3928	FLAG- and tandem Strep-tag II expression plasmid pN-SF-TAP with BZLF1 (aa 149 to 245) (Wolfgang Hammerschmidt and Martin Bergbauer)
p4816	pRTR, oriP expression vector with EBNA1, reverse tetracycline controlled transactivator rtTA2(S)-M2 and Tet repressor tTS (PLDLS-135-L) as a silencer, puromycin resistance, luciferase reporter gene of vector was substituted by BZLF1 as gene of interest (SfiI sites), NGF-R-IRES-GFP for monitoring inserted with AscI/SwaI (Martin Bergbauer and Marisa Schöffner)
p5406	FLAG- and tandem Strep-tag II expression plasmid pN-SF-TAP with BZLF1 (aa 1 to 245)
p5594	pUC18 plasmid containing Asp718I-flanked BRLF1 ZRE 0 multimers
p5595	pUC18 plasmid containing Asp718I-flanked BBLF4 ZRE 3 multimers
p5596	pUC18 plasmid containing Asp718I-flanked BBLF4 ZRE 3+4 multimers
p5597	pUC18 plasmid containing Asp718I-flanked BBLF4 ZRE 4 multimers
p5686	FLAG- and tandem Strep-tag II expression plasmid pN-SF-TAP with BZLF1 (aa 175 to 236)

p5693	pRTR, oriP expression vector with EBNA1, reverse tetracycline controlled transactivator rtTA2(S)-M2 and Tet repressor tTS (PLDLS-135-L) as a silencer, puromycin resistance, luciferase reporter gene of vector was substituted by Flag-tandem Strep-BZLF1 (aa1 to 245) as gene of interest (SfiI sites), NGF-R-IRES-GFP for monitoring inserted with AscI/SwaI
p5694	RTR, oriP expression vector with EBNA1, reverse tetracycline controlled transactivator rtTA2(S)-M2 and Tet repressor tTS (PLDLS-135-L) as a silencer, puromycin resistance, luciferase reporter gene of vector was substituted by Flag-tandem Strep-BZLF1 (aa175 to 236) as gene of interest (SfiI sites), NGF-R-IRES-GFP for monitoring inserted with AscI/SwaI
p5748	pUC18 plasmid containing Asp718I-flanked BBLF4 ZRE 0+4 multimers
p5749	pUC18 plasmid containing Asp718I-flanked BBLF4 ZRE 3+0 multimers
p5836	pUC18 plasmid containing Asp718I-flanked BBLF4 ZRE 3+0 -5nt multimers
p5837	pUC18 plasmid containing Asp718I-flanked BBLF4 ZRE 3+0 +5nt multimers
p5838	pUC18 plasmid containing Asp718I-flanked BBLF4 ZRE 3+0 +10nt multimers
p5839	pUC18 plasmid containing Asp718I-flanked BBLF4 ZRE 3+0 +15nt multimers
p5840	pUC18 plasmid containing Asp718I-flanked BBLF4 ZRE 3+0 +30nt multimers
p5906	pEGFP-N3 + SNF2H
p5916	pmCherryC1 + LacI-BZLF1 (aa 1-245)
p5985	pEGFP-C1 + hIno80
p6013	FLAG- and tandem Strep-tag II expression plasmid pN-SF-TAP with BZLF1 (aa 175-245)
p6014	FLAG- and tandem Strep-tag II expression plasmid pN-SF-TAP with BZLF1 (aa 1-236)

## 2.3 Antibodies

All antibodies used in this work are listed below.

Specificity	Species	Distributor	Application	Amount
Anti-acetyl-Histone H3	Rabbit	Millipore (#06-599)	ChIP	3 µg
Anti-BZLF1	Mouse	E. Kremmer (HMGU)	Western	1:50
Anti-Flag	Mouse	Stratagene (#200474-21)	Western/EMSA	1:5000/1 µg
Anti-GFP	Rat	Chromotek (#3H9)	Western	1:1000
Anti-Histone H3 mono methyl Lys4	Mouse	Abcam (#ab8895)	ChIP	3 µg
Anti-INO80	Rabbit	Abcam (#ab118787)	Western	1:2000
Anti-mouse IgG, HRP	Goat	Cell Signaling (#7076S)	Western	1:5000
Anti-rabbit IgG	Rabbit	Millipore (#PP64B)	ChIP	3 µg
Anti-rabbit IgG, HRP	Rabbit	Cell Signaling (#7074S)	Western	1:5000
Anti-rat IgG, HRP	Goat	Cell Signaling (#7077)	Western	1:5000
Anti-RNA polymerase II (N20)	Mouse	Santa Cruz (#sc-39097)	ChIP	10 µl
Anti-SNF2h	Mouse	Active Motif (#39543)	Western	1:2000
Anti-tubulin	Mouse	Santa Cruz (#sc-23948)	Western	1:5000
Anti-ZEBRA	Goat	Santa Cruz (#sc-17503)	ChIP/ReChIP	3 µg/15 µg

## 2.4 Bacterial strains

For all cloning purposes and the preparation of plasmid DNA, the strain DH5- $\alpha$  (F<sup>-</sup>, lacI<sup>-</sup>, recA1, endA1, hsdR17,  $\Delta$ (lacZYA-argF), U169, F80d lacZ $\Delta$ M15, supE44, thi-1, gyrA96, relA1; Hanahan, 1985) was used.

## 2.5 Eukaryotic cell lines

All used cell lines stem from the collection of the Research Unit Gene Vectors or were established (\*) in the course of my work and are recorded below. In case of established cell lines the stably transfected plasmid is noted.

Name	Description
HEK293	Human embryonic kidney cells transformed after transfection with DNA from human Adenovirus Type 5 (Graham <i>et al.</i> , 1977)
Raji	Human EBV-positive Burkitt-lymphoma cell line (Pulvertaft, 1964)
Raji/4816*	Raji cells carrying a tet-inducible plasmid for BZLF1 (aa 1-245)
Raji/5693*	Raji cells carrying a tet-inducible plasmid for flag- and tandem strep-tagged BZLF1 (aa 1-245)
Raji/5694*	Raji cells carrying a tet-inducible plasmid for flag- and tandem strep-tagged BZLF1 (aa 175-236)

## 2.6 Cell culture media and additives

### 2.6.1 Media for the cultivation of bacteria

Bacteria were either cultivated with LB-medium in liquid culture for large-scale production or on solid agar plates if single clones were cultured.

Appellation	Ingredients	Distributor
LB-medium	1 % (w/v) tryptone, 1 % (w/v) NaCl, 0.5 % (w/v) yeast extract	Invitrogen, Karlsruhe
Select agar	LB-medium with 1.5 % (w/v) select agar	Invitrogen, Karlsruhe

### 2.6.2 Media for the cultivation of eukaryotic cells

Media and additives for eukaryotic cell culture used in this work are listed below.

Appellation	Application	Distributor
RPMI-1640	Cell culture medium for cultivation of HEK293 and Raji cell lines used in this study	Invitrogen, Karlsruhe
DMEM	Cell culture medium for cultivation of U2OS cell lines used in this study	Sigma-Aldrich, Munich
Opti-MEM I	Minimal culture medium for transfection reactions	Invitrogen, Karlsruhe
$\alpha$ -thioglycerole	Antioxidant agents (additive for RPMI-1640)	Sigma-Aldrich, Munich
Bathocuproine-disulfonic acid	Antioxidant agents (additive for RPMI-1640)	Sigma-Aldrich, Munich
Fetal bovine serum	Nutritive substance (additive for RPMI-1640)	Invitrogen, Karlsruhe
Sodium pyruvate	Antioxidant agent (additive for RPMI-1640)	Invitrogen, Karlsruhe
Sodium selenite	Antioxidant agent (additive for RPMI-1640)	Sigma-Aldrich, Munich
Penicillin/streptomycin	Antibiotics (additives for RPMI-1640)	Invitrogen, Karlsruhe
Puromycin	Antibiotic for the selection of stably transfected cell lines	Invitrogen, Karlsruhe

## 2.7 Chemicals and enzymes

The following list shows the used chemicals and enzymes in this work.

Distributor	Appellation
Affymetrix, Santa Clara, USA	T4 DNA Ligase
Applichem, Darmstadt	Lysozyme, RNase A, Tris ( $C_4H_{11}NO_3$ )
Biochrome AG, Berlin	PBS
Bio Rad, Munich	Bradford solution
Carl Roth GmbH, Karlsruhe	Bovine serum albumin fraction V (BSA) powder, chloroform ( $CHCl_3$ ), phenol ( $C_6H_6O$ ), powdered milk, Rotiphorese Gel30 (acrylamide), Rotiphorese Gel40 (acrylamide)
Difco Laboratories, Detroit, USA	Bacto-agar, trypton, yeast extract
Fermentas, St. Leon-Roth	DNA ladders, loading dye for gel electrophoresis, restriction enzymes, T4 Polynucleotide Kinase
Finnzymes, Vantaa, Finland	Phusion polymerase
GE Healthcare, Munich	Amersham ECL Select Western Blotting Detection Reagent, Hybond-ECL membrane
Hartmann Analytik, Braunschweig	$[\gamma\text{-}^{32}P]$ ATP
IBA GmbH, Göttingen	Desthiobiotin elution buffer (10x), Strep-Tactin Sepharose, wash buffer (10x)
Invitrogen, Karlsruhe	Agarose, calf thymus DNA, DNase I, trypsin-EDTA
Merck, Darmstadt	Acetic acid ( $C_2H_4O_2$ ), ammonium sulfate ( $(NH_4)_2SO_4$ ), Benzonase Nuclease, boric acid ( $H_3BO_3$ ), caesium chloride ( $CsCl$ ), calcium chloride ( $CaCl_2$ ), disodium phosphate ( $Na_2HPO_4$ ), ethanol ( $C_2H_6O$ ), ethidium bromide ( $C_{21}H_{20}BrN_3$ ), ethylenediaminetetraacetic acid (EDTA, $C_{10}H_{16}N_2O_8$ ), ethylene glycol tetraacetic acid (EGTA, $C_{14}H_{24}N_2O_{10}$ ), glucose ( $C_6H_{12}O_6$ ), glycerol ( $C_3H_8O_3$ ), glycine ( $C_2H_5NO_2$ ), HEPES ( $C_8H_{18}N_2O_4S$ ), hydrochloric acid (HCl), isopropanol ( $C_3H_8O$ ), lithium chloride (LiCl), magnesium chloride ( $MgCl_2$ ), magnesium sulfate ( $MgSO_4$ ), methanol ( $CH_4O$ ), monopotassium phosphate ( $KH_2PO_4$ ), paraformaldehyde ( $OH(CH_2O)_nH$ ( $n = 8-100$ )), N-lauroyl sarcosine ( $C_{15}H_{29}NO_3$ ), potassium acetate ( $C_2H_3KO_2$ ), potassium chloride (KCl), sodium acetate ( $C_2H_3NaO_2$ ), sodium chloride (NaCl), sodium dodecyl sulfate (SDS, $NaC_{12}H_{25}SO_4$ ), sodium hydroxide (NaOH), sucrose ( $C_{12}H_{22}O_{11}$ ), tetramethylethylenediamin (TEMED, $C_6H_{16}N_2$ ), Triton X-100 ( $C_{14}H_{22}O(C_2H_4O)_n$ ( $n = 9-10$ )), zink sulfate ( $ZnSO_4$ )
New England Biolabs, Frankfurt	Alkaline Phosphatase Calf Intestinal (CIP), CpG Methyltransferase (M.SssI), restriction enzymes (AvaI, RsaI, XmnI)
Promega, Mannheim	RNAasin plus RNase inhibitor
Roche Diagnostics GmbH, Mannheim	Asp718 restriction enzyme, Complete Mini Protease Inhibitor, desoxy-nucleotides, LightCycler 480 SYBR Green I Master, Micrococcal Nuclease S7, PhosStop Phosphatase Inhibitor, poly(dI/dC)
SERVA Electrophoresis GmbH, Heidelberg	Ammonium persulfate (APS, $(NH_4)_2S_2O_8$ )
Sigma-Aldrich, Munich	Ampicillin ( $C_{16}H_{19}N_3O_4S$ ), beta-mercaptoethanol ( $C_2H_6SO$ ), bromophenol blue ( $C_{19}H_{10}Br_4O_5S$ ), dimethyl sulfoxide (DMSO, $C_2H_6OS$ ), dithiothreitol (DTT, $C_4H_{10}O_2S_2$ ), doxycycline (DOX, $C_{22}H_{24}N_2O_8$ ), kanamycin ( $C_{18}H_{36}N_4O_{11}$ ), NP-40 ( $(C_2H_4O)_nC_{14}H_{22}O$ ), phenylmethanesulfonylfluoride (PMSF, $C_7H_7FO_2S$ ), polyethylenimine (PEI, $(C_2H_5N)_n$ ), Ponceau S ( $C_{22}H_{16}N_4O_{13}S_4$ ), Proteinase K, puromycin ( $C_{22}H_{29}N_7O_5$ ), silver nitrate ( $AgNO_3$ ), sodium carbonate ( $Na_2CO_3$ ), sodium deoxycholate ( $C_{24}H_{39}NaO_4$ ), sodium metabisulfite ( $Na_2S_2O_5$ ), sodium thiosulfate ( $Na_2S_2O_3$ ), xylene cyanol ( $C_{25}H_{27}N_2NaO_6S_2$ )
Thermo Scientific, Waltham, USA	PageRuler Plus Prestained Protein Ladder, Phusion High-Fidelity DNA Polymerase

## 2.8 Buffers and solutions

The following lists records the buffers and solutions used in my work.

Buffer/solution	Ingredients	Application
Agarose loading dye	1 mg/ml bromophenol blue, 1 mg/ml xylene cyanol, 50 % sucrose	General lab techniques
Alkaline phosphatase buffer (10x)	500 mM Tris-HCl pH9.3, 10 mM MgCl <sub>2</sub> , 1 mM ZnSO <sub>4</sub>	
Ampicillin (1000x)	100 mg/ml ampicillin in 50 % ethanol, sterile filtered	
Kanamycin (1000x)	30 mg/ml kanamycin in ddH <sub>2</sub> O, sterile filtered	
M-STET	50 mM Tris-HCl pH8.0, 25 mM EDTA, 5 % sucrose, 0.5 % Triton X-100	
PBS, pH7.3	10 mM Na <sub>2</sub> HPO <sub>4</sub> , 1.8 mM KH <sub>2</sub> PO <sub>4</sub> , 140 mM NaCl, 2.7 mM KCl	
TAE	40 mM Tris-acetate, 1 mM EDTA	
TBE	89 mM Tris, 89 mM boric acid, 2 mM EDTA	
TE, pH8.0	10 mM Tris-HCl, 1 mM EDTA,	
ChIP lysis buffer	10 mM Tris-HCl pH7.5, 10 mM NaCl, 3 mM MgCl <sub>2</sub> , 0.5 % NP-40	ChIP
ChIP sonication buffer	50 mM Tris-HCl pH7.5, 10 mM EDTA, 1 % SDS, 1 % NP-40, 1x "Complete" proteinase inhibitor cocktail (Roche)	
ChIP dilution buffer	20 mM Tris-HCl pH8.0, 2 mM EDTA, pH 8.0, 1 % Triton X-100, 150 mM NaCl, 1x "Complete" proteinase inhibitor cocktail (Roche)	
ChIP low salt buffer	20 mM Tris-HCl pH8.0, 2 mM EDTA pH8.0, 1 % Triton X-100, 150 mM NaCl, 0.1 % SDS	
ChIP high salt buffer	20 mM Tris-HCl pH8.0, 2 mM EDTA pH8.0, 1 % Triton X-100, 500 mM NaCl, 0.1 % SDS	
ChIP LiCl buffer	10 mM Tris-HCl pH8.0, 1 mM EDTA pH8.0, 250 mM LiCl, 0.5 % NP-40, 0.5 % sodium deoxycholate	
ChIP elution buffer	25 mM Tris-HCl pH7.5, 10 mM EDTA pH8.0, 0.5 % SDS	
ReChIP lysis buffer 1	50 mM HEPES pH7.5, 140 mM NaCl, 1 mM EDTA pH8.0, 0.5 mM EGTA pH8.0, 10 % glycerol, 0.5 % NP-40, 0.25 % Triton X-100, 1x "Complete" proteinase inhibitor cocktail (Roche)	ReChIP
ReChIP Lysis buffer 2	25 mM HEPES pH7.5, 200 mM NaCl, 1 mM EDTA pH8.0, 0.5 mM EGTA pH8.0, 1x "Complete" proteinase inhibitor cocktail (Roche)	
ReChIP lysis buffer 3	25 mM HEPES pH7.5, 140 mM NaCl, 1 mM EDTA pH8.0, 0.5 mM EGTA pH8.0, 0.25 % N-lauroyl sarcosine, 0.1 % sodium deoxycholate, 0.25 % Triton X-100, 1x "Complete" proteinase inhibitor cocktail (Roche)	
ReChIP wash buffer 1	50 mM Tris-HCl pH8.0, 150 mM NaCl, 1 mM EDTA pH8.0, 0.1 % SDS, 0.5 % sodium deoxycholate, 1 % NP-40	
ReChIP wash buffer 2	50 mM Tris-HCl pH8.0, 300 mM NaCl, 1 mM EDTA pH8.0, 0.1 % SDS, 0.5 % sodium deoxycholate, 1 % NP-40	
ReChIP wash buffer 3	50 mM Tris-HCl pH8.0, 250 mM LiCl, 0.1 % SDS, 0.5 % sodium deoxycholate, 1 % NP-40	
ReChIP elution buffer	10 mM Tris-HCl pH8.0, 1 mM EDTA pH8.0, 1 % SDS	
EMSA binding buffer (10x)	100 mM Tris-HCl pH7.6, 10 mM MgCl <sub>2</sub> , 600 mM KCl, 30 mg/ml BSA, 10 % glycerol, 10 % Ficoll, 10 mM DTT	EMSA
Native separation gel (10 %)	16.6 ml Rotiphorese 30 (37.5:1), 2.5 ml 10x TBE, 400 µl 10 % APS, 50 µl TEMED	
Native shift gel (5 %)	5 ml Rotiphorese 30 (37.5:1), 5 ml Rotiphorese 40 (19:1), 3.2 ml 10x TBE, 66 ml ddH <sub>2</sub> O, 50 µl TEMED, 400 µl 10 % APS	
EMSA loading dye	20 mM Tris-HCl pH7.5, 8 mM EDTA, 25 % glycerol, 0.1 % NP-40	
Fixing solution	10 % acetic acid, 20 % methanol in ddH <sub>2</sub> O	

RIPA buffer	50 mM Tris-HCl pH8.0, 150 mM NaCl, 0.1 % SDS, 0.5 % sodium deoxycholate, 1 % NP-40, 1x “Complete” proteinase inhibitor cocktail (Roche)	Protein purification
Wash buffer (10x)	100 mM Tris-HCl pH8.0, 150 mM NaCl, 1 mM EDTA, 1x “Complete” proteinase inhibitor cocktail (Roche)	
Desthiobiotin elution buffer (10x)	100 mM Tris-HCl pH8.0, 150 mM NaCl, 1 mM EDTA, 2.5 mM desthiobiotin, 1x “Complete” proteinase inhibitor cocktail (Roche)	
Lysis buffer	15 mM HEPES-KOH pH7.5, 10 mM KCl, 5 mM MgCl <sub>2</sub> , 0.1 mM EDTA, 0.5 mM EGTA, 17.5 % (w/v) sucrose, 1 mM DTT, 0.2 mM PMSF, 1 mM sodium metabisulfite	Histone octamer preparation
Suc buffer	15 mM HEPES-KOH pH7.5, 10 mM KCl, 5 mM MgCl <sub>2</sub> , 0.05 mM EDTA, 0.25 mM EGTA, 1.2 % (w/v) sucrose, 1 mM DTT, 0.1 mM PMSF	
Hypotonic buffer	10 mM HEPES pH7.9, 1.5 mM MgCl <sub>2</sub> , 10 mM KCl, 340 mM sucrose, 1x “Complete” proteinase inhibitor cocktail (Roche)	Mass spectrometry analysis
High salt buffer	10 mM HEPES pH7.9, 1.5 mM MgCl <sub>2</sub> , 1260 mM NaCl, 1x “Complete” proteinase inhibitor cocktail (Roche)	
Wash buffer	100 mM Tris-HCl pH8.0, 150 mM NaCl, 1 mM EDTA, 1x “Complete” proteinase inhibitor cocktail (Roche)	
Impregnating solution	50 µl sodium thiosulfate solution (2.15 g in 5 ml ddH <sub>2</sub> O), 70 µl 37 % formaldehyde, ad 100 ml ddH <sub>2</sub> O	Silver staining
Staining solution	0.2 g silver nitrate, 70 µl 37 % formaldehyde, ad 100 ml ddH <sub>2</sub> O	
Developing solution	6 g Na <sub>2</sub> CO <sub>3</sub> (water-free), 2 µl sodium thiosulfate solution (2.15 g in 5 ml ddH <sub>2</sub> O), 50 µl 37 % formaldehyde, ad 100 ml ddH <sub>2</sub> O	
CoIP lysis buffer	10 mM Tris-HCl pH7.5, 150 mM NaCl, 0.5 mM EDTA, 0.2 % NP-40, 1x “Complete” proteinase inhibitor cocktail (Roche)	CoIP
CoIP dilution/wash buffer	10 mM Tris-HCl pH7.5, 150 mM NaCl, 0.5 mM EDTA, 1x “Complete” proteinase inhibitor cocktail (Roche)	

## 2.9 Commercial kits

Commercial kits used in this work are listed below.

Distributor	Appellation
GE-Healthcare, Munich	ECL Select Western Blotting Detection Reagent, Illustra MicroSpin G50 columns
Genomed, Bad Oeynhausen	Jet-Star Plasmid purification Kit
Invitrogen GmbH, Karlsruhe	SuperScript III First Strand Synthesis SuperMix
Macherey-Nagel, Düren	NucleoSpin Extract II Kit, NTB Buffer
Metabion, Planegg/Steinkirchen	mi-Plasmid Miniprep Kit
Qiagen, Hilden	Endofree Plasmid Maxi Kit, QIAamp DNA Mini Kit, Rneasy MiniKit, QiaShredder
Roche Diagnostics GmbH, Erlangen	Rapid DNA Dephos and Ligation Kit
Thermo Scientific, Waltham, USA	CloneJET PCR Cloning Kit
Whatman, Dassel	ELUTRAP BT1000 STARTERKIT



## 2.10 Software

Software tools that contributed to this work are listed below.

Distributor	Appellation
Accelrys, Cambridge, UK	MacVector 12.6
Adobe Systems Inc., San Jose (USA)	Illustrator CS5, Photoshop CS5
Graphpad Software, La Jolla, USA	Prism 6
Microsoft, Redmond (USA)	Microsoft Office 2008
Raytest Isotopenmessgeräte GmbH, Straubenhardt	AIDA Alias Software
The R Foundation for Statistical Computing Vienna, Austria	R 3.1.1
Thomson Reuters, New York (USA)	EndNote X2
TreeStar Inc., Ashland (USA)	FlowJo 9.1
Vilber Lourmat, Marne-la-Vallée, France	Quantum ST4 software

## 2.11 Devices and consumables

The list below comprises devices and consumables that were used in this work.

Distributor	Appellation
AGFA, Cologne	CP1000 developer machine, Medical X-Ray Screen
Beckman, Heidelberg	Centrifuge Avanti J-25 and Avanti-26XP
Becton Dickinson GmbH, Heidelberg	FACS-Calibur, cell culture flasks, 6-/12-/24-/48- and 96-well plates
Bio-Rad, Munich	Mini Protean II Tetra Gelelectrophoresis Unit, Gene-Pulser II electroporation device
Brand, Wertheim	Glass pipettes 5 ml, 10 ml, 20 ml and 25 ml
Branson, Danbury, USA	Branson Sonifier S-250D
Diagenode, Liège, Belgium	Bioruptor (UCD-200)
Eppendorf, Hamburg	BioPhotometer, PCR machine Mastercycler Personal, reaction tubes, desk centrifuge 5415, thermomixer comfort
Eurofins MWG Operon, Ebersberg	DNA sequencing
Hartenstein, Würzburg	Cover slips, glass slides, forceps, Whatman paper, Neubauer chamber
Hewlett Packard, USA	HP Scan-Jet G4050
G. Heinemann, Schwäbisch Gmünd	Sonifier nozzle 5 mM for Branson sonifier
FujiFilm, Kleve	Phosphorimager FLA 5100, film cassettes, intensifier screen
Invitrogen GmbH, Karlsruhe	Qubit 2.0 Fluorometer, Neon Transfection System
GE Healthcare, Munich	High performance autoradiography film
Gilson Inc., Villiers le Bel	Peristaltic Pump Minipuls 2, 2 µl, 20 µl, 200 µl and 1000 µl pipettes
Greiner Bio One, Solingen	Plastic consumables for cell culture and laboratory work
Metabion, Martinsried	DNA oligonucleotides and primers
Millipore, Schwalbach	Water deionizing device Milli-RO 60 PLUS
Montreal Biotec Inc., Montreal, Canada	Vacuum centrifuge univapo H150
Nunc GmbH, Wiesbaden	Cell culture dishes, 6-/12-/24-/48- and 96-well plates, cryotubes
Peqlab, Erlangen	Agarose gel electrophoresis chambers, NanoDrop ND-1000
Roche Diagnostics GmbH, Erlangen	Light Cyclers 480 Real Time PCR System, Xcelligence RTCA DP
Schleicher & Schüll, Dassel	0.8 µm and 1.2 µm filter
Schott, Mainz	Glass ware
Stratagene, Heidelberg	Robocycler Gradient 96
Thermo Scientific, USA	Heracus Multifuge 3L-R, orbital shakers, incubators
Vilber Lourmat, Marne-la-Vallée, France	Quantum ST4
Zeiss, Göttingen	Axiovert 40C, Axiovert 200M

# 3. METHODS

## 3.1 Bacterial culture

### 3.1.1 Growth and storage of bacterial cultures

*Escherichia coli* (*E.coli*) suspensions were cultured in LB-medium at 37 °C and 200 rpm in orbital shakers. Single cell clones were isolated by streaking the bacteria on LB-agar using an inoculating loop or a glass spreader and incubating the agar plates at 37 °C over night. Antibiotics (100 µg/ml ampicillin or 30 µg/ml kanamycin) were added to autoclaved LB-medium to select for bacteria harboring plasmid DNA with resistance genes. For long-term storage, bacterial stocks of over night cultures supplemented with 25 % glycerol were frozen at -80 °C.

### 3.1.2 Transformation of bacteria

According to the protocol of Hanahan *et al.* (1985) chemical competent *E.coli* cells were generated. For long-term storage, 200 µl aliquots were made, frozen immediately in liquid nitrogen and transferred to a -80 °C freezer. For a single transformation reaction, bacteria were thawed on ice, 50-100 µl were incubated with 2 µl (equivalent to 5-10 ng) of a ligation reaction or 1 ng of purified plasmid DNA on ice for 30 minutes. Heat shock reaction was performed by incubating on 42 °C for 90 seconds. Subsequently, the bacteria were transferred back on ice and 900 µl of LB-medium was added. The mixture was incubated at 37 °C allowing the expression of resistance genes. After 30 minutes bacteria were centrifuged at

3000 g for 30 seconds, resuspended in 100  $\mu$ l and plated on LB-agar containing the adequate antibiotic. The LB-agar plates were incubated at 37 °C over night.

## **3.2 Eukaryotic cell culture**

### **3.2.1 Cell culture conditions**

Eukaryotic cell culture was performed in lamina hoods using sterile pipettes, solutions and culture dishes. Cells were cultivated in 37 °C incubators in an atmosphere of 5 % CO<sub>2</sub> and 95 % air humidity. Centrifugation steps were carried out at 300 g for 5 minutes. Cells were washed with sterile PBS. Cell number was determined using a Neubauer cell chamber. All cell lines used in this work were cultured in RPMI-1640 medium supplemented with 10 % fetal bovine serum (FBS), 1 mM sodium pyruvate, 100 nM sodium selenite, 20  $\mu$ M bathocupproine-disulfonic acid, 0.433 %  $\alpha$ -thioglycerole, 100  $\mu$ g/ml streptomycin and 100 Units/ml penicillin (full medium). When the adherent HEK293 cells reached a confluency of 70-80 % they were washed with 10 ml PBS and subsequently incubated with 2 ml of 0.05 % trypsin and 0.02 % EDTA. The detached cells were resuspended in 10 ml medium and 1 ml was transferred to a new culture vessel. Raji cells were cultivated in suspension at an average density of  $3\text{-}5 \times 10^5$  cells/ml. The Raji cell lines 4816, 5693, or 5694 were all selected with 1  $\mu$ g/ml puromycin.

### **3.2.2 Storage of eukaryotic cells**

For long term storage cells were trypsinized, washed and resuspended in a mixture of 90 % FBS and 10 % DMSO at a concentration of  $1 \times 10^7$  cells/ml. Cells were transferred to a 2 ml CryoTube (Nunc) and gentle freezing was guaranteed by slowly cooling in a “Nalge Nunc Cryo 1 °C Mr. Frosty Freezing Container” (Nunc) with a cooling rate of -1 °C/min. In order to test cell viability, one vial was thawed after one week at -80 °C. The other vials were transferred to liquid nitrogen tanks and stored in the gas phase. For thawing, cells were warmed to 37 °C, washed with 50 ml of full medium, and taken up in 5 ml full medium. If required, an antibiotic for selection pressure was applied the day after thawing.

### **3.2.3 Transient transfection of HEK293 cells**

HEK293 cells were transiently transfected with plasmid DNA using PEI (Sigma-Aldrich).

For a 6-well scale,  $5 \times 10^5$  cells were seeded per well one day before transfection. The

upcoming day the culture medium was replaced with 1 ml Opti-MEM I (Invitrogen) and following mixtures were set up:

100  $\mu$ l Opti-MEM I + 1  $\mu$ g DNA

100  $\mu$ l Opti-MEM I + 6  $\mu$ l PEI (1 mg/ml)

For a 13 cm cell culture dish scale,  $2 \times 10^7$  cells were seeded per dish one day before transfection. The upcoming day the culture medium was replaced with 10 ml Opti-MEM I (Invitrogen) and following mixtures were set up:

3.6 ml Opti-MEM I + 30  $\mu$ g DNA

3.6 ml Opti-MEM I + 180  $\mu$ l PEI (1 mg/ml)

Both solutions were mixed, incubated for 15 minutes at room temperature and then added to the cells. After an incubation time of 4 hours, the transfection mixture was replaced either by 2 ml (6-well) or 20 ml (13 cm dish) of full medium.

### **3.2.4 Electroporation of eukaryotic cells**

Raji cells were electroporated with the gene pulser II electroporator (Biorad).  $5 \times 10^6$  cells were spun down and resuspended in 250  $\mu$ l Opti-MEM I. 5-10  $\mu$ g plasmid DNA were added and cells were incubated on ice for 15 minutes. Electroporation was performed in 4 mM cuvettes at 230 V and 975  $\mu$ F. After pulsing, cells were supplied with 400  $\mu$ l FBS, transferred to 5 ml full medium, and cultivated at 37 °C.

### **3.2.5 Establishment of stable cell lines**

For the generation of single cell clones electroporated cells (see chapter 3.2.4) were first grown in bulk culture for two days and then diluted in 96-well plates. The cells were cultivated under selection for four weeks, medium was changed if necessary, and outgrowing cells were expanded continuously. Expression of the transgene was evaluated using flow cytometry (see chapter 3.2.6).

### **3.2.6 Flow cytometry**

Cells of the stable Raji cell lines 4816, 5693, or 5694 were washed with PBS and analyzed in a FACS Calibur (Beckton Dickinson) to detect and count GFP-positive cells. Data was evaluated with the FlowJo 9.1 software.

### 3.3 Nucleic acid techniques

General methods like phenol/chloroform extraction, DNA precipitation with ethanol or isopropanol, electrophoretic separation of DNA, enzymatic restriction hydrolysis, ligation of free DNA ends, or radioactive labeling of DNA were performed according to standard protocols (Sambrook *et al.*, 2001).

#### 3.3.1 DNA purification from *E.coli*

Small-scale purification of plasmids was performed according to two different protocols. For evaluating a cloning procedure by enzymatic restriction digest, 2 ml of bacteria culture in the stationary phase were harvested, resuspended in M-STET buffer (50 mM Tris-HCl pH8.0, 25 mM EDTA, 5 % sucrose, 0.5 % Triton X-100), incubated at 95 °C for 2 minutes and centrifuged for 10 minutes at 15000 rpm. 2 µl of plasmid DNA were used for an enzymatic control digest. Instead for evaluating a cloning procedure by sequencing, 2 ml of bacteria culture in the stationary phase was used to purify plasmid DNA according to the manufacturer's protocol of the mi-Plasmid Miniprep Kit (Metabion).

For large-scale purification of plasmid DNA, 400 ml of bacteria culture in the stationary phase was used. The purification was performed using either the Jet Star Plasmid Purification Kit (Genomed) for cloning or the EndoFree Plasmid Maxi Kit (Qiagen) for transfection of cells.

#### 3.3.2 DNA purification from eukaryotic cells

Genomic DNA from eukaryotic cells was purified using the QIAamp DNA Mini Kit (Qiagen) according to the manufacturer's protocol.

#### 3.3.3 Purification of DNA from PCR products and agarose gels

Purification of DNA from PCR products or agarose gels was performed with the NucleoSpin Extract II Kit (Macherey-Nagel) following the manufacturer's protocol. SDS containing samples were purified with five volumes of NTB buffer instead of the standard binding buffer.

### 3.3.4 Electroelution of DNA from native gels

Large-scale purification of DNA fragments was performed by native gel electrophoresis. Using a UV lamp, the fragment of interest was visualized, excised with a scalpel and the DNA was electroeluted with the ELUTRAP BT1000 STARTERKIT (Whatman) according to the manufacturer's recommendations. DNA concentration was measured by the Nanodrop method.

### 3.3.5 Dephosphorylation and ligation

For cloning procedures DNA fragments were dephosphorylated and ligated using the Rapid DNA Dephos and Ligation Kit (Roche) according to the company's recommendations.

### 3.3.6 Polymerase chain reaction (PCR)

PCR amplifies defined nucleic acid fragments exponentially (Mullis *et al.*, 1986). In this work the protocol of the Phusion High-Fidelity DNA polymerase (Finnzymes) was used. The components of a PCR reaction and a typical PCR program are listed below.

Component	50 µl reaction
H <sub>2</sub> O	ad to 50 µl
5x Phusion HF Buffer	10 µl
10 mM dNTPs	1 µl (10 mM)
Forward primer	0.5 µl (100 µM)
Reverse primer	0.5 µl (100 µM)
Template DNA	1 to 50 ng
Phusion DNA polymerase	0.5 µl (0.02 U/µl)

Cycle step	Temperature	Time	Cycles
Initial denaturation	98 °C	3 min	1
Denaturation	98 °C	30 s	30
Annealing	50-60 °C (depending on primer pair)	30 s	
Extension	72 °C	30 s – 1 min/kb	
Final extension	72 °C	10 min	1

Amplified DNA was separated on a 1 % TBE agarose gel to control the size of the PCR product or for preparative gel purification (see chapter 3.3.3).

### 3.3.7 Quantitative real time PCR (qPCR)

Immunoprecipitated DNA (see chapter 3.5.2) or cDNA (see chapter 3.3.10) was quantified with a Roche LightCycler 480 device. During DNA synthesis the fluorescent dye SYBR-

Green I is incorporated into double-stranded DNA and therefore the amount of DNA can be quantified after each elongation cycle (Higuchi *et al.*, 1993).

The amount of DNA was analyzed with “absolute quantification”. This method allows the calculation of the sample concentration by comparing the crossing points (Cp) of the unknown sample with a defined standard curve, which encompasses different dilutions of either input (immunoprecipitated DNA) or a known amount of transcripts (cDNA). The analysis was done automatically with the LightCycler 480 software according to the second derivative maximum method.

The PCR mix and the PCR program for qPCR are listed below.

Component	Amount
Template DNA	1 µl immunoprecipitated DNA or cDNA
Primer	5 pm each
SYBR Green I Master (2x)	5 µl
H <sub>2</sub> O	3.5 µl

Program	Target temperature (°C)	Hold (sec)	Acquisition mode	RampRate (°C/sec)	Cycles	Analysis mode
Pre-incubation	95	600	None	4.4	1	None
Amplification	95	1	None	4.4	45	Quantification
	62	10	None	2.2		
	72	10	None	4.4		
	75	3	Single	4.4		
	97	1	None	4.4		
Melting curve	67	10	None	2.2	1	Melting curve
	97	/	Continuous	0.11		
Cooling	37	15	None	2.2	1	None

### 3.3.8 Mutagenesis PCR

Single point mutations were introduced in plasmid DNA using the Phusion High-Fidelity DNA polymerase (Finnzymes). Primers were designed such that their 5' ends are located close to each other, resulting in an amplification of the whole plasmid except the sequence between the primers. The sequence between the 5' ends of the primers was replaced by adding the desired sequence to the 5' end of one primer. The PCR procedure is described in chapter 3.3.6.

### 3.3.9 Isolation of RNA from cells

Isolation of RNA from cells was performed using the RNase Mini Kit (Qiagen). Per each sample the lysate of  $1 \times 10^7$  cells was prepared and homogenized with QiaShredder columns

(Qiagen). All subsequent steps were performed according to the manufacturer's recommendations. RNA was eluted in 80 µl of RNase-free water and stored at -80 °C.

### **3.3.10 Reverse transcription of RNA**

RNA was transcribed into cDNA to determine expression levels of genes of interest. The removal of contaminating DNA from the RNA preparation was performed using the enzyme Desoxyribonuclease I (DNase I, Invitrogen). Therefore, 2 µg of extracted RNA were incubated at 37 °C with 2 U DNase I, 40 U RNase inhibitor and 1x DNase buffer in a 20 µl approach for 90 minutes. Remaining DNase I was heat inactivated by incubating at 65 °C for 10 minutes and the efficiency of DNase treatment was controlled by PCR (see chapter 3.3.6). Reverse transcription of RNA was performed with the SuperScript III First Strand Synthesis SuperMix Kit (Invitrogen) according to the manufacturer's protocol. cDNA was analyzed quantitatively using qPCR (see chapter 3.3.7).

## **3.4 Protein analysis techniques**

### **3.4.1 Preparation of whole cell extracts**

For the preparation of whole cell extracts,  $5 \times 10^7$  HEK293 cells were washed (7 min at 300 g and 4 °C) twice with ice-cold PBS and lysed in a volume of 1 ml RIPA buffer (50 mM Tris-HCl pH8.0, 150 mM NaCl, 0.1 % SDS, 0.5 % sodium deoxycholate, 1 % NP-40, 1x "Complete" proteinase inhibitor cocktail (Roche)) for 20 minutes on ice. The lysate was sonified using a Branson sonifier 250-D (10 sec on/50 sec off, 1 min, 20 % amplitude, on ice). Cell debris was pelleted by centrifugation (15 min at 20000 g and 4 °C). The supernatant was transferred to a new tube and the protein concentration was measured with Bradford solution (Bio-Rad) in a BioPhotometer (Eppendorf).

### **3.4.2 Preparation of nuclear cell extracts**

Nuclear cell extracts were prepared by harvesting  $1 \times 10^8$  Raji cells (7 min at 1200 rpm and 4 °C). Cells were washed twice with ice-cold PBS (7 min at 1200 rpm and 4 °C) and the pellet was resuspended in 2 ml hypotonic buffer (10 mM HEPES pH7.9, 1.5 mM MgCl<sub>2</sub>, 10 mM KCl, 340 mM sucrose, 1x "Complete" proteinase inhibitor cocktail (Roche)). Swelling of the cells was checked after incubation on ice for 15 minutes under the microscope. Cell lysis was performed using a final concentration of 0.1 % Triton X-100.



After vortexing for 15 seconds, grey colored nuclei were controlled under the microscope. Nuclei were pelleted (5 min at 2000 rpm and 4 °C) and resuspended in 300 µl hypotonic buffer. To extract the nuclei, 150 µl of high salt buffer (10 mM HEPES pH7.9, 1.5 mM MgCl<sub>2</sub>, 1260 mM NaCl, 1x “Complete” proteinase inhibitor cocktail (Roche)) was added and incubated while rotating for 1 hour at 4 °C. After centrifugation (15 min at 13200 rpm and 4 °C), the protein concentration of the nuclear extract containing supernatant was measured with Bradford solution (Bio-Rad) in a BioPhotometer (Eppendorf).

### **3.4.3 Purification of Strep-tag fusion proteins**

The purification of Strep-tag fusion proteins in HEK293 cells was accomplished using Strep-Tactin affinity chromatography according to the manufacturer’s recommendations (IBA). Briefly, four to six 13 cm culture dishes were transiently transfected with the expression plasmid coding for the desired tandem strep-tagged protein (see chapter 3.2.3). After 48 hours, the cells were harvested (7 min at 1400 rpm and 4 °C) and whole cell extracts were prepared in 5 ml RIPA buffer (see chapter 3.4.1). A poly-prep chromatography column was loaded with a 200 µl column volume (CV) of Strep-Tactin sepharose beads and equilibrated with two CVs washing buffer (100 mM Tris-HCl pH8.0, 150 mM NaCl, 1 mM EDTA, 1x “Complete” proteinase inhibitor cocktail (Roche)). The protein lysate was loaded onto the column three times followed by five washing steps with one CV washing buffer each. The protein was eluted in six fractions by adding half a CV elution buffer (100 mM Tris-HCl pH8.0, 150 mM NaCl, 1 mM EDTA, 2.5 mM desthiobiotin, 1x “Complete” proteinase inhibitor cocktail (Roche)) each. The protein concentration was first measured with Bradford solution (BioRad) and then verified on a SDS gel by Coomassie staining in comparison to different amounts of a bovine serum albumin (BSA) standard.

### **3.4.4 Electromobility shift assay (EMSA) for detecting protein-DNA interactions**

EMSAs were performed for analyzing protein-DNA interactions. According to Fried and Crothers (1981), the assay is based on altered migration behavior of a protein-DNA complex in comparison to unbound DNA in a native polyacrylamide gel. The electrophoretic separation of a protein DNA complex is determined by their size, charge and shape. Proteins were purified using Strep-Tactin affinity chromatography (see chapter 3.4.3). As DNA templates 156 bp fragments derived from digested, methylated plasmid DNAs (see chapter 3.7.2) were used. The DNA fragments were radioactively labeled in a T4 polynucleotide

kinase reaction (T4-PNK) with [ $\gamma$ - $^{32}$ P] ATP as the phosphate group donor. Therefore, the following reaction was set up and incubated at 37 °C for 30 minutes to one hour.

Component	Amount
Template DNA	1 $\mu$ g
PNK buffer A (10x)	5 $\mu$ l
T4-PNK (Fermentas)	2 $\mu$ l [10 U/ $\mu$ l]
[ $\gamma$ - $^{32}$ P] ATP (30 mCi/ml)	3 $\mu$ l
ddH <sub>2</sub> O	ad 50 $\mu$ l

The labeled fragments were purified using G50-Sephadex columns (GE Healthcare) and radioactive emission was measured. The protein-DNA interaction was performed for ten minutes at room temperature with following binding conditions.

Component	Amount
Protein solution	4 $\mu$ l
EMSA binding buffer (10x)	2 $\mu$ l
Poly (dI/dC) [1 $\mu$ g/ $\mu$ l]	1 $\mu$ l
Labeled template	0.8 ng (5000-20000 dpm)
ddH <sub>2</sub> O	ad 20 $\mu$ l

After incubation, EMSA loading dye (20 mM Tris-HCl pH7.5, 8 mM EDTA, 25 % glycerol, 0.1 % NP-40) was added to the samples to a final concentration of 1x and the samples were loaded onto a 5 % native shift gel (5 ml Rotiphorese 30 (37.5:1), 5 ml Rotiphorese 40 (19:1), 3.2 ml 10x TBE, 66 ml ddH<sub>2</sub>O, 50  $\mu$ l TEMED, 400  $\mu$ l 10 % APS), which had been pre-run for at least 60 minutes. Bromophenol blue in EMSA loading dye was loaded in one empty lane for estimating the run length. The gel was run at 4 °C and 130 V for five to six hours. The gel was incubated for 15 minutes in fixing solution (10 % acetic acid, 20 % methanol in ddH<sub>2</sub>O) and then dried in a vacuum gel dryer on Whatman paper.

DNA was visualized using a high performance autoradiography film (GE Healthcare). For densitometric quantification of protein-DNA complexes an image plate (Fujifilm) was exposed and read with the aid of a Phosphoimager (Fujifilm). Quantitation of radioactive emission was done using the program AIDA (Raytest).

### 3.4.5 Determination of the equilibrium dissociation constant ( $K_d$ value)

According to Ryder *et al.* (2008), the  $K_d$  value defines the protein concentration needed to achieve a half-maximum binding at equilibrium, expressed here in nM concentration. The  $K_d$  value was experimentally assessed using EMSAs (see chapter 3.4.4). The amount of protein needed in nmol was converted in ng with the help of the website [http://www.molbiol.ru/eng/scripts/01\\_04.html](http://www.molbiol.ru/eng/scripts/01_04.html) and the ratio of protein-DNA complex to

unbound DNA was determined. The  $K_d$  value was calculated using the program Prism6 (Graphpad). The bound fraction was plotted against the protein concentration and the  $K_d$  value was calculated using the equation “One site – Specific binding with Hill slope”.

### **3.4.6 Sodium dodecyl sulfate polyacrylamide gel electrophoresis (SDS-PAGE)**

SDS-PAGE was performed using a Mini Protean Tetra Cell (Bio-Rad). Acrylamide gels were cast as described in the table of chapter 2.8. Samples were prepared as described below and heat denatured for five minutes at 100 °C in a sand bath.

Component	Amount
Protein lysate	max. 30 µg
Laemmli buffer (5x)	4 µl
ddH <sub>2</sub> O	ad 20 µl

Proteins were separated at 100-130 V until the bromophenol blue dye migrated out of the gel.

### **3.4.7 Western blot**

Western blot was performed using a Mini Trans-Blot Cell (Bio-Rad). Proteins separated by SDS-PAGE were transferred onto a Hybond ECL membrane (GE Healthcare) at 100 V for 80 minutes. Afterwards, the membrane was incubated for 30 minutes in blocking solution (5 g milk powder in 100 ml PBS-T) at room temperature and then with the primary antibody, diluted in blocking solution, at 4 °C overnight. The next day, the membrane was washed five times for five minutes each in PBS-T and incubated with the HRP-conjugated secondary antibody, diluted in blocking solution, for 45 minutes at room temperature. The membrane was again washed five times for five minutes each in PBS-T. After incubating the membrane with ECL reagent (GE Healthcare) for five minutes, the bands were detected using a x-ray film. Used antibody dilutions are listed in the table of chapter 2.3.

### **3.4.8 Silver staining**

The silver staining of SDS-PAGEs (see chapter 3.4.6) was performed at room temperature and constant shaking as follows. Incubating for 60 minutes in 50 % methanol and 12 % acetic acid, followed by washing with 50 % ethanol and 30 % ethanol for 20 minutes each, fixed the gel. Impregnation was performed using freshly made impregnation solution (50 µl sodium thiosulfate solution (2.15 g in 5 ml ddH<sub>2</sub>O), 70 µl 37 % formaldehyde, ad 100 ml ddH<sub>2</sub>O) for two minutes. After three washing steps with ddH<sub>2</sub>O the gel was stained in freshly made

staining solution (0.2 g silver nitrate, 70  $\mu$ l 37% formaldehyde, ad 100 ml ddH<sub>2</sub>O) for 20 minutes. Silver excess was removed by washing two times with ddH<sub>2</sub>O. Staining reaction was initiated by incubating in freshly made developing solution (6 g Na<sub>2</sub>CO<sub>3</sub> (water-free), 2  $\mu$ l sodium thiosulfate solution (2.15 g in 5 ml ddH<sub>2</sub>O), 50  $\mu$ l 37 % formaldehyde, ad 100 ml ddH<sub>2</sub>O) until all bands were visible and stopped by 50 % methanol and 12 % acetic acid.

## **3.5 Chromatin Immunoprecipitation (ChIP)**

### **3.5.1 Chromatin preparation**

For chromatin preparation  $4 \times 10^7$  Raji 4816 cells were harvested (7 min at 300 g at 4 °C) and washed twice with ice-cold PBS (7 min at 300 g and 4 °C). Cross-linking was carried out in a total volume of 20 ml PBS (room temperature) and 1 % formaldehyde for seven minutes at room temperature with constant rotating. The reaction was stopped with 2.5 ml of 1 M glycine while incubating and inverting for five minutes at room temperature. Afterwards all steps were performed on ice. The cells were pelleted and washed twice with ice-cold PBS (5 min at 500 g and 4 °C). The isolation of nuclei was accomplished by washing (10 min at 300 g and 4 °C) the pellet three times with 10 ml ice-cold ChIP lysis puffer (10 mM Tris-HCl, pH7.5, 10 mM NaCl, 3 mM MgCl<sub>2</sub>, 0.5 % NP-40). After checking the grey colored nuclei under the microscope, the pellet was resuspended in 2 ml of ice-cold ChIP sonication buffer (50 mM Tris-HCl, pH7.5, 10 mM EDTA, 1 % SDS, 1 % NP-40, 1x “Complete” proteinase inhibitor cocktail (Roche)). Chromatin was fragmented by sonication with a BRANSON sonifier W-250 D (amplitude = 35 %, total pulse time 180 sec with 36 cycles of 5 sec pulse and 25 sec pause). The sonicated samples were centrifuged (10 min at maximum speed and 4 °C), their protein concentration was measured with the Bradford method and subsequently frozen at -80 °C. The fraction size of the chromatin was analyzed after treatment of 10  $\mu$ g chromatin with proteinase K at 68 °C for three hours and checked on a 1 % TBE agarose gel upon DNA purification with the NucleoSpin Extract kit II (Macherey-Nagel).

### **3.5.2 Chromatin immunoprecipitation and purification of ChIP DNA**

For chromatin immunoprecipitation 100  $\mu$ g of chromatin solution was adjusted with ChIP dilution buffer (20 mM Tris-HCl, pH8.0, 2 mM EDTA, pH8.0, 1 % TritonX-100, 150 mM NaCl, 1x “Complete” proteinase inhibitor cocktail (Roche)) to a final volume of 1 ml and a final concentration of 0.1 % SDS. After addition of the antibody, the chromatin was incubated

at 4 °C over night with constant overhead rotating. Used antibody concentrations are listed in the table of chapter 2.3. 100 µl of protein G or protein A resin (50 % slurry) were pre-equilibrated with ChIP dilution buffer and incubated at 4 °C over night with overhead shaking. The next day, beads were spun down at 2000 rpm for two minutes, added to the antibody-chromatin mixture, and incubated at 4 °C for two hours by overhead rotating. To remove unspecific DNA and proteins, the beads were washed (2 min at 2000 rpm and RT) each time with 1 ml in the order of following buffers: ChIP low salt buffer (20 mM Tris-HCl, pH8.0, 2 mM EDTA, pH8.0, 1 % Triton X-100, 150 mM NaCl, 0.1 % SDS), ChIP high salt buffer (20 mM Tris-HCl, pH8.0, 2 mM EDTA, pH8.0, 1 % Triton X-100, 500 mM NaCl, 0.1 % SDS), ChIP LiCl buffer (10 mM Tris-HCl, pH8.0, 1 mM EDTA, pH8.0, 250 mM LiCl, 0.5 % NP-40, 0.5 % sodium deoxycholate) and TE buffer (10 mM Tris-HCl, pH8.0, 1 mM EDTA). Elution and removal of the cross-link was accomplished in 200 µl ChIP elution buffer (25 mM Tris-HCl, pH7.5, 10 mM EDTA, pH8.0, 0.5 % SDS) containing 20 µg proteinase K for three hours at 68 °C while shaking. DNA was purified with the NucleoSpin Extract II Kit (Macherey-Nagel) according to manufacturer's protocol and eluted in 60 µl elution buffer. ChIP samples were immediately analyzed or stored at -20 °C.

### 3.5.3 Quantitation of ChIP DNA by qPCR

To quantify the DNA content of ChIP samples, qPCR with the LightCycler 480 system was performed (see chapter 3.3.7). Stepwise dilutions of total input DNA ranging from 0.1 % to 10 % and ChIP DNA were analyzed with primer pairs specific for different loci of latent, early lytic and late lytic EBV regions. Oligonucleotides and their sequences are listed in the appendix.

## 3.6 Sequential ChIP (ReChIP)

The ReChIP method is a relatively new technique that enables sequential chromatin immunoprecipitations to be performed using two different antibodies to prove the co-occupancy of two proteins or distinct histone modifications at the same genomic region of interest (Geisberg and Struhl, 2004).

### 3.6.1 Chromatin preparation for BZLF1-directed ChIP

For chromatin preparation  $1 \times 10^8$  Raji 4816 cells were harvested (7 min at 300 g and 4 °C) and washed twice with ice-cold PBS (7 min at 300 g and 4 °C). Cross-linking was carried out in a

total volume of 40 ml PBS (room temperature) and a final concentration of 1 % formaldehyde for eight minutes at room temperature with constant rotating. The reaction was stopped with 5 ml of 1 M glycine while incubating and rotating for one minute at room temperature, followed by incubation on ice for five minutes. Afterwards all steps were performed on ice. The cells were pelleted and washed twice with ice-cold PBS (5 min at 500 g and 4 °C). The isolation of nuclei was accomplished by washing (10 min at 300 g and 4 °C) the pellet with 10 ml in the order of following buffers: ReChIP lysis buffer 1 (50 mM HEPES, pH7.5, 140 mM NaCl, 1 mM EDTA, pH8.0, 0.5 mM EGTA, pH8.0, 10 % glycerol, 0.5 % NP-40, 0.25 % Triton X-100, 1x “Complete” proteinase inhibitor cocktail (Roche)) and ReChIP lysis buffer 2 (25 mM HEPES, pH7.5, 200 mM NaCl, 1 mM EDTA, pH8.0, 0.5 mM EGTA, pH8.0, 1x “Complete” proteinase inhibitor cocktail (Roche)). Further, the nuclei containing pellet was resuspended in 5 ml ReChIP lysis buffer 3 (25 mM HEPES, pH7.5, 140 mM NaCl, 1 mM EDTA, pH8.0, 0.5 mM EGTA, pH8.0, 0.25 % N-lauryl sarcosine, 0.1 % sodium deoxycholate, 0.25 % Triton X-100, 1x “Complete” proteinase inhibitor cocktail (Roche) and the grey colored nuclei were checked under the microscope. To obtain mononucleosomal fragment-sized chromatin, acid-washed glass beads (212-300 µm, Sigma-Aldrich) were added and chromatin was sonicated with a BRANSON sonifier W-250 D (amplitude = 35 %, total pulse time 240 sec with 120 cycles of 1 sec pulse and 1 sec pause). The sonicated samples were centrifuged (10 min at maximum speed and 4 °C) and chromatin was further digested with Micrococcal Nuclease (MNase) S7 (10 U/µl, Roche) and a final concentration of 4 mM CaCl for ten minutes at 37 °C. Adding EGTA pH8.0 to a final concentration of 40 mM stopped the reaction. The DNA concentration of the chromatin was measured with the Nanodrop method, the chromatin solution was adjusted to an amount of 1 mg/ml with a final concentration of 0.5 % Triton X-100, 10 % glycerol and ReChIP lysis buffer 3 and subsequently frozen at -80 °C. The mononucleosomal fraction size of the chromatin was analyzed after treatment of 30 µg chromatin with 20 µg proteinase K at 68 °C for three hours and checked on a 1 % TBE agarose gel upon DNA purification with the NucleoSpin Extract kit II (Macherey-Nagel).

### **3.6.2 ReChIP starting with a BLZF1-directed antibody**

For the first round of chromatin immunoprecipitation 1500 µg of chromatin solution (see chapter 3.6.1) was adjusted with ReChIP lysis buffer 3 to a final volume of 5 ml. 25 µg of ZEBRA antibody (Santa Cruz) was added and incubated at 4 °C over night with constant overhead rotating. 500 µl of protein G resin (50 % slurry) were pre-equilibrated with 4.5 ml

ReChIP lysis buffer 3 and incubated at 4 °C over night with constant overhead rotating. The next day, beads were spun down at 2000 rpm for two minutes, added to the antibody-chromatin mixture, and incubated at 4 °C for two hours by overhead rotating. To remove unspecific DNA and proteins, the beads were washed (2 min at 2000 rpm and RT) each time with 1 ml in the order of following buffers: ReChIP wash buffer 1 (50 mM Tris-HCl, pH8.0, 150 mM NaCl, 1 mM EDTA, pH8.0, 0.1 % SDS, 0.5 % sodium deoxycholate, 1 % NP-40), ReChIP wash buffer 2 (50 mM Tris-HCl, pH8.0, 300 mM NaCl, 1 mM EDTA, pH8.0, 0.1 % SDS, 0.5 % sodium deoxycholate, 1 % NP-40), ReChIP LiCl buffer (50 mM Tris-HCl, pH8.0, 250 mM LiCl, 0.1 % SDS, 0.5 % sodium deoxycholate, 1 % NP-40) and TE buffer (10 mM Tris-HCl, pH8.0, 1 mM EDTA). Elution of the BZLF1-ChIPed chromatin was performed with 100 µl ChIP sonication buffer by incubating for two hours at 37 °C under constant shaking.

For the second round of chromatin immunoprecipitation, the first ChIPed chromatin solution was adjusted with ChIP sonication buffer to a final volume of 1 ml and a final concentration of 0.1 % SDS. 1 µg of H3K4me1 antibody (Abcam) was added and incubated at 4 °C over night with constant overhead rotating. 100 µl of protein A resin (50 % slurry) were pre-equilibrated with 1 ml ChIP sonication buffer and incubated at 4 °C over night with constant overhead rotating. The next day, beads were spun down at 2000 rpm for two minutes, added to the antibody-chromatin mixture, and incubated at 4 °C for two hours by overhead rotating. To remove unspecific DNA and proteins, the beads were washed (2 min at 2000 rpm and RT) each time with 1 ml in the order of following buffers: ChIP low salt buffer (20 mM Tris-HCl, pH8.0, 2 mM EDTA, pH8.0, 1 % Triton X-100, 150 mM NaCl, 0.1 % SDS), ChIP high salt buffer (20 mM Tris-HCl, pH8.0, 2 mM EDTA, pH8.0, 1 % Triton X-100, 500 mM NaCl, 0.1 % SDS), ChIP LiCl buffer (10 mM Tris-HCl, pH8.0, 1 mM EDTA, pH8.0, 250 mM LiCl, 0.5 % NP-40, 0.5 % sodium deoxycholate) and TE buffer (10 mM Tris-HCl, pH8.0, 1 mM EDTA). Elution and removal of the cross-link was accomplished in 200 µl ChIP elution buffer (25 mM Tris-HCl, pH7.5, 10 mM EDTA, pH8.0, 0.5 % SDS) containing 20 µg proteinase K for three hours at 68 °C while shaking. The double ChIPed DNA was purified with the NucleoSpin Extract II Kit (Macherey-Nagel) according to manufacturer's protocol and eluted in 60 µl elution buffer. ChIP samples were immediately analyzed or stored in the freezer at -20 °C.

### 3.6.3 ReChIP starting with an H3K4me1-directed antibody

For the first round of chromatin immunoprecipitation 100 µg of chromatin solution (see chapter 3.5.1) was adjusted with ChIP sonication buffer to a final volume of 1 ml and a final concentration of 0.1 % SDS. 5 µg of H3K4me1 antibody (Abcam) was added and incubated at 4 °C over night with constant overhead rotating. 100 µl of protein A resin (50 % slurry) were pre-equilibrated with 1 ml ChIP dilution buffer and incubated at 4 °C over night with constant overhead rotating. The next day, beads were spun down at 2000 rpm for two minutes, added to the antibody-chromatin mixture, and incubated at 4 °C for two hours by overhead rotating. To remove unspecific DNA and proteins, the beads were washed (2 min at 2000 rpm and RT) each time with 1 ml in the order of following buffers: ChIP low salt buffer, ChIP high salt buffer, ChIP LiCl buffer and TE buffer. Elution of the H3K4me1-ChIPed chromatin was accomplished with 100 µl ReChIP lysis buffer 3 and 1 % SDS by incubating for two hours at 37 °C under constant shaking.

For the second round of chromatin immunoprecipitation, the first H3K4me1-ChIPed chromatin solution was adjusted with ReChIP buffer 3 to a final volume of 1 ml and a final concentration of 0.1 % SDS. 1 µg of ZEBRA antibody (Santa Cruz) was added and incubated at 4 °C over night with constant overhead rotating. 15 µl of protein G resin (50 % slurry) were pre-equilibrated with 1 ml ReChIP buffer 3 and incubated at 4 °C over night with constant overhead rotating. The next day, beads were spun down at 2000 rpm for two minutes, added to the antibody-chromatin mixture, and incubated at 4 °C for two hours by overhead rotating. To remove unspecific DNA and proteins, the beads were washed (2 min at 2000 rpm and RT) each time with 1 ml in the order of following buffers: ReChIP wash buffer 1, ReChIP wash buffer 2, ReChIP LiCl buffer and TE buffer. Elution and removal of the cross-link was accomplished in 200 µl ChIP elution buffer containing 20 µg proteinase K for three hours at 68 °C while shaking. The double ChIPed DNA was purified with the NucleoSpin Extract II Kit (Macherey-Nagel) according to the manufacturer's protocol and eluted in 60 µl elution buffer. ChIP samples were immediately analyzed or stored at -20 °C.



## 3.7 Co-Immunoprecipitation (CoIP)

### 3.7.1 CoIPs of GFP-tagged bait proteins

For Co-IPs the GFP-Trap\_A for immunoprecipitation of GFP-fusion proteins (Chromotek) was used according to the manufacturer's recommendations. Briefly, for one IP reaction,  $1 \times 10^7$  co-transfected HEK293 cells were harvested and washed three times with ice-cold PBS (7 min at 1200 rpm and 4 °C). The pellet was resuspended in 200  $\mu$ l CoIP lysis buffer (10 mM Tris-HCl, pH7.5, 150 mM NaCl, 0.5 mM EDTA, 0.2 % NP-40, 1x "Complete" proteinase inhibitor cocktail (Roche) +/- 5 U/ $\mu$ l Benzonase and 0.5  $\mu$ g/ $\mu$ l DNase I (Invitrogen)) and incubated on ice for 30 minutes with extensively pipetting every 10 minutes. The cell lysate was spun down and the protein-containing supernatant was adjusted with CoIP wash/dilution buffer (10 mM Tris-HCl, pH7.5, 150 mM NaCl, 0.5 mM EDTA, 1x "Complete" proteinase inhibitor cocktail (Roche)) to a final volume of 500  $\mu$ l. For immunoblot analysis 5-10 % input material was used. 20  $\mu$ l of GFP-Trap\_A bead slurry was pre-equilibrated in 500  $\mu$ l ice cold CoIP dilution/wash buffer and washed two more times with 500  $\mu$ l of CoIP buffer dilution/wash buffer (2 min at 2500 g and 4 °C). The cell lysate was added to the pre-equilibrated beads and incubated under constant rotating for two hours at 4 °C. Further, beads were spun down and washed five times with 500  $\mu$ l CoIP dilution/wash buffer (2 min at 2500 g and 4 °C). To dissociate the immunocomplexes the beads were boiled for five minutes at 95 °C in 1x Laemmli buffer.

To check the interaction of GFP-coupled bait proteins and prey candidates, western blot immunodetection (see chapter 3.4.7) with an anti-GFP antibody (Chromotek) as well as an antibody against the protein of interest were performed.

### 3.7.2 CoIPs of Strep-tagged bait proteins

For CoIPs of Strep-tag fusion proteins, Strep-Tactin affinity chromatography was performed using Strep-Tactin sepharose beads (IBA) according to the manufacturer's recommendations. Briefly, for one reaction,  $5 \times 10^7$  to  $1 \times 10^8$  Raji 5693 or Raji 5694 cells were induced with 100 ng/ml doxycycline over night for BZLF1 or bZIP expression, respectively. The next day cells were harvested and washed three times with ice-cold PBS (7 min at 1200 rpm and 4 °C). The pellet was resuspended in 200  $\mu$ l CoIP lysis buffer and incubated on ice for 30 minutes

with extensively pipetting every ten minutes. The cell lysate was spun down and the protein-containing supernatant was adjusted with CoIP wash/dilution buffer to a final volume of 500  $\mu$ l. For immunoblot analysis 5-10 % input material was used. 100  $\mu$ l of Strep-Tactin sepharose beads were pre-equilibrated in 500  $\mu$ l ice cold 1x wash buffer and washed two other times with 500  $\mu$ l of 1x wash buffer (2 min at 2500 g and 4 °C). The cell lysate was added to the pre-equilibrated beads and incubated under constant rotating for two hours at 4 °C. Further, beads were spun down and washed five times with 500  $\mu$ l 1x wash buffer (2 min at 2500 g and 4 °C). To dissociate the immunocomplexes the beads were boiled for five minutes at 95 °C in 1x Laemmli buffer.

To check the interaction of the Strep-tagged BZLF1 bait proteins and prey candidates, western blot immunodetection (see chapter 3.4.7) with antibodies against BZLF1 ( $\alpha$ -BZ1, Elisabeth Kremmer) as well as an antibody against the protein of interest were performed.

### 3.8 *In vitro* reconstitution of chromatin

#### 3.8.1 Histone octamer preparation from *Drosophila* embryos

Histone octamers from *Drosophila* embryos were prepared according to Krietenstein *et al.* (2012). A long-term storage of histone octamers is possible at -20 °C in a final concentration of 50 % glycerol.

#### 3.8.2 Purification of 156 bp DNA fragments

DNA templates of interests with Asp718I restriction site flanks were cloned as multimers in pUC18 vector. The methylation of CpG dinucleotides was accomplished using the CpG Methyltransferase M.SssI (NEB) with following protocol.

Component	Amount
Plasmid DNA	100 $\mu$ g
NeBuffer 2 (10x)	100 $\mu$ l
SAM (32 mM)	5 $\mu$ l
M.SssI [4 U/ $\mu$ l]	10 $\mu$ l
ddH <sub>2</sub> O	ad 1000 $\mu$ l

After an over-night incubation at 37 °C, the methylation reaction was refreshed with 5  $\mu$ l M.SssI [4 U/ $\mu$ l] and 5  $\mu$ l 32 mM S-Adenosyl methionine (SAM) and further incubated at 37 °C for two hours. According to standard protocols of Sambrook *et al.* (2001) phenol/chloroform extraction and DNA precipitation with ethanol was performed. The

precipitated, methylated plasmid DNA was resuspended in 100 µl ddH<sub>2</sub>O. To control the methylation degree of CpG dinucleotides, a control digest using methylation sensitive restriction enzymes (NEB) was carried out as follows.

Component	Amount
Methylated plasmid DNA	500 ng
NeBuffer 4 (10x)	20 µl
BSA (100x)	0.2 µl
AvaI [10 U/µl]	0.50 µl
XmnI [20 U/µl]	0.25 µl
ddH <sub>2</sub> O	ad 20 µl

After incubation for two hours at 37 °C, the restriction was controlled on an agarose gel.

To liberate the monomeric fragments of the methylated plasmids and to obtain blunt ends, a methylation-insensitive restriction digest with RsaI (NEB) was performed.

Component	Amount
Methylated plasmid DNA	100 µl
NeBuffer 4 (10x)	50 µl
RsaI [10 U/µl]	10 µl
ddH <sub>2</sub> O	ad 500 µl

Complete digestion was achieved after two hours at 37 °C. A subsequent dephosphorylation of DNA was carried out with a buffer change to 1x Alkaline Phosphatase buffer (50 mM Tris-HCl pH9.3, 1 mM MgCl<sub>2</sub>, 0.1 mM ZnSO<sub>4</sub>) and Alkaline Phosphatase Calf Intestinal (CIP, NEB) according to the following protocol.

Component	Amount
Methylated, digested plasmid DNA	500 µl
Alkaline Phosphatase buffer (10x)	50 µl
CIP [10 U/µl]	10 µl

Incubation was carried out for 30 minutes at 37 °C in the water bath and the reaction was stopped at 65 °C for several minutes. According to standard protocols of Sambrook *et al.* (2001) phenol/chloroform extraction and DNA precipitation with ethanol was performed. The precipitated, methylated plasmid DNA fragments were resuspended in 100 µl ddH<sub>2</sub>O and electrophoretically separated on a 10 % native separation gel (16.6 ml Rotiphorese 30 (37.5:1), 2.5 ml 10x TBE, 400 µl 10 % APS, 50 µl TEMED) at 90 V for 15 hours. Electroelution of the 156 bp DNA fragment from the native gel was performed according to chapter 3.3.4.

### 3.8.3 Preparation of chromatin via salt gradient dialysis

The *in vitro* reconstitution of DNA of interest with histone octamers was accomplished according to Krietenstein *et al.* (2012) via salt gradient dialysis.

## 3.9 Mass spectrometry analysis

Nuclear cell extracts of each Raji cell line (either 5693 or 5694) were prepared (see chapter 3.4.2) and analyzed in triplicates (1,2,3) for mass spectrometry analysis. After centrifugation (15 min at 13200 rpm and 4 °C), proteins of the supernatant were precipitated using a purification protocol of Strep-tag fusion proteins with Strep-Tactin matrices (IBA). Briefly, the nuclear extract with a final volume of 450 µl was incubated with wash buffer (100 mM Tris-HCl pH8.0, 150 mM NaCl, 1 mM EDTA, 1x “Complete” proteinase inhibitor cocktail (Roche)) pre-equilibrated Streptavidin beads with a CV of 200 µl for two hours at 4 °C while rotating. The column was washed five times with five CVs of wash buffer. The analysis of lysate, wash fractions, and beads of each mass spectrometry sample was accomplished by silver staining (see chapter 3.4.8) and western blot immunodetection (see chapter 3.4.7) with an anti-BZLF1 antibody. Beads were frozen directly on dry ice and send for mass spectrometry analysis to the Zentrallabor für Proteinanalytik (ZfP, Munich).

In order to remove detergents and unspecific binders, the beads were washed three times with 100 µl of 50 mM NH<sub>4</sub>HCO<sub>3</sub>. Digestion of the beads was performed with 100 µl of 10 ng/µl trypsin in 1 M urea and 50 mM NH<sub>4</sub>HCO<sub>3</sub> for 30 minutes at 25 °C and 800 rpm. The supernatant was collected, the beads were washed again two times with 50 µl 50 mM NH<sub>4</sub>HCO<sub>3</sub> and all supernatants were pooled. Digestion of the supernatant was performed in a final concentration of 1 mM DTT at 25 °C and 800 rpm over night. The next day, 10 µl of 5 mg/ml iodoacetamide (27 mM) was added and incubated for 30 minutes in the dark at 25 °C. 1 µl of 1 M DTT was added and incubated for ten minutes at 25 °C. Upon addition of 2.5 µl trifluoroacetic acid, the samples were desalted using 2x C18 stagetips. Liquid chromatography tandem mass spectrometry (LC-MS/MS) was performed with the ion trap mass analyzer Orbitrap. With the aid of the Mascot software the colleagues of the ZfP (Munich) identified BZLF1’s interacting proteins in the viral and human protein databases.

# 4. RESULTS

## 4.1 BZLF1 changes the epigenetic landscape in viral chromatin

The Epstein-Barr Virus (EBV) life cycle is characterized by three major phases: the pre-latent, latent and lytic phase. EBV persists lifelong in B cells of the host and is maintained during the latent phase. In this phase a number of latent viral genes is expressed but infectious virions are never synthesized. Only the lytic phase supports viral synthesis, which is mandatory for the virus to spread to uninfected cells. The EBV-encoded transcription factor BZLF1 governs the switch from the latent to the lytic phase and activates the expression of EBV's lytic genes, which encode the enzymes for viral DNA replication and structural proteins of the virion. BZLF1 is not only expressed in latently infected cells, when it initiates lytic reactivation, but also during the pre-latent prior to the latent phase. BZLF1 binds sequence-specifically to two classes of (viral) DNA motifs. One class is exceptional in that it consists of BZLF1 Responsive Elements (ZREs) with a CpG dinucleotide. The binding of BZLF1 depends on the methylated state of this class of ZREs, which are prevalent in viral promoters of early lytic genes (Bergbauer *et al.*, 2010; Kalla *et al.*, 2010; Woellmer *et al.*, 2012). Paradoxically, methylation of viral DNA in the latent state is no hindrance but a must for lytic reactivation. During latency, a high nucleosomal occupancy and Polycomb silencing, responsible for the repressive histone mark H3K27me3, epigenetically silence the promoter regions of viral lytic genes. Upon lytic reactivation, BZLF1 binding induces a nucleosomal

loss, the removal of Polycomb repression, and the recruitment of RNA polymerase II (Woellmer *et al.*, 2012).

The epigenetic code of EBV's DNA is not yet completely understood and needs further analysis. It is unclear, how BZLF1 reactivates silenced viral chromatin after induction of EBV's lytic phase. It is equally unclear, how BZLF1 gets access to compacted heterochromatin, binds its ZRE motifs and induces the transition to open activated euchromatin of viral DNA. I wished to address these open questions in my PhD work.

The initial aim of my thesis was the establishment of an improved conditional system for the induced expression of *BZLF1*. The Raji cell line is a good model to study epigenetic changes of viral DNA during the latent and lytic phases. Raji cells carry strict latent EBV genomes. The cells can be easily activated by a tetracycline-controlled BZLF1 expression system to initiate the viral lytic phase. Raji cells lack the viral *BALF2* locus, which encodes the BALF2 protein essential for the lytic DNA replication of the viral genome. As a consequence, the lytic phase ensues but viral genes downstream of the class of early lytic genes are blocked preventing the synthesis of viral progeny DNA. This aspect is important for the analysis of epigenetic modifications on EBV's DNA upon lytic induction, because viral progeny DNA is epigenetically naïve, lacks histones or nucleosomes and is free of methylated cytosine residues. If Raji cells synthesized this type of viral DNA, the molecular analysis of viral DNA and its epigenetic modifications in the lytic phase would be close to impossible.

My group reported a conditional expression system for BZLF1 (Woellmer *et al.*, 2012). The problem of this previous conditional system was the epigenetic silencing of the inducible plasmid by the host cell machinery over time. The newly constructed conditional BZLF1 expression plasmid (p4816, Fig. 4.1 panel A) contains the bicistronic coding sequence of the tetracycline controlled repressor *rTS* (instead of the previous *KRAB* repressor) and the transactivator *rtTA2S-M2*. In the absence of tetracycline (or the analogue doxycycline), the repressor binds tightly to the so-called *tet* promoter preventing its activation. After addition of doxycycline to the cells, the repressor rTS is replaced by the activator rtTA2S-M2, which induces bidirectional transcription and concomitant expression of three transgenes: *enhanced green fluorescent protein (eGFP)*, the human *truncated nerve growth factor-receptor (tNGF-R)* and *BZLF1*. BZLF1 expression can be monitored by flow cytometry and the detection of GFP-positive cells (Fig. 4.1 panel B). Additionally, the co-expressed *tNGF-R* transgene allows cell sorting by magnetic activated cell sorting (MACS).

Raji cells were stably transfected with the plasmid 4816. Single cell clones were selected with puromycin under condition of limiting dilution and analyzed for inducibility of the transgenes by flow cytometry. The single cell clone with the most robust and highest expression of the *eGFP* gene (about 90 %) was used for all my experiments (Fig. 4.1 panel B). The expression of BZLF1 protein in the Raji 4816 cells was monitored in a time kinetic experiment (Fig. 4.1 panel C). The parental Raji cell line and Raji 4816 cells were induced with 100 ng/ml doxycycline at certain time points post induction and checked for BZLF1 expression by western blot immunodetection. BZLF1 protein became detectable as early as two hours post induction and reached its maximal expression after 15 hours. No spontaneous BZLF1 expression could be detected in the parental Raji cell line or in Raji 4816 cells in the absence of tetra- or doxycycline. Quantitative RT-PCR experiments were performed in Raji 4816 cells in the time course of lytic induction to analyze the expression of selected transcripts (Fig. 4.1 panel D). Raji 4816 cells were induced with 100 ng/ml doxycycline for different intervals as indicated. RNA was prepared and treated with DNase I to eliminate contaminating DNA from the samples, which was controlled by PCR. RNA was reversely transcribed into cDNA and the relative amount of transcripts per cell was quantified by qPCR. Expression of a set of early and late lytic genes was analyzed together with the housekeeping gene *Cytochrome C* (*CytC*). The kinetics of induction differed among the early lytic genes. The expression of the transgene *BZLF1* responded immediately to doxycycline induction. The expression of *BMRF1* and *BNLF2a* was equally fast and responded within three hours post induction. The levels of transcripts of the *BRLF1* and *BBLF4* genes were induced with a delayed kinetic. The expression levels of the viral late lytic gene *BcLF1* and the cellular *CytC* genes were not influenced by BZLF1 and served as negative controls. The time course revealed different kinetics of activation suggesting functional grouping of the viral genes confirming an earlier report (Woellmer *et al.*, 2012).

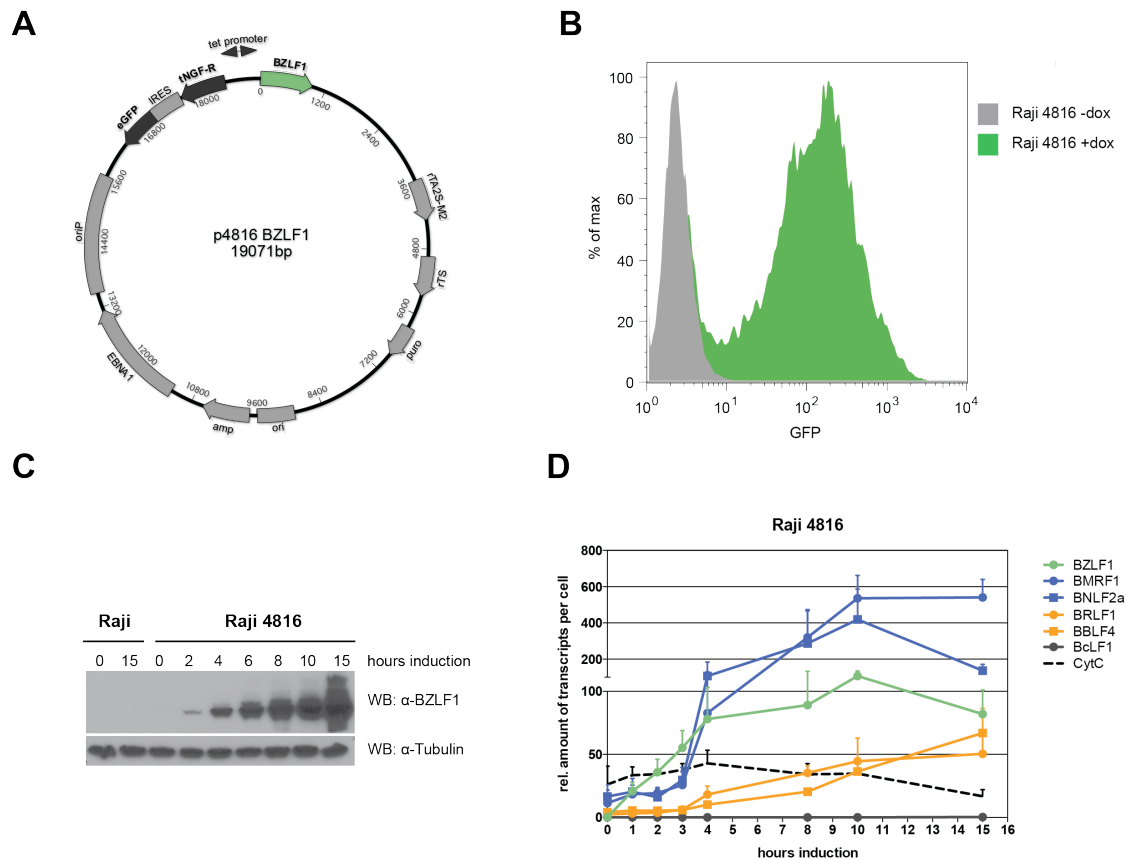


**Fig. 4.1 Conditional expression of BZLF1 in Raji cells**

(A) The plasmid p4816 contains the bicistronic coding sequences of the tetracycline controlled repressor *rTS* and transactivator *rtTA2S-M2*. In the absence of tetracycline or its analogue doxycycline, the *rTS* repressor binds tightly to the *tet* promoter preventing its activation. After addition of doxycycline to the cells, the repressor *rTS* is replaced by the activator *rtTA2S-M2*, which induces bidirectional transcription and concomitant expression of three transgenes: *enhanced green fluorescent protein (eGFP)*, the human *truncated nerve growth factor-receptor (tNGF-R)* and *BZLF1*. An internal ribosomal entry site (*IRES*) separates *tNGF-R* and *BZLF1*.  $\beta$ -lactamase (*amp*) and *puromycin N-acetyl-transferase (puro)* serve as resistance genes in bacteria and Raji cells, respectively. DNA replication in *E.coli* initiates at the prokaryotic origin of replication (*ori*). Epstein-Barr nuclear antigen 1 (*EBNA1*) activates replication of the plasmid DNAs through binding to the origin of plasmid replication (*oriP*) and governs plasmid segregation.

(B) GFP expression in Raji cells was a measure of the induced expression of BZLF1. Upon addition of 100 ng/ml doxycycline to the cells for 15 hours, about 90 % turned GFP-positive.

(C) BZLF1 protein expression was analyzed by western blot immunodetection upon lytic phase induction. Protein lysates of either parental or Raji 4816 cells were analyzed with an antibody recognizing BZLF1 (top panel) at different time points post induction. Tubulin served as a loading control (bottom panel). As early as two hours post induction, BZLF1 protein became detectable, reaching its maximum at 15 hours. No BZLF1 expression could be detected in the parental Raji cell line.

(D) Expression levels of selected transcripts were analyzed upon induction of the lytic phase in a time kinetic experiment. Raji 4816 cells were induced with doxycycline for different intervals as indicated, RNA was prepared, reverse transcribed, and analyzed by qPCR. The relative amount of transcripts per cell indicates the expression levels of individual transcripts. The temporal expression of different EBV genes suggests three different functional groups of viral genes: *BZLF1* expression responds immediately to the addition of doxycycline (group 1, green), *BMRF1* and *BNLF2a* respond within three hours (group 2, blue), *BRLF1* and *BBLF4* respond with a delayed kinetic (group 3, orange). The levels of mRNA induction of group 2 members are about tenfold higher than of group 3 members. The viral *BcLF1* and the cellular *Cytochrom C (CytC)* genes served as negative controls. BZLF1 did not induce their expression.



A chromatin immunoprecipitation (ChIP) protocol was established with cross-linked chromatin and a BZLF1-specific antibody. BZLF1 binds preferentially to the promoters of early lytic genes (*Q/F*, *BRLF1*, *BZLF1*, *BMRF1*, *BBLF4* and *BSRF1*) upon lytic reactivation (Fig. 4.2 panel A). BZLF1 enhances especially the transcriptional activation of *BMRF1* (ten-fold), *BBLF4* (13-fold) and *BSRF1* (eight-fold). Control promoter regions of the cellular *cen* and *GAPDH* genes and the viral late lytic gene *BcLF1* were not affected by BZLF1. In line with BZLF1 binding, I could detect the recruitment of the RNA polymerase II in the promoter regions of the above-mentioned early lytic genes (*Q/F*, *BRLF1*, *BZLF1*, *BMRF1*, *BBLF4* and *BSRF1*) after the onset of the lytic phase (Fig. 4.2 panel B). RNA polymerase II binding could be detected at the promoters of *Q/F*, *BRLF1*, *BMRF1*, *BBLF4* and *BSRF1* with a 26-, seven-, eight-, six-, and four-fold enrichment, respectively. Control promoter regions did not show the BZLF1-induced recruitment of the RNA polymerase II.

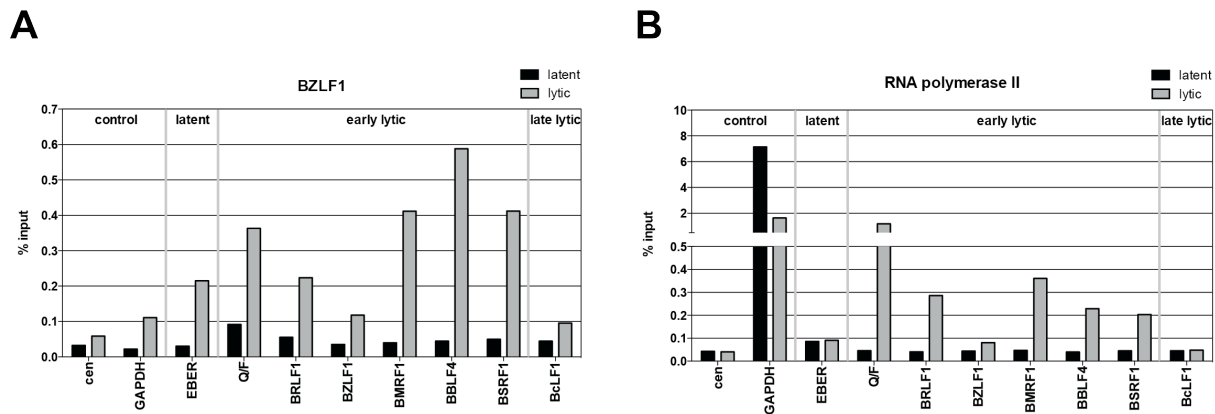


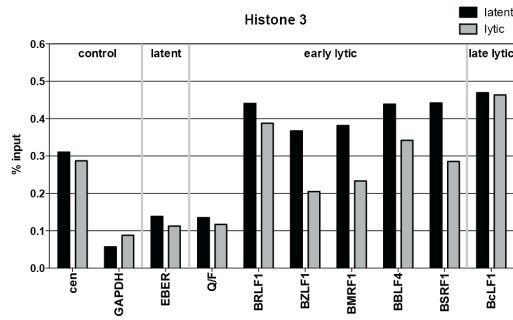
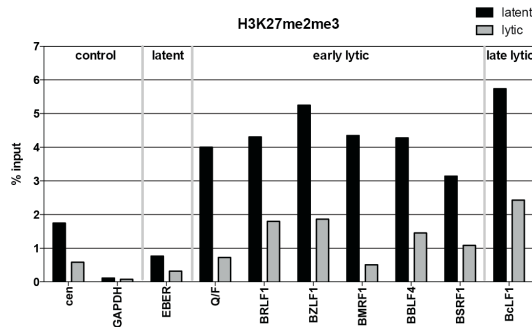
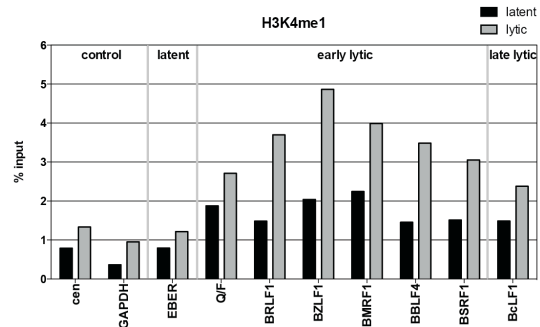
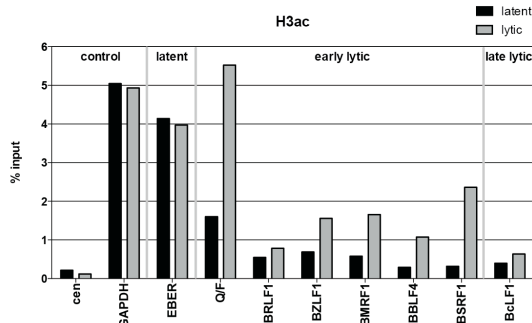
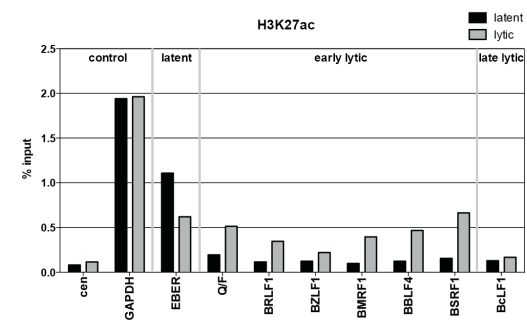
**Fig. 4.2 Chromatin immunoprecipitations of BZLF1 and RNA polymerase II in Raji cells**

Shown are the results of ChIP experiments with BZLF1 and RNA polymerase II specific antibodies and formaldehyde cross-linked chromatin of Raji 4816 cells in latently infected cells and 15 hours post induction of EBV's lytic cycle. Enrichment of EBV DNA was assessed with primer pairs covering latent, early lytic, and late lytic promoters as indicated. Controls encompassed two cellular loci, *cen* and *GAPDH*, which represent inactive and active cellular chromatin, respectively. The late lytic promoter *BcLF1* served as a viral negative control. The y-axis shows the recovery of DNA in percentage [%] after ChIP as a function of input. Mean of three independent experiments are shown. The results of the three individual experiments can be found in the appendix.

**(A)** BZLF1 preferentially binds to viral chromatin of early lytic promoters 15 hours after induction of the lytic phase.

**(B)** BZLF1 induces the recruitment of RNA polymerase II at early lytic promoters 15 hours after induction of the lytic phase.

In previous studies Woellmer *et al.* (2012) analyzed histone modifications and chromatin-modifying enzymes in EBV DNA by ChIP experiments. Early and late lytic promoters showed a high occupancy of histone H3 during latency. The control of lytic promoters was found to be mediated by Polycomb proteins, which introduced the repressive histone mark H3K27me3 during latency. Induction of the lytic phase caused a selective histone H3 loss at early lytic promoters, only, but also introduced the active histone mark H3K4me3, whereas the H3K27me3 marks were lost. Upon induction of EBV's lytic phase the active histone mark H3K4me3 predominated whereas H3K27me3 was lost (Woellmer *et al.*, 2012). With the aid of the newly established Raji 4816 cell line I could confirm these findings but wanted to look for additional dynamics of N-terminal histone modifications. As shown in Fig. 4.3 panel A, lytic induction causes the loss of histone octamers as indicated by the loss of histone H3 at early lytic gene promoters confirming our earlier report (Woellmer *et al.*, 2012). The repressive N-terminal modification H3K27me2me3 (Fig. 4.3 panel B) strongly correlates with repressed early lytic promoters during latency. Upon BZLF1 expression and onset of the lytic phase, the repressive mark H3K27me2me3 is removed and replaced by the activation mark H3K4me1 (Fig. 4.3 panel C). There is also a strong correlation of the N-terminal acetylation level of total histone H3 (Fig. 4.3 panel D) and the modification H3K27ac (Fig. 4.3 panel E) with the activation of early lytic gene promoters upon reactivation. The cellular and viral control promoters showed no or only a weak regulation. Taken together epigenetic changes, which lead to the activation of repressed viral chromatin, represent the switch from the latent to the lytic phase by BZLF1.

**A****B****C****D****E**

**Fig. 4.3 Chromatin immunoprecipitations of histone H3 and its N-terminal modifications in Raji cells**

Shown are the results of ChIP experiments with histone 3 specific antibodies and formaldehyde cross-linked chromatin of Raji 4816 cells in latently infected cells and 15 hours post induction of EBV's lytic cycle. Enrichment of EBV DNA was assessed with primer pairs covering latent, early lytic, and late lytic promoters as indicated. Controls encompassed two cellular loci, *cen* and *GAPDH*, which represent inactive and active cellular chromatin, respectively. The late lytic promoter *BcLF1* served as a viral negative control. The y-axis shows the recovery of DNA in percentage [%] after ChIP as a function of input. Mean of three independent experiments are shown. The results of the three individual experiments can be found in the appendix.

(A) Lytic induction caused the loss of histone octamers represented by histone H3 at early lytic gene promoters. BZLF1 expression showed no effect on cellular and viral control promoters as expected.

(B) The repressive posttranslational modification H3K27me2me3 correlated with repressed early lytic and late lytic gene promoters in the latent phase. Upon lytic phase induction, the repressive mark was reduced. The cellular and viral control promoters showed no or only a weak regulation.

(C) The posttranslational modification H3K4me1 correlated with active early lytic gene promoters in the lytic phase. The active mark was increased after the onset of the lytic phase.

(D) and (E) The induction of the lytic phase by BZLF1 resulted in an increase of the N-terminal acetylation level of total histone H3 in (D) and the gain of the H3K27ac modification in (E) in the promoter regions of early lytic genes. The acetylation status correlated with active early lytic gene promoters upon lytic phase induction. Histone acetylation of the cellular and viral control promoters did not change in the course of this experiment.

## 4.2 BZLF1's molecular role in chromatin remodeling *in vitro* and *in vivo*

The viral transcription factor BZLF1 is an immediate-early gene product. In latently EBV-infected cells it induces the switch to the lytic cycle and initiates the synthesis of virions. It is a transactivator, binds to viral promoters and induces the expression of essential early lytic genes. The structure of BZLF1 is modular and consists of three domains: the TAD, the bZIP domain containing the DNA-binding and dimerization domain, and the C-terminal domain with a so far unknown function (Petosa *et al.*, 2006). As a homodimer BZLF1 binds two classes of BZLF1 Responsive Elements (ZREs), termed meZREs and ZREs, with or without a CpG-pair, respectively (Bergbauer *et al.*, 2010). BZLF1's dimerization ability of ZRE and meZRE sites is comparable, but in the latter the CpG dinucleotides must contain methylated cytosines for BZLF1 to bind efficiently (Bergbauer *et al.*, 2010). BZLF1 has evolved to transactivate cytosine-methylated, hence repressed, silent promoters as a rule to overcome epigenetic silencing (Bergbauer *et al.*, 2010; Kalla *et al.*, 2012; Woellmer *et al.*, 2012).

In previous studies, Woellmer *et al.* (2012) found that a high nucleosome occupancy in the promoter regions of BZLF1 target genes correlated with their repressed state during latency. Upon induced expression of BZLF1 and its binding, the chromatin structures of BZLF1 target genes were altered and the density of high nucleosomal occupancy decreased. Based on these observations, I hypothesized that BZLF1 is capable of binding to its ZRE and/or meZRE motifs even when they are located within repressed chromatin in promoter regions of lytic genes. Binding of BZLF1 might cause the repositioning or even the eviction of nucleosomes to make the chromatin accessible for components of the transcription machinery.

My first aim was to find out, if the viral transcription factor BZLF1 binds to or even evicts nucleosomes with or without the help of additional molecular machines. To address this question I performed electromobility shift assays (EMSAs), a common affinity electrophoresis technique used to study protein–DNA interactions. I adopted this technique to analyze the interaction of BZLF1 protein with mononucleosomal DNA. In order to mimic repressed chromatin, the binding reactions were conducted with mononucleosomes and template DNA that contained part of a BZLF1-regulated promoter with one or two meZRE motifs.

I prepared BZLF1 protein from HEK293 cells. I transiently transfected these cells with a CMV-promoter controlled expression vector system, where a Flag- and tandem Strep-tag is fused to the coding sequences of BZLF1 full-length (aa1-245) or the truncated BZLF1 version Z $\Delta$ TAD (aa149-245) (Fig. 4.4 panel A). The purification of Strep-tag fusion proteins in HEK293 cells was accomplished using Strep-Tactin affinity chromatography. Fig. 4.4 panel B shows the results after the single steps of the purification process (lysate preparation, flow-through check, washing and elution steps) of the Strep-tagged fusion proteins BZLF1 and Z $\Delta$ TAD in HEK293 by western blot immunodetection with an antibody directed against Flag. Coomassie staining after SDS-PAGE (Fig. 4.4 panel C) visualized the quality of BZLF1 and Z $\Delta$ TAD protein purifications and allowed to estimate the protein concentrations as compared to serial dilutions of BSA.

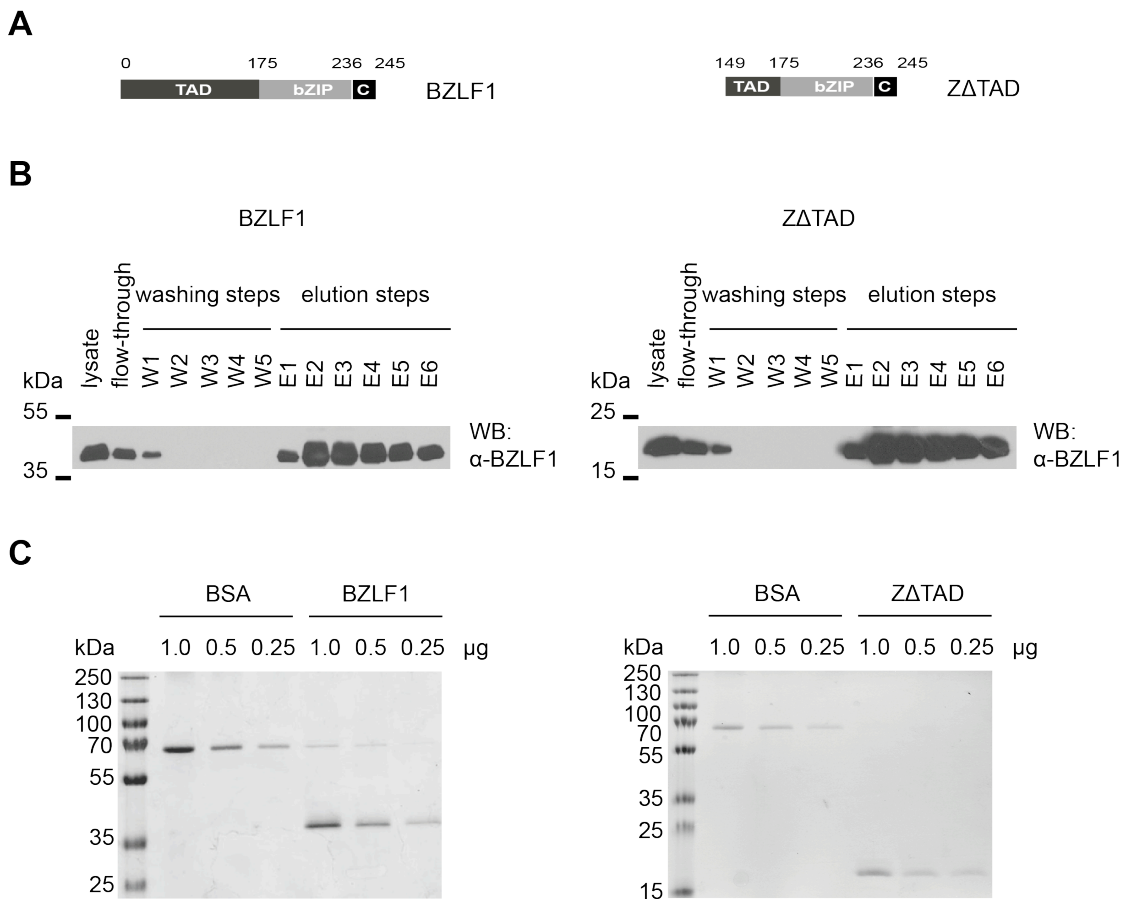


**Fig. 4.4 BZLF1 protein expression in HEK293 cells and its purification**

Expression plasmids encoding BZLF1 and its truncated version Z $\Delta$ TAD were transiently transfected into HEK293 cells and the BZLF1 proteins were purified for the later use in EMSAs.

(A) Shown is the modular structure of the BZLF1 full-length protein and the truncated version Z $\Delta$ TAD used in my work. Numbers indicate the amino acid residues.

(B) BZLF1 and Z $\Delta$ TAD are Flag- and tandem Strep-tagged proteins, which can be purified by Strep-Tactin affinity chromatography. The figure shows the results after the different steps along the purification process (lysate preparation, flow-through check, washing and elution steps) of Strep-tag fusion proteins by immunodetection using an anti-Flag antibody.

(C) Coomassie staining after SDS-PAGE shows the quality of BZLF1 and Z $\Delta$ TAD protein purification and estimates the concentrations of BZLF1 proteins as compared to serial dilutions of BSA.

For the functional analysis of ZRE-containing nucleosomal templates, I chose the promoter of the early lytic gene *BBLF4* encoding the viral DNA replication helicase. The *BBLF4* promoter harbors five methylation-dependent CpG-pair containing meZREs that consist of nine nucleotides (Bergbauer *et al.*, 2010). I generated a number of DNA templates of a total length of 156 bps each, which differ in the positioning of ZRE 3 and ZRE 4 or contain non-functional mutations in these sites (Fig. 4.5).

Histone octamers from *Drosophila* embryos, which can be easily prepared with high yield, high purity and already in form of histone octamers, i.e. with the exact 1:1:1:1 ratio of all four histones, are an essential component for the chromatin reconstitution of the ZRE-containing *BBLF4* templates (Krietenstein *et al.*, 2012). They contain certain histone modifications and histone variants (Bonaldi *et al.*, 2004). Histone octamer preparations used in all subsequent experiments are shown in Fig. 4.6 panel A. In the next step, I performed salt gradient dialysis to assemble mononucleosomal DNA with the *Drosophila* histone octamers and the ZRE-containing templates. The histone octamers interact with DNA mainly through electrostatic interactions (Luger *et al.*, 1997). Both histones and DNA are highly charged molecules. Therefore, the chromatin assembly at physiological ionic strength would lead to aggregation. To prevent the electrostatic interactions, histones and DNA are mixed at high salt concentration. The slow, gradual dialysis with the aid of a salt gradient generates conditions that allow the histone DNA-interactions to be strong enough for nucleosome formation but weak enough to prevent aggregation (Krietenstein *et al.*, 2012). Fig. 4.6 panel B illustrates the assembly of mononucleosomal chromatin with a DNA template and the *Drosophila* histone octamers by salt gradient dialysis. The titration of the histone octamer preparation and a given amount of DNA template identified the optimal conditions for the complete assembly of nucleosomal DNA. This was important for my following EMSA experiments, because the nucleosome-free DNA template would always interfere with the binding reactions of BZLF1 protein and nucleosomal DNA.

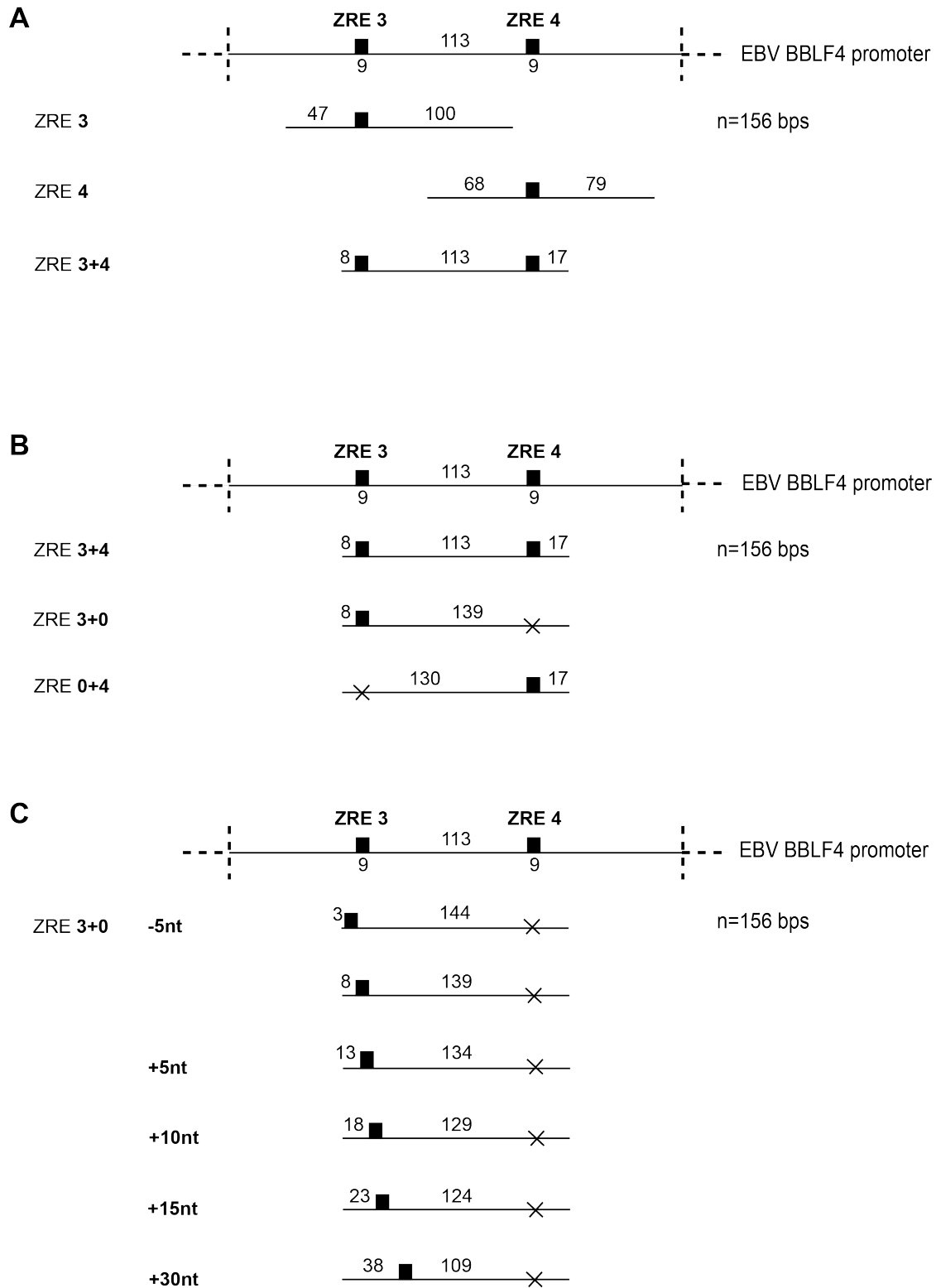


**Fig. 4.5 Functional analysis of two BZLF1 responsive elements (ZREs) in the promoter of *BBLF4***

The figure schematically shows a part of the *BBLF4* promoter with two ZRE sites, ZRE 3 and 4 (Bergbauer *et al.*, 2010). Both ZRE sequences consist of nine nucleotides and encompass CpG motifs, which must be methylated in order to bind BZLF1. A number of DNA templates of a total length of 156 bps each were generated, which differ in the positioning of ZRE 3 and ZRE 4 or contain non-functional mutations in these sites. (A) The top line represents a part of the *BBLF4* promoter with two ZREs. The numbers indicate the length of the elements shown. The ZRE motifs are 9 bps long and 113 bps apart.

(B) ZRE 3 or ZRE 4 were inactivated by PCR-mediated mutagenesis to obtain the DNA templates shown.

(C) A series of DNA templates with a “walking” ZRE 3 motif are depicted. The templates differ in the relative positions of ZRE 3 as indicated.

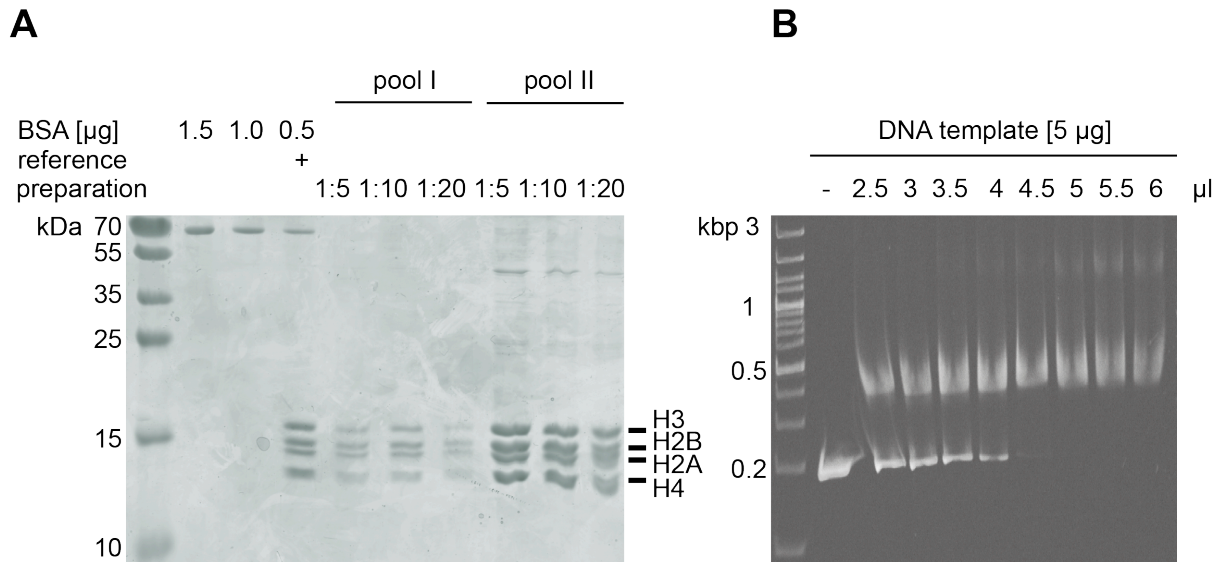


**Fig. 4.6 Histone octamer preparation and chromatin assembly**

The preparation of histone octamers from *Drosophila* embryos and the chromatin assembly after salt gradient dialysis were performed according to Krietenstein *et al.* (2012).

**(A)** The figure depicts two of my histone octamer preparations, pool II was used in all my experiments. The Coomassie stained gel after SDS-PAGE showed the correct ratio of all four histones (1:1:1:1) in the histone octamer. The concentrations of the histone octamer preparations were estimated with the aid of serial dilutions of BSA and a reference histone preparation.

**(B)** The figure illustrates the assembly of mononucleosomal chromatin with a DNA template (ZRE 3+4) and *Drosophila* histone octamers by salt gradient dialysis. An ethidium bromide stained agarose gel shows the titration of the histone octamer preparation and a given amount of the DNA template (5 μg). 4.5 μl of histone octamer pool II, diluted 1:2, and 5 μg of DNA were used for the assembly of mononucleosomal DNA templates in all my subsequent experiments.

First, I performed EMSAs with wild-type BZLF1 (aa1-245) and three different DNA templates of the *BBLF4* promoter with one (ZRE 3, ZRE 4) or two (ZRE 3+4) functional ZREs, which differ in the lengths of the flanks distal to the ZREs as indicated in Fig. 4.5 panel A. A region of the *BRLF1* coding sequence, which lacks ZRE motifs and which is not bound by BZLF1, served as a negative control. I compared the binding of BZLF1 (Fig 4.7 panel A) with the DNA templates in their naked (upper row of panels) and compacted, nucleosomal (lower row of panels) state by measuring the equilibrium dissociation constant ( $K_D$ ). BZLF1 bound to naked DNA templates (ZRE 3, ZRE 4, and ZRE 3+4) with a similar  $K_D$  of 15 nM on average, independent of the number of ZRE motifs. The negative control showed hardly any interaction with BZLF1.

The interaction of BZLF1 protein with mononucleosomal DNA templates differed. BZLF1 did not bind to mononucleosomal DNA templates containing no (control) or only one ZRE (ZRE 3 or ZRE 4), but BZLF1 did interact with the ZRE 3+4 template with a 13 nM  $K_D$  on average. The migration of complexes consisting of BZLF1 protein and naked DNA templates differed from the migration of complexes with BZLF1 and mononucleosomal DNA.



I repeated the same set of EMSA experiments with the BZLF1 version Z $\Delta$ TAD (aa149-245) to investigate the importance of BZLF1's TAD in this binding assay (Fig. 4.7 panel B). Again, BZLF1 binding to naked ZRE-containing DNA templates (upper row of panels) did not differ much and showed a similar  $K_D$  of 16 nM on average. The negative control showed hardly any interaction with Z $\Delta$ TAD. As seen with BZLF1 full-length protein, Z $\Delta$ TAD bound only the mononucleosomal DNA template (lower row of panels) with two ZREs (ZRE 3+4), but not the mononucleosomal DNA templates ZRE 3 or ZRE 4. The  $K_D$  of Z $\Delta$ TAD was 22 nM with the ZRE 3+4 template and similar to the binding constant with the naked DNAs. My results indicated that the TAD is not critical for BZLF1's property to bind to mononucleosomal DNA.

Fig 4.8 panel A summarizes the  $K_d$  values of three independent shift experiments of full-length BZLF1 protein and the truncated BZLF1 version Z $\Delta$ TAD with naked DNA (top panel) or mononucleosomal DNA (bottom panel). In addition, I performed super shift assays (Fig 4.8 panel B) with BZLF1 full-length (upper panel) and the BZLF1 version Z $\Delta$ TAD (bottom panel) with naked and mononucleosomal DNA templates containing two ZREs (ZRE 3+4). Very slowly migrating bands identified BZLF1 protein in the protein-nucleosomal DNA shift complexes. This trimeric complex (\*\*) migrated differently as compared to bands of the BZLF1-nucleosomal DNA (\*), BZLF1-naked DNA and the antibody-bound BZLF1-naked DNA complexes.

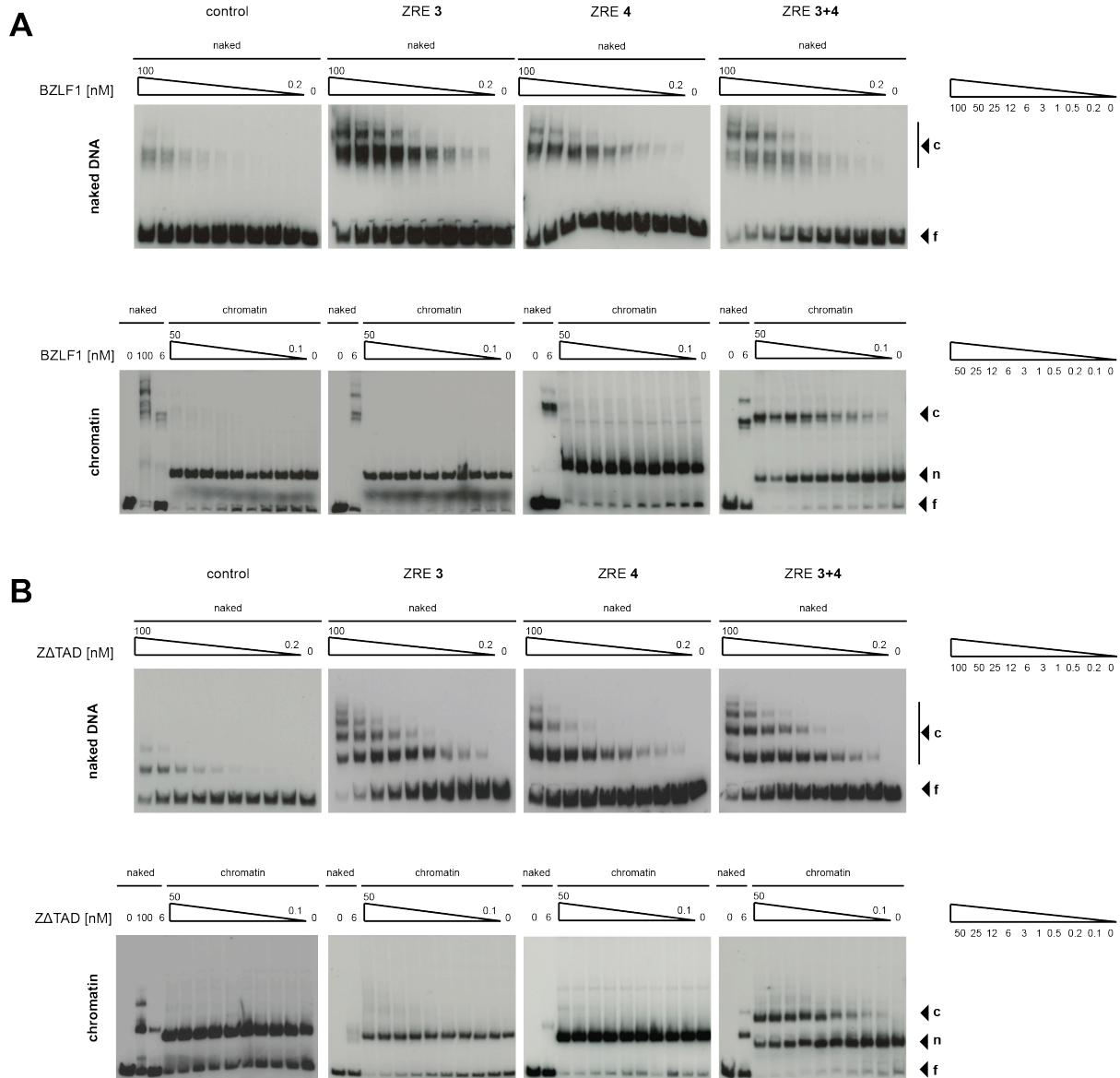


**Fig. 4.7 BZLF1's binding characteristics to mononucleosomal DNA templates *in vitro***

The figure depicts the *in vitro* binding of BZLF1 protein to four different 156 bp DNA templates in their naked or compacted, mononucleosomal states. The DNA templates are derived of the viral *BBLF4* promoter and encompass one or two meZRE motifs (see Figure 4.4 A). A region of the *BRLF1* coding sequence, which lacks a ZRE motif and is not bound by BZLF1, served as a negative control. Mononucleosomal DNA templates were obtained after salt gradient dialysis.

(f – free DNA; n – mononucleosomal DNA; c – complex of BZLF1 with free DNA or mononucleosomal DNA)

**(A)** The upper row of panels shows the interaction of BZLF1 protein with naked DNA templates. BZLF1 binding to templates containing only one ZRE (ZRE 3 or ZRE 4) or two ZREs (ZRE 3+4) showed a similar  $K_d$  of 15 nM on average. The negative control showed hardly any interaction with BZLF1. The lower row of panels shows the interaction of BZLF1 protein with mononucleosomal DNA templates. BZLF1 did not bind to mononucleosomal DNA templates containing only one ZRE (ZRE 3 or ZRE 4) but did interact with the ZRE 3+4 template with two ZRE motifs. The  $K_d$  of this ZRE template was 13 nM in three independent experiments. Binding reactions with BZLF1 protein and naked DNA templates were performed to clearly identify the different complexes.

**(B)** The upper row of panels shows the interaction of BZLF1's truncated version lacking the TAD (ZΔTAD) with naked DNA templates. Binding to templates with two ZREs (ZRE 3+4) or with only one ZRE (ZRE 3 or ZRE 4) showed a  $K_d$  similar to full-length BZLF1. The negative control showed hardly any interaction with ZΔTAD. The lower row of panels shows the interaction of ZΔTAD protein with mononucleosomal DNA templates. ZΔTAD did bind to the template with two ZREs (ZRE 3+4) but not to these with one ZRE, only. The  $K_d$  was about 22 nM with the mononucleosomal DNA containing two ZREs and similar to the dissociation constant with naked DNA templates. Control binding reactions with ZΔTAD protein and naked DNA templates were performed to clearly distinguish the migration of the different complexes.

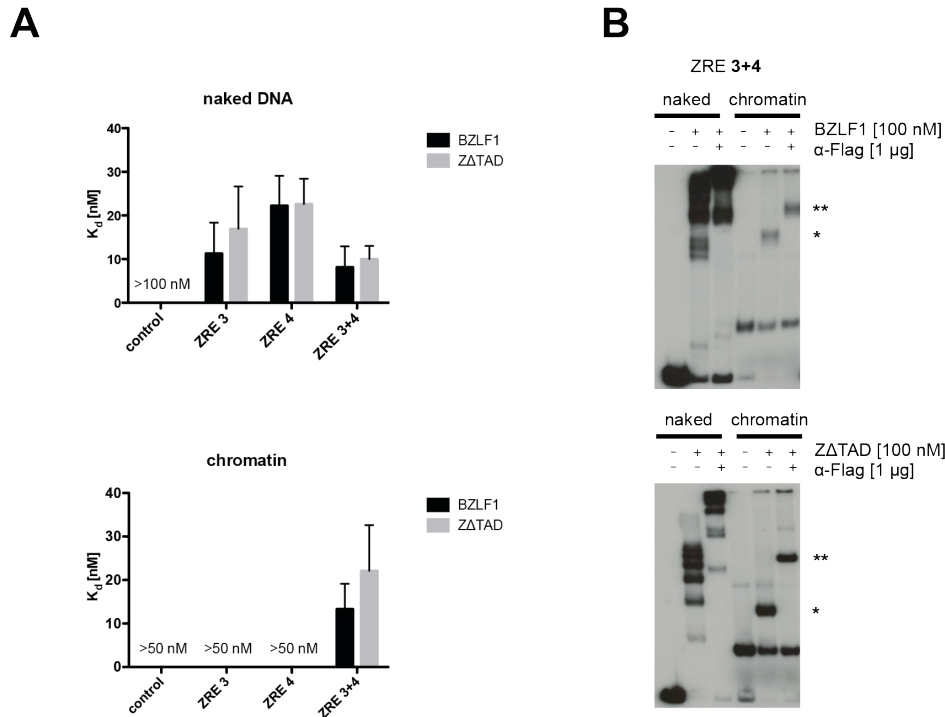


**Fig. 4.8 Half maximum binding and supershift assay of BZLF1 and ZATAD protein to mononucleosomal DNA templates *in vitro***

(A) The figure summarizes the  $K_d$  values of three independent shift experiments of full-length BZLF1 protein and ZATAD with naked DNA (top panel) or mononucleosomal DNA (bottom panel). EMSAs were performed with a final salt concentration of 90 mM and in the presence of competitor DNA. The  $K_d$  value was determined with a serial dilution of protein, a binding reaction without BZLF1 served as a negative control. The  $K_d$  values were calculated using the equation “One site – Specific binding with Hill slope” (Prism, Graphpad). The binding characteristics of BZLF1 full-length and its truncated version ZATAD are similar. The  $K_d$  values with naked DNA templates with one (ZRE 3 or ZRE 4) or two (ZRE 3+4) ZREs were 15 nM on average. Both proteins bind to mononucleosomal DNA with two ZREs (ZRE 3+4), only, with a  $K_d$  of about 18 nM similar to the  $K_D$  values obtained with naked DNA templates.

(B) The figure depicts the super shift assays of BZLF1 (top panel) and ZATAD (bottom panel) with naked and mononucleosomal DNA templates containing two ZREs (ZRE 3+4). As in Figure 4.6 (A) and (B), BZLF1 and ZATAD bind to the mononucleosomal ZRE 3+4 template as indicated by a slower migrating shift band (\*). Addition of an  $\alpha$ -Flag antibody shifted the complex (\*\*), which migrated very slowly as expected. The detected BZLF1-mononucleosomal DNA complex as well as the antibody-bound BZLF1-mononucleosomal DNA complex could be clearly distinguished from shift bands of BZLF1-naked DNA and the antibody-bound BZLF1-naked DNA complexes.

Next, I assessed the specificity of my experimental setup with a well-studied transcription factor, known to be incapable of binding to nucleosomal DNA. The binding of the budding yeast transcription factor Pho4 (Fig. 4.9 panel A) to its target sites is significantly restricted by nucleosomes (Zhou and O’Shea, 2011) and served therefore as a negative control. The nucleosomal positioning sequence ‘601’ (Lowary and Widom, 1998; kindly provided by Daniela Rhodes, NTU, Singapore) is 197 bps long and contains a five nucleotide-long Pho4 binding motif as indicated (Fig. 4.9 panel B). The ‘601’ DNA template was reconstituted with histone octamers after salt gradient dialysis and used with Pho4 protein (kindly provided by Philipp Korber, LMU, München) in EMSA experiments. The binding reactions with Pho4 and

naked DNA template revealed a  $K_D$  of 240 nM on average (Fig. 4.9 panel C). I could not detect binding of Pho4 to the mononucleosomal DNA template.

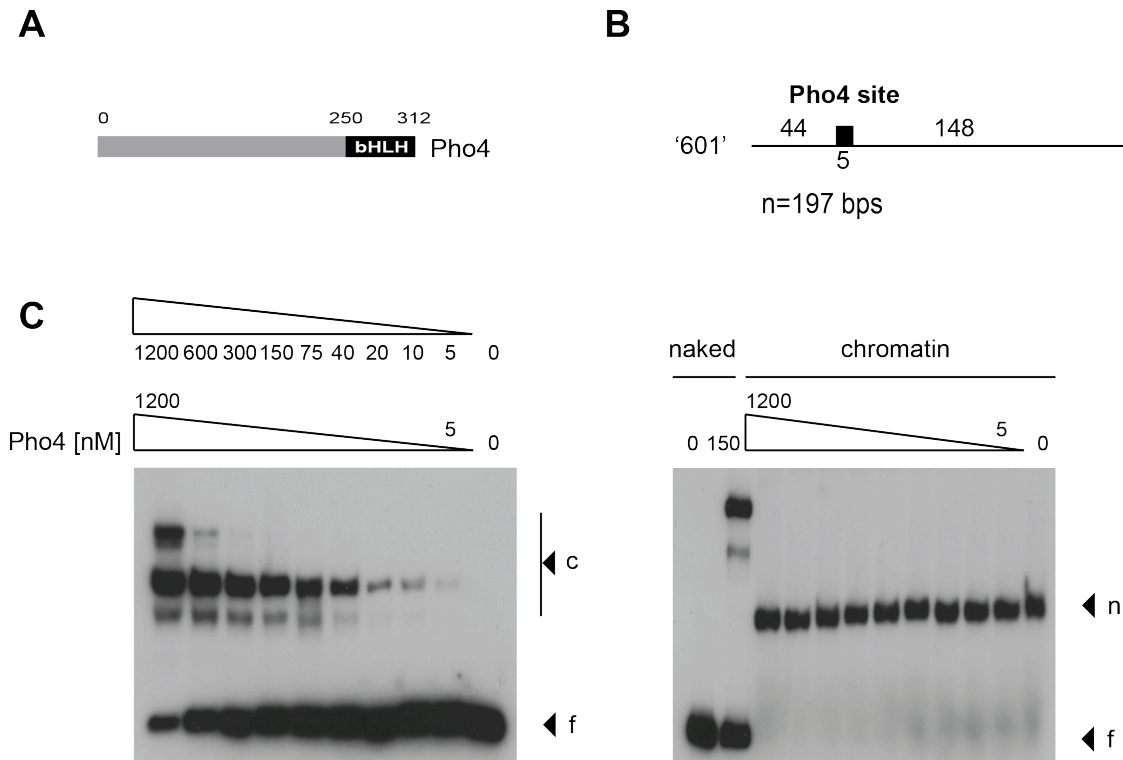


**Fig. 4.9 The transcription factor Pho4 does not bind nucleosomal DNA *in vitro***

Nucleosomes significantly restrict binding of the budding yeast transcription factor Pho4, which served as a negative control in EMSAs (Zhou and O'Shea, 2011).

(A) Shown is the modular structure of Pho4 with its basic helix-loop-helix (bHLH) domain.

(B) The figure depicts the nucleosomal positioning sequence '601' (Lowary and Widom, 1998). The '601' sequence is a 197 bps long DNA template and contains a single Pho4 binding site.

(C) The left and right panels show the interaction of Pho4 protein with the naked and the mononucleosomal '601' DNA templates, respectively. Mononucleosomal DNA templates were obtained after salt gradient dialysis. EMSAs were performed with a final salt concentration of 90 mM and in the presence of competitor DNA. Pho4's  $K_d$  value was determined with serial dilutions of Pho4 protein, a binding reaction without any Pho4 protein served as a negative control. The  $K_d$  of Pho4 protein with naked DNA template was 240 nM on average in three independent experiments. The  $K_D$  with mononucleosomal DNA template could not be determined, as Pho4 did not bind the mononucleosomal DNA template.

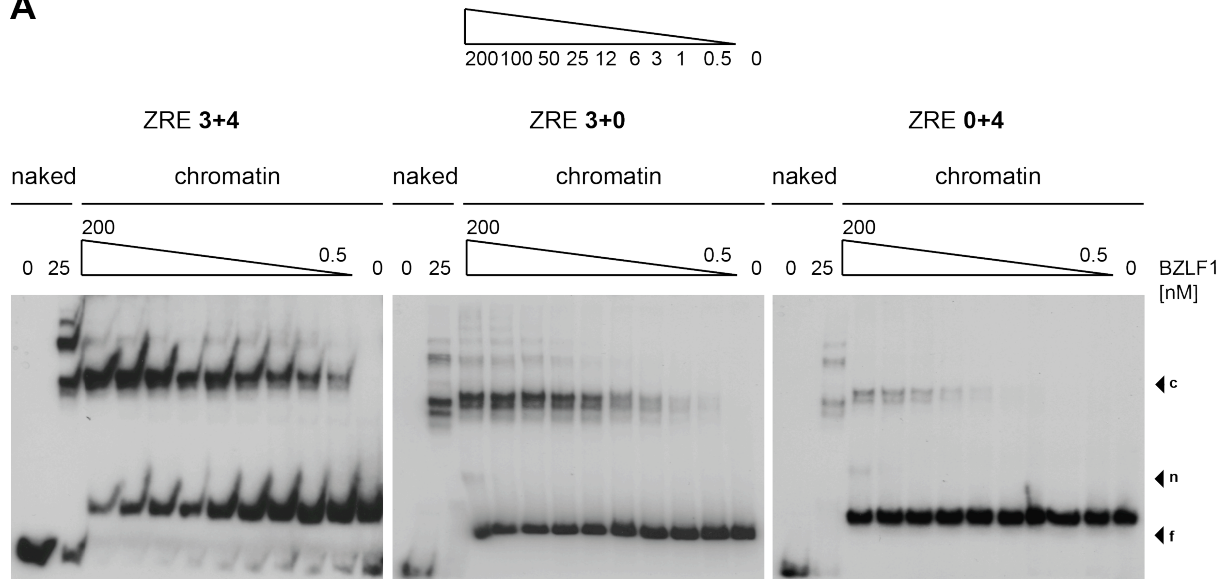
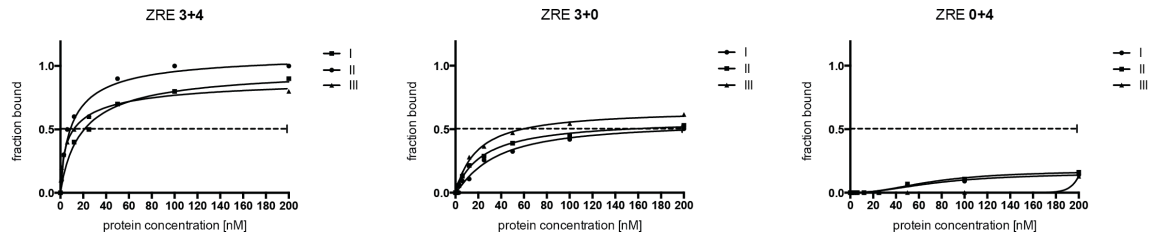
(f – free DNA; n – mononucleosomal DNA; c – complex of Pho4 with free DNA)

BZLF1 does not bind mononucleosomal DNA templates containing only one ZRE (ZRE 3, ZRE 4) but it does bind a template with two ZRE motifs (ZRE 3+4) (Fig. 4.7). This finding could mean that the positions of ZREs in the mononucleosomal template are critical. As shown in Fig. 4.5 panel A, the location of the single ZRE motifs ZRE 3 and ZRE 4 is more in the center of the mononucleosomal DNA templates in contrast to the two ZREs of the ZRE 3+4 template. There, the two ZREs are more distal, which could favor the access of BZLF1 to the mononucleosomal DNA template. To test this hypothesis, I performed EMSA experiments with synthetic DNA templates based on the ZRE 3+4 prototype. First, I mutated the sequences of ZRE 3 or ZRE 4 by PCR mutagenesis, which yielded the two new DNA

templates ZRE 3+0 and ZRE 0+4, respectively (Fig. 4.5 panel B). I chromatinized the DNA templates and investigated the binding of BZLF1 (Fig. 4.10 panel A). As in Fig 4.7, the EMSAs revealed that BZLF1 binds robustly ZRE 3+4, but interacts less efficiently with ZRE 3+0 and weakly with ZRE 0+4. Fig. 4.10 panel B shows the deduced and calculated Hill slopes of BZLF1's binding to the three mononucleosomal DNA templates. The half maximum binding of the mononucleosomal DNA template ZRE 3+4 was about 13 nM, ZRE 3+0 had a  $K_D$  of  $\geq 100$  nM but no dissociation constant could be obtained with ZRE 0+4. The  $K_d$  values of BZLF1 with the naked DNA templates ZRE 3+4, ZRE 3+0 and ZRE 0+4 are 8 nM, 22 nM and 18 nM, respectively. Apparently, in the *BBLF4* promoter ZRE 3 and ZRE 4 cooperate in binding BZLF1.

The location of individual ZRE motifs within a mononucleosomal structure might be critical for the access and binding of BZLF1. To address this still open question, I generated a series of DNA templates with a "walking" ZRE 3 motif with the ZRE 3+0 DNA template as the prototype. The templates differ in the relative positions of ZRE 3 as indicated in Fig. 4.5 panel C. The 9 bps long ZRE 3 motif was positioned at -5 nt upstream and +5, +10, +5, or +30 nt downstream with respect to its original location. I reconstituted the DNA templates with histone octamers after salt gradient dialysis and analyzed the binding of BZLF1 to the six different mononucleosomes (Fig. 4.11). BZLF1 bound the mononucleosomal ZRE 3+0 DNA templates -5 nt, +15 nt, and +30 nt but not +5 nt or +10 nt. The results documented that BZLF1 is capable of binding ZRE sites in compacted DNA even if the ZRE motifs are located towards the center of a mononucleosome. Using the six naked DNA templates, the binding of BZLF1 did not differ much (Fig 4.11).

Summarizing all my EMSA results, I could show that the viral transcription factor BZLF1 binds the histone octamer of a compacted binding site *in vitro*. Interestingly, BZLF1 binding to mononucleosomes did not evict the histone octamer *in vitro*.

**A****B**

**Fig. 4.10 BZLF1 shows cooperative binding to mononucleosomal DNA templates *in vitro***

The figure depicts the EMSA results of BZLF1 protein with three different 156 bps long DNA templates (see Figure 4.5 panel B) in their naked or mononucleosomal and compacted state. The DNA templates are derived from the viral *BBLF4* promoter and encompass the third and forth identified ZRE motifs (ZRE 3+4 in Bergbauer *et al.* (2010)). PCR mutagenesis eliminated the ZRE 3 or ZRE 4 motifs in the DNA templates ZRE 0+4 or ZRE 3+0, respectively. Naked DNA templates were used and compared to templates, which had been chromatinized forming a single nucleosome.

(A) EMSA results of BZLF1 protein and the DNA templates ZRE 3+4, ZRE 3+0 and ZRE 0+4 suggested a cooperative binding of ZRE 3 and ZRE 4 within the *BBLF4* promoter region. The ZRE 3+4 template was robustly bound by BZLF1, which interacted less efficiently with ZRE 3+0 and weakly with ZRE 0+4.

(B) Individual Hill slope curves of BZLF1's binding characteristics to the mononucleosomal DNA templates ZRE 3+4, ZRE 3+0 and ZRE 0+4 summarize three independent experiments. The half maximum binding of the mononucleosomal DNA template ZRE 3+4 was about 13 nM. No half maximum binding could be determined with ZRE 0+4 but ZRE 3+0 had a  $K_D$  about 100 nM. The  $K_d$  values of BZLF1 with the naked DNA templates ZRE 3+4, ZRE 3+0 and ZRE 0+4 were 8 nM, 22 nM and 18 nM, respectively. EMSAs were performed with a final salt concentration of 90 mM and in the presence of competitor DNA. BZLF1's  $K_d$  value was determined with serial dilutions of purified BZLF1 protein, a binding reaction without BZLF1 protein served as a negative control.  $K_d$  value was calculated using the equation "One site – Specific binding with Hill slope" (Prism, Graphpad).



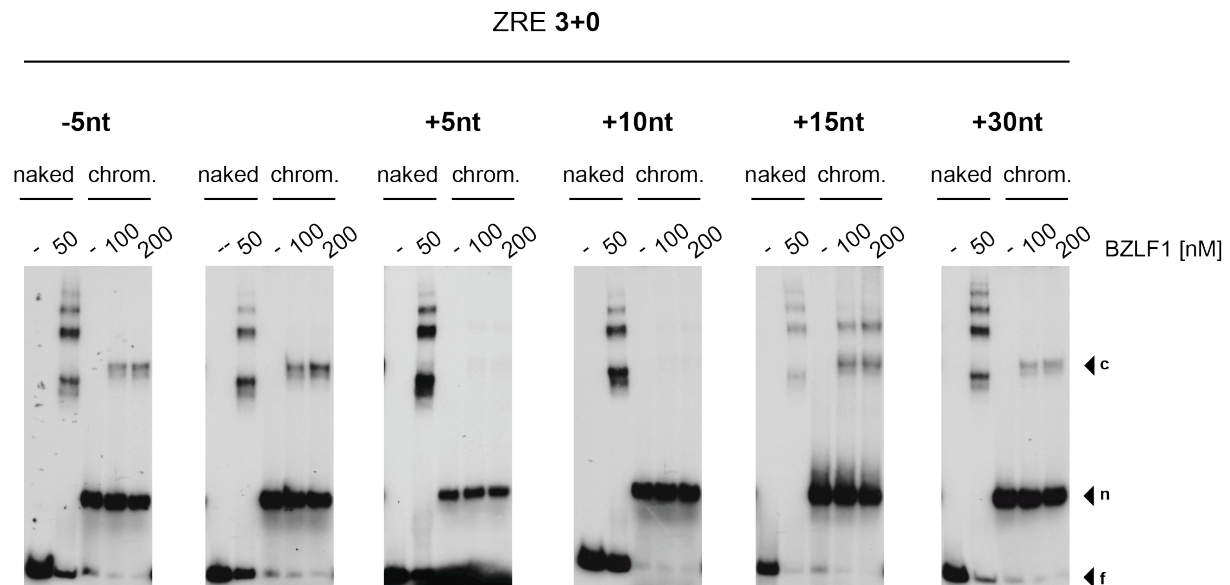


**Fig. 4.11 The positions of ZREs in mononucleosomal DNA are critical for BZLF1's cooperative binding to chromatin**

The figure depicts the EMSA results of BZLF1 protein with six different 156 bps long DNA templates (see Figure 4.5 panel C) in their naked or mononucleosomal and compacted state. The DNA templates are derived from the viral *BBLF4* promoter and encompass the third ZRE motif (ZRE 3 in Bergbauer *et al.* (2010)). PCR mutagenesis eliminated the ZRE 4 motif obtaining the DNA template ZRE 3+0. The DNA template ZRE 3+0 was modified to alter the position of the ZRE 3 motif. The 9 bps long ZRE 3 motif was positioned at -5 nt upstream or +5, +10, +5, or +30 nt downstream with respect to its original location. BZLF1 was capable of binding the modified mononucleosomal ZRE 3+0 DNA templates -5 nt, +15 nt, and +30 nt but not +5 nt or +10nt indicating that the factor can bind nucleosomally structured DNA. The binding of BZLF1 with the six naked DNA templates did not apparently differ.

My *in vitro* assays with reconstituted mononucleosomes and BZLF1 protein indicated the function of a trimeric complex consisting of DNA, histone octamer and BZLF1. I wanted to scrutinize BZLF1's binding characteristic to chromatin and mononucleosomes *in vivo* and performed ReChIPs meaning re-immunoprecipitations with two different antibodies. ReChIP is a relatively new technique and is used to assess the co-occupancy of two proteins at the same genomic region of interest in two consecutive ChIPs. The workflow and individual steps of the ChIP and ReChIP methods are shown in Fig. 4.12.

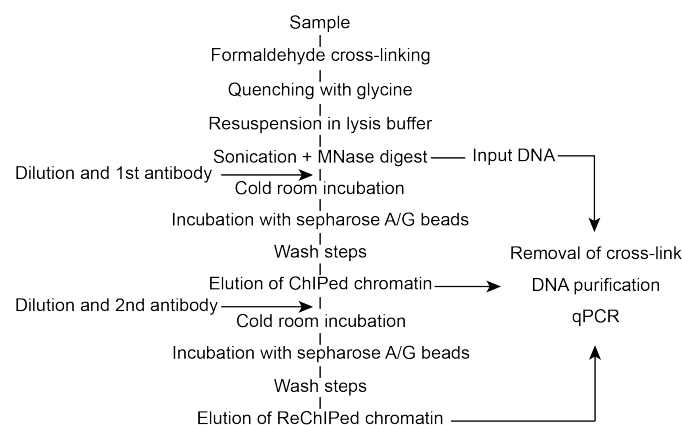


**Fig. 4.12 Workflow and individual steps of the ChIP and ReChIP methods**

For my aims, I wanted to investigate if BZLF1 can bind to DNA in mononucleosomal structures *in vivo*. First, I performed ChIP experiments with antibodies directed against BZLF1 or H3K4me1 (Fig. 4.13 panel A). I chose the H3K4me1 modification-specific antibody because it proved to be very efficient in ChIP experiments in very contrast to cell pan H3 antibodies I tested. Upon addition of doxycycline and induction of the lytic phase, BZLF1 binding was detected at the early lytic gene promoters (*Q/F*, *BRLF1*, *BZLF1*, *BMRF1*, *BBLF4* and *BSRF1*) as early as four hours after induction. The increase of H3K4me1 became detectable after seven hours post induction at the very same promoters. Late lytic (*BcLF1*) and latent (*EBER*) promoters showed little change, the cellular control promoters (*cen*, *GAPDH*) were not affected. Second, two ReChIP experiments were done, which differed in the order of antibodies used (Fig. 4.13 panel B). In the left panel, BZLF1 and H3K4me1 specific antibodies were used in the first and second ChIP experiments, respectively. The right panel shows the reverse order. Third, I performed control ReChIPs using a non-specific IgG antibody as an unspecific second ReChIP antibody (Fig. 4.13 panel C). These controls are important to demonstrate that carry-over of the antigen-specific antibodies used in the first ChIP experiments does not take place in the following ReChIP experiment, which would lead to noninterpretable or false positive results. Specificity controls of the BZLF1+IgG and H3K4me1+IgG ReChIP experiments documented low (left panel) and no (right panel) carry-over, respectively, resulting in the very low background in the second ChIP.

The results of my ReChIP experiments documented the co-occupancy of BZLF1 and the histone octamer represented by histone mark H3K4me1 in the promoter regions of early lytic genes (*Q/F*, *BRLF1*, *BZLF1*, *BMRF1*, *BBLF4* and *BSRF1*) as early as seven hours post induction. The late lytic gene (*BcLF1*) and the cellular control promoters (*cen*, *GAPDH*) did not show co-occupancy of BZLF1 and histones.

Taken together, I could demonstrate that the viral transcription factor BZLF1 binds to nucleosomes *in vitro* and *in vivo*, which occupy the promoter regions of early lytic genes.



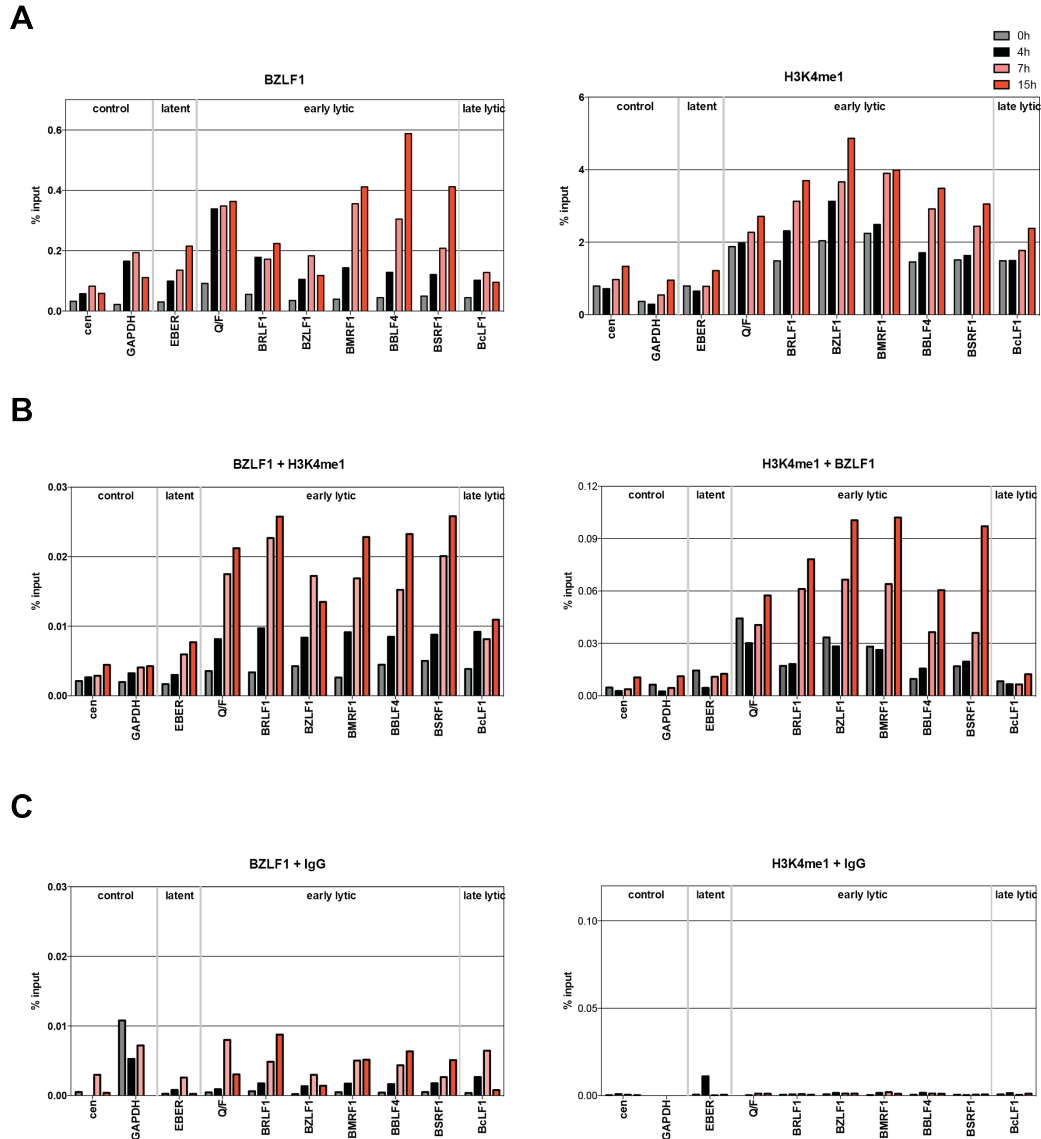


**Fig. 4.13 Sequential chromatin immunoprecipitation (ReChIP) of BZLF1 and H3K4me1**

ChIPs and ReChIPs were performed with antibodies directed against BZLF1 and the histone mark H3K4me1 in a time kinetic experiment. DNA was analyzed by qPCR for enrichment at different loci in the human or the EBV genomes. PCR with *Centromer1* (*cen*) specific primers served as control of an epigenetically repressed locus, the promoter of the housekeeping gene *GAPDH* is indicative of chromatin with active epigenetic marks. Enrichment of EBV DNA was assessed with primer pairs covering latent, early lytic, and late lytic promoters as indicated. Results of the individual experiments can be found in the appendix.

**(A)** ChIP experiments with antibodies directed against BZLF1 or H3K4me1 are shown. Upon addition of doxycycline, BZLF1 was detected at certain promoters (e.g. *BRLF1*) as early as four hours after induction of EBV's lytic phase. The increase of H3K4me1 became detectable after seven hours post induction at all promoters of early lytic genes (*Q/F*, *BRLF1*, *BZLF1*, *BMRF1*, *BBLF4* and *BSRF1*). Late lytic (*BcLF1*) and latent (*EBER*) promoters showed little change, the cellular control promoters (*cen*, *GAPDH*) were not affected. The means of three independent experiments are shown.

**(B)** Two ReChIP experiments are shown, which differ in the order of antibodies used. In the left panel, BZLF1 and H3K4me1 specific antibodies were used in the first and second ChIP experiments, respectively. The right panel shows the reverse order. ReChIP experiments documented the co-occupancy of BZLF1 and the histone octamer represented by histone mark H3K4me1 in the promoter regions of early lytic genes (*Q/F*, *BRLF1*, *BZLF1*, *BMRF1*, *BBLF4* and *BSRF1*) as early as seven hours post induction. The late lytic gene (*BcLF1*) and the cellular control promoters (*cen*, *GAPDH*) did not show co-occupancy of BZLF1 and histones. The means of three independent experiments are shown.

**(C)** Specificity controls of the ReChIP experiments documented the low (left panel) and no (right panel) carry-over of the antigen-specific antibodies used in the first ChIP experiments resulting in the very low background in the second ChIP shown in (C). The control ReChIPs were performed with a non-specific IgG antibody as an unspecific secondary antibody. The results of representative experiments are shown.

### 4.3 BZLF1 interacts with chromatin regulatory proteins *in vivo*

The viral transcription factor BZLF1 binds compacted and chromatinized DNA binding motifs *in vitro* and co-locates with histone octamers in the promoter regions of early lytic genes *in vivo* upon lytic reactivation. The previous time kinetic experiments pointed out that BZLF1 binding precedes the loss of histones in the promoter regions of early lytic genes (Fig. 4.3 panel A; Woellmer *et al.*, 2012). Based on these observations, I hypothesized that BZLF1 binds nucleosomal DNA in lytic gene promoter regions but is incapable of evicting nucleosomes without recruiting additional factors. Obviously, BZLF1 might recruit cellular chromatin remodelers directly or indirectly, which can reposition or eject nucleosomes and support the recruitment of the cellular transcriptional machinery and the expression of the lytic gene products.

Chromatin remodeling complexes are ATP-driven molecular machines that introduce structural changes in chromatin. They disrupt histone-DNA contacts, slide or even move nucleosomes, and change the nucleosomal histone composition. These structural modifications change the accessibility of compacted DNA and promote the local recruitment of regulatory cellular protein complexes that support subsequent transcription, DNA replication and DNA repair. Chromatin remodelers are highly abundant in the cell and numerous different complexes exist that display distinct activity patterns. All eukaryotic cells contain at least four families of chromatin remodelers: SWI/SNF, ISWI, INO80, and CHD (Clapier and Cairns, 2009).

In a candidate approach I analyzed the protein-protein interactions of BZLF1 with the catalytic ATPase subunits of two of the four chromatin remodeler families: SNF2H (ISWI) and hIno80 (INO80). I performed co-immunoprecipitations (coIPs) with BZLF1 and the key components of the two remodeler families acting as bait and prey proteins. In two different types of experiments I analyzed these interactions in transient co-transfection experiments in HEK293 cells (Fig. 4.14 panel A and B), but also checked for the presumed interactions in Raji cells in a more physiological setting (Fig. 4.14 panel C).

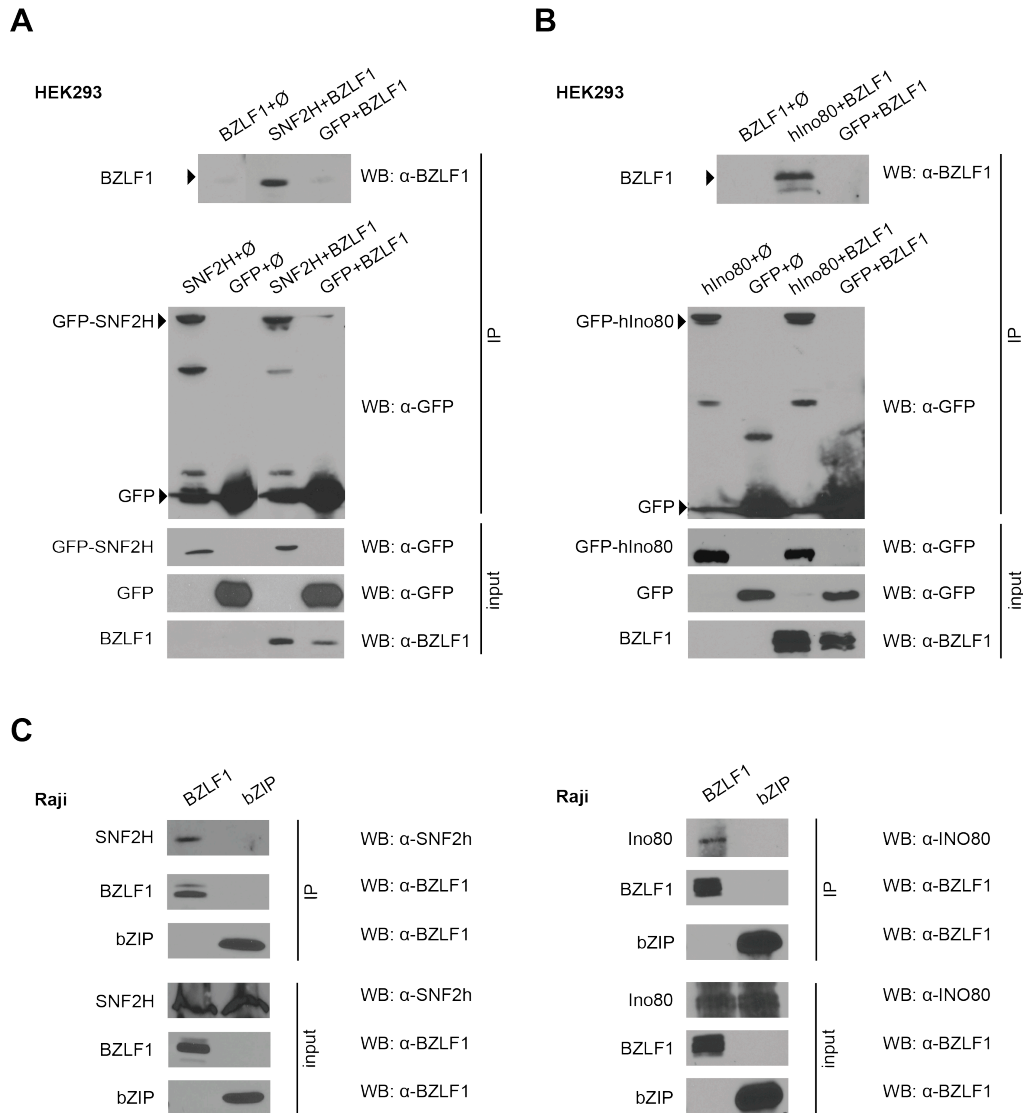


**Fig. 4.14 Immunoprecipitations of the viral transcription factor BZLF1 and the cellular chromatin remodelers SNF2H or hIno80**

BZLF1 interacts *in vivo* with the core subunits of the cellular chromatin remodelers SNF2H and hIno80. The interaction was shown with GFP-tagged chromatin remodeler in HEK293 and in Raji cells with endogenous levels of SNF2H and hIno80. Western blot immunodetection with antibodies specific for BZLF1 and GFP or the chromatin remodeler core subunits identified the interacting proteins.

**(A)** Expression plasmids encoding GFP (p1925), BZLF1 (p509) and GFP-SNF2H (p5906) were transfected or co-transfected into HEK293 cells as indicated. Protein lysates were prepared and analyzed for protein expression (input). After two days, immunoprecipitations with GFP-binder (Chromotek) coupled to sepharose beads were performed and the samples were analyzed with antibodies directed against GFP (second panel from the top, IP) and BZLF1 (upper panel, IP). BZLF1 co-precipitated with GFP-SNF2H but not with GFP, which served as a negative control.

**(B)** Expression plasmids encoding GFP (p1925), BZLF1 (p509) and GFP-hIno80 (p5985) were transfected or co-transfected into HEK293 cells as indicated. Protein lysates were prepared and analyzed for protein expression (input). After two days, immunoprecipitations with GFP-binder (Chromotek) coupled to sepharose beads were performed and the samples were analyzed with antibodies directed against GFP (second panel from the top, IP) and BZLF1 (upper panel, IP). BZLF1 co-precipitated with GFP-hIno80 but not with GFP alone.

**(C)** Raji cell lines stably transfected with the tetracycline regulated expression plasmids encoding the Strep-tagged BZLF1 full-length (p5693) or bZIP (p5694) protein. bZIP contains aa175 to aa236 carrying the DNA binding and dimerization domains of BZLF1, only. Cells were induced with doxycycline over night. Protein lysates were prepared and immunoprecipitations of Strep-tag fusion proteins were performed with Strep-Tactin sepharose beads. The interaction of the Strep-tagged BZLF1 proteins and cellular proteins were analyzed with antibodies directed against SNF2H (left panel) and hIno80 (right panel). The results indicated that only the Strep-tagged BZLF1 full-length protein (p5693) but not the truncated bZIP protein (p5694) interacts with the endogenous chromatin remodeler SNF2H and hIno80.

In transiently transfected HEK293 cells immunoprecipitations were performed with GFP as the bait protein. The chromatin remodeler catalytic ATPase subunits SNF2H and hIno80 were GFP-tagged and precipitated with GFP-binder coupled sepharose beads. The interactions of GFP-SNF2H and GFP-hIno80 with BZLF1 were analyzed by western blot immunodetection using an antibody directed against BZLF1. Unmodified GFP protein served as a negative control. BZLF1 co-precipitated with GFP-SNF2H (Fig. 4.14 panel A) and GFP-hIno80 (Fig. 4.14 panel B). BZLF1 did not show unspecific binding to the GFP-binder beads or GFP alone. The study of protein-protein interactions in HEK293 cells with the over-expression of both bait and prey proteins might be prone to artifacts. Hence, the interactions of BZLF1 with the chromatin remodeler components were also analyzed in Raji cells, in which the chromatin remodeler complexes are expressed at endogenous levels. I stably transfected Raji cells with conditional expression plasmids encoding the Strep-tagged BZLF1 wild-type protein or the BZLF1 bZIP domain (aa175-236) to yield the two cell lines Raji 5693 and Raji 5694, respectively. Upon induction with doxycycline over night, the cells expressed the Strep-tagged BZLF1 proteins, which were used as bait proteins in immunoprecipitations using Strep-Tactin sepharose beads. Western blot immunodetection with antibodies directed against the chromatin remodeler components analyzed the interactions of Strep-tagged BZLF1 proteins with endogenous SNF2H or hIno80. The immunoprecipitation results (Fig. 4.14 panel C) showed the protein-protein interaction of BZLF1 wild-type protein with endogenous SNF2H and hIno80 confirming the findings in HEK293 cells. The BZLF1 bZIP protein did not show any interaction with the ATPase catalytic subunits of both chromatin remodelers. My experiments revealed that BZLF1 interacts with at least two of the known chromatin remodeler to accomplish the process of lytic reactivation.

Next, I performed additional immunoprecipitations to identify BZLF1's domains, which mediate the interaction with the chromatin remodeler SNF2H. The modular structures that are part of the different BZLF1 variants are shown in Fig. 4.15 panel A. HEK293 cells were co-transfected with GFP-SNF2H and the BZLF1 variants. Immunoprecipitations were performed again with GFP-SNF2H as bait and BZLF1 mutants as prey. In addition, cell lysates were treated with the enzymes benzonase and DNase I prior to immunoprecipitation in order to disrupt complexes that might be stabilized by protein-DNA-protein interactions. Precipitations were performed with GFP-binder coupled sepharose beads and the possible interactions were visualized by western blot immunodetection with an antibody directed against BZLF1. The GFP protein alone served as a negative control.

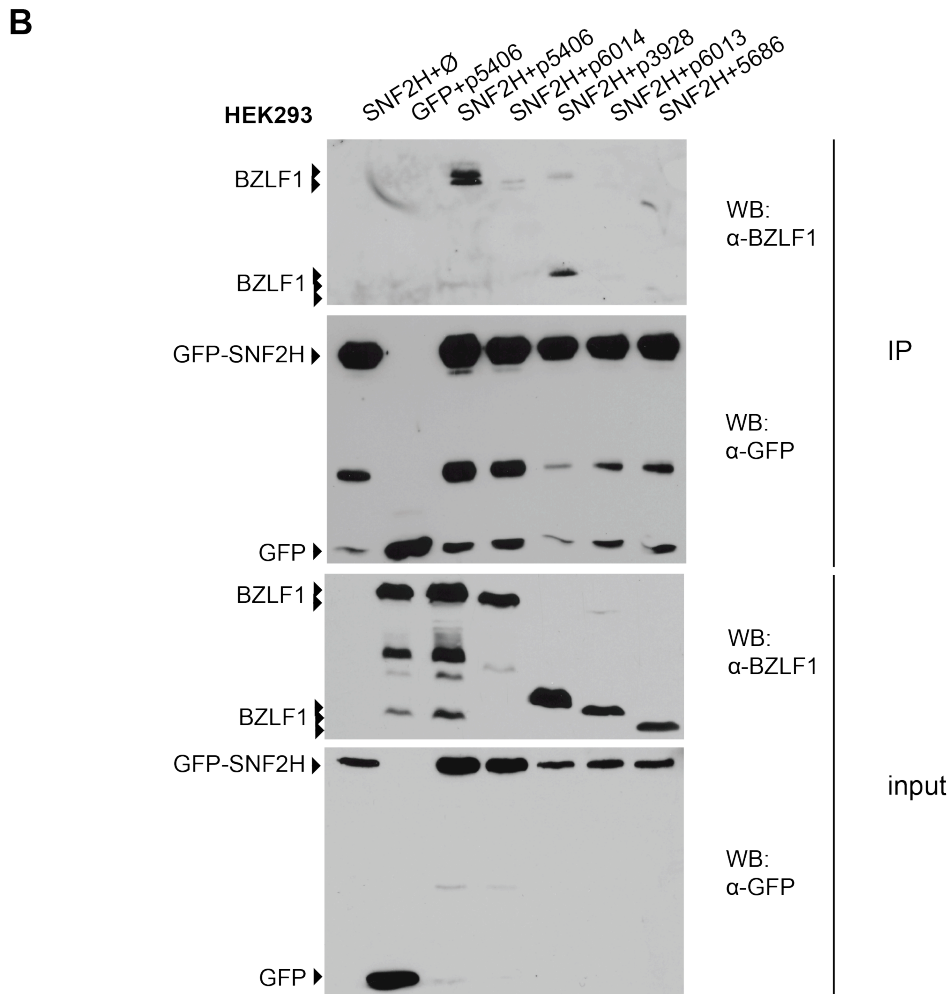
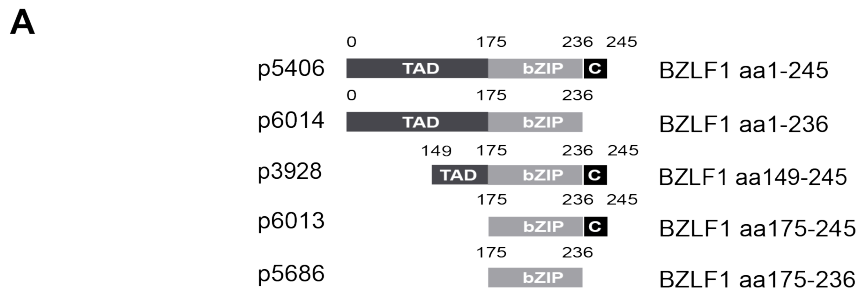


**Fig. 4.15 Immunoprecipitations of the cellular chromatin remodeler SNF2H with BZLF1 full-length and truncated versions of BZLF1**

(A) The figure depicts the modular structures of the truncated BZLF1 variants used in the subsequent experiments.

(B) BZLF1's TAD but also the C-terminus are involved in the protein interaction with the cellular chromatin remodeler SNF2H. The expression plasmid of the GFP-tagged chromatin remodelers SNF2H (p5906) was co-transfected in HEK293 cells together with expression plasmids encoding BZLF1 versions (p5406, p6014, p3928, p6013 and p5686) as shown in (A). Cell lysates were treated with the enzymes benzonase and DNase I prior to immunoprecipitation in order to disrupt complexes that might occur via protein-DNA-protein interactions. Immunoprecipitation of the GFP-tagged chromatin remodeler SNF2H was performed with GFP-binder beads. The analysis of input and immunoprecipitated material was done by western blot immunodetection with antibodies directed against GFP or BZLF1. The immunoblots showed the interaction of cellular SNF2H with wild-type BZLF1 (BZLF1 aa1-245) and the BZLF1 mutant (BZLF1 aa149-245). No interaction could be seen with BZLF1 aa1-236, BZLF1 aa175-245 or BZLF1 aa175-236 proteins. BZLF1 did not show unspecific binding to the GFP-binder beads or GFP (p1925) alone.

The immunoblots showed the interaction of cellular SNF2H with wild-type BZLF1 (BZLF1 aa1-245) and the BZLF1 mutant (BZLF1 aa149-245). No interaction could be detected between SNF2H and the BZLF1 versions aa1-236, BZLF1 aa175-245 or BZLF1 aa175-236. BZLF1 did not show unspecific binding to the GFP-binder beads or GFP alone. The results in Fig. 4.15 panel B indicated that the interactions of the viral transcription factor BZLF1 and the cellular chromatin remodeler SNF2H are mediated by a combination of BZLF1's TAD and its C-terminus. This is an interesting finding because the importance of BZLF1's C-terminus has been described (Petosa *et al.*, 2006) but its molecular function has been elusive so far.

My candidate approach was successful but is limited to the presumed interactors, only. In order to identify additional and unknown chromatin factors, which interact with BZLF1 *in vivo*, I performed mass spectrometry analysis. I made use of the conditional expression system in Raji 4816 cell line described in Fig. 4.1 panel A. I constructed two conditional expression plasmids with BZLF1 wild-type (p5693, BZLF1 aa1-245) or BZLF1's bZIP domain (p5694, BZLF1 aa175-236) fused to functional Flag- and tandem Strep-tags as shown in Fig. 4.16 panel A. BZLF1 or bZIP expression was monitored with the detection of GFP positive cells by flow cytometry (Fig. 4.16 panel C). First, protein expression of the conditional expression plasmids (p5693 and p5694) was confirmed in HEK293 cells by western blot immunodetection upon lytic phase induction. Both proteins (BZLF1 and bZIP) were equally expressed with a functional Flag-tag (Fig. 4.16 panel B). Second, Raji cells were stably transfected with the plasmids 5693 and 5694. Single cell clones were analyzed for viability and inducibility of the transgenes by flow cytometry. The single cell clones with the most robust and highest expression of the *eGFP* gene (about 70 %) were used for all my following experiments (Fig. 4.16 panel C). Immunoprecipitations of nuclear extracts were performed with Strep Tactin sepharose beads. I did immunoprecipitations of each cell line in triplicates. Fig. 4.16 panel D shows single steps along the mass spectrometry sample preparation indicating an (barely visible) enrichment of the bait proteins BZLF1 and bZIP. I sent these samples for mass spectrometry analysis to the Zentrallabor für Proteinanalytik (ZfP, Munich), where liquid chromatography tandem mass spectrometry (LC-MS/MS) with the ion trap mass analyzer Orbitrap was performed. With the aid of the Mascot software the colleagues identified BZLF1's interacting proteins in the viral and human protein databases.

The data that I received from ZfP were analyzed as follows. The two data sets with three experiments each (5693 (1,2,3) and 5694 (1,2,3)) were analyzed by the R program. First, the protein names were made unique, deleting multiple entries. Second, the triplicates (1,2,3)

were checked for proteins, which were identified in at least two out of three samples. As expected the protein scores of distinct samples differed. Therefore, the mean of the protein scores were calculated in a pair-wise comparison. The pair with the highest mean was used. The outputs were sorted by mean values in decreasing order. Only if the highest mean had a score  $\geq 100$ , the interaction was considered as credible. Third, all proteins that turned up in the data sets from 5693 and 5694 samples were sorted in three different lists (including viral and cellular interactors) in the following manner: The first list (BZLF1\_5693\_minus\_5694) contains proteins present in 5693 but not in 5694 data sets. This list should encompass proteins that interact with BZLF1's TAD or C-terminus, only. The second list (BZLF1\_5694\_minus\_5693) contains proteins present in 5694 but not in 5693 data sets. This list should encompass proteins that bound exclusively to BZLF1's bZIP domain but did not interact with other BZLF1 domains. The third list (BZLF1\_5693\_intersect\_5694) contains proteins present in 5693 and 5694 samples. This list encompasses all proteins that were found to interact with all BZLF1 domains. All lists can be found in the appendix.

The viral proteins BMRF1 (DNA polymerase processivity factor), BALF5 (DNA polymerase catalytic subunit), TK (thymidine kinase), and BSLF2 (mRNA export factor) were identified as BZLF1 interaction partners. With the exception of TK all these interactions are known from the literature (Baumann *et al.*, 1999) supporting my experimental setup and the credibility of the mass spectrometry data of cellular interactors. BZLF1 wild-type (but not the bZIP domain alone) interacts with the histones H2B type 1-C (score: 364.0) and H2A type 1-D (score: 160.5). This finding is in line with my previous data of BZLF1 binding to mononucleosomal DNA *in vitro* (Fig. 4.7) and co-locating with histone octamers in the lytic promoter regions *in vivo* (Fig. 4.13). The interaction of BZLF1 with the histone-binding protein RBBP4 (RbBP4, score: 95.5) and chromodomain helicase DNA-binding protein 4 (CHD4, score: 55.5) supports the assumption that BZLF1 interacts with various chromatin remodelers in the nucleus but the low score values in these cases argue for independent experimental confirmation. From the preliminary data I can conclude that the N- and C-terminal domains of BZLF1 are responsible for these interactions. Unexpectedly three chromatin regulatory proteins exclusively interact with the bZIP domain of BZLF1 but not with full-length BZLF1: the nucleosome assembly protein 1-like 1 (NP1L1, score: 502.0), the histone linker protein histone H1.2 (score: 167.5) and the histone H3.3C (score: 81.5). Histone H4 (score: 242.5) and histone H1.5 (score: 121.5) interacted with BZLF1 full-length version and also the bZIP domain. Again these data need independent experimental confirmation but my mass spectrometry results strongly confirmed BZLF1's role as an

important chromatin player, which activates the viral chromatin and enables the rapid and strong expression of EBV's lytic genes.

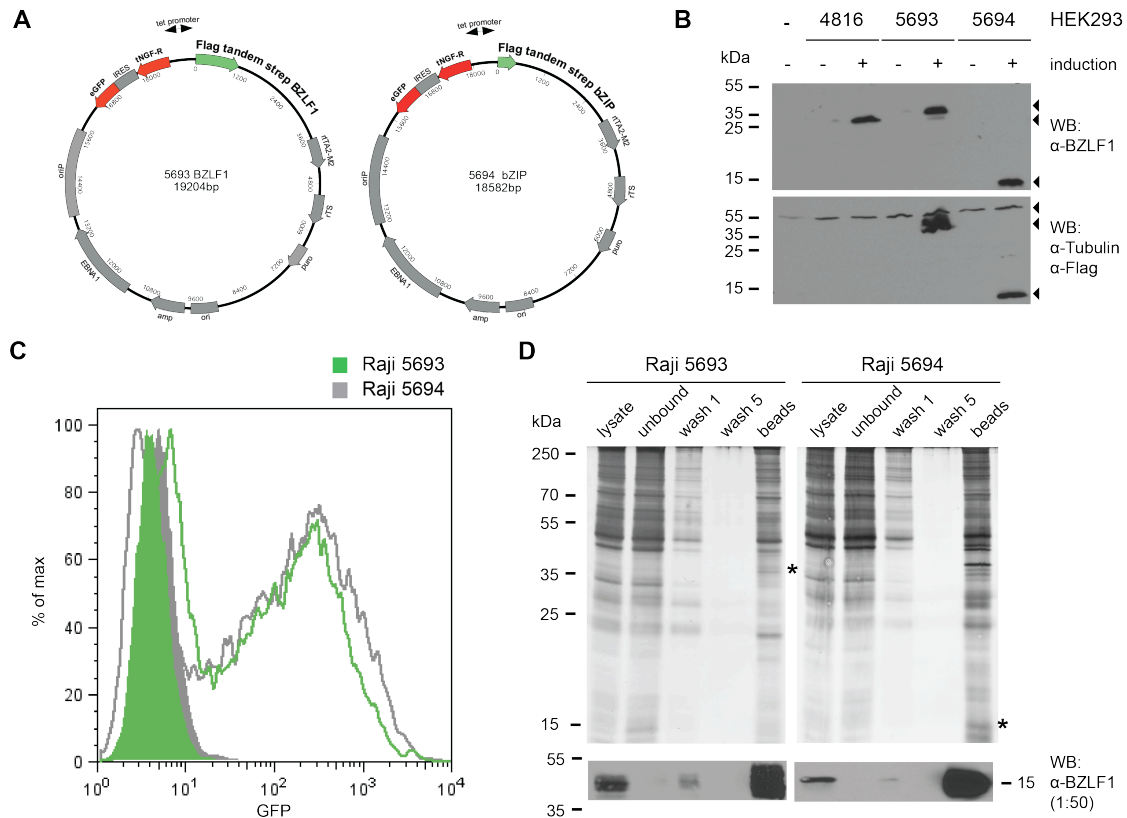


**Fig. 4.16 Mass spectrometry analysis identified chromatin regulatory proteins as potential BZLF1 interaction partners**

**(A)** Conditional expression plasmids of Flag- and tandem strep-tagged versions of BZLF1 full-length (aa1-245, p5693) and its bZIP domain (aa175-236, p5694) were cloned. The plasmids contain the bicistronic coding sequence of the tetracycline controlled repressor *rTS* and transactivator *rtTA2-M2*. In the absence of tetracycline (or its analogue doxycycline), the repressor binds tightly to the so-called *tet* promoter preventing its activation. After addition of doxycycline to the cells, the repressor *rTS* is replaced by the activator *rtTA2-M2*, which induces bidirectional transcription and simultaneous expression of three transgenes: *enhanced green fluorescent protein* (*eGFP*), the human *truncated nerve growth factor-receptor* (*tNGF-R*) and *BZLF1* (or *bZIP*). An internal ribosomal entry site (*IRES*) separates *tNGF-R* and *BZLF1* or *bZIP*.  $\beta$ -lactamase (*amp*) and *puromycin N-acetyltransferase* (*puro*) serve as resistance genes in bacteria and Raji cells, respectively. DNA replication in *E. coli* initiates at the prokaryotic origin of replication (*ori*). Epstein-Barr nuclear antigen 1 (*EBNA1*) activates replication of the plasmid DNAs through binding to the origin of plasmid replication (*oriP*) and governs their segregation by mediating attachment to host cell metaphase chromosomes.

**(B)** Protein expression of the conditional expression plasmids (p5693 and p5694) was confirmed by western blot immunodetection in HEK293 cells upon lytic phase induction. Protein lysates were analyzed with an antibody recognizing either BZLF1 (top panel) or Flag-tag (bottom panel) 15 hours post induction. The plasmid p4816 served as a control for BZLF1 expression. Tubulin was used as a loading control (bottom panel). Both proteins (BZLF1 and bZIP) were equally expressed with a functional Flag-tag.

**(C)** The conditional expression plasmids (p5693 and p5694) were stably introduced to Raji cells and single cell clones were selected by limiting dilution, expanded and analyzed further. GFP expression in Raji cells was a measure of the induced expression of BZLF1 or bZIP. Upon addition of 100 ng/ml doxycycline to the cells for 15 hours, about 70 % of the cells turned GFP-positive.

**(D)** Nuclear cell extracts of Raji 5693 or 5694 cells were prepared and BZLF1 was precipitated using a purification protocol of Strep-tag fusion proteins with Strep-Tactin matrices. Streptavidin beads were incubated with the nuclear extracts and washed five times. Beads were frozen directly on dry ice and used for mass spectrometry analysis. The results can be found in the appendix. Lysates, first and last washing fractions, and beads were controlled for BZLF1 or bZIP expression (\*) by silver staining after SDS-PAGE (top panel) and western blot immunodetection with an  $\alpha$ -BZLF1 antibody (bottom panel).



# 5. DISCUSSION

## 5.1 Scope and aim of my thesis work

The Epstein-Barr Virus (EBV) is a very successful human tumor virus that infects more than 95 % of the adult population worldwide with a lifelong persistence in human B cells. The key to EBV's success lies in its ingenious life cycle consisting of three major phases. Upon cellular infection the virus enters the pre-latent phase, in which the expression of latent genes, repression of lytic genes and the short-term transcriptional activation of cellular target genes by BZLF1 help the virus to activate the resting infected B lymphocyte and escape from the human immune system (Kalla *et al.*, 2010). Viral interaction activates quiescent B lymphocytes but induces their proliferation *in vitro*. After one to two weeks, the virus establishes a strictly latent infection, in which no virus is synthesized and the viral genome is maintained in the infected and proliferating cells as nuclear plasmid copies. Only latent genes supporting proliferation and genome maintenance are expressed, all lytic genes are repressed. Upon induction of the lytic phase, all three classes of viral lytic genes are expressed: immediate-early, early and late lytic genes. The lytic phase is accomplished within 48 hours and results in viral synthesis and spread of viral progeny to uninfected cells (Kieff and Rickinson, 2007; Rickinson and Kieff, 2007).

All three phases of EBV's life cycle rely on the different epigenetic states of viral DNA and the availability of viral and cellular factors (Woellmer and Hammerschmidt, 2013). In a smart way, the virus takes advantage of the host cell's epigenetic machinery to establish a stable latent infection but is still capable to escape from it. Upon infection, the viral DNA is first

completely naïve, i.e. free of histones and devoid of methylated CpG dinucleotides (Kintner and Sugden, 1981; Fernandez *et al.*, 2009; Kalla *et al.*, 2010). In the course of the pre-latent phase, the host cell's epigenetic machinery compacts the viral DNA into nucleosomal arrays, modifies the histones over time and intensively methylates the majority of all viral CpG dinucleotides (Kalla *et al.*, 2010). Apart from the promoters of a few latent genes, all other viral promoters are silenced during latency. Densely positioned nucleosomes, the establishment of repressive histone marks by Polycomb proteins and extensive DNA methylation keep the virus in the strictly latent, dormant mode (Ramasubramanyan *et al.*, 2011; Woellmer *et al.*, 2012).

Surprisingly, DNA methylation is a prerequisite for the induction of EBV's lytic phase in order to escape from latency and initiate the lytic reactivation process (Bergbauer *et al.*, 2010; Kalla *et al.*, 2010; Woellmer *et al.*, 2012). In the lytic phase, the loss of nucleosomes increases the accessibility of the viral DNA. The removal of repressive histone marks and the establishments of active histone marks reactivate the promoter regions of viral lytic genes and enable the virus to replicate and produce viral progeny to infect new B cells (Woellmer *et al.*, 2012).

It is well accepted that the viral transcription factor BZLF1 triggers the switch from the latent to the lytic phase (Countryman and Miller, 1985; Chevallier-Greco *et al.*, 1986; Takada *et al.*, 1986; Countryman *et al.*, 1987). First, BZLF1 enhances the expression of more than 50 early lytic genes by binding sequence-specifically to BZLF1 Responsive Elements (ZREs), which are located in promoter regions of certain lytic genes (Miller, 1989; Speck *et al.*, 1997; Schwarzmann *et al.*, 1998). Second, BZLF1 enables viral DNA replication via two mechanisms: it binds to the lytic origin of DNA replication and promotes the recruitment of components of the viral DNA replication machinery (Schepers *et al.*, 1993a, b; Schepers *et al.*, 1996; Zhang *et al.*, 1996; Gao *et al.*, 1998; Baumann *et al.*, 1999; Liao *et al.*, 2001). Third, BZLF1 indirectly or directly causes the loss of nucleosomes in the promoter region of viral lytic genes, which correlates with their expression (Woellmer *et al.*, 2012). It has been hypothesized that the observed reactivation of silenced, inactive chromatin is forced by a pioneer function of the BZLF1 transcription factor (Woellmer *et al.*, 2012) and/or the additional recruitment of chromatin remodelers (Adamson and Kenney, 1999; Zerby *et al.*, 1999; Schelcher *et al.*, 2007; McDonald *et al.*, 2009; Woellmer *et al.*, 2012).

Pioneer factors belong to a special class of transcription factors, which establish competence for gene expression (Magnani *et al.*, 2011; Zaret and Carroll, 2011). Peculiar structural characteristics of pioneer factors promote binding to their cognate binding motifs even in

nucleosome-dense regions and cause the remodeling of the silenced chromatin. Remodeling can be the consequence of DNA binding and opening of chromatin or of site-specific recruitment of cellular chromatin remodelers. Only very few examples of this type of factors have been identified and studied so far, among them FoxA, PBX1 and PU.1.

The central hypothesis of my PhD work was, if the viral transcription factor BZLF1 might have functions similar or identical to known pioneer factors during the process of lytic gene activation. If BZLF1 itself could act as a chromatin remodeler or, alternatively, could recruit cellular chromatin regulatory factors, which might assist in the reactivation process of silenced chromatin.

In the subsequent chapters, I shall discuss my data in the light of these questions and discuss and integrate my new findings in the context of the known epigenetic mechanisms and principles of EBV's life style.

## **5.2 Novel findings of BZLF1 and the regulation of meZREs**

### **5.2.1 BZLF1 shows characteristics of a pioneer factor**

Pioneer factors find access to their DNA binding sites in nucleosome-dense chromatin prior to other factors binding and prior to the time of transcriptional activation. These factors are defined as nucleosome-binding proteins that pioneer the subsequent binding of other transcription factors, chromatin modifiers, and nucleosome remodelers involved in chromatin remodeling. Alternatively, certain pioneer factors can actively open local chromatin by themselves (Zaret and Carroll, 2011). The regulation of cell development and differentiation is often mediated by pioneer factors that promote cell type-specific transcriptional programs (Magnani *et al.*, 2011).

The preliminary work for my PhD project was conducted in my group (Woellmer *et al.*, 2012), when Anne Woellmer analyzed the nucleosomal occupancy at various ZRE sites of lytic promoters in latently infected versus lytically induced Raji cells. During latency, Anne found very dense nucleosomes at and in close vicinity of ZRE sites. The high nucleosomal occupancy was interpreted to mean that nucleosomes shield the ZRE sites within the lytic promoters during latency preventing their transcriptional activation. Upon expression of BZLF1 and the onset of the lytic phase, the nucleosomal occupancy abruptly diminishes resulting in a more open conformation of viral chromatin. Based on these observations, we

hypothesized that the viral transcription factor BZLF1 is involved in chromatin remodeling. BZLF1 could actively eject nucleosomes or recruit cellular chromatin remodeler. I performed a number of *in vitro* and *in vivo* experiments to scrutinize if BZLF1 acts as a pioneer factor.

First, I performed *in vitro* electro mobility shift assays (EMSAs) with purified BZLF1 protein and compacted, 156 bps long mononucleosomal DNA templates containing one or two ZRE sites. I made use of the principle that the stable complex of BZLF1 and the mononucleosome would migrate more slowly than the mononucleosome alone. I used a number of DNA templates, which differ in the number of ZRE sites and their positioning within the mononucleosomal-sized DNA templates. My EMSA results documented that the viral transcription factor BZLF1 does bind the histone octamer of a compacted binding site *in vitro*, but BZLF1's binding does not seem to reposition or even eject the mononucleosome without the help of other molecular machines (Fig. 4.7 panel A). Under certain conditions, even ZRE sites located within the core of the histone octamer can be accessed by the BZLF1 protein (Fig. 4.11). In addition, I could show that the nucleosome-binding activity does not depend on BZLF1's transactivation domain (TAD) but is encoded within the C-terminal part of BZLF1 encompassing the bZIP domain and C-terminus (Fig. 4.7 panel B). Only very few of the many known and studied DNA binding transaction factors are capable of binding their cognate sites *in vitro* in a nucleosomal context underlining the exceptional property of BZLF1.

Second, using two sequential chromatin immunoprecipitations (ReChIPs) I could document that BZLF1 binds to histone octamers *in vivo* at certain viral lytic promoters upon lytic reactivation of Raji cells. BZLF1's binding to the viral lytic promoter regions and the loss of nucleosomes are two distinct events that can be detected at four and 15 hours post induction, respectively (Fig. 4.13 panel A and unpublished data of A. Woellmer), indicating that BZLF1 binds to nucleosomal DNA prior to the removal of the histone octamer *in vivo*.

Third, I performed mass spectrometry analysis to identify BZLF1's interaction partner involved in the formation and regulation of chromatin. I could confirm the *in vivo* interaction of BZLF1 with the histone octamer and identify the responsible domains of BZLF1 (see according lists in the appendix). My results suggested that BZLF1's TAD and/or C-terminus bind the histone H2A-H2B dimer, whereas the bZIP domain interacts with the linker histone H1.2 and the histone variant H3.3. H2A and H2B histones are core components of the histone octamer (Kornberg, 1977). The linker histone H1.2 is responsible for the higher packaging of chromatin (Kornberg, 1974). The interaction of BZLF1 with H1.2 likely supports the access of BZLF1 to silenced, repressed chromatin. The substitution of the canonical core histone H3 with the histone variant H3.3 provides a mechanism for the immediate activation of genes,

which are silenced by histone modifications (Ahmad and Henikoff, 2002). The presence of H3.3 might assist BZLF1 to recognize its ZRE motifs within repressed chromatin.

The nucleosome-binding activity of known pioneer factors is based on their peculiar structural features that are more or less understood in chromatin opening. The fork head-like transcription factor FoxA regulates the transcriptional activation of the *albumin* gene, which is indispensable for liver cell function. Nucleosomal occupancy in the promoter region of albumin results in an equal or even favored binding of FoxA (Cirillo *et al.*, 1998) suggesting that the complex formation of FoxA with nucleosomes serves as a positive architectural signal for the recruitment of complexes of gene regulation (Chaya *et al.*, 2001). The N-terminus of FoxA contains a binding motif for core histones (Cirillo *et al.*, 2002), but the pioneer factor activity stems from its C-terminus. The winged helix DNA-binding domain contains a helix-turn-helix (HTH) motif, which mediates DNA contacts and structurally resembles the linker histone H1 (Cirillo *et al.*, 1998). In that way the DBD is capable to disrupt internucleosomal interactions (Cirillo *et al.*, 2002; Sekiya *et al.*, 2009).

The Pre-B-cell leukemia homeobox 1 (PBX1) plays crucial roles in cell type-specific transcriptional regulation of genes involved in organogenesis (Magnani *et al.*, 2011). PBX1 occupies chromatin prior to other factors, mediates nucleosome depletion, and recruits additional chromatin factors involved in transcriptional regulation. As a member of three amino acid loop extension (TALE)-class homeodomain family, PBX1 contains also a HTH motif for DNA binding. The nucleosome binding characteristics have been reported to drive from its charge that promotes chromatin openness at specific genomic locations but the exact binding mechanistic is not reported yet (Magnani *et al.*, 2011).

PU.1 belongs to the family of ETS-domain transcription factors that regulates gene expression during growth and development (Kodandapani *et al.*, 1996; Sharrocks, 2001). The factor plays an important role in the cell-type specific transcriptional program that promotes B cell or macrophage differentiation (Magnani *et al.*, 2011). At early stages of B cell differentiation and development PU.1 binds the enhancer of the *Paired box protein Pax-5* gene in multipotent hematopoietic progenitors (Zaret and Carroll, 2011). The structure of PU.1 contains an ETS DNA-binding domain with a variant of the winged HTH motif. As a pioneer factor it expands the linker region, initiates nucleosome repositioning and chromatin opening in the course of macrophage and B cell differentiation (Ghisletti *et al.*, 2010; Heinz *et al.*, 2010).

The viral transcription factor BZLF1 belongs to the basic leucine-zipper (bZIP) family of transcription factors (Farrell *et al.*, 1989; Chang *et al.*, 1990; Lieberman and Berk, 1990). The

DNA-binding domain of BZLF1 does not contain a HTH motif, but a variant of the leucine zipper motif responsible for the coiled-coil structure. BZLF1 forms homodimers and binds the DNA via its two long bZIP helices (Morand *et al.*, 20006; Petosa *et al.*, 2006). The basic region of each helix contacts the major groove and the zipper region forms a coiled-coil. The C-terminal tail forms an additional structured motif stabilizing the coiled-coil.

It seems that a HTH motif mimicking the structure of a linker histone facilitates the remodeling activity of a pioneer factor. No pioneer factor with a bZIP domain is known, but I want to discuss the similarities and differences of a HTH motif and a leucine zipper motif compared to the structure of a linker histone to provide a possible explanation and a model for BZLF1's nucleosome-binding activity.

The HTH motif contains two  $\alpha$ -helices connected by a short extended chain of amino acids, which constitutes the "turn". The two helices interact and are held together at a fixed angle. The more C-terminal recognition helix fits into the major groove of DNA and its residues play an important part in recognizing the specific DNA sequence to which the protein binds.

In contrast the leucine zipper motif contains two  $\alpha$ -helices (one from each monomer), which are joined to form a short coiled-coil. The helices are held together by interactions between hydrophobic amino acid side chains, primarily leucines. Beyond the dimerization interface the two  $\alpha$ -helices separate from each other to form a Y-shaped structure allowing their side chains to contact the major groove of the DNA molecule.

Most eukaryotic linker histones H1 share a similar, tripartite structure. A globular domain is flanked by a short N-terminal and long C-terminal lysine-rich domain (Kasinsky *et al.*, 2001). Linker histones H1 attach close to the entry and exit sites of linker DNA on the nucleosome core, bringing together the two linker DNA segments (Allan *et al.*, 1980; Wolffe *et al.*, 1997; Thomas, 1999). The globular domain contains a three-helix bundle with structural homology to HTH DNA-binding proteins and is essential for binding of H1 with the nucleosome (Ramakrishnan *et al.*, 1993). With the help of the highly positively charged C-terminal domain, the linker histone H1 binds to linker DNA through nonspecific electrostatic interactions (Allan *et al.*, 1980; Allan *et al.*, 1986; Subirana, 1990).

According to the linker histone H1's positively charged C-terminus, the viral transcription factor BZLF1 could facilitate binding to the linker DNA through its basic bZIP domain. My results from the mass spectrometry analysis revealed that the bZIP domain of BZLF1 interacts with the linker histone H1.2, which would support the hypothesis that BZLF1 acts on linker regions of silenced chromatin. The N- or C-terminal ends of the  $\alpha$ -helices of BZLF1's dimer could provide the interaction with the nucleosome. Since the C-terminal tail is known to

stabilize the coiled-coil through numerous interactions (Petosa *et al.*, 2006), it could also be involved in the binding to the nucleosome. The mass spectrometry data revealed that BZLF1's TAD or C-terminus bind to the histone dimer H2A-H2B supporting the hypothesized nucleosome-binding function. My speculations of BZLF1's binding characteristics to nucleosomes have to be structurally verified by approaches such as electron microscopy of the BZLF1-monomonucleosome complex in the future.

### 5.2.2 BZLF1 might read epigenetic modifications in silenced chromatin

Recent reports support the assumption that pioneer factors can penetrate repressive chromatin to recognize and bind their DNA-binding sites and regulate the transcriptional activation of the relevant genes. The cell type-specific distribution of the histone marks H3K4me1 and H3K4me2 plays an important role in the recruitment of pioneer factors, as they are capable of reading them.

The recruitment of FoxA to enhancers is dependent on epigenetic changes of enhancer hallmarks (Serandour *et al.*, 2011). The nucleosome-binding activity of FoxA is facilitated by the histone marks H3K4me1 and H3K4me2 but not by histone acetylation (Cirillo and Zaret, 1999; Lupien *et al.*, 2008). FoxA can even favor H3K4me2 deposition (Smale, 2010). The pioneer factor PBX1 is also capable of reading specific epigenetic signatures like H3K4me2 (Berkes *et al.*, 2004; Magnani *et al.*, 2011), and PU.1 reprograms the chromatin landscape through the induced deposition of H3K4me1 (Magnani *et al.*, 2011).

Summarizing my chromatin immunoprecipitation (ChIP) data regarding the histone H3 and its N-terminal modifications in latent and lytically induced Raji cells, I speculate that the pioneer factor BZLF1 can read and decipher epigenetic modifications and penetrate repressive chromatin. Upon lytic reactivation, BZLF1 binds to viral promoters as early as four hours post induction (Fig. 4.13 panel A). The nucleosomal loss shown by the decrease of histone H3 in the viral promoters appears later about 15 hours post induction (unpublished data of Anne Woellmer). During latency, viral lytic genes are repressed by very densely positioned nucleosomes and repressive histone marks like H3K27me3 in the promoters of lytic genes (Woellmer *et al.*, 2012). Upon lytic phase induction, the repressive histone mark is removed as early as seven hours post induction (data not shown) and replaced by active histone marks. The activation of viral lytic promoters starts with the establishment of the active histone marks H3K4me1 (Fig. 4.13 panel A) and H3K27ac (data not shown) as early as seven hours post induction followed by H3K4me3 (unpublished data, Anne Woellmer) about 15 hours post induction. One could hypothesize that initially the viral transcription factor BZLF1 reads

its target sites in nucleosome-dense and H3K27me3-enriched promoter regions and penetrates the repressive chromatin. In a second step, BZLF1 promotes the removal of repressive histone marks and the deposition of active histone marks like H3K4me1, H3K27ac and H3K4me3. The change of histone modifications increases the accessibility of the viral DNA for the transcriptional machinery and enables gene expression of the viral lytic genes.

### 5.2.3 BZLF1' s binding to meZREs in silenced chromatin

The crystal structure of the nucleosome core particle and all its protein-protein as well as protein-DNA interactions has been solved (Luger *et al.*, 1997). A common conserved structural motif, termed the histone fold, has been identified in all four core histones (Arents and Moudrianakis, 1995). This motif exists also in eukaryotic transcription factors e.g. TFII TATA box-binding protein-associated factors (TAF's) (Xie *et al.*, 1996). In 1.65 turns of a left-handed superhelix, DNA is wrapped around the histone octamer, termed the nucleosomal DNA. DNA bases that are not directly in contact with the protein guarantee a high degree of mobility. In the nucleosome core particle the histone fold dimers of the H3-H4 and H2A-H2B pairs mediate the structural unit for the protein-protein and protein-DNA interactions. Each histone fold dimer has three independent DNA-binding sites. As a consequence, the histone folds are responsible for DNA binding at twelve of the 14 minor groove locations that face the histone octamer (Luger and Richmond, 1998). Over 121 bps within the inner face of the DNA supercoil establish all the interactions of the histone folds. The 13 bps at each entry and exit point of the superhelix are bound by an  $\alpha$ -helical histone fold extension of H3 and its N-terminal tail. Structural variability stems from the regions flanking the histone fold motif. Histone-fold extensions form an integral part of the histone octamer and provide specific formation of the histone octamer. Histone tails contact the DNA outside of the nucleosome core particle contributing to six of the 14 DNA-binding sites (Luger and Richmond, 1998). Neighboring nucleosome core particles can make contact via their tails of H3 and H4 (Luger *et al.*, 1997). There are 142 hydrogen bond interactions between histone and DNA within the 14 binding sites. The protein main-chain and the phosphodiester backbone atoms provide the first half of these interactions (Luger *et al.*, 1997). Lysine and arginine residues of histones maintain the second half.

The energetic cost of DNA bending into a superhelix must be partially compensated. This is done through the neutralization of the phosphate charge by the basic side chains and the N-termini of  $\alpha$ -helices located only on one side of the double helix (Strauss and Maher, 1994).



The number and nature of the protein main-chain interactions are very similar in nucleosome core particles containing different DNA sequences. The protein main-chain interactions dominate the intrinsic sequence variability in the structure of DNA. As a consequence, nucleosomes can form independent of the underlying DNA sequence (Luger *et al.*, 1997). How the histone octamer positions according to DNA sequence preferences depends on three issues. First, the energetic cost that arises of DNA bending at each of the 14 histone contact sites. Second, the distortion of the DNA bridging between binding sites that lead to fewer direct histone-DNA contacts. Third, the hydrogen bond interactions mediated by side chains reaching into the minor groove.

Recapitulating all my EMSA results, I can postulate that BZLF1 shows pioneer factor activity and binds nucleosomal DNA *in vitro*, even if the ZRE is located in the nucleosomal core particle (Fig. 4.7; Fig. 4.11). Nevertheless, it seems that the exact ZRE location within the nucleosomal core particle is critical for BZLF1 binding in silenced chromatin (Fig. 4.11). Since the 156 bps long DNA templates are longer than the normally 147 bps long nucleosomal DNA, the exact nucleosome position within the used DNA templates is uncertain. With the help of the nucleosome positioning prediction engine (NuPOP; <http://nucleosome.stats.northwestern.edu/>), I tried to predict the nucleosome occupancy within the DNA templates. NuPOP is built upon a duration hidden Markov model, in which the linker DNA length is explicitly modeled. The nucleosome or linker DNA state model was chosen as a 4th order Markov chain (Wang *et al.*, 2008; Xi *et al.*, 2010).

**Table 6.1 Overview of the DNA templates, their ZRE, CpG dinucleotides, and predicted nucleosome positions and their BZLF1 binding in my EMSA experiments**

DNA template (156 bps)	ZRE position	CpG position	Nucleosome prediction	BZLF1 binding
Control	-	-	2-148	No
ZRE 3	48-56	53-54	6-152	No
ZRE 4	69-77	74-75	9-155	No
ZRE 3+4	9-17; 131-139	14-15; 136-137	7-153	Yes
ZRE 0+4	131-139	136-137	7-153	Reduced
ZRE 3+0 -5nt	4-12	9-10	6-152	Yes
ZRE 3+0	9-17	14-15	7-153	Yes
ZRE 3+0 +5nt	14-22	19-20	7-153	No
ZRE 3+0 +10nt	19-27	24-25	7-153	No
ZRE 3+0 +15nt	24-32	29-30	7-153	Yes
ZRE 3+0 +30nt	39-47	44-45	7-153	Yes

All mononucleosomal DNA templates used in EMSA experiments were 156 bps long. The precise location of ZRE motifs and CpG dinucleotides within the 156 bps are noted. The nucleosome prediction was performed using the NuPOP engine. The result of BZLF1 binding in EMSAs is noted.

Except for the DNA template ZRE 3+0 -5 nt, all ZRE sites seem to be located within the nucleosome core particle supporting the findings that BZLF1 does bind to nucleosomal DNA.

It has been reported that pioneer factors bind their compacted binding sites in the major groove, which makes them more accessible for factor binding in the chromatin context. Unfortunately, it is not clear from my data, if the ZRE is located in the major or minor groove for the access of BZLF1. The analysis of the EMSA data does not show a five-bp-periodicity, which would explain the BZLF1 binding constriction for some ZRE locations. Further analysis has to clarify these questions. It would be interesting to know, if BZLF1's binding to nucleosomal DNA moves or slides the histone octamer. To address this question further EMSA experiments coupled with enzymatic digestion should be performed. In that way the sliding process of the histone octamer upon BZLF1 binding could be captured using longer multi-nucleosomal DNA templates.

Additionally, it appears that two ZRE sites in the lytic promoters may have a cooperative or, at least, an additive effect for BZLF1's binding (Fig. 4.10). In contrast to the ZRE template ZRE 3+4 with two functional ZRE motifs, the non-functional mutations in the DNA templates ZRE 3+0 and ZRE 4+0 resulted in reduced and almost eliminated nucleosome-binding activity of BZLF1, respectively. It seems that not only the ZRE location within the nucleosome core particle but also the number of ZRE's and probably the distance between two ZRE sites play a role in the efficiency of BZLF1's pioneer factor activity. The promoter regions of lytic EBV genes usually contain several ZREs but I could not delineate a clear distinct and consensed ZRE spacing, which would underline this hypothesis.

#### **5.2.4 BZLF1 and its interactions with chromatin regulatory proteins**

The viral transcription factor BZLF1 binds nucleosome-dense regions in the promoter regions of viral lytic genes but does not evict nucleosomes. Previous data showed that the nucleosomal occupancy of these promoter sites drops later upon lytic induction (Woellmer *et al.*, 2012). This let me hypothesize that BZLF1 might recruit chromatin remodelers explaining the removal of histones. I addressed this uncertainty with two *in vivo* approaches: co-immunoprecipitation and mass spectrometry analysis.

Since there are four major remodeler families (SWI/SNF, ISWI, INO80 and CHD), I first decided to examine the *in vivo* interactions of BZLF1 using SNF2H of the ISWI family and hIno80 of the INO80 family in a candidate approach. The ISWI family is involved in chromatin assembly and nucleosomal spacing (Cairns, 2005; Clapier and Cairns, 2009). ISWI has been shown to regulate transcription and is involved in DNA replication and chromatin assembly. SNF2H has been previously reported to promote herpes simplex virus 1 (HSV-1) immediate-early gene expression and replication. SNF2H might also interact with VP16, the

cousin of BZLF1 and immediate-early gene product in herpes simplex virus 1 (HSV-1; Bryant *et al.*, 2011). The INO80 remodelers are able to slide nucleosomes and exchange histones (Shen *et al.*, 2003; Tsukuda *et al.*, 2005; van Attikum *et al.*, 2007). INO80 remodelers regulate transcription and are involved in DNA repair and cell cycle checkpoint adaption. So far there is no report that this chromatin remodeler family plays a role in the reactivation process of herpes viruses, but EBV nuclear proteins EBNA-LP and EBNA2 were found associated with a INO80 remodeler complex necessary for lymphoblastoid cell line growth and survival (Portal *et al.*, 2013). Performing co-immunoprecipitations I could prove that BZLF1 interacts with SNF2H (Fig. 4.14 panel A and C) and also with hIno80 (Fig. 4.14 panel B and C) in two different experimental models and two cell types. In preliminary experiments, I could narrow down the responsible domains for the interaction of BZLF1 with SNF2H to the N- and C-terminus of BZLF1 (Fig. 4.15 panel B).

Next, I performed immunoprecipitations followed by mass spectrometry analysis at the ZfP (Munich) in order to identify chromatin regulatory factors as BZLF1's interaction partners. The data showed an interaction of BZLF1 with CHD4 and RBBP4, components of the CHD family (data see appendix). This family is involved in nucleosome sliding and histone deacetylation important for transcriptional regulation (Brehm *et al.*, 2000; Guschin *et al.*, 2000; Bowen *et al.*, 2004). BZLF1's TAD, C-terminus or a combination of both mediate the interaction of BZLF1 with the components of the CHD remodeler family. I identified yet another chromatin regulatory protein as an interaction partner of BZLF1. The nucleosome assembly protein 1-like 1 (NP1L1) seems to interact exclusively with the bZIP domain of BZLF1 (data see appendix). The histone chaperone NP1L1 stimulates transcription factor binding to nucleosomal DNA and histone displacement (Walter *et al.*, 1995). An additional report showed that NP1L1 positively contributes to EBV reactivation through the induction of BZLF1 expression (Mansouri *et al.*, 2013).

Summarizing the newly identified interaction partners, it appears that BZLF1 recruits not only one but several chromatin regulatory factors to disrupt the nucleosome-dense regions of the viral promoters upon lytic reactivation. Interestingly, the C-terminus of BZLF1 seems to play a substantial role in this remodeling process. The C-terminal tail folds towards the coiled-coil to stabilize it (Petosa *et al.*, 2006). In that way the C-terminus could also contribute to the interaction with chromatin remodelers. If confirmed this finding would identify the first molecular function of BZLF1's C-terminus.

## 6. SUMMARY

The Epstein-Barr Virus (EBV), a member of the herpes virus family, is a human tumor virus that efficiently infects and immortalizes human B cells to yield proliferating B cell lines *in vitro*. Infection is initially non-productive and only after several weeks the infected cells support *de novo* viral synthesis. EBV uses cellular epigenetic processes of the host to establish latency in infected B cells and an exceptional mechanism to escape from it.

Upon infection, the host cell machinery packages the viral DNA in nucleosomal arrays and methylates it extensively resulting in silenced viral chromatin in order to maintain the state of latent infection. EBV's transcription factor BZLF1 is crucial and unique in overcoming the repressed latent state and inducing epigenetic reprogramming to allow transactivation of all viral lytic genes. BZLF1 binds to its preferred target motif, which is a cytosine-methylated meZRE sequence embedded in epigenetically silenced heterochromatin, in order to overcome transcriptional repression.

The aim of my PhD thesis was to investigate the molecular mechanisms of the viral transcription factor BZLF1 during the process of lytic reactivation. I wanted to address the question, if BZLF1 alone is capable of binding nucleosomes to open regulatory regions of viral genes, reactivate them and induce the lytic cycle. My results suggested that BZLF1 binds *in vitro* and *in vivo* to meZRE motifs even if they are embedded in nucleosomes. BZLF1's modular structure supports the access to histone octamers and histone linker regions. The transactivation domain and/or the C-terminus of BZLF1 bind the H2A-H2B histone dimer, whereas the bZIP domain is capable of binding the linker histone H1.2 and the histone variant H3.3. The binding of BZLF1 to nucleosomes does not result in their ejection, but rather

BZLF1 recruits cellular chromatin regulatory factors, which open these regions and facilitate access of the transcription machinery. With the help of its transactivation domain and/or C-terminus BZLF1 binds the catalytic subunits of the chromatin remodeler families ISWI, INO80 and CHD. In addition, the bZIP domain of BZLF1 provides an interaction with a member of the nucleosome assembly protein (NP1L1) family, which might positively regulate the viral reactivation process.

According to my findings, the viral transcription factor BZLF1 can be defined as a pioneer factor, it fulfills all peculiar characteristics of this special class of transcription factors. First, BZLF1 finds access to its target sites in condensed chromatin prior to other factors binding and prior to the time of transcriptional activation. Second, it enables the subsequent binding of chromatin modifiers and nucleosome remodelers involved in chromatin reprogramming and transcriptional activation. Together with BZLF1, these factors co-operatively contribute to the induction of EBV's lytic phase and promote viral synthesis. The structural details, how the transcription factor BZLF1 binds its target sites in condensed chromatin, if it modulates nucleosomal positioning and how exactly it interacts with chromatin regulatory factors will be of interest in the future.

## 7. ABBREVIATIONS

$\alpha$	anti (in context of antibody specificity)
A	adenosine (in context of nucleotides)
A	alanine (in context of amino acids)
aa	amino acid
ac	acetylation
ad	adde
ACF	ATP-utilizing chromatin assembly and remodeling factor
amp	$\beta$ -lactamase
AP-1	activator protein 1
ATF	activating transcription factor
ATP	adenosine-5'-triphosphate
bHLH	basic helix-loop-helix
bp	base pair
BSA	bovine serum albumin
bZIP	basic leucine zipper
C	cysteine (in context of amino acids)
C	cytosine (in context of nucleotides)
C/EBP $\alpha$	CCAAT/enhancer-binding protein alpha
C-terminus	carboxy-terminus
CBP	CREB binding protein
cDNA	complementary DNA
cen	centromer
CHD	chromodomain helicase DNA-binding
ChIP	chromatin immunoprecipitation
CHRAc	chromatin accessibility complex
chromo	chromatin organization modifier
CMV	cytomegalovirus
coIP	co-immunoprecipitation
Cp	crossing point
CpG	cytosine-phosphatidyl-guanosine
CREB	cAMP response element binding protein
CTCF	CCCTC-binding factor
CV	column volume
CytC	cytochrome C
DBD	DNA-binding domain

DMEM	Dulbecco's modified eagle medium
DMSO	dimethylsulfoxid
DNA	deoxyribonucleic acid
DNase	deoxyribonuclease
dox	doxycycline
DTT	dithiothreitol
E. coli	Escherichia coli
e.g.	exempli gratia
EBER	EBV-encoded RNA
EBNA	EBV-encoded nuclear antigen
EBV	Epstein-Barr virus
ECL	enhanced chemiluminescence
EDTA	ethyldiamintetraacetic acid
eGFP	enhanced green fluorescent protein
EGTA	ethylene glycol tetraacetic acid
EMSA	electromobility shift assay
ER $\alpha$	estrogen receptor alpha
et al.	et alii
ETS	E-twenty-six
F	farad
FBS	fetal bovine serum
Fig.	figure
g	gram
G	guanosine (in context of nucleotides)
GAPDH	glyceraldehyde 3-phosphate dehydrogenase
GFP	green fluorescent protein
h	hour
H2A	histone H2A
H2AX	histone H2AX
H2A.Z	histone H2A.Z
H2B	histone H2B
H <sub>2</sub> O	water
H3	histone H3
H3ac	acteylated histone H3
H3K9ac	acteylated histone H3 at lysine 9
H3K9me1	monomethylated histone H3 at lysine 9
H3K27	histone H3 lysine 27
H3K27ac	acteylated histone H3 at lysine 27
H3K27me2me3	di/trimethylated histone H3 at lysine 27
H3K27me3	trimethylated histone H3 at lysine 27
H3K36me3	trimethylated histone H3 at lysine 36
H3K4	histone H3 lysine 4
H3K4me1	monomethylated histone H3 at lysine 4
H3K4me2	dimethylated histone H3 at lysine 4
H3K4me3	trimethylated histone H3 at lysine 4
H3K79me2	dimethylated histone H3 at lysine 79
H3K9	histone H3 lysine 9
H3K9me2	dimethylated histone H3 at lysine 9
H3K9me3	trimethylated histone H3 at lysine 9
H4	histone H4
H4K16ac	acteylated histone H4 at lysine 16
H4K20me1	monomethylated histone H4 at lysine 20
H4K20me3	trimethylated histone H4 at lysine 20
HAT	histone acetyltransferase

HDAC	histone deacetylase
HEK293	human embryonic kidney 293
HEPES	(4-(2-hydroxyethyl)-1-piperazineethanesulfonic acid
HP1	heterochromatin protein 1
HSA	helicase/SANT-associated
HRP	horseradish peroxidase
HSV-1	herpes simplex virus 1
HTH	helix-turn-helix
i.e.	id est
IgG	immune globuline G
INO80	inositol requiring 80
IRES	internal ribosomal entry site
ISWI	imitation switch
JDP2	Jun dimerization protein 2
K	lysine (in context of amino acids)
K <sub>D</sub>	equilibrium dissociation constant
kDa	kilo dalton
l	litre
LB	Luria broth
LCL	lymphoblastoid cell line
LC-MS/MS	liquid chromatography tandem mass spectrometry
LMP	latent membrane protein
M	molar
MACS	magnetic activated cell sorting
MBD	methyl-CpG binding domain
me	methylation
meZRE	methylated BZLF1 responsive element
min	minute
mM	millimolar
mRNA	messenger RNA
MTA	metastasis associated
ng	nanogram
nm	nanometre
nmol	nanomole
NF <sub>κ</sub> B	nuclear factor „kappa-light-chain-enhancer“ of activated B cells
NoRC	nucleolar remodeling complex
NP1L1	nucleosome assembly protein 1-like 1
nt	nucleotide
N-terminus	amino-terminus
NuPOP	nucleosome positioning prediction
NURF	nucleosome remodeling factor
ori	prokaryotic origin of replication
oriP	origin of plasmid replication
PAA	polyacrylamide
Pax	paired box protein
PBS	phosphate buffered saline
PBX1	pre-B cell leukemia homeobox 1
PCR	polymerase chain reaction
PEI	polyethylenimine
PHD	plant homeodomain
PHO	phosphate metabolism
PKC	protein kinase C
PML	promyelocytic leukemia protein
PMSF	phenylmethanesulfonylfluoride



---

PNK	polynucleotide kinase
puro	puromycin N-acetyl-transferase
qPCR	quantitative PCR
R	arginine (in context of amino acids)
RbAp	retinoblastoma associated protein
RNA	ribonucleic acid
RNA Pol II	RNA polymerase II
rpm	rounds per minute
RPMI	Roswell Park Memorial Institute
RT	room temperature
RT-PCR	reverse transcriptase PCR
S	serine (in context of amino acids)
SDS	sodium dodecyl sulfate
SDS-PAGE	SDS polyacrylamide gel electrophoresis
sec	second
SUMO	small ubiquitin-like modifier
SWI/SNF	switch/sucrose nonfermentable
T	threonine (in context of amino acids)
T	thymine (in context of nucleotides)
TAD	transactivation domain
TALE	three amino acid loop extension
TBE	buffer containing Tris base, boric acid and EDTA
TBP	TATA box binding protein
TEMED	tetramethylethylenediamine
tet	ten-eleven translocation proteins
tNGF-R	truncated nerve growth factor-receptor
TORC	transducer of regulated CREB activity
Tris	2-amino-2-hydroxymethyl-propane-1,3-diol
TSS	transcription start site
U	units
UV	ultra violet
V	volt
WB	western blot
WD	tryptophan/aspartic acid
w/v	weight per volume
ZEB	zinc finger E-box-binding homeobox
ZRE	BZLF1 responsive element

## 8. LITERATURE

- Adams, C.C., and Workman, J.L. (1995). Binding of disparate transcriptional activators to nucleosomal DNA is inherently cooperative. *Mol Cell Biol* 15, 1405-1421.
- Adamson, A.L., and Kenney, S. (1999). The Epstein-Barr virus BZLF1 protein interacts physically and functionally with the histone acetylase CREB-binding protein. *J Virol* 73, 6551-6558.
- Adamson, A.L., Wright, N., and LaJeunesse, D.R. (2005). Modeling early Epstein-Barr virus infection in *Drosophila melanogaster*: the BZLF1 protein. *Genetics* 171, 1125-1135.
- Ahmad, K., and Henikoff, S. (2002). The histone variant H3.3 marks active chromatin by replication-independent nucleosome assembly. *Mol Cell* 9, 1191-1200.
- Aho, S., Buisson, M., Pajunen, T., Ryoo, Y.W., Giot, J.F., Gruffat, H., Sergeant, A., and Uitto, J. (2000). Ubinuclein, a novel nuclear protein interacting with cellular and viral transcription factors. *J Cell Biol* 148, 1165-1176.
- Allan, J., Hartman, P.G., Crane-Robinson, C., and Aviles, F.X. (1980). The structure of histone H1 and its location in chromatin. *Nature* 288, 675-679.
- Allan, J., Mitchell, T., Harborne, N., Bohm, L., and Crane-Robinson, C. (1986). Roles of H1 domains in determining higher order chromatin structure and H1 location. *J Mol Biol* 187, 591-601.
- Altmann, M., and Hammerschmidt, W. (2005). Epstein-Barr virus provides a new paradigm: a requirement for the immediate inhibition of apoptosis. *PLoS Biol* 3, e404.
- Anderson, J.D., Lowary, P.T., and Widom, J. (2001). Effects of histone acetylation on the equilibrium accessibility of nucleosomal DNA target sites. *J Mol Biol* 307, 977-985.
- Arents, G., and Moudrianakis, E.N. (1995). The histone fold: a ubiquitous architectural motif utilized in DNA compaction and protein dimerization. *Proc Natl Acad Sci USA* 92, 11170-11174.
- Arvey, A., Tempera, I., Tsai, K., Chen, H.S., Tikhmyanova, N., Klichinsky, M., Leslie, C., and Lieberman, P.M. (2012). An atlas of the Epstein-Barr virus transcriptome and epigenome reveals host-virus regulatory interactions. *Cell Host Microbe* 12, 233-245.

- Asai, R., Kato, A., Kato, K., Kanamori-Koyama, M., Sugimoto, K., Sairenji, T., Nishiyama, Y., and Kawaguchi, Y. (2006). Epstein-Barr virus protein kinase BGLF4 is a virion tegument protein that dissociates from virions in a phosphorylation-dependent process and phosphorylates the viral immediate-early protein BZLF1. *J Virol* 80, 5125-5134.
- Asai, R., Kato, A., and Kawaguchi, Y. (2009). Epstein-Barr virus protein kinase BGLF4 interacts with viral transactivator BZLF1 and regulates its transactivation activity. *J Gen Virol* 90, 1575-1581.
- Babcock, G.J., Decker, L.L., Volk, M., and Thorley-Lawson, D.A. (1998). EBV persistence in memory B cells in vivo. *Immunity* 9, 395-404.
- Baer, R., Bankier, A.T., Biggin, M.D., Deininger, P.L., Farrell, P.J., Gibson, T.J., Hatfull, G., Hudson, G.S., Satchwell, S.C., Seguin, C., *et al.* (1984). DNA sequence and expression of the B95-8 Epstein-Barr virus genome. *Nature* 310, 207-211.
- Bai, L., and Morozov, A.V. (2010). Gene regulation by nucleosome positioning. *Trends Genet* 26, 476-483.
- Bannister, A.J., and Kouzarides, T. (2011). Regulation of chromatin by histone modifications. *Cell Res* 21, 381-395.
- Bao, Y., and Shen, X. (2011). SnapShot: Chromatin remodeling: INO80 and SWR1. *Cell* 144, 158-158 e152.
- Barski, A., Cuddapah, S., Cui, K., Roh, T.Y., Schones, D.E., Wang, Z., Wei, G., Chepelev, I., and Zhao, K. (2007). High-resolution profiling of histone methylations in the human genome. *Cell* 129, 823-837.
- Baumann, M., Feederle, R., Kremmer, E., and Hammerschmidt, W. (1999). Cellular transcription factors recruit viral replication proteins to activate the Epstein-Barr virus origin of lytic DNA replication, oriLyt. *EMBO J* 18, 6095-6105.
- Baumann, M., Gires, O., Kolch, W., Mischak, H., Zeidler, R., Pich, D., and Hammerschmidt, W. (2000). The PKC targeting protein RACK1 interacts with the Epstein-Barr virus activator protein BZLF1. *Eur J Biochem* 267, 3891-3901.
- Bergbauer, M., Kalla, M., Schmeinck, A., Gobel, C., Rothbauer, U., Eck, S., Benet-Pages, A., Strom, T.M., and Hammerschmidt, W. (2010). CpG-methylation regulates a class of Epstein-Barr virus promoters. *PLoS Pathog* 6, e1001114.
- Berkes, C.A., Bergstrom, D.A., Penn, B.H., Seaver, K.J., Knoepfler, P.S., and Tapscott, S.J. (2004). Pbx marks genes for activation by MyoD indicating a role for a homeodomain protein in establishing myogenic potential. *Mol Cell* 14, 465-477.
- Bernstein, E., and Hake, S.B. (2006). The nucleosome: a little variation goes a long way. *Biochem Cell Biol* 84, 505-517.
- Bhende, P.M., Seaman, W.T., Delecluse, H.J., and Kenney, S.C. (2004). The EBV lytic switch protein, Z, preferentially binds to and activates the methylated viral genome. *Nat Genet* 36, 1099-1104.
- Billon, P., and Cote, J. (2012). Precise deposition of histone H2A.Z in chromatin for genome expression and maintenance. *Biochim Biophys Acta* 1819, 290-302.
- Binne, U.K., Amon, W., and Farrell, P.J. (2002). Promoter sequences required for reactivation of Epstein-Barr virus from latency. *J Virol* 76, 10282-10289.

- Birney, E., Stamatoyannopoulos, J.A., Dutta, A., Guigo, R., Gingeras, T.R., Margulies, E.H., Weng, Z., Snyder, M., Dermitzakis, E.T., Thurman, R.E., *et al.* (2007). Identification and analysis of functional elements in 1% of the human genome by the ENCODE pilot project. *Nature* *447*, 799-816.
- Blackwood, E.M., and Kadonaga, J.T. (1998). Going the distance: a current view of enhancer action. *Science* *281*, 60-63.
- Blow, M.J., McCulley, D.J., Li, Z., Zhang, T., Akiyama, J.A., Holt, A., Plajzer-Frick, I., Shoukry, M., Wright, C., Chen, F., *et al.* (2010). ChIP-Seq identification of weakly conserved heart enhancers. *Nat Genet* *42*, 806-810.
- Bodescot, M., Perricaudet, M., and Farrell, P.J. (1987). A promoter for the highly spliced EBNA family of RNAs of Epstein-Barr virus. *J Virol* *61*, 3424-3430.
- Bonaldi, T., Imhof, A., and Regula, J.T. (2004). A combination of different mass spectroscopic techniques for the analysis of dynamic changes of histone modifications. *Proteomics* *4*, 1382-1396.
- Bowen, N.J., Fujita, N., Kajita, M., and Wade, P.A. (2004). Mi-2/NuRD: multiple complexes for many purposes. *Biochim Biophys Acta* *1677*, 52-57.
- Bowling, B.L., and Adamson, A.L. (2006). Functional interactions between the Epstein-Barr virus BZLF1 protein and the promyelocytic leukemia protein. *Virus Res* *117*, 244-253.
- Brackertz, M., Boeke, J., Zhang, R., and Renkawitz, R. (2002). Two highly related p66 proteins comprise a new family of potent transcriptional repressors interacting with MBD2 and MBD3. *J Biol Chem* *277*, 40958-40966.
- Brackertz, M., Gong, Z., Leers, J., and Renkawitz, R. (2006). p66alpha and p66beta of the Mi-2/NuRD complex mediate MBD2 and histone interaction. *Nucleic Acids Res* *34*, 397-406.
- Brehm, A., Langst, G., Kehle, J., Clapier, C.R., Imhof, A., Eberharter, A., Muller, J., and Becker, P.B. (2000). dMi-2 and ISWI chromatin remodelling factors have distinct nucleosome binding and mobilization properties. *EMBO J* *19*, 4332-4341.
- Brown, C.E., Lechner, T., Howe, L., and Workman, J.L. (2000). The many HATs of transcription coactivators. *Trends Biochem Sci* *25*, 15-19.
- Brownell, J.E., Zhou, J., Ranalli, T., Kobayashi, R., Edmondson, D.G., Roth, S.Y., and Allis, C.D. (1996). Tetrahymena histone acetyltransferase A: a homolog to yeast Gcn5p linking histone acetylation to gene activation. *Cell* *84*, 843-851.
- Bryant, K.F., Colgrove, R.C., and Knipe, D.M. (2011). Cellular SNF2H chromatin-remodeling factor promotes herpes simplex virus 1 immediate-early gene expression and replication. *MBio* *2*, e00330-00310.
- Bulger, M., and Groudine, M. (1999). Looping versus linking: toward a model for long-distance gene activation. *Genes Dev* *13*, 2465-2477.
- Cairns, B.R. (2005). Chromatin remodeling complexes: strength in diversity, precision through specialization. *Curr Opin Genet Dev* *15*, 185-190.
- Cayrol, C., and Flemington, E. (1996). G0/G1 growth arrest mediated by a region encompassing the basic leucine zipper (bZIP) domain of the Epstein-Barr virus transactivator Zta. *J Biol Chem* *271*, 31799-31802.

- Chang, Y.N., Dong, D.L., Hayward, G.S., and Hayward, S.D. (1990). The Epstein-Barr virus Zta transactivator: a member of the bZIP family with unique DNA-binding specificity and a dimerization domain that lacks the characteristic heptad leucine zipper motif. *J Virol* 64, 3358-3369.
- Chaya, D., Hayamizu, T., Bustin, M., and Zaret, K.S. (2001). Transcription factor FoxA (HNF3) on a nucleosome at an enhancer complex in liver chromatin. *J Biol Chem* 276, 44385-44389.
- Chen, C.J., Deng, Z., Kim, A.Y., Blobel, G.A., and Lieberman, P.M. (2001). Stimulation of CREB binding protein nucleosomal histone acetyltransferase activity by a class of transcriptional activators. *Mol Cell Biol* 21, 476-487.
- Chen, H.S., Martin, K.A., Lu, F., Lupey, L.N., Mueller, J.M., Lieberman, P.M., and Tempera, I. (2014). Epigenetic deregulation of the LMP1/LMP2 locus of Epstein-Barr virus by mutation of a single CTCF-cohesin binding site. *J Virol* 88, 1703-1713.
- Chen, L., Conaway, R.C., and Conaway, J.W. (2013). Multiple modes of regulation of the human Ino80 SNF2 ATPase by subunits of the INO80 chromatin-remodeling complex. *Proc Natl Acad Sci U S A* 110, 20497-20502.
- Chevallier-Greco, A., Manet, E., Chavrier, P., Mosnier, C., Daillie, J., and Sergeant, A. (1986). Both Epstein-Barr virus (EBV)-encoded trans-acting factors, EB1 and EB2, are required to activate transcription from an EBV early promoter. *EMBO J* 5, 3243-3249.
- Chi, T., and Carey, M. (1993). The ZEBRA activation domain: modular organization and mechanism of action. *Mol Cell Biol* 13, 7045-7055.
- Chi, T., and Carey, M. (1996). Assembly of the isomerized TFIIA--TFIID--TATA ternary complex is necessary and sufficient for gene activation. *Genes Dev* 10, 2540-2550.
- Chi, T., Lieberman, P., Ellwood, K., and Carey, M. (1995). A general mechanism for transcriptional synergy by eukaryotic activators. *Nature* 377, 254-257.
- Cirillo, L.A., Lin, F.R., Cuesta, I., Friedman, D., Jarnik, M., and Zaret, K.S. (2002). Opening of compacted chromatin by early developmental transcription factors HNF3 (FoxA) and GATA-4. *Mol Cell* 9, 279-289.
- Cirillo, L.A., McPherson, C.E., Bossard, P., Stevens, K., Cherian, S., Shim, E.Y., Clark, K.L., Burley, S.K., and Zaret, K.S. (1998). Binding of the winged-helix transcription factor HNF3 to a linker histone site on the nucleosome. *EMBO J* 17, 244-254.
- Cirillo, L.A., and Zaret, K.S. (1999). An early developmental transcription factor complex that is more stable on nucleosome core particles than on free DNA. *Mol Cell* 4, 961-969.
- Clapier, C.R., and Cairns, B.R. (2009). The biology of chromatin remodeling complexes. *Annu Rev Biochem* 78, 273-304.
- Consortium, T.E.P. (2012). An integrated encyclopedia of DNA elements in the human genome. *Nature* 489, 57-74.
- Countryman, J., Jenson, H., Seibl, R., Wolf, H., and Miller, G. (1987). Polymorphic proteins encoded within BZLF1 of defective and standard Epstein-Barr viruses disrupt latency. *J Virol* 61, 3672-3679.
- Countryman, J., and Miller, G. (1985). Activation of expression of latent Epstein-Barr herpesvirus after gene transfer with a small cloned subfragment of heterogeneous viral DNA. *Proc Natl Acad Sci U S A* 82, 4085-4089.

- Countryman, J.K., Gradoville, L., and Miller, G. (2008). Histone hyperacetylation occurs on promoters of lytic cycle regulatory genes in Epstein-Barr virus-infected cell lines which are refractory to disruption of latency by histone deacetylase inhibitors. *J Virol* 82, 4706-4719.
- Creyghton, M.P., Cheng, A.W., Welstead, G.G., Kooistra, T., Carey, B.W., Steine, E.J., Hanna, J., Lodato, M.A., Frampton, G.M., Sharp, P.A., *et al.* (2010). Histone H3K27ac separates active from poised enhancers and predicts developmental state. *Proc Natl Acad Sci USA* 107, 21931-21936.
- Davey, C., Pennings, S., Meersseman, G., Wess, T.J., and Allan, J. (1995). Periodicity of strong nucleosome positioning sites around the chicken adult beta-globin gene may encode regularly spaced chromatin. *Proc Natl Acad Sci U S A* 92, 11210-11214.
- Day, L., Chau, C.M., Nebozhyn, M., Rennekamp, A.J., Showe, M., and Lieberman, P.M. (2007). Chromatin profiling of Epstein-Barr virus latency control region. *J Virol* 81, 6389-6401.
- de Laat, W., Klous, P., Kooren, J., Noordermeer, D., Palstra, R.J., Simonis, M., Splinter, E., and Grosveld, F. (2008). Three-dimensional organization of gene expression in erythroid cells. *Curr Top Dev Biol* 82, 117-139.
- Delmas, V., Stokes, D.G., and Perry, R.P. (1993). A mammalian DNA-binding protein that contains a chromodomain and an SNF2/SWI2-like helicase domain. *Proc Natl Acad Sci U S A* 90, 2414-2418.
- Deng, Z., Chen, C.J., Zerby, D., Delecluse, H.J., and Lieberman, P.M. (2001). Identification of acidic and aromatic residues in the Zta activation domain essential for Epstein-Barr virus reactivation. *J Virol* 75, 10334-10347.
- Denslow, S.A., and Wade, P.A. (2007). The human Mi-2/NuRD complex and gene regulation. *Oncogene* 26, 5433-5438.
- Dickerson, S.J., Xing, Y., Robinson, A.R., Seaman, W.T., Gruffat, H., and Kenney, S.C. (2009). Methylation-dependent binding of the Epstein-Barr virus BZLF1 protein to viral promoters. *PLoS Pathog* 5, e1000356.
- Downs, J.A., Allard, S., Jobin-Robitaille, O., Javaheri, A., Auger, A., Bouchard, N., Kron, S.J., Jackson, S.P., and Cote, J. (2004). Binding of chromatin-modifying activities to phosphorylated histone H2A at DNA damage sites. *Mol Cell* 16, 979-990.
- Dreyfus, D.H., Nagasawa, M., Kelleher, C.A., and Gelfand, E.W. (2000). Stable expression of Epstein-Barr virus BZLF-1-encoded ZEBRA protein activates p53-dependent transcription in human Jurkat T-lymphoblastoid cells. *Blood* 96, 625-634.
- Eisen, J.A., Sweder, K.S., and Hanawalt, P.C. (1995). Evolution of the SNF2 family of proteins: subfamilies with distinct sequences and functions. *Nucleic Acids Res* 23, 2715-2723.
- Eissenberg, J.C., and Shilatifard, A. (2010). Histone H3 lysine 4 (H3K4) methylation in development and differentiation. *Dev Biol* 339, 240-249.
- Ellis, A.L., Wang, Z., Yu, X., and Mertz, J.E. (2010). Either ZEB1 or ZEB2/SIP1 can play a central role in regulating the Epstein-Barr virus latent-lytic switch in a cell-type-specific manner. *J Virol* 84, 6139-6152.
- Farrell, P.J., Rowe, D.T., Rooney, C.M., and Kouzarides, T. (1989). Epstein-Barr virus BZLF1 trans-activator specifically binds to a consensus AP-1 site and is related to c-fos. *EMBO J* 8, 127-132.

- Feng, Q., Cao, R., Xia, L., Erdjument-Bromage, H., Tempst, P., and Zhang, Y. (2002). Identification and functional characterization of the p66/p68 components of the MeCP1 complex. *Mol Cell Biol* 22, 536-546.
- Fernandez, A.F., Rosales, C., Lopez-Nieva, P., Grana, O., Ballestar, E., Ropero, S., Espada, J., Melo, S.A., Lujambio, A., Fraga, M.F., *et al.* (2009). The dynamic DNA methylomes of double-stranded DNA viruses associated with human cancer. *Genome Res* 19, 438-451.
- Field, Y., Kaplan, N., Fondufe-Mittendorf, Y., Moore, I.K., Sharon, E., Lubling, Y., Widom, J., and Segal, E. (2008). Distinct modes of regulation by chromatin encoded through nucleosome positioning signals. *PLoS Comput Biol* 4, e1000216.
- Flaus, A., Martin, D.M., Barton, G.J., and Owen-Hughes, T. (2006). Identification of multiple distinct Snf2 subfamilies with conserved structural motifs. *Nucleic Acids Res* 34, 2887-2905.
- Flemington, E., and Speck, S.H. (1990). Evidence for coiled-coil dimer formation by an Epstein-Barr virus transactivator that lacks a heptad repeat of leucine residues. *Proc Natl Acad Sci USA* 87, 9459-9463.
- Fried, M., and Crothers, D.M. (1981). Equilibria and kinetics of lac repressor-operator interactions by polyacrylamide gel electrophoresis. *Nucleic Acids Res* 9, 6505-6525.
- Gao, Z., Krithivas, A., Finan, J.E., Semmes, O.J., Zhou, S., Wang, Y., and Hayward, S.D. (1998). The Epstein-Barr virus lytic transactivator Zta interacts with the helicase-primase replication proteins. *J Virol* 72, 8559-8567.
- Geisberg, J.V., and Struhl, K. (2004). Quantitative sequential chromatin immunoprecipitation, a method for analyzing co-occupancy of proteins at genomic regions in vivo. *Nucleic Acids Res* 32, e151.
- Ghisletti, S., Barozzi, I., Mietton, F., Polletti, S., De Santa, F., Venturini, E., Gregory, L., Lonie, L., Chew, A., Wei, C.L., *et al.* (2010). Identification and characterization of enhancers controlling the inflammatory gene expression program in macrophages. *Immunity* 32, 317-328.
- Graham, F.L., Smiley, J., Russell, W.C., and Nairn, R. (1977). Characteristics of a human cell line transformed by DNA from human adenovirus type 5. *J Gen Virol* 36, 59-74.
- Grigoryev, S.A. (2012). Nucleosome spacing and chromatin higher-order folding. *Nucleus* 3, 493-499.
- Guschin, D., Wade, P.A., Kikyo, N., and Wolffe, A.P. (2000). ATP-Dependent histone octamer mobilization and histone deacetylation mediated by the Mi-2 chromatin remodeling complex. *Biochemistry* 39, 5238-5245.
- Gutsch, D.E., Holley-Guthrie, E.A., Zhang, Q., Stein, B., Blonar, M.A., Baldwin, A.S., and Kenney, S.C. (1994). The bZIP transactivator of Epstein-Barr virus, BZLF1, functionally and physically interacts with the p65 subunit of NF-kappa B. *Mol Cell Biol* 14, 1939-1948.
- Hahn, S. (2004). Structure and mechanism of the RNA polymerase II transcription machinery. *Nat Struct Mol Biol* 11, 394-403.
- Hammerschmidt, W., and Sugden, B. (1988). Identification and characterization of oriLyt, a lytic origin of DNA replication of Epstein-Barr virus. *Cell* 55, 427-433.
- Hanahan, D. (1985). Techniques for transformation of *E. coli*. In Glover, D. (ed.), *DNA Cloning: A Practical Approach*. 1: 109-135.

- Heintzman, N.D., Stuart, R.K., Hon, G., Fu, Y., Ching, C.W., Hawkins, R.D., Barrera, L.O., Van Calcar, S., Qu, C., Ching, K.A., *et al.* (2007). Distinct and predictive chromatin signatures of transcriptional promoters and enhancers in the human genome. *Nat Genet* 39, 311-318.
- Heinz, S., Benner, C., Spann, N., Bertolino, E., Lin, Y.C., Laslo, P., Cheng, J.X., Murre, C., Singh, H., and Glass, C.K. (2010). Simple combinations of lineage-determining transcription factors prime cis-regulatory elements required for macrophage and B cell identities. *Mol Cell* 38, 576-589.
- Heston, L., El-Guindy, A., Countryman, J., Dela Cruz, C., Delecluse, H.J., and Miller, G. (2006). Amino acids in the basic domain of Epstein-Barr virus ZEBRA protein play distinct roles in DNA binding, activation of early lytic gene expression, and promotion of viral DNA replication. *J Virol* 80, 9115-9133.
- Higuchi, R., Fockler, C., Dollinger, G., and Watson, R. (1993). Kinetic PCR analysis: real-time monitoring of DNA amplification reactions. *Biotechnology (N Y)* 11, 1026-1030.
- Holdorf, M.M., Cooper, S.B., Yamamoto, K.R., and Miranda, J.J. (2011). Occupancy of chromatin organizers in the Epstein-Barr virus genome. *Virology* 415, 1-5.
- Holmes, K.A., Hurtado, A., Brown, G.D., Launchbury, R., Ross-Innes, C.S., Hadfield, J., Odom, D.T., and Carroll, J.S. (2011). Transducin-like enhancer protein 1 mediates estrogen receptor binding and transcriptional activity in breast cancer cells. *Proc Natl Acad Sci U S A* 109, 2748-2753.
- Hou, C., Dale, R., and Dean, A. (2010). Cell type specificity of chromatin organization mediated by CTCF and cohesin. *Proc Natl Acad Sci USA* 107, 3651-3656.
- Hudson, G.S., Farrell, P.J., and Barrell, B.G. (1985). Two related but differentially expressed potential membrane proteins encoded by the EcoRI Dhet region of Epstein-Barr virus B95-8. *J Virol* 53, 528-535.
- Ioshikhes, I.P., Albert, I., Zanton, S.J., and Pugh, B.F. (2006). Nucleosome positions predicted through comparative genomics. *Nat Genet* 38, 1210-1215.
- Jenkins, P.J., Binne, U.K., and Farrell, P.J. (2000). Histone acetylation and reactivation of Epstein-Barr virus from latency. *J Virol* 74, 710-720.
- Jiang, C., and Pugh, B.F. (2009). Nucleosome positioning and gene regulation: advances through genomics. *Nat Rev Genet* 10, 161-172.
- Kalla, M., Gobel, C., and Hammerschmidt, W. (2012). The lytic phase of Epstein-Barr virus requires a viral genome with 5-methylcytosine residues in CpG sites. *J Virol* 86, 447-458.
- Kalla, M., and Hammerschmidt, W. (2011). Human B cells on their route to latent infection--early but transient expression of lytic genes of Epstein-Barr virus. *Eur J Cell Biol* 91, 65-69.
- Kalla, M., Schmeink, A., Bergbauer, M., Pich, D., and Hammerschmidt, W. (2010). AP-1 homolog BZLF1 of Epstein-Barr virus has two essential functions dependent on the epigenetic state of the viral genome. *Proc Natl Acad Sci USA* 107, 850-855.
- Kamakaka, R.T., and Biggins, S. (2005). Histone variants: deviants? *Genes Dev* 19, 295-310.
- Karlsson, Q.H., Schelcher, C., Verrall, E., Petosa, C., and Sinclair, A.J. (2008). Methylated DNA recognition during the reversal of epigenetic silencing is regulated by cysteine and serine residues in the Epstein-Barr virus lytic switch protein. *PLoS Pathog* 4, e1000005.



- Kasinsky, H.E., Lewis, J.D., Dacks, J.B., and Ausio, J. (2001). Origin of H1 linker histones. *FASEB J* 15, 34-42.
- Katz, D.A., Baumann, R.P., Sun, R., Kolman, J.L., Taylor, N., and Miller, G. (1992). Viral proteins associated with the Epstein-Barr virus transactivator, ZEBRA. *Proc Natl Acad Sci USA* 89, 378-382.
- Kieff, E., and Rickinson, A. (2007). Epstein-Barr Virus and its replication, Vol Fifth ed. (Philadelphia, Lippincott-Williams Wilkins).
- Kintner, C., and Sugden, B. (1981). Conservation and progressive methylation of Epstein-Barr viral DNA sequences in transformed cells. *J Virol* 38, 305-316.
- Koch, C.M., Andrews, R.M., Flicek, P., Dillon, S.C., Karaoz, U., Clelland, G.K., Wilcox, S., Beare, D.M., Fowler, J.C., Couttet, P., *et al.* (2007). The landscape of histone modifications across 1% of the human genome in five human cell lines. *Genome Res* 17, 691-707.
- Kodandapani, R., Pio, F., Ni, C.Z., Piccialli, G., Klemsz, M., McKercher, S., Maki, R.A., and Ely, K.R. (1996). A new pattern for helix-turn-helix recognition revealed by the PU.1 ETS-domain-DNA complex. *Nature* 380, 456-460.
- Kornberg, R.D. (1974). Chromatin structure: a repeating unit of histones and DNA. *Science* 184, 868-871.
- Kornberg, R.D. (1977). Structure of chromatin. *Annu Rev Biochem* 46, 931-954.
- Kornberg, R.D., and Stryer, L. (1988). Statistical distributions of nucleosomes: nonrandom locations by a stochastic mechanism. *Nucleic Acids Res* 16, 6677-6690.
- Kouzarides, T. (2007). Chromatin modifications and their function. *Cell* 128, 693-705.
- Kouzarides, T., Packham, G., Cook, A., and Farrell, P.J. (1991). The BZLF1 protein of EBV has a coiled coil dimerisation domain without a heptad leucine repeat but with homology to the C/EBP leucine zipper. *Oncogene* 6, 195-204.
- Krietenstein, N., Wippo, C.J., Lieleg, C., and Korber, P. (2012). Genome-wide in vitro reconstitution of yeast chromatin with in vivo-like nucleosome positioning. *Methods Enzymol* 513, 205-232.
- Krogan, N.J., Dover, J., Wood, A., Schneider, J., Heidt, J., Boateng, M.A., Dean, K., Ryan, O.W., Golshani, A., Johnston, M., *et al.* (2003). The Paf1 complex is required for histone H3 methylation by COMPASS and Dot1p: linking transcriptional elongation to histone methylation. *Mol Cell* 11, 721-729.
- Li, Z., Gadue, P., Chen, K., Jiao, Y., Tuteja, G., Schug, J., Li, W., and Kaestner, K.H. (2012). Foxa2 and H2A.Z mediate nucleosome depletion during embryonic stem cell differentiation. *Cell* 151, 1608-1616.
- Liao, G., Wu, F.Y., and Hayward, S.D. (2001). Interaction with the Epstein-Barr virus helicase targets Zta to DNA replication compartments. *J Virol* 75, 8792-8802.
- Lieberman, P.M. (2006). Chromatin regulation of virus infection. *Trends Microbiol* 14, 132-140.
- Lieberman, P.M., and Berk, A.J. (1990). In vitro transcriptional activation, dimerization, and DNA-binding specificity of the Epstein-Barr virus Zta protein. *J Virol* 64, 2560-2568.
- Lieberman, P.M., and Berk, A.J. (1991). The Zta trans-activator protein stabilizes TFIID association with promoter DNA by direct protein-protein interaction. *Genes Dev* 5, 2441-2454.

- Lieberman, P.M., and Berk, A.J. (1994). A mechanism for TAFs in transcriptional activation: activation domain enhancement of TFIID-TFIIA--promoter DNA complex formation. *Genes Dev* 8, 995-1006.
- Lieberman, P.M., Ozer, J., and Gursel, D.B. (1997). Requirement for transcription factor IIA (TFIIA)-TFIID recruitment by an activator depends on promoter structure and template competition. *Mol Cell Biol* 17, 6624-6632.
- Lindner, S.E., and Sugden, B. (2007). The plasmid replicon of Epstein-Barr virus: mechanistic insights into efficient, licensed, extrachromosomal replication in human cells. *Plasmid* 58, 1-12.
- Lowary, P.T., and Widom, J. (1998). New DNA sequence rules for high affinity binding to histone octamer and sequence-directed nucleosome positioning. *J Mol Biol* 276, 19-42.
- Loyola, A., and Almouzni, G. (2004). Histone chaperones, a supporting role in the limelight. *Biochim Biophys Acta* 1677, 3-11.
- Luger, K., Mader, A.W., Richmond, R.K., Sargent, D.F., and Richmond, T.J. (1997). Crystal structure of the nucleosome core particle at 2.8 Å resolution. *Nature* 389, 251-260.
- Luger, K., and Richmond, T.J. (1998). DNA binding within the nucleosome core. *Curr Opin Struct Biol* 8, 33-40.
- Lukas, J., Bohr, V.A., and Halazonetis, T.D. (2006). Cellular responses to DNA damage: current state of the field and review of the 52nd Benzon Symposium. *DNA Repair (Amst)* 5, 591-601.
- Lupien, M., Eeckhoutte, J., Meyer, C.A., Wang, Q., Zhang, Y., Li, W., Carroll, J.S., Liu, X.S., and Brown, M. (2008). FoxA1 translates epigenetic signatures into enhancer-driven lineage-specific transcription. *Cell* 132, 958-970.
- Magnani, L., Eeckhoutte, J., and Lupien, M. (2011). Pioneer factors: directing transcriptional regulators within the chromatin environment. *Trends Genet* 27, 465-474.
- Manavathi, B., and Kumar, R. (2007). Metastasis tumor antigens, an emerging family of multifaceted master coregulators. *J Biol Chem* 282, 1529-1533.
- Manelyte, L., and Langst, G. (2013). Chromatin Remodelers and Their Way of Action, Chromatin Remodelling, Dr. Danuta Radzioch (Ed.), ISBN: 978-953-51-1087-3, InTech, DOI: 10.5772/55683. Available from: <http://www.intechopen.com/books/chromatin-remodelling/chromatin-remodelers-and-their-way-of-action>.
- Mansouri, S., Wang, S., and Frappier, L. (2013). A role for the nucleosome assembly proteins TAF-Ibeta and NAP1 in the activation of BZLF1 expression and Epstein-Barr virus reactivation. *PLoS One* 8, e63802.
- Marhold, J., Brehm, A., and Kramer, K. (2004). The Drosophila methyl-DNA binding protein MBD2/3 interacts with the NuRD complex via p55 and MI-2. *BMC Mol Biol* 5, 20.
- Mausser, A., Saito, S., Appella, E., Anderson, C.W., Seaman, W.T., and Kenney, S. (2002). The Epstein-Barr virus immediate-early protein BZLF1 regulates p53 function through multiple mechanisms. *J Virol* 76, 12503-12512.
- McArthur, M., and Thomas, J.O. (1996). A preference of histone H1 for methylated DNA. *EMBO J* 15, 1705-1714.

- McDonald, C.M., Petosa, C., and Farrell, P.J. (2009). Interaction of Epstein-Barr virus BZLF1 C-terminal tail structure and core zipper is required for DNA replication but not for promoter transactivation. *J Virol* 83, 3397-3401.
- McPherson, C.E., Horowitz, R., Woodcock, C.L., Jiang, C., and Zaret, K.S. (1996). Nucleosome positioning properties of the albumin transcriptional enhancer. *Nucleic Acids Res* 24, 397-404.
- Mikaelian, I., Manet, E., and Sergeant, A. (1993). The bZIP motif of the Epstein-Barr virus (EBV) transcription factor EB1 mediates a direct interaction with TBP. *C R Acad Sci III* 316, 1424-1432.
- Miller, G. (1989). The switch between EBV latency and replication. *Yale J Biol Med* 62, 205-213.
- Miller, G., El-Guindy, A., Countryman, J., Ye, J., and Gradoville, L. (2007). Lytic cycle switches of oncogenic human gammaherpesviruses. *Adv Cancer Res* 97, 81-109.
- Miyashita, E.M., Yang, B., Babcock, G.J., and Thorley-Lawson, D.A. (1997). Identification of the site of Epstein-Barr virus persistence in vivo as a resting B cell. *J Virol* 71, 4882-4891.
- Miyashita, E.M., Yang, B., Lam, K.M., Crawford, D.H., and Thorley-Lawson, D.A. (1995). A novel form of Epstein-Barr virus latency in normal B cells in vivo. *Cell* 80, 593-601.
- Mizuguchi, G., Shen, X., Landry, J., Wu, W.H., Sen, S., and Wu, C. (2004). ATP-driven exchange of histone H2AZ variant catalyzed by SWR1 chromatin remodeling complex. *Science* 303, 343-348.
- Morand, P., Budayova-Spano, M., Perrissin, M., Muller, C.W., and Petosa, C. (2006). Expression, purification, crystallization and preliminary X-ray analysis of a C-terminal fragment of the Epstein-Barr virus ZEBRA protein. *Acta Crystallogr Sect F Struct Biol Cryst Commun* 62, 210-214.
- Morozov, A.V., Fortney, K., Gaykalova, D.A., Studitsky, V.M., Widom, J., and Siggia, E.D. (2009). Using DNA mechanics to predict in vitro nucleosome positions and formation energies. *Nucleic Acids Res* 37, 4707-4722.
- Morrison, A.J., Highland, J., Krogan, N.J., Arbel-Eden, A., Greenblatt, J.F., Haber, J.E., and Shen, X. (2004). INO80 and gamma-H2AX interaction links ATP-dependent chromatin remodeling to DNA damage repair. *Cell* 119, 767-775.
- Mullis, K., Faloona, F., Scharf, S., Saiki, R., Horn, G., and Erlich, H. (1986). Specific enzymatic amplification of DNA in vitro: the polymerase chain reaction. *Cold Spring Harb Symp Quant Biol* 51 Pt 1, 263-273.
- Murata, T., Hotta, N., Toyama, S., Nakayama, S., Chiba, S., Isomura, H., Ohshima, T., Kanda, T., and Tsurumi, T. (2010). Transcriptional repression by sumoylation of Epstein-Barr virus BZLF1 protein correlates with association of histone deacetylase. *J Biol Chem* 285, 23925-23935.
- Murata, T., Kondo, Y., Sugimoto, A., Kawashima, D., Saito, S., Isomura, H., Kanda, T., and Tsurumi, T. (2012). Epigenetic histone modification of Epstein-Barr virus BZLF1 promoter during latency and reactivation in Raji cells. *J Virol* 86, 4752-4761.
- Murata, T., Noda, C., Saito, S., Kawashima, D., Sugimoto, A., Isomura, H., Kanda, T., Yokoyama, K.K., and Tsurumi, T. (2011). Involvement of Jun dimerization protein 2 (JDP2) in the maintenance of Epstein-Barr virus latency. *J Biol Chem* 286, 22007-22016.

- Murata, T., Sato, Y., Nakayama, S., Kudoh, A., Iwahori, S., Isomura, H., Tajima, M., Hishiki, T., Ohshima, T., Hijikata, M., *et al.* (2009). TORC2, a coactivator of cAMP-response element-binding protein, promotes Epstein-Barr virus reactivation from latency through interaction with viral BZLF1 protein. *J Biol Chem* 284, 8033-8041.
- Murata, T., and Tsurumi, T. (2013). Epigenetic modification of the Epstein-Barr virus BZLF1 promoter regulates viral reactivation from latency. *Front Genet* 4, 53.
- Nathan, D., and Crothers, D.M. (2002). Bending and flexibility of methylated and unmethylated EcoRI DNA. *J Mol Biol* 316, 7-17.
- Nikitin, P.A., Yan, C.M., Forte, E., Bocedi, A., Tourigny, J.P., White, R.E., Allday, M.J., Patel, A., Dave, S.S., Kim, W., *et al.* (2010). An ATM/Chk2-mediated DNA damage-responsive signaling pathway suppresses Epstein-Barr virus transformation of primary human B cells. *Cell Host Microbe* 8, 510-522.
- Papamichos-Chronakis, M., and Peterson, C.L. (2008). The Ino80 chromatin-remodeling enzyme regulates replisome function and stability. *Nat Struct Mol Biol* 15, 338-345.
- Papamichos-Chronakis, M., Watanabe, S., Rando, O.J., and Peterson, C.L. (2011). Global regulation of H2A.Z localization by the INO80 chromatin-remodeling enzyme is essential for genome integrity. *Cell* 144, 200-213.
- Park, Y.J., Chodaparambil, J.V., Bao, Y., McBryant, S.J., and Luger, K. (2005). Nucleosome assembly protein 1 exchanges histone H2A-H2B dimers and assists nucleosome sliding. *J Biol Chem* 280, 1817-1825.
- Pennings, S., Allan, J., and Davey, C.S. (2005). DNA methylation, nucleosome formation and positioning. *Brief Funct Genomic Proteomic* 3, 351-361.
- Petosa, C., Morand, P., Baudin, F., Moulin, M., Artero, J.B., and Muller, C.W. (2006). Structural basis of lytic cycle activation by the Epstein-Barr virus ZEBRA protein. *Mol Cell* 21, 565-572.
- Pfitzner, E., Becker, P., Rolke, A., and Schule, R. (1995). Functional antagonism between the retinoic acid receptor and the viral transactivator BZLF1 is mediated by protein-protein interactions. *Proc Natl Acad Sci U S A* 92, 12265-12269.
- Phillips, J.E., and Corces, V.G. (2009). CTCF: master weaver of the genome. *Cell* 137, 1194-1211.
- Polach, K.J., Lowary, P.T., and Widom, J. (2000). Effects of core histone tail domains on the equilibrium constants for dynamic DNA site accessibility in nucleosomes. *J Mol Biol* 298, 211-223.
- Portal, D., Zhou, H., Zhao, B., Kharchenko, P.V., Lowry, E., Wong, L., Quackenbush, J., Holloway, D., Jiang, S., Lu, Y., *et al.* (2013). Epstein-Barr virus nuclear antigen leader protein localizes to promoters and enhancers with cell transcription factors and EBNA2. *Proc Natl Acad Sci U S A* 110, 18537-18542.
- Pulvertaft, J.V. (1964). Cytology of Burkitt's Tumour (African Lymphoma). *Lancet* 1, 238-240.
- Rada-Iglesias, A., Bajpai, R., Swigut, T., Brugmann, S.A., Flynn, R.A., and Wysocka, J. (2010). A unique chromatin signature uncovers early developmental enhancers in humans. *Nature* 470, 279-283.
- Ramakrishnan, V., Finch, J.T., Graziano, V., Lee, P.L., and Sweet, R.M. (1993). Crystal structure of globular domain of histone H5 and its implications for nucleosome binding. *Nature* 362, 219-223.

- Ramasubramanyan, S., Osborn, K., Flower, K., and Sinclair, A.J. (2011). Dynamic chromatin environment of key lytic cycle regulatory regions of the Epstein-Barr virus genome. *J Virol* 86, 1809-1819.
- Rickinson, A., and Kieff, E. (2007). Epstein-Barr virus, Vol Fifth ed. (Philadelphia, Lippincott-Williams Wilkins).
- Robinson, A.R., Kwek, S.S., and Kenney, S.C. (2012). The B-cell specific transcription factor, Oct-2, promotes Epstein-Barr virus latency by inhibiting the viral immediate-early protein, BZLF1. *PLoS Pathog* 8, e1002516.
- Rodriguez, A., Armstrong, M., Dwyer, D., and Flemington, E. (1999). Genetic dissection of cell growth arrest functions mediated by the Epstein-Barr virus lytic gene product, Zta. *J Virol* 73, 9029-9038.
- Rubio, E.D., Reiss, D.J., Welch, P.L., Disteche, C.M., Filippova, G.N., Baliga, N.S., Aebersold, R., Ranish, J.A., and Krumm, A. (2008). CTCF physically links cohesin to chromatin. *Proc Natl Acad Sci U S A* 105, 8309-8314.
- Ryder, S.P., Recht, M.I., and Williamson, J.R. (2008). Quantitative analysis of protein-RNA interactions by gel mobility shift. *Methods Mol Biol* 488, 99-115.
- Sambrook, and Russell (2001). *Molecular Cloning: A Laboratory Manual*, Third Edition edn (CSHL press).
- Sarma, K., and Reinberg, D. (2005). Histone variants meet their match. *Nat Rev Mol Cell Biol* 6, 139-149.
- Sato, Y., Shirata, N., Kudoh, A., Iwahori, S., Nakayama, S., Murata, T., Isomura, H., Nishiyama, Y., and Tsurumi, T. (2009). Expression of Epstein-Barr virus BZLF1 immediate-early protein induces p53 degradation independent of MDM2, leading to repression of p53-mediated transcription. *Virology* 388, 204-211.
- Schelcher, C., Al Mehairi, S., Verrall, E., Hope, Q., Flower, K., Bromley, B., Woolfson, D.N., West, M.J., and Sinclair, A.J. (2007). Atypical bZIP domain of viral transcription factor contributes to stability of dimer formation and transcriptional function. *J Virol* 81, 7149-7155.
- Schepers, A., Pich, D., and Hammerschmidt, W. (1993a). A transcription factor with homology to the AP-1 family links RNA transcription and DNA replication in the lytic cycle of Epstein-Barr virus. *EMBO J* 12, 3921-3929.
- Schepers, A., Pich, D., and Hammerschmidt, W. (1996). Activation of oriLyt, the lytic origin of DNA replication of Epstein-Barr virus, by BZLF1. *Virology* 220, 367-376.
- Schepers, A., Pich, D., Mankertz, J., and Hammerschmidt, W. (1993b). cis-acting elements in the lytic origin of DNA replication of Epstein-Barr virus. *J Virol* 67, 4237-4245.
- Schwarzmann, F., Jager, M., Prang, N., and Wolf, H. (1998). The control of lytic replication of Epstein-Barr virus in B lymphocytes (Review). *Int J Mol Med* 1, 137-142.
- Segal, E., Fondufe-Mittendorf, Y., Chen, L., Thastrom, A., Field, Y., Moore, I.K., Wang, J.P., and Widom, J. (2006). A genomic code for nucleosome positioning. *Nature* 442, 772-778.
- Segal, E., and Widom, J. (2009). What controls nucleosome positions? *Trends Genet* 25, 335-343.

- Sekiya, T., Muthurajan, U.M., Luger, K., Tulin, A.V., and Zaret, K.S. (2009). Nucleosome-binding affinity as a primary determinant of the nuclear mobility of the pioneer transcription factor FoxA. *Genes Dev* 23, 804-809.
- Sekiya, T., and Zaret, K.S. (2007). Repression by Groucho/TLE/Grg proteins: genomic site recruitment generates compacted chromatin in vitro and impairs activator binding in vivo. *Mol Cell* 28, 291-303.
- Serandour, A.A., Avner, S., Percevault, F., Demay, F., Bizot, M., Lucchetti-Miganeh, C., Barloy-Hubler, F., Brown, M., Lupien, M., Metivier, R., *et al.* (2011). Epigenetic switch involved in activation of pioneer factor FOXA1-dependent enhancers. *Genome Res* 21, 555-565.
- Serio, T.R., Angeloni, A., Kolman, J.L., Gradoville, L., Sun, R., Katz, D.A., Van Grunsven, W., Middeldorp, J., and Miller, G. (1996). Two 21-kilodalton components of the Epstein-Barr virus capsid antigen complex and their relationship to ZEBRA-associated protein p21 (ZAP21). *J Virol* 70, 8047-8054.
- Sharrocks, A.D. (2001). The ETS-domain transcription factor family. *Nat Rev Mol Cell Biol* 2, 827-837.
- Shen, X., Mizuguchi, G., Hamiche, A., and Wu, C. (2000). A chromatin remodelling complex involved in transcription and DNA processing. *Nature* 406, 541-544.
- Shen, X., Ranallo, R., Choi, E., and Wu, C. (2003). Involvement of actin-related proteins in ATP-dependent chromatin remodeling. *Mol Cell* 12, 147-155.
- Shogren-Knaak, M., Ishii, H., Sun, J.M., Pazin, M.J., Davie, J.R., and Peterson, C.L. (2006). Histone H4-K16 acetylation controls chromatin structure and protein interactions. *Science* 311, 844-847.
- Sims, J.K., and Wade, P.A. (2011). SnapShot: Chromatin remodeling: CHD. *Cell* 144, 626-626 e621.
- Sinclair, A.J., and Farrell, P.J. (1992). Epstein-Barr virus transcription factors. *Cell Growth Differ* 3, 557-563.
- Sista, N.D., Barry, C., Sampson, K., and Pagano, J. (1995). Physical and functional interaction of the Epstein-Barr virus BZLF1 transactivator with the retinoic acid receptors RAR alpha and RXR alpha. *Nucleic Acids Res* 23, 1729-1736.
- Sista, N.D., Pagano, J.S., Liao, W., and Kenney, S. (1993). Retinoic acid is a negative regulator of the Epstein-Barr virus protein (BZLF1) that mediates disruption of latent infection. *Proc Natl Acad Sci U S A* 90, 3894-3898.
- Smale, S.T. (2010). Pioneer factors in embryonic stem cells and differentiation. *Curr Opin Genet Dev* 20, 519-526.
- Smale, S.T., and Kadonaga, J.T. (2003). The RNA polymerase II core promoter. *Annu Rev Biochem* 72, 449-479.
- Speck, S.H., Chatila, T., and Flemington, E. (1997). Reactivation of Epstein-Barr virus: regulation and function of the BZLF1 gene. *Trends Microbiol* 5, 399-405.
- Stokes, D.G., and Perry, R.P. (1995). DNA-binding and chromatin localization properties of CHD1. *Mol Cell Biol* 15, 2745-2753.
- Strauss, J.K., and Maher, L.J., 3rd (1994). DNA bending by asymmetric phosphate neutralization. *Science* 266, 1829-1834.

- Subirana, J.A. (1990). Analysis of the charge distribution in the C-terminal region of histone H1 as related to its interaction with DNA. *Biopolymers* 29, 1351-1357.
- Takacs, M., Banati, F., Koroknai, A., Segesdi, J., Salamon, D., Wolf, H., Niller, H.H., and Minarovits, J. (2010). Epigenetic regulation of latent Epstein-Barr virus promoters. *Biochim Biophys Acta* 1799, 228-235.
- Takada, K. (1984). Cross-linking of cell surface immunoglobulins induces Epstein-Barr virus in Burkitt lymphoma lines. *Int J Cancer* 33, 27-32.
- Takada, K., Shimizu, N., Sakuma, S., and Ono, Y. (1986). trans activation of the latent Epstein-Barr virus (EBV) genome after transfection of the EBV DNA fragment. *J Virol* 57, 1016-1022.
- Thoma, F., Koller, T., and Klug, A. (1979). Involvement of histone H1 in the organization of the nucleosome and of the salt-dependent superstructures of chromatin. *J Cell Biol* 83, 403-427.
- Thomas, J.O. (1999). Histone H1: location and role. *Curr Opin Cell Biol* 11, 312-317.
- Thorley-Lawson, D.A., Miyashita, E.M., and Khan, G. (1996). Epstein-Barr virus and the B cell: that's all it takes. *Trends Microbiol* 4, 204-208.
- Tong, J.K., Hassig, C.A., Schnitzler, G.R., Kingston, R.E., and Schreiber, S.L. (1998). Chromatin deacetylation by an ATP-dependent nucleosome remodelling complex. *Nature* 395, 917-921.
- Tovey, M.G., Lenoir, G., and Begon-Lours, J. (1978). Activation of latent Epstein-Barr virus by antibody to human IgM. *Nature* 276, 270-272.
- Tsukuda, T., Fleming, A.B., Nickoloff, J.A., and Osley, M.A. (2005). Chromatin remodelling at a DNA double-strand break site in *Saccharomyces cerevisiae*. *Nature* 438, 379-383.
- van Attikum, H., Fritsch, O., and Gasser, S.M. (2007). Distinct roles for SWR1 and INO80 chromatin remodeling complexes at chromosomal double-strand breaks. *EMBO J* 26, 4113-4125.
- van Attikum, H., Fritsch, O., Hohn, B., and Gasser, S.M. (2004). Recruitment of the INO80 complex by H2A phosphorylation links ATP-dependent chromatin remodeling with DNA double-strand break repair. *Cell* 119, 777-788.
- van Attikum, H., and Gasser, S.M. (2005). The histone code at DNA breaks: a guide to repair? *Nat Rev Mol Cell Biol* 6, 757-765.
- Vignali, M., Hassan, A.H., Neely, K.E., and Workman, J.L. (2000). ATP-dependent chromatin-remodeling complexes. *Mol Cell Biol* 20, 1899-1910.
- Wade, P.A., Geronze, A., Jones, P.L., Ballestar, E., Aubry, F., and Wolffe, A.P. (1999). Mi-2 complex couples DNA methylation to chromatin remodelling and histone deacetylation. *Nat Genet* 23, 62-66.
- Wade, P.A., Jones, P.L., Vermaak, D., and Wolffe, A.P. (1998). A multiple subunit Mi-2 histone deacetylase from *Xenopus laevis* cofractionates with an associated Snf2 superfamily ATPase. *Curr Biol* 8, 843-846.
- Walter, P.P., Owen-Hughes, T.A., Cote, J., and Workman, J.L. (1995). Stimulation of transcription factor binding and histone displacement by nucleosome assembly protein 1 and nucleoplasmin requires disruption of the histone octamer. *Mol Cell Biol* 15, 6178-6187.

- Wang, J.P., Fondufe-Mittendorf, Y., Xi, L., Tsai, G.F., Segal, E., and Widom, J. (2008). Preferentially quantized linker DNA lengths in *Saccharomyces cerevisiae*. *PLoS Comput Biol* 4, e1000175.
- Wang, Z., Zang, C., Rosenfeld, J.A., Schones, D.E., Barski, A., Cuddapah, S., Cui, K., Roh, T.Y., Peng, W., Zhang, M.Q., *et al.* (2008). Combinatorial patterns of histone acetylations and methylations in the human genome. *Nat Genet* 40, 897-903.
- Watson, A.A., Mahajan, P., Mertens, H.D., Deery, M.J., Zhang, W., Pham, P., Du, X., Bartke, T., Edlich, C., Berridge, G., *et al.* (2012). The PHD and chromo domains regulate the ATPase activity of the human chromatin remodeler CHD4. *J Mol Biol* 422, 3-17.
- Wendt, K.S., Yoshida, K., Itoh, T., Bando, M., Koch, B., Schirghuber, E., Tsutsumi, S., Nagae, G., Ishihara, K., Mishiro, T., *et al.* (2008). Cohesin mediates transcriptional insulation by CCCTC-binding factor. *Nature* 451, 796-801.
- West, S.C. (1997). Processing of recombination intermediates by the RuvABC proteins. *Annu Rev Genet* 31, 213-244.
- Widlund, H.R., Vitolo, J.M., Thiriet, C., and Hayes, J.J. (2000). DNA sequence-dependent contributions of core histone tails to nucleosome stability: differential effects of acetylation and proteolytic tail removal. *Biochemistry* 39, 3835-3841.
- Widom, J. (1992). A relationship between the helical twist of DNA and the ordered positioning of nucleosomes in all eukaryotic cells. *Proc Natl Acad Sci U S A* 89, 1095-1099.
- Widom, J. (2001). Role of DNA sequence in nucleosome stability and dynamics. *Q Rev Biophys* 34, 269-324.
- Wilson, B.G., and Roberts, C.W. (2011). SWI/SNF nucleosome remodellers and cancer. *Nat Rev Cancer* 11, 481-492.
- Woellmer, A., Arteaga-Salas, J.M., and Hammerschmidt, W. (2012). BZLF1 governs CpG-methylated chromatin of Epstein-Barr Virus reversing epigenetic repression. *PLoS Pathog* 8, e1002902.
- Woellmer, A., and Hammerschmidt, W. (2013). Epstein-Barr virus and host cell methylation: regulation of latency, replication and virus reactivation. *Curr Opin Virol* 3, 260-265.
- Woisetschlaeger, M., Yandava, C.N., Furmanski, L.A., Strominger, J.L., and Speck, S.H. (1990). Promoter switching in Epstein-Barr virus during the initial stages of infection of B lymphocytes. *Proc Natl Acad Sci U S A* 87, 1725-1729.
- Wolffe, A.P., Khochbin, S., and Dimitrov, S. (1997). What do linker histones do in chromatin? *Bioessays* 19, 249-255.
- Woodage, T., Basrai, M.A., Baxevanis, A.D., Hieter, P., and Collins, F.S. (1997). Characterization of the CHD family of proteins. *Proc Natl Acad Sci USA* 94, 11472-11477.
- Wu, F.Y., Chen, H., Wang, S.E., ApRhys, C.M., Liao, G., Fujimuro, M., Farrell, C.J., Huang, J., Hayward, S.D., and Hayward, G.S. (2003). CCAAT/enhancer binding protein alpha interacts with ZTA and mediates ZTA-induced p21(CIP-1) accumulation and G(1) cell cycle arrest during the Epstein-Barr virus lytic cycle. *J Virol* 77, 1481-1500.



- Wu, F.Y., Wang, S.E., Chen, H., Wang, L., Hayward, S.D., and Hayward, G.S. (2004). CCAAT/enhancer binding protein alpha binds to the Epstein-Barr virus (EBV) ZTA protein through oligomeric interactions and contributes to cooperative transcriptional activation of the ZTA promoter through direct binding to the ZII and ZIIIB motifs during induction of the EBV lytic cycle. *J Virol* 78, 4847-4865.
- Wu, S., Shi, Y., Mulligan, P., Gay, F., Landry, J., Liu, H., Lu, J., Qi, H.H., Wang, W., Nickoloff, J.A., *et al.* (2007). A YY1-INO80 complex regulates genomic stability through homologous recombination-based repair. *Nat Struct Mol Biol* 14, 1165-1172.
- Xi, H., Shulha, H.P., Lin, J.M., Vales, T.R., Fu, Y., Bodine, D.M., McKay, R.D., Chenoweth, J.G., Tesar, P.J., Furey, T.S., *et al.* (2007). Identification and characterization of cell type-specific and ubiquitous chromatin regulatory structures in the human genome. *PLoS Genet* 3, e136.
- Xi, L., Fondufe-Mittendorf, Y., Xia, L., Flatow, J., Widom, J., and Wang, J.P. (2010). Predicting nucleosome positioning using a duration Hidden Markov Model. *BMC Bioinformatics* 11, 346.
- Xie, X., Kokubo, T., Cohen, S.L., Mirza, U.A., Hoffmann, A., Chait, B.T., Roeder, R.G., Nakatani, Y., and Burley, S.K. (1996). Structural similarity between TAFs and the heterotetrameric core of the histone octamer. *Nature* 380, 316-322.
- Xu, Y.Z., Kanagaratham, C., and Radzioch, D. (2013). Chromatin Remodelling During Host-Bacterial Pathogen Interaction, Chromatin Remodelling, Dr. Danuta Radzioch (Ed.), ISBN: 978-953-51-1087-3, InTech, DOI: 10.5772/55977. Available from: <http://www.intechopen.com/books/chromatin-remodelling/chromatin-remodelling-during-host-bacterial-pathogen-interaction>.
- Xue, Y., Wong, J., Moreno, G.T., Young, M.K., Cote, J., and Wang, W. (1998). NURD, a novel complex with both ATP-dependent chromatin-remodeling and histone deacetylase activities. *Mol Cell* 2, 851-861.
- Yang, Z., Zheng, C., and Hayes, J.J. (2007). The core histone tail domains contribute to sequence-dependent nucleosome positioning. *J Biol Chem* 282, 7930-7938.
- Yao, J., Lowary, P.T., and Widom, J. (1991). Linker DNA bending induced by the core histones of chromatin. *Biochemistry* 30, 8408-8414.
- Young, L.S., and Rickinson, A.B. (2004). Epstein-Barr virus: 40 years on. *Nat Rev Cancer* 4, 757-768.
- Yu, X., McCarthy, P.J., Lim, H.J., Iempridee, T., Kraus, R.J., Gorlen, D.A., and Mertz, J.E. (2011). The ZIIR element of the Epstein-Barr virus BZLF1 promoter plays a central role in establishment and maintenance of viral latency. *J Virol* 85, 5081-5090.
- Yu, X., Wang, Z., and Mertz, J.E. (2007). ZEB1 regulates the latent-lytic switch in infection by Epstein-Barr virus. *PLoS Pathog* 3, e194.
- Zaret, K.S., and Carroll, J.S. (2011). Pioneer transcription factors: establishing competence for gene expression. *Genes Dev* 25, 2227-2241.
- Zerby, D., Chen, C.J., Poon, E., Lee, D., Shiekhatar, R., and Lieberman, P.M. (1999). The amino-terminal C/H1 domain of CREB binding protein mediates zta transcriptional activation of latent Epstein-Barr virus. *Mol Cell Biol* 19, 1617-1626.
- Zhang, Q., Gutsch, D., and Kenney, S. (1994). Functional and physical interaction between p53 and BZLF1: implications for Epstein-Barr virus latency. *Mol Cell Biol* 14, 1929-1938.

- Zhang, Q., Hong, Y., Dorsky, D., Holley-Guthrie, E., Zalani, S., Elshiekh, N.A., Kiehl, A., Le, T., and Kenney, S. (1996). Functional and physical interactions between the Epstein-Barr virus (EBV) proteins BZLF1 and BMRF1: Effects on EBV transcription and lytic replication. *J Virol* 70, 5131-5142.
- Zhang, Y., Ng, H.H., Erdjument-Bromage, H., Tempst, P., Bird, A., and Reinberg, D. (1999). Analysis of the NuRD subunits reveals a histone deacetylase core complex and a connection with DNA methylation. *Genes Dev* 13, 1924-1935.
- Zhao, J., Jin, H., Cheung, K.F., Tong, J.H., Zhang, S., Go, M.Y., Tian, L., Kang, W., Leung, P.P., Zeng, Z., *et al.* (2011). Zinc finger E-box binding factor 1 plays a central role in regulating Epstein-Barr virus (EBV) latent-lytic switch and acts as a therapeutic target in EBV-associated gastric cancer. *Cancer* 118, 924-936.
- Zhou, X., and O'Shea, E.K. (2011). Integrated approaches reveal determinants of genome-wide binding and function of the transcription factor Pho4. *Mol Cell* 42, 826-836.
- Zippo, A., Serafini, R., Rocchigiani, M., Pennacchini, S., Krepelova, A., and Oliviero, S. (2009). Histone crosstalk between H3S10ph and H4K16ac generates a histone code that mediates transcription elongation. *Cell* 138, 1122-1136.

# 9. APPENDIX

## 9.1 Oligonucleotides

### 9.1.1 RT-PCR primer

**Tab. A1 Primer pairs for reverse transcript PCR (RT-PCR)**

Locus	Forward Primer	Reverse Primer
BZLF1	GGTTTCCGTGTGCGTCGTG	AGCCTGCTCCTGAGAATGCTT
BMRF1	TTGAGGTTTACAGGTCTGGCATC	GGTGGCGGAGGTGAAGGAG
BNLF2a	TGCTGACGTCTGGGTCCT	TGCTTTGCTAGAGCAGCAGT
BRLF1	CCTGTCTTGGACGAGACCAT	AAGGCCTCCTAAGCTCCAAG
BBLF4	GTCCTCCGTGGCTAAAAGCG	CAAGACCAAAAAGTCCATCTG
BcLF1	CCTCCCTGACCGTTCCCAG	GCAGTTTGAGACCGCCACATC
CytC	CAATGCTCCGTTGTTGGCAG	CCTGGTGGGCGTGTGCTAC

### 9.1.2 qPCR primer

**Tab. A2 Primer pairs for quantitative PCR (qPCR) analysis**

Locus	Forward Primer	Reverse Primer
cen	AAGGTCAATGGCAGAAAAGGA	CAACGAAGGCCACAAGATGTC
GAPDH	CCCCGGTTTCTATAAATTGAGC	GGCTGACTGTGCAACAGGA
EBER	CGCTACATCAAAACAGGACAGC	AGCCGAATACCCTTCTCCCAG
Q/F	TGTCACCACCTCCCTGATAATGTC	CATACACCGTGCGAAAAGAAGC
BRLF1	CCGGCTGACATGGATTACTGG	AGGAACCAAAAATAACCGAGCCTC
BZLF1	GGTGCAATGTTTAGTGAGTTACCTGTC	TGACACCAGCTTATTTTAGACACTTCTG
BMRF1	CACACCACCCCCAAGGAC	GCAGCAGCAGAAGCCAACG
BBLF4	GAGGCAGGTGTTTACCCATTTG	CAGGTCACGCACGGTCAGC
BSRF1	CCAAAAATAGTAAGCAGCCGTGA	GAAACAGCCACAGGGGGATG
BcLF1	AATCAAATGGTTGGACACGGC	TCAGGGTGGGCAGAGGACC

### 9.1.3 EMSA DNA template primer

**Tab. A3 Primer pairs for EMSA DNA templates generation by common, mutagenesis and nucleotide shift PCR**

Locus	Forward Primer	Reverse Primer
BRLF1 ZRE 0 Asp718	GGTACCGGTCTCTCATCGCTC	GGTACCAGAGGCCAGGGCCGA
BBLF4 ZRE 3 Asp718	GGTACCAAGTTCGAGGCCTGC	GGTACCGCTGTGTAGCACTCG
BBLF4 ZRE 3+4 Asp718	GGTACCGACTCGTGTGCGAGC	GGTACCGATCCAGTCCACATA
BBLF4 ZRE 4 Asp718	GGTACCGACCGTGCGTGACCT	GGTACCATCTTGGAGTGGAGC
BBLF4 ZRE 0+4 Asp718	P-ATACACGAGTCGGTACCATCT	CAGCCGGTTTCGTGAGTCCAC
BBLF4 ZRE 3+0 Asp718	P-ATTCATAGGAGAGCACGGAGC	CTTATGTGGACTGGATCGGTA
BBLF4 ZRE 3+0 -5 nt Asp718	GGTACCGTGTGCGAGATCAGCCGGTTTC GTGAGTCCACCTTC	GGTACCGATCCAGTCCACATAAAGAT TC
BBLF4 ZRE 3+0 +5 nt Asp718	GGTACCGACTCGTGTAGTGTGCGAGTTC GTGAGTCCACCTTCGAG	GGTACCGATCCAGTCCACATAAAGAT TC
BBLF4 ZRE 3+0 +10 nt Asp718	GGTACCGACTCGTGTATCAGCGTGTGCG AGGAGTCCACCTTCGAGTCGTG	GGTACCGATCCAGTCCACATAAAGAT TC
BBLF4 ZRE 3+0 +15 nt Asp718	GGTACCGACTCGTGTATCAGCCGGTTGT GTGCGAGCACCTTCGAGTCGTGGTCCAC	GGTACCGATCCAGTCCACATAAAGAT TC
BBLF4 ZRE 3+0 +30 nt Asp718	GGTACCGACTCGTGTATCAGCCGGTTTC GTGAGTCCACCTTGTGTGCGAGGTCCAC GACCATGAAGCTGAC	GGTACCGATCCAGTCCACATAAAGAT TC

## 9.2 Sequences of EMSA DNA templates (156 bps long)

### *Control:*

ACCGGTCTCTCATCGCTCTCTTGGTGGACCGCTGCTATCCAAGGCTGTTCAGGTTC  
CGCCGCGTTGGAAGGACATGGAGTTTGACCACGGTTGGGCCTGGATGTCCGGCGC  
GACTTTGGGGCCCGCAGGCGCGGGGCCTCGGCCCTGGCCTCTGGT

### *BBLF4 ZRE 3:*

ACCAAGTTCGAGGCCTGCATCCAGAAGCGATGGCCGAGCGATGACTCgtgtgcgagCC  
GGTTTCGTGAGTCCACCTTCGAGTCGTGGTCCACGACCATGAAGCTGACCGTGCG  
TGACCTGCTGACCACCAACATCTACCGAGTGCTACACAGCGGT

*BBLF4 ZRE 3+4:*

ACCGACTCgtgtgagCGGGTTTCGTGAGTCCACCTTCGAGTCGTGGTCCACGACCAT  
GAAGCTGACCGTGCGTGACCTGCTGACCACCAACATCTACCGAGTGCTACACAGC  
CGCTCCGTGCTCTCCTatgagcgttATGTGGACTGGATCGGT

*BBLF4 ZRE 4:*

ACCGACCGTGCGTGACCTGCTGACCACCAACATCTACCGAGTGCTACACAGCCGC  
TCCGTGCTCTCCTatgagcgttATGTGGACTGGATCTGCGCCACCGGCATGGTGCCCGC  
CGTTAAGAAGCCCATAACCCAAGAGCTCCACTCCAAGATGGT

*BBLF4 ZRE 0+4:*

ACCGACTCgtgtatcagCGGGTTTCGTGAGTCCACCTTCGAGTCGTGGTCCACGACCAT  
GAAGCTGACCGTGCGTGACCTGCTGACCACCAACATCTACCGAGTGCTACACAGC  
CGCTCCGTGCTCTCCTatgagcgttATGTGGACTGGATCGGT

*BBLF4 ZRE 3+0:*

ACCGACTCgtgtgagCGGGTTTCGTGAGTCCACCTTCGAGTCGTGGTCCACGACCAT  
GAAGCTGACCGTGCGTGACCTGCTGACCACCAACATCTACCGAGTGCTACACAGC  
CGCTCCGTGCTCTCCTatgaatcttATGTGGACTGGATCGGT

*BBLF4 ZRE 3+0 -5nt:*

ACCgtgtgagATCAGCCGGTTTCGTGAGTCCACCTTCGAGTCGTGGTCCACGACCA  
TGAAGCTGACCGTGCGTGACCTGCTGACCACCAACATCTACCGAGTGCTACACAG  
CCGCTCCGTGCTCTCCTatgaatcttATGTGGACTGGATCGGT

*BBLF4 ZRE 3+0 +5nt:*

ACCGACTCGTGTAggtgagTTCGTGAGTCCACCTTCGAGTCGTGGTCCACGACCAT  
GAAGCTGACCGTGCGTGACCTGCTGACCACCAACATCTACCGAGTGCTACACAGC  
CGCTCCGTGCTCTCCTatgaatcttATGTGGACTGGATCGGT

*BBLF4 ZRE 3+0 +10nt:*

ACCGACTCGTGTATCAGCgtgtgagGAGTCCACCTTCGAGTCGTGGTCCACGACCA  
TGAAGCTGACCGTGCGTGACCTGCTGACCACCAACATCTACCGAGTGCTACACAG  
CCGCTCCGTGCTCTCCTatgaatcttATGTGGACTGGATCGGT

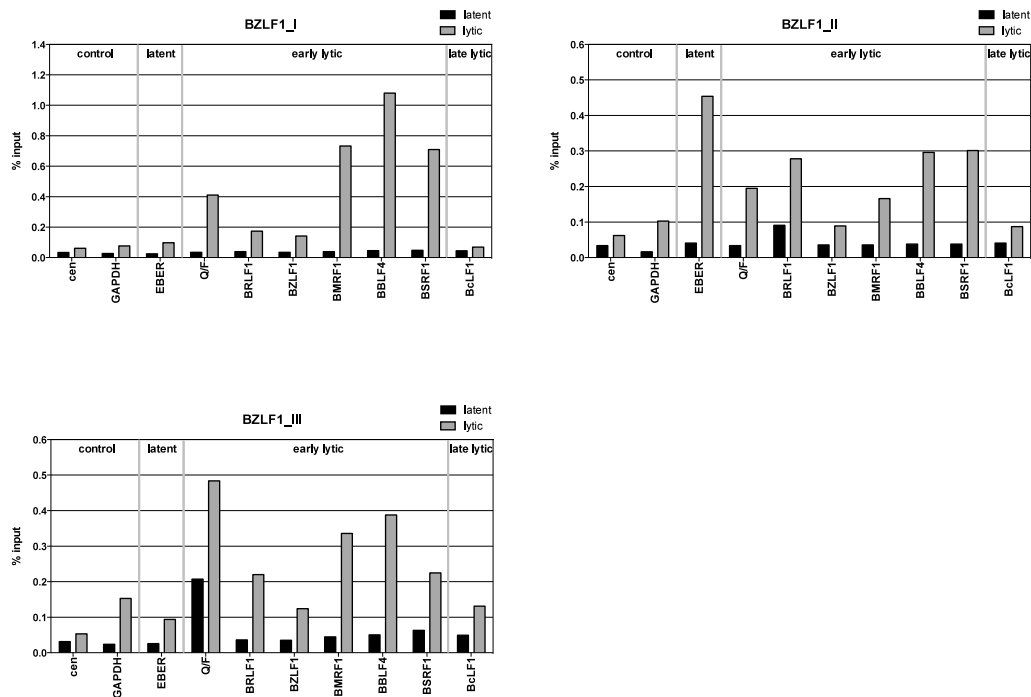
*BBLF4 ZRE 3+0 +15nt:*

ACCGACTCGTGTATCAGCCGGTTgtgtgcgagCACCTTCGAGTCGTGGTCCACGACCA  
 TGAAGCTGACCGTGCGTGACCTGCTGACCACCAACATCTACCGAGTGCTACACAG  
 CCGCTCCGTGCTCTCCTatgaatcttATGTGGACTGGATCGGT

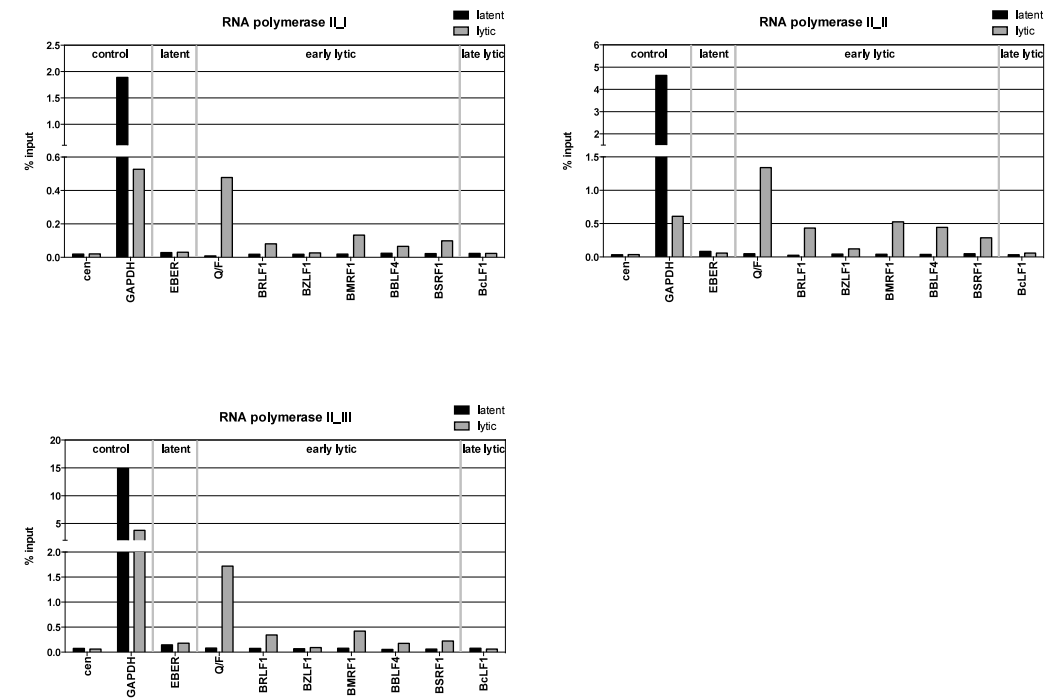
*BBLF4 ZRE 3+0 +30nt:*

ACCGACTCGTGTATCAGCCGGTTTCGTGAGTCCACCTTgtgtgcgagGTCCACGACCAT  
 GAAGCTGACCGTGCGTGACCTGCTGACCACCAACATCTACCGAGTGCTACACAGC  
 CGCTCCGTGCTCTCCTatgaatcttATGTGGACTGGATCGGT

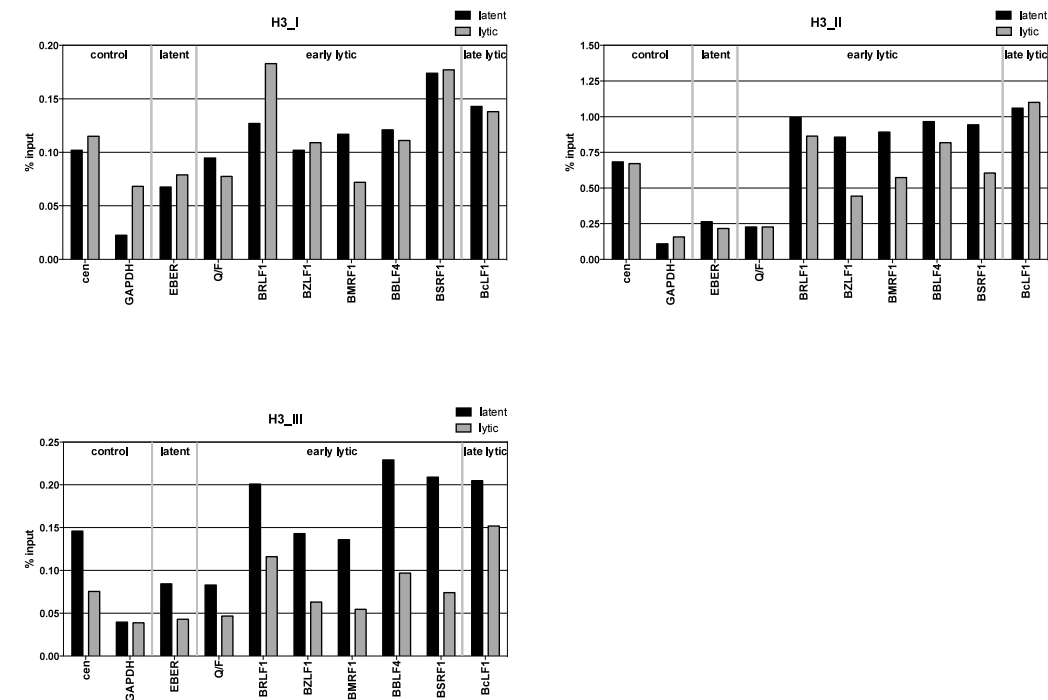
### 9.3 (Re)ChIP qPCR triplicates

*BZLF1 ChIPs:*

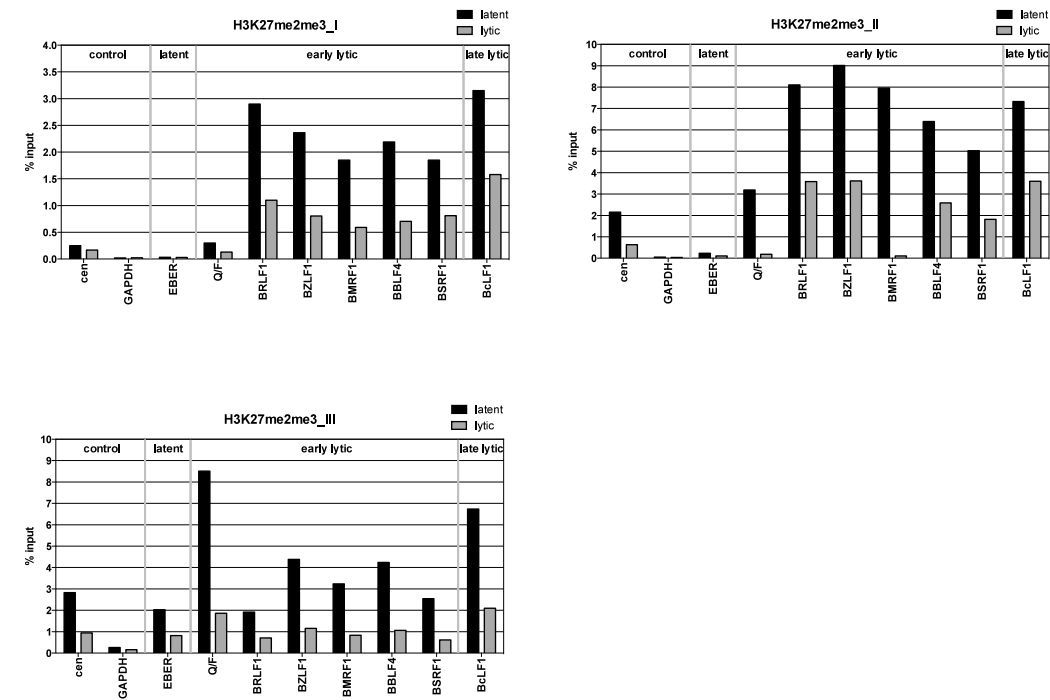
RNA polymerase II ChIPs:



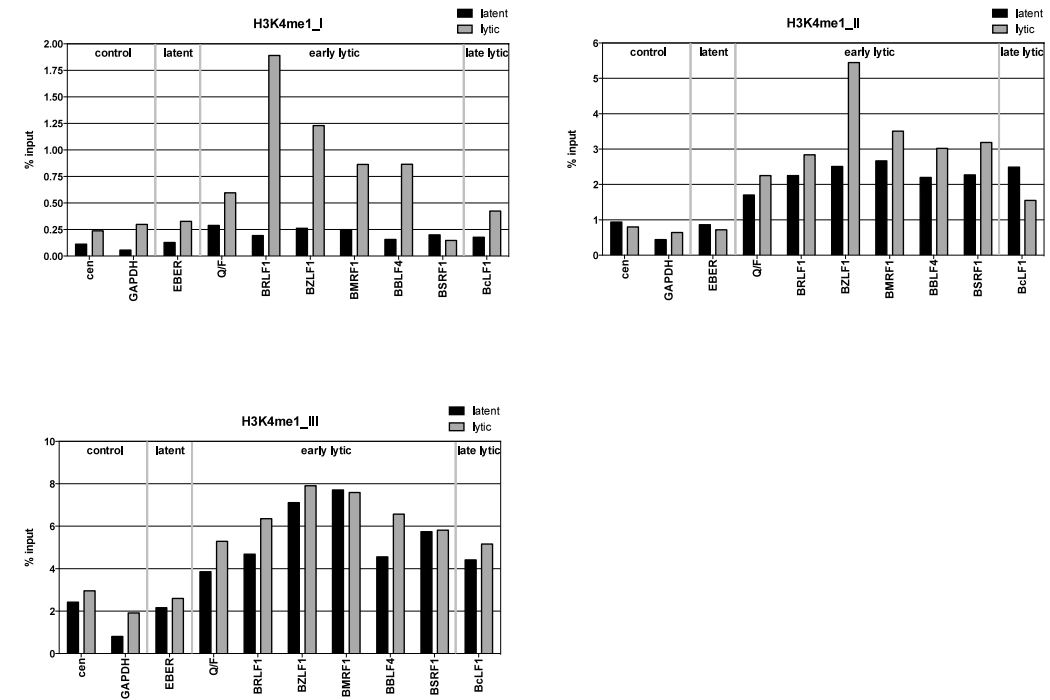
H3 ChIPs:



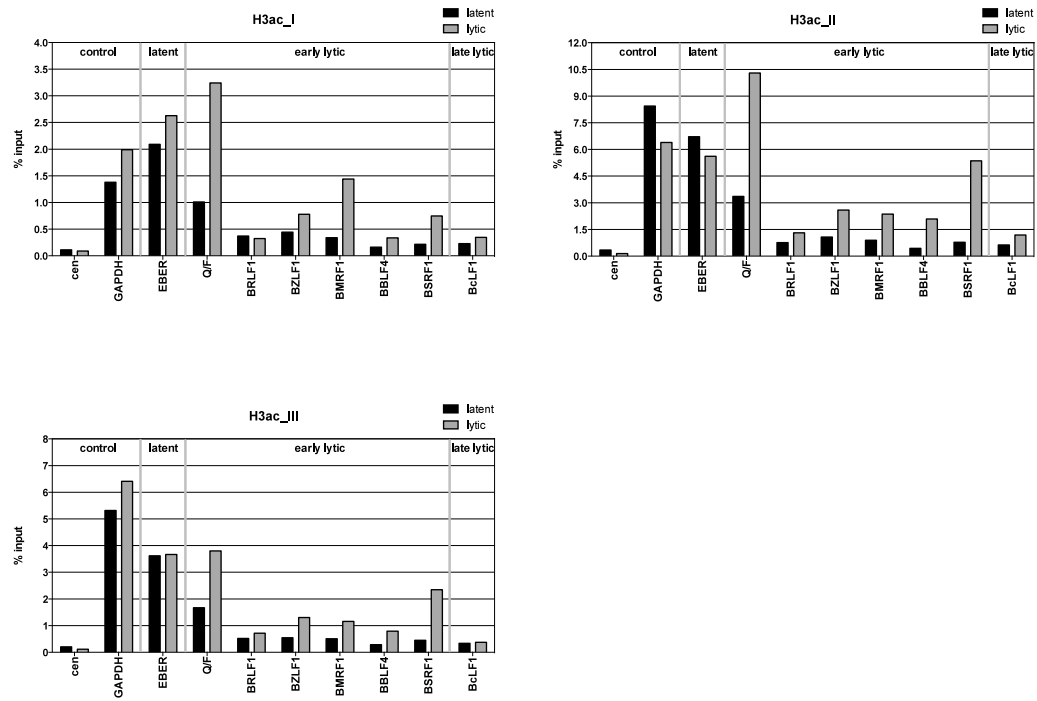
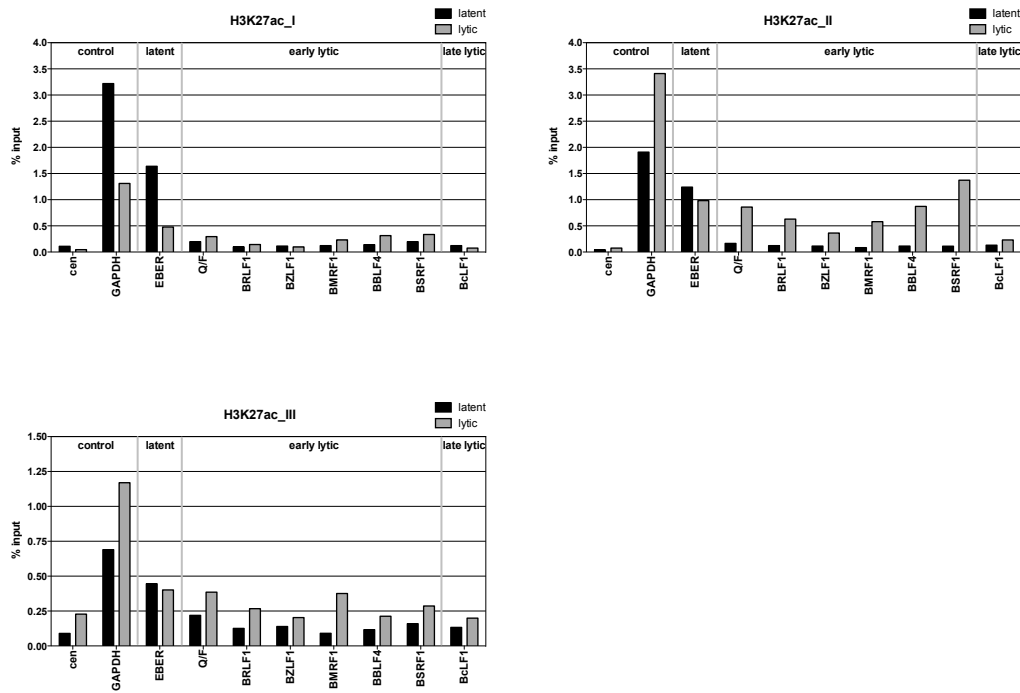
H3K27me2me2 ChIPs:



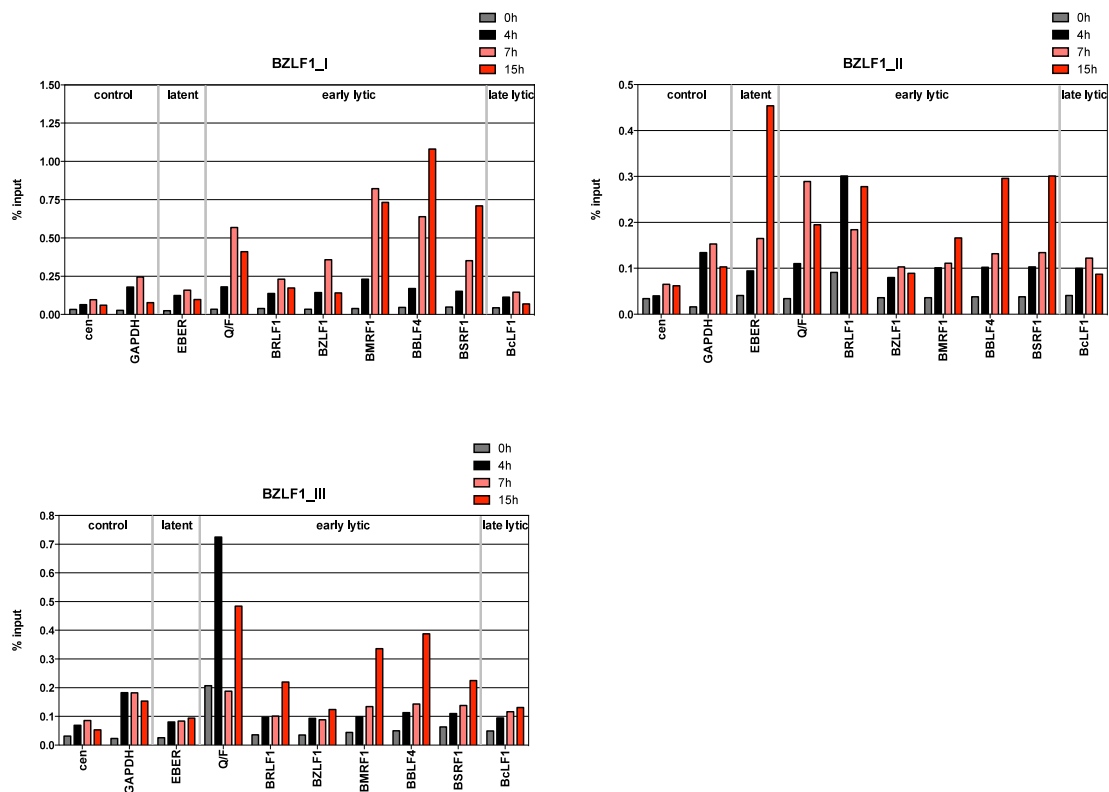
H3K4me1 ChIPs:



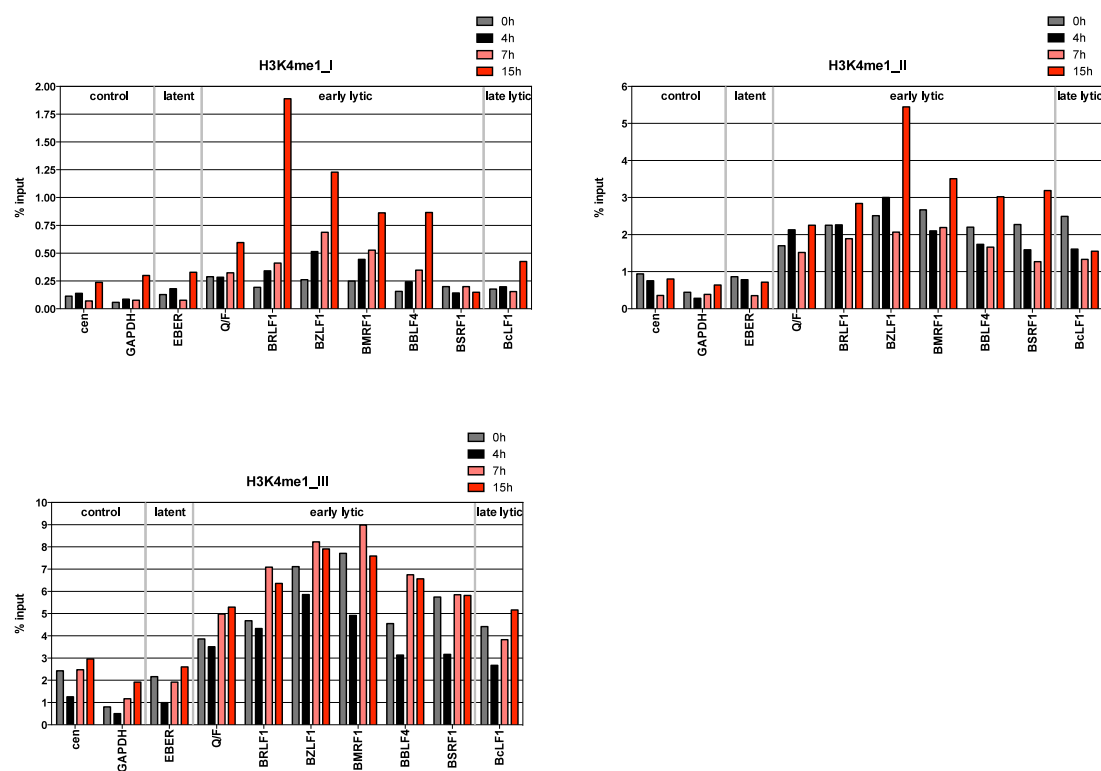


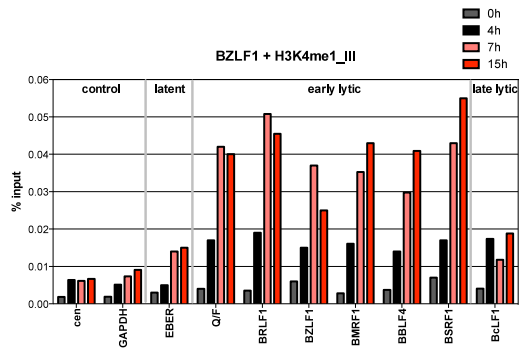
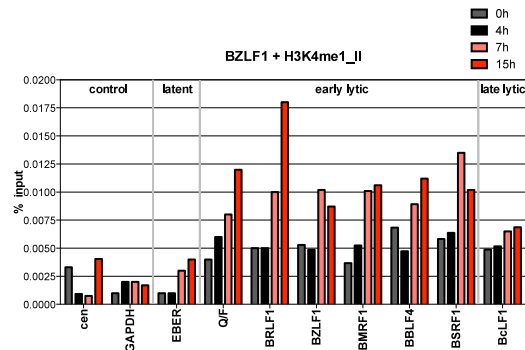
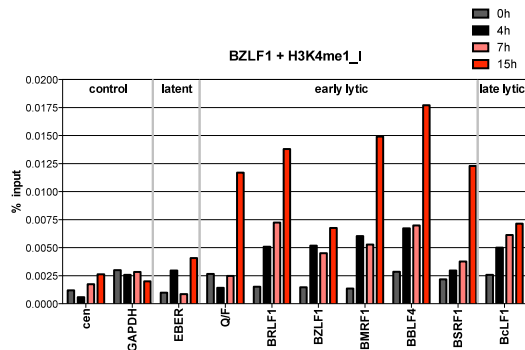
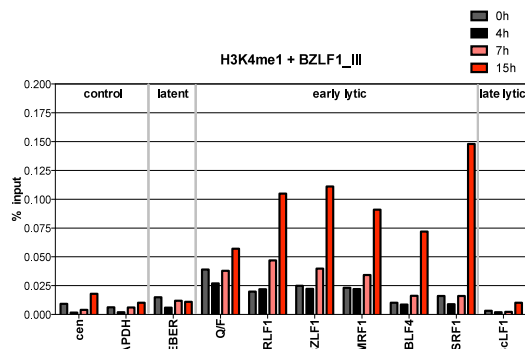
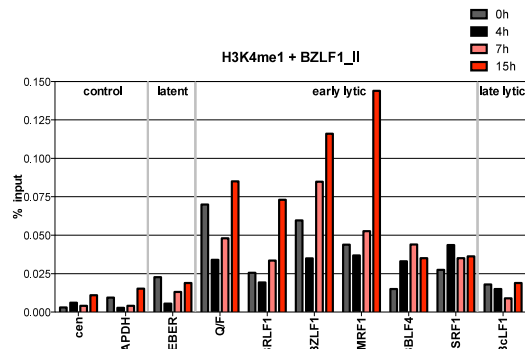
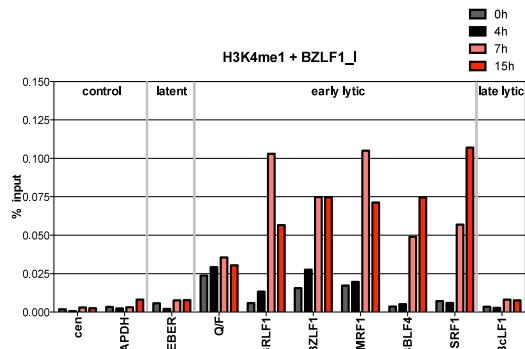
*H3ac ChIPs:**H3K27ac ChIPs:*

*BZLF1* time kinetic ChIPs:



*H3K4me1* time kinetic ChIPs:



*BZLF1+H3K4me1 time kinetic ReChIPs:**H3K4me1+BZLF1 time kinetic ReChIPs:*

## 9.4 Mass spectrometry analysis (data tables)

*Viral interaction partners of BZLF1:*

**Tab. A4 BZLF1\_5693\_minus\_5694**

prot_acc	BZLF1_5693_minus_5694_prot_desc	highest_mean
EAD_EBVG	DNA polymerase processivity factor BMRF1 OS=Epstein-Barr virus (strain GD1) GN=BMRF1 PE=3 SV=1	401,5
DPOL_EBVG	DNA polymerase catalytic subunit OS=Epstein-Barr virus (strain GD1) GN=BALF5 PE=3 SV=1	162,0
KITH_EBVG	Thymidine kinase OS=Epstein-Barr virus (strain GD1) GN=TK PE=1 SV=1	100,0
EB2_EBVA8	mRNA export factor EB2 OS=Epstein-Barr virus (strain AG876) GN=BSLF2 PE=3 SV=1	96,0
HSP70_MIMIV	Heat shock 70 kDa protein homolog OS=Acanthamoeba polyphaga mimivirus GN=HSP70 PE=3 SV=1	78,5
RDRP_PRV	RNA-directed RNA polymerase OS=Pieris rapae virus PE=3 SV=1	66,0
CASPD_HP VKA	Capsid protein OS=High plains virus (isolate Kansas 2004) PE=1 SV=2	52,5
Y094_OSHVF	Uncharacterized protein ORF94 OS=Ostreid herpesvirus 1 (isolate France) GN=ORF94 PE=4 SV=1	51,0
VP6_ROT HC	Intermediate capsid protein VP6 OS=Rotavirus C (isolate Human/United Kingdom/Bristol/1989) PE=2 SV=1	49,0
VF706_ASFB7	Putative ATP-dependent RNA helicase Q706L OS=African swine fever virus (strain Badajoz 1971 Vero-adapted) GN=Ba71V-122 PE=3 SV=1	48,5
PB2_I97A0	Polymerase basic protein 2 (Fragment) OS=Influenza A virus (strain A/Chicken/Hong Kong/220/1997 H5N1 genotype Gs/Gd) GN=PB2 PE=3 SV=1	47,0
POL_CERV	Enzymatic polyprotein OS=Carnation etched ring virus GN=ORF V PE=3 SV=1	44,0
U79_HHV7J	Protein U79 OS=Human herpesvirus 7 (strain JI) GN=U79 PE=3 SV=1	43,0
POLG_YEFV8	Genome polyprotein (Fragment) OS=Yellow fever virus (isolate Peru/1899/1981) PE=3 SV=1	40,5
POLG_YEFVA	Genome polyprotein OS=Yellow fever virus (strain Ghana/Asibi/1927) PE=1 SV=1	38,0
RDRP_ROTGI	RNA-directed RNA polymerase OS=Rotavirus B (isolate Rat/United States/IDIR/1984) PE=3 SV=1	37,0
YORF1_NORAV	Uncharacterized ORF1 protein OS=Nora virus GN=ORF1 PE=4 SV=1	36,5
RPOA_PRRSL	Replicase polyprotein 1ab OS=Porcine reproductive and respiratory syndrome virus (strain Lelystad) GN=rep PE=1 SV=3	36,0
VP4_ROT F1	Outer capsid protein VP4 OS=Rotavirus A (isolate Cat/Japan/FRV-1/1986 G3-P3[9]-Ix-Rx-Cx-Mx-Ax-Nx-Tx-E3-Hx) PE=2 SV=1	34,5
SUNT_BPSPB	Sublancin-168-processing and transport ATP-binding protein sunT OS=Bacillus phage SPbeta GN=sunT PE=3 SV=1	34,0
INTG_SSV1	Probable integrase OS=Sulfolobus virus-like particle SSV1 GN=d335 PE=3 SV=1	33,5
VA51_VACCA	Protein A51 OS=Vaccinia virus (strain Ankara) GN=MVA164R PE=3 SV=1	33,5
Y014_AMEPV	Uncharacterized leucine-rich repeat-containing protein AMV014/Q3 OS=Amsacta moorei entomopoxvirus GN=AMV014 PE=4 SV=2	33,5
LT_POVMA	Large T antigen OS=Murine polyomavirus (strain A2) PE=3 SV=1	29,5
VF358_IIV6	Uncharacterized protein 358L OS=Invertebrate iridescent virus 6 GN=IIV6-358L PE=3 SV=1	28,0
VF113_ASFK5	Putative ATP-dependent RNA helicase D1133L OS=African swine fever virus (isolate Pig/Kenya/KEN-50/1950) GN=Ken-118 PE=3 SV=1	27,0

Tab. A5 BZLF1\_5694\_minus\_5693

prot_acc	BZLF1_5694_minus_5693_prot_desc	highest_mean
U17_HHV6U	Protein U17 OS=Human herpesvirus 6A (strain Uganda-1102) GN=U17/U16 PE=4 SV=1	65,5
POLG_RTSVA	Genome polyprotein OS=Rice tungro spherical virus (strain A) PE=1 SV=1	52,5
POLG_RTSVT	Genome polyprotein OS=Rice tungro spherical virus (strain Vt6) PE=1 SV=1	52,5
NCAP_CVMDV	Nucleoprotein OS=Murine coronavirus (strain DVIM) GN=N PE=3 SV=1	46,0
L_PIRVV	RNA-directed RNA polymerase L OS=Pirital virus (isolate Rat/Venezuela/VAV-488/1995) GN=L PE=3 SV=1	44,5
IBMP_CERV	Transactivator/viroplasm protein OS=Carnation etched ring virus GN=ORF VI PE=3 SV=1	44,0
L_HENDH	RNA-directed RNA polymerase L OS=Hendra virus (isolate Horse/Australia/Hendra/1994) GN=L PE=3 SV=2	44,0
1A_BBMV	Replication protein 1a OS=Broad bean mottle virus GN=ORF1a PE=3 SV=1	43,0
VGLC_GAHVB	Secretory glycoprotein GP57-65 OS=Gallid herpesvirus 2 (strain bc-1) GN=GA PE=3 SV=1	39,5
L_HRSVB	RNA-directed RNA polymerase L OS=Human respiratory syncytial virus B (strain B1) GN=L PE=3 SV=1	38,0
YR508_MIMIV	Putative SWIB domain-containing protein R508 OS=Acanthamoeba polyphaga mimivirus GN=MIMI_R508 PE=4 SV=1	37,5
Z_JUNIN	RING finger protein Z OS=Junin arenavirus GN=Z PE=3 SV=1	37,5
VA51_VACCV	Protein A51 OS=Vaccinia virus (strain Western Reserve) GN=VACWR177 PE=3 SV=1	37,0
VP4B_FOWPV	Major core protein P4b OS=Fowlpox virus GN=FPV167 PE=3 SV=1	36,5
VP2_BT3V	Outer capsid protein VP2 OS=Bluetongue virus 3 (isolate South Africa vaccine) GN=S2 PE=3 SV=1	36,0
PHOSP_CDVO	Phosphoprotein OS=Canine distemper virus (strain Onderstepoort) GN=P/V PE=3 SV=1	35,0
PHOSP_PHODV	Phosphoprotein OS=Phocine distemper virus GN=P/V PE=2 SV=1	35,0
POL1_GCMV	RNA1 polyprotein OS=Grapevine chrome mosaic virus PE=3 SV=1	34,5
TOP2_MIMIV	DNA topoisomerase 2 OS=Acanthamoeba polyphaga mimivirus GN=TOP2 PE=3 SV=1	33,5
VP5_BT1A	Outer capsid protein VP5 OS=Bluetongue virus 1 (isolate Australia) GN=S6 PE=3 SV=1	32,5
DPOL_ADE40	DNA polymerase OS=Human adenovirus F serotype 40 GN=POL PE=3 SV=1	32,0
DEN_EBVG	Deneddylase BPLF1 OS=Epstein-Barr virus (strain GD1) GN=BPLF1 PE=3 SV=1	30,5
R1AB_CVBM	Replicase polyprotein 1ab OS=Bovine coronavirus (strain Mebus) GN=rep PE=3 SV=1	28,0
GAG_FUJSV	Gag polyprotein OS=Fujinami sarcoma virus GN=gag PE=4 SV=1	26,5
POL_RSVP	Gag-Pro-Pol polyprotein OS=Rous sarcoma virus (strain Prague C) GN=gag-pro-pol PE=1 SV=2	26,5
POLG_BSTV1	Genome polyprotein OS=Brome streak virus (strain 11-Cal) PE=3 SV=1	22,5
TEGU_HHV7J	Large tegument protein OS=Human herpesvirus 7 (strain JI) GN=U31 PE=3 SV=1	21,5

**Tab. A6 BZLF1\_5693\_intersect\_5694**

prot_acc	BZLF1_5694_intersect_5693_prot_desc_only	highest_mean
BZLF1_EBVB9	Trans-activator protein BZLF1 OS=Epstein-Barr virus (strain B95-8) GN=BZLF1 PE=1 SV=2	810,5
FGR_FSVGR	Tyrosine-protein kinase transforming protein Fgr OS=Feline sarcoma virus (strain Gardner-Rasheed) GN=V-FGR PE=3 SV=1	259,0
VE6_HP41	Protein E6 OS=Human papillomavirus type 41 GN=E6 PE=3 SV=1	40,5
YL630_MIMIV	Uncharacterized protein L630 OS=Acanthamoeba polyphaga mimivirus GN=MIMI_L630 PE=4 SV=1	40,5
084L_IIV6	Uncharacterized protein 084L OS=Invertebrate iridescent virus 6 GN=IIV6- 084L PE=4 SV=1	36,5
VF030_IIV6	Uncharacterized protein 030L OS=Invertebrate iridescent virus 6 GN=IIV6- 030L PE=3 SV=1	36,0
RPO1_VACCA	DNA-directed RNA polymerase 147 kDa polypeptide OS=Vaccinia virus (strain Ankara) GN=RPO147 PE=4 SV=1	35,0
NSP1_ROTHL	Non-structural protein 1 OS=Rotavirus A (strain Human/Philippines/L26/1987 G12-P1B[4]-I2-R2-C2-M1/M2-A2-N1-T2- E2-H1) PE=3 SV=1	33,5
36011_ASFK5	Protein MGF 360-11L OS=African swine fever virus (isolate Pig/Kenya/KEN-50/1950) GN=Ken-034 PE=3 SV=1	32,0
VP3_ROTHC	Protein VP3 OS=Rotavirus C (isolate Human/United Kingdom/Bristol/1989) PE=2 SV=1	31,5
ICP22_HHV11	Transcriptional regulator ICP22 OS=Human herpesvirus 1 (strain 17) GN=US1 PE=1 SV=1	27,5
VG51_ICHVA	Putative membrane protein ORF51 OS=Ictalurid herpesvirus 1 (strain Auburn) GN=ORF51 PE=4 SV=1	27,5

*Cellular interaction partners of BZLF1:***Tab. A7 BZLF1\_5693\_minus\_5694**

prot_acc	BZLF1_5693_minus_5694_prot_desc	highest_mean
TBA1A_HUMAN	Tubulin alpha-1A chain OS=Homo sapiens GN=TUBA1A PE=1 SV=1	617,0
MCCA_HUMAN	Methylcrotonoyl-CoA carboxylase subunit alpha, mitochondrial OS=Homo sapiens GN=MCCC1 PE=1 SV=3	402,0
HS71L_HUMAN	Heat shock 70 kDa protein 1-like OS=Homo sapiens GN=HSPA1L PE=1 SV=2	397,5
H2B1C_HUMAN	Histone H2B type 1-C/E/F/G/I OS=Homo sapiens GN=HIST1H2BC PE=1 SV=4	364,0
TBA8_HUMAN	Tubulin alpha-8 chain OS=Homo sapiens GN=TUBA8 PE=1 SV=1	312,5
HNRH2_HUMAN	Heterogeneous nuclear ribonucleoprotein H2 OS=Homo sapiens GN=HNRNPH2 PE=1 SV=1	231,0
ILF2_HUMAN	Interleukin enhancer-binding factor 2 OS=Homo sapiens GN=ILF2 PE=1 SV=2	224,5
MCCB_HUMAN	Methylcrotonoyl-CoA carboxylase beta chain, mitochondrial OS=Homo sapiens GN=MCCC2 PE=1 SV=1	223,5
K1C9_HUMAN	Keratin, type I cytoskeletal 9 OS=Homo sapiens GN=KRT9 PE=1 SV=3	213,5
HNRPF_HUMAN	Heterogeneous nuclear ribonucleoprotein F OS=Homo sapiens GN=HNRNPF PE=1 SV=3	202,0
CH60_HUMAN	60 kDa heat shock protein, mitochondrial OS=Homo sapiens GN=HSPD1 PE=1 SV=2	161,5
H2A1D_HUMAN	Histone H2A type 1-D OS=Homo sapiens GN=HIST1H2AD PE=1 SV=2	160,5
TERA_HUMAN	Transitional endoplasmic reticulum ATPase OS=Homo sapiens GN=VCP PE=1 SV=4	158,0

GRPE1_HUMAN	GrpE protein homolog 1, mitochondrial OS=Homo sapiens GN=GRPEL1 PE=1 SV=2	151,5
RNPS1_HUMAN	RNA-binding protein with serine-rich domain 1 OS=Homo sapiens GN=RNPS1 PE=1 SV=1	136,0
GRP75_HUMAN	Stress-70 protein, mitochondrial OS=Homo sapiens GN=HSPA9 PE=1 SV=2	128,5
LRC59_HUMAN	Leucine-rich repeat-containing protein 59 OS=Homo sapiens GN=LRR59 PE=1 SV=1	115,0
RBM33_HUMAN	RNA-binding protein 33 OS=Homo sapiens GN=RBM33 PE=1 SV=3	109,0
RLA0L_HUMAN	60S acidic ribosomal protein P0-like OS=Homo sapiens GN=RPLP0P6 PE=5 SV=1	102,5
CALX_HUMAN	Calnexin OS=Homo sapiens GN=CANX PE=1 SV=2	101,5
TCOF_HUMAN	Treacle protein OS=Homo sapiens GN=TCOF1 PE=1 SV=3	99,5
PCBP1_HUMAN	Poly(rC)-binding protein 1 OS=Homo sapiens GN=PCBP1 PE=1 SV=2	96,5
RBBP4_HUMAN	Histone-binding protein RBBP4 OS=Homo sapiens GN=RBBP4 PE=1 SV=3	95,5
RBM39_HUMAN	RNA-binding protein 39 OS=Homo sapiens GN=RBM39 PE=1 SV=2	93,0
BCLF1_HUMAN	Bcl-2-associated transcription factor 1 OS=Homo sapiens GN=BCLAF1 PE=1 SV=2	75,5
TFAM_HUMAN	Transcription factor A, mitochondrial OS=Homo sapiens GN=TFAM PE=1 SV=1	75,0
RSMB_HUMAN	Small nuclear ribonucleoprotein-associated proteins B and B~ OS=Homo sapiens GN=SNRBP PE=1 SV=2	73,5
ERH_HUMAN	Enhancer of rudimentary homolog OS=Homo sapiens GN=ERH PE=1 SV=1	72,5
K2C8_HUMAN	Keratin, type II cytoskeletal 8 OS=Homo sapiens GN=KRT8 PE=1 SV=7	71,0
ELAV1_HUMAN	ELAV-like protein 1 OS=Homo sapiens GN=ELAVL1 PE=1 SV=2	70,0
PIMT_HUMAN	Protein-L-isoaspartate(D-aspartate) O-methyltransferase OS=Homo sapiens GN=PCMT1 PE=1 SV=4	68,0
XPO2_HUMAN	Exportin-2 OS=Homo sapiens GN=CSE1L PE=1 SV=3	68,0
LRC53_HUMAN	Leucine-rich repeat-containing protein 53 OS=Homo sapiens GN=LRR53 PE=4 SV=2	64,5
PTPRK_HUMAN	Receptor-type tyrosine-protein phosphatase kappa OS=Homo sapiens GN=PTPRK PE=1 SV=2	62,0
F1892_HUMAN	Protein FAM189A2 OS=Homo sapiens GN=FAM189A2 PE=2 SV=3	57,5
NEK10_HUMAN	Serine/threonine-protein kinase Nek10 OS=Homo sapiens GN=NEK10 PE=2 SV=2	57,5
CBLN4_HUMAN	Cerebellin-4 OS=Homo sapiens GN=CBLN4 PE=1 SV=1	55,5
CHD4_HUMAN	Chromodomain-helicase-DNA-binding protein 4 OS=Homo sapiens GN=CHD4 PE=1 SV=2	55,5
SRRM2_HUMAN	Serine/arginine repetitive matrix protein 2 OS=Homo sapiens GN=SRRM2 PE=1 SV=2	53,5
BZW2_HUMAN	Basic leucine zipper and W2 domain-containing protein 2 OS=Homo sapiens GN=BZW2 PE=1 SV=1	53,0
TMEDA_HUMAN	Transmembrane emp24 domain-containing protein 10 OS=Homo sapiens GN=TMED10 PE=1 SV=2	52,0
CALCA_HUMAN	Calcitonin gene-related peptide 1 OS=Homo sapiens GN=CALCA PE=1 SV=3	49,5
CU129_HUMAN	Uncharacterized protein C21orf129 OS=Homo sapiens GN=C21orf129 PE=2 SV=2	49,5
MINA_HUMAN	MYC-induced nuclear antigen OS=Homo sapiens GN=MINA PE=1 SV=1	49,5
RUXF_HUMAN	Small nuclear ribonucleoprotein F OS=Homo sapiens GN=SNRPF PE=1 SV=1	49,5
ZBED1_HUMAN	Zinc finger BED domain-containing protein 1 OS=Homo sapiens GN=ZBED1 PE=1 SV=1	46,5
SNUT1_HUMAN	U4/U6.U5 tri-snRNP-associated protein 1 OS=Homo sapiens GN=SART1 PE=1 SV=1	45,0
COQ6_HUMAN	Ubiquinone biosynthesis monooxygenase COQ6 OS=Homo sapiens GN=COQ6 PE=1 SV=2	44,5

PRDX1_HUMAN	Peroxisredoxin-1 OS=Homo sapiens GN=PRDX1 PE=1 SV=1	44,0
RAB7A_HUMAN	Ras-related protein Rab-7a OS=Homo sapiens GN=RAB7A PE=1 SV=1	44,0
FEN1_HUMAN	Flap endonuclease 1 OS=Homo sapiens GN=FEN1 PE=1 SV=1	41,5
DKC1_HUMAN	H/ACA ribonucleoprotein complex subunit 4 OS=Homo sapiens GN=DKC1 PE=1 SV=3	40,5
DYH11_HUMAN	Dynein heavy chain 11, axonemal OS=Homo sapiens GN=DNAH11 PE=1 SV=3	40,5
KDSR_HUMAN	3-ketodihydrosphingosine reductase OS=Homo sapiens GN=KDSR PE=1 SV=1	40,5
RHES_HUMAN	GTP-binding protein Rhes OS=Homo sapiens GN=RASD2 PE=1 SV=1	39,5
YB052_HUMAN	Putative uncharacterized protein LOC100130201 OS=Homo sapiens PE=5 SV=1	39,5
EST3_HUMAN	Carboxylesterase 3 OS=Homo sapiens GN=CES3 PE=1 SV=1	39,0
MOS_HUMAN	Proto-oncogene serine/threonine-protein kinase mos OS=Homo sapiens GN=MOS PE=1 SV=1	38,5
GPR62_HUMAN	Probable G-protein coupled receptor 62 OS=Homo sapiens GN=GPR62 PE=2 SV=2	37,0
SYNE1_HUMAN	Nesprin-1 OS=Homo sapiens GN=SYNE1 PE=1 SV=3	37,0
CN102_HUMAN	UPF0614 protein C14orf102 OS=Homo sapiens GN=C14orf102 PE=1 SV=3	36,5
SAFB1_HUMAN	Scaffold attachment factor B1 OS=Homo sapiens GN=SAFB PE=1 SV=4	36,0
TTC5_HUMAN	Tetratricopeptide repeat protein 5 OS=Homo sapiens GN=TTC5 PE=1 SV=2	35,5
CV031_HUMAN	Uncharacterized protein C22orf31 OS=Homo sapiens GN=C22orf31 PE=2 SV=1	35,0
RBM3_HUMAN	Putative RNA-binding protein 3 OS=Homo sapiens GN=RBM3 PE=1 SV=1	30,0

**Tab. A8 BZLF1\_5694 minus 5693**

prot_acc	BZLF1_5694_minus_5693_prot_desc	highest_mean
TBA1B_HUMAN	Tubulin alpha-1B chain OS=Homo sapiens GN=TUBA1B PE=1 SV=1	721,0
NP1L1_HUMAN	Nucleosome assembly protein 1-like 1 OS=Homo sapiens GN=NAP1L1 PE=1 SV=1	502,0
RL12_HUMAN	60S ribosomal protein L12 OS=Homo sapiens GN=RPL12 PE=1 SV=1	380,5
RLA0_HUMAN	60S acidic ribosomal protein P0 OS=Homo sapiens GN=RPLP0 PE=1 SV=1	357,5
RL22_HUMAN	60S ribosomal protein L22 OS=Homo sapiens GN=RPL22 PE=1 SV=2	345,5
RLA2_HUMAN	60S acidic ribosomal protein P2 OS=Homo sapiens GN=RPLP2 PE=1 SV=1	323,0
TBB2C_HUMAN	Tubulin beta-2C chain OS=Homo sapiens GN=TUBB2C PE=1 SV=1	288,0
RS9_HUMAN	40S ribosomal protein S9 OS=Homo sapiens GN=RPS9 PE=1 SV=3	280,5
PTBP1_HUMAN	Polypyrimidine tract-binding protein 1 OS=Homo sapiens GN=PTBP1 PE=1 SV=1	262,5
G3BP1_HUMAN	Ras GTPase-activating protein-binding protein 1 OS=Homo sapiens GN=G3BP1 PE=1 SV=1	201,0
RL36_HUMAN	60S ribosomal protein L36 OS=Homo sapiens GN=RPL36 PE=1 SV=3	200,5
RL26L_HUMAN	60S ribosomal protein L26-like 1 OS=Homo sapiens GN=RPL26L1 PE=1 SV=1	200,0
RL31_HUMAN	60S ribosomal protein L31 OS=Homo sapiens GN=RPL31 PE=1 SV=1	176,0
EZRI_HUMAN	Ezrin OS=Homo sapiens GN=EZR PE=1 SV=4	172,5
H12_HUMAN	Histone H1.2 OS=Homo sapiens GN=HIST1H1C PE=1 SV=2	167,5
NOG1_HUMAN	Nucleolar GTP-binding protein 1 OS=Homo sapiens GN=GTPBP4 PE=1 SV=3	166,0
SND1_HUMAN	Staphylococcal nuclease domain-containing protein 1 OS=Homo sapiens GN=SND1 PE=1 SV=1	163,0
PP1A_HUMAN	Serine/threonine-protein phosphatase PP1-alpha catalytic subunit OS=Homo sapiens GN=PPP1CA PE=1 SV=1	161,5



IF2B3_HUMAN	Insulin-like growth factor 2 mRNA-binding protein 3 OS=Homo sapiens GN=IGF2BP3 PE=1 SV=2	161,0
PABP4_HUMAN	Polyadenylate-binding protein 4 OS=Homo sapiens GN=PABPC4 PE=1 SV=1	159,0
RCC2_HUMAN	Protein RCC2 OS=Homo sapiens GN=RCC2 PE=1 SV=2	158,5
RRP1B_HUMAN	Ribosomal RNA processing protein 1 homolog B OS=Homo sapiens GN=RRP1B PE=1 SV=3	157,5
RRMJ3_HUMAN	Putative rRNA methyltransferase 3 OS=Homo sapiens GN=FTSJ3 PE=1 SV=2	155,5
ACTBM_HUMAN	Putative beta-actin-like protein 3 OS=Homo sapiens GN=POTEKP PE=5 SV=1	154,5
DHX15_HUMAN	Putative pre-mRNA-splicing factor ATP-dependent RNA helicase DHX15 OS=Homo sapiens GN=DHX15 PE=1 SV=2	152,0
RS26L_HUMAN	Putative 40S ribosomal protein S26-like 1 OS=Homo sapiens GN=RPS26P11 PE=5 SV=1	151,5
RS13_HUMAN	40S ribosomal protein S13 OS=Homo sapiens GN=RPS13 PE=1 SV=2	151,0
WIBG_HUMAN	Partner of Y14 and mago OS=Homo sapiens GN=WIBG PE=1 SV=1	145,0
MOES_HUMAN	Moesin OS=Homo sapiens GN=MSN PE=1 SV=3	141,5
RADI_HUMAN	Radixin OS=Homo sapiens GN=RDX PE=1 SV=1	141,5
NPM3_HUMAN	Nucleoplasmin-3 OS=Homo sapiens GN=NPM3 PE=1 SV=3	140,5
POTEE_HUMAN	POTE ankyrin domain family member E OS=Homo sapiens GN=POTEE PE=1 SV=3	140,0
TCPA_HUMAN	T-complex protein 1 subunit alpha OS=Homo sapiens GN=TCP1 PE=1 SV=1	126,5
PPIB_HUMAN	Peptidyl-prolyl cis-trans isomerase B OS=Homo sapiens GN=PPIB PE=1 SV=2	124,5
ACACB_HUMAN	Acetyl-CoA carboxylase 2 OS=Homo sapiens GN=ACACB PE=1 SV=3	123,5
GNL3_HUMAN	Guanine nucleotide-binding protein-like 3 OS=Homo sapiens GN=GNL3 PE=1 SV=2	123,5
RS12_HUMAN	40S ribosomal protein S12 OS=Homo sapiens GN=RPS12 PE=1 SV=3	123,5
YBOX1_HUMAN	Nuclease-sensitive element-binding protein 1 OS=Homo sapiens GN=YBX1 PE=1 SV=3	120,0
NOP56_HUMAN	Nucleolar protein 56 OS=Homo sapiens GN=NOP56 PE=1 SV=4	118,0
RL35A_HUMAN	60S ribosomal protein L35a OS=Homo sapiens GN=RPL35A PE=1 SV=2	113,5
IMA2_HUMAN	Importin subunit alpha-2 OS=Homo sapiens GN=KPNA2 PE=1 SV=1	110,0
HG2A_HUMAN	HLA class II histocompatibility antigen gamma chain OS=Homo sapiens GN=CD74 PE=1 SV=3	109,0
CPSF2_HUMAN	Cleavage and polyadenylation specificity factor subunit 2 OS=Homo sapiens GN=CPSF2 PE=1 SV=2	105,5
RLA1_HUMAN	60S acidic ribosomal protein P1 OS=Homo sapiens GN=RPLP1 PE=1 SV=1	105,5
G3BP2_HUMAN	Ras GTPase-activating protein-binding protein 2 OS=Homo sapiens GN=G3BP2 PE=1 SV=2	104,0
ERF1_HUMAN	Eukaryotic peptide chain release factor subunit 1 OS=Homo sapiens GN=ETF1 PE=1 SV=3	103,5
RL3L_HUMAN	60S ribosomal protein L3-like OS=Homo sapiens GN=RPL3L PE=1 SV=3	103,5
DDX3X_HUMAN	ATP-dependent RNA helicase DDX3X OS=Homo sapiens GN=DDX3X PE=1 SV=3	102,5
IF2B2_HUMAN	Insulin-like growth factor 2 mRNA-binding protein 2 OS=Homo sapiens GN=IGF2BP2 PE=1 SV=2	98,5
PA2G4_HUMAN	Proliferation-associated protein 2G4 OS=Homo sapiens GN=PA2G4 PE=1 SV=3	98,5
TOP2B_HUMAN	DNA topoisomerase 2-beta OS=Homo sapiens GN=TOP2B PE=1 SV=3	98,5
PHF8_HUMAN	Histone lysine demethylase PHF8 OS=Homo sapiens GN=PHF8 PE=1 SV=3	97,5
DRA_HUMAN	HLA class II histocompatibility antigen, DR alpha chain OS=Homo sapiens GN=HLA-DRA PE=1 SV=1	94,5
SF3A3_HUMAN	Splicing factor 3A subunit 3 OS=Homo sapiens GN=SF3A3 PE=1 SV=1	94,0

MSH6_HUMAN	DNA mismatch repair protein Msh6 OS=Homo sapiens GN=MSH6 PE=1 SV=2	91,5
BRX1_HUMAN	Ribosome biogenesis protein BRX1 homolog OS=Homo sapiens GN=BRX1 PE=1 SV=2	89,0
PTBP2_HUMAN	Polypyrimidine tract-binding protein 2 OS=Homo sapiens GN=PTBP2 PE=1 SV=1	88,5
EF2_HUMAN	Elongation factor 2 OS=Homo sapiens GN=EEF2 PE=1 SV=4	87,0
RS27_HUMAN	40S ribosomal protein S27 OS=Homo sapiens GN=RPS27 PE=1 SV=3	86,5
BA2L2_HUMAN	Protein BAT2-like 2 OS=Homo sapiens GN=BAT2L2 PE=1 SV=3	85,5
RL28_HUMAN	60S ribosomal protein L28 OS=Homo sapiens GN=RPL28 PE=1 SV=3	83,0
H3C_HUMAN	Histone H3.3C OS=Homo sapiens GN=H3F3C PE=1 SV=3	81,5
RS27A_HUMAN	Ubiquitin-40S ribosomal protein S27a OS=Homo sapiens GN=RPS27A PE=1 SV=2	81,5
TIF1B_HUMAN	Transcription intermediary factor 1-beta OS=Homo sapiens GN=TRIM28 PE=1 SV=5	80,5
CNTP4_HUMAN	Contactin-associated protein-like 4 OS=Homo sapiens GN=CNTNAP4 PE=1 SV=3	76,0
GTF2I_HUMAN	General transcription factor II-I OS=Homo sapiens GN=GTF2I PE=1 SV=2	75,5
RCC1_HUMAN	Regulator of chromosome condensation OS=Homo sapiens GN=RCC1 PE=1 SV=1	75,0
EDF1_HUMAN	Endothelial differentiation-related factor 1 OS=Homo sapiens GN=EDF1 PE=1 SV=1	74,0
DTD2_HUMAN	Probable D-tyrosyl-tRNA(Tyr) deacylase 2 OS=Homo sapiens GN=C14orf126 PE=2 SV=1	70,0
MND1_HUMAN	Meiotic nuclear division protein 1 homolog OS=Homo sapiens GN=MND1 PE=1 SV=1	67,5
SR140_HUMAN	U2-associated protein SR140 OS=Homo sapiens GN=SR140 PE=1 SV=2	67,5
RRP15_HUMAN	RRP15-like protein OS=Homo sapiens GN=RRP15 PE=1 SV=2	64,5
APOB_HUMAN	Apolipoprotein B-100 OS=Homo sapiens GN=APOB PE=1 SV=2	60,0
CHM4A_HUMAN	Charged multivesicular body protein 4a OS=Homo sapiens GN=CHMP4A PE=1 SV=3	60,0
RIC8A_HUMAN	Synembryon-A OS=Homo sapiens GN=RIC8A PE=1 SV=3	60,0
GTR12_HUMAN	Solute carrier family 2, facilitated glucose transporter member 12 OS=Homo sapiens GN=SLC2A12 PE=2 SV=1	58,0
SEPT6_HUMAN	Septin-6 OS=Homo sapiens GN=SEPT6 PE=1 SV=4	58,0
SEPT7_HUMAN	Septin-7 OS=Homo sapiens GN=SEPT7 PE=1 SV=2	58,0
VPRBP_HUMAN	Protein VPRBP OS=Homo sapiens GN=VPRBP PE=1 SV=3	58,0
ROA0_HUMAN	Heterogeneous nuclear ribonucleoprotein A0 OS=Homo sapiens GN=HNRNPA0 PE=1 SV=1	57,0
EF1D_HUMAN	Elongation factor 1-delta OS=Homo sapiens GN=EEF1D PE=1 SV=5	54,0
K1C10_HUMAN	Keratin, type I cytoskeletal 10 OS=Homo sapiens GN=KRT10 PE=1 SV=6	53,0
RRP5_HUMAN	Protein RRP5 homolog OS=Homo sapiens GN=PDCD11 PE=1 SV=3	53,0
SMD3_HUMAN	Small nuclear ribonucleoprotein Sm D3 OS=Homo sapiens GN=SNRPD3 PE=1 SV=1	53,0
COJA1_HUMAN	Collagen alpha-1(XIX) chain OS=Homo sapiens GN=COL19A1 PE=1 SV=3	52,0
MAZ_HUMAN	Myc-associated zinc finger protein OS=Homo sapiens GN=MAZ PE=1 SV=1	50,0
RL7L_HUMAN	60S ribosomal protein L7-like 1 OS=Homo sapiens GN=RPL7L1 PE=1 SV=1	50,0
MYBPP_HUMAN	MYCBP-associated protein OS=Homo sapiens GN=MYCBPAP PE=1 SV=2	49,5
LARP1_HUMAN	La-related protein 1 OS=Homo sapiens GN=LARP1 PE=1 SV=2	48,5
SC31A_HUMAN	Protein transport protein Sec31A OS=Homo sapiens GN=SEC31A PE=1 SV=3	48,5
PESC_HUMAN	Pescadillo homolog OS=Homo sapiens GN=PES1 PE=1 SV=1	48,0

ROCK2_HUMAN	Rho-associated protein kinase 2 OS=Homo sapiens GN=ROCK2 PE=1 SV=4	46,5
CUL2_HUMAN	Cullin-2 OS=Homo sapiens GN=CUL2 PE=1 SV=2	45,5
LSM12_HUMAN	Protein LSM12 homolog OS=Homo sapiens GN=LSM12 PE=1 SV=2	45,5
RL40_HUMAN	Ubiquitin-60S ribosomal protein L40 OS=Homo sapiens GN=UBA52 PE=1 SV=2	45,5
CD63_HUMAN	CD63 antigen OS=Homo sapiens GN=CD63 PE=1 SV=2	45,0
PPOX_HUMAN	Protoporphyrinogen oxidase OS=Homo sapiens GN=PPOX PE=1 SV=1	45,0
TNIK_HUMAN	TRAF2 and NCK-interacting protein kinase OS=Homo sapiens GN=TNIK PE=1 SV=1	45,0
RBM28_HUMAN	RNA-binding protein 28 OS=Homo sapiens GN=RBM28 PE=1 SV=3	44,5
FACD2_HUMAN	Fanconi anemia group D2 protein OS=Homo sapiens GN=FANCD2 PE=1 SV=1	41,5
UBF1_HUMAN	Nucleolar transcription factor 1 OS=Homo sapiens GN=UBTF PE=1 SV=1	41,5
ANO2_HUMAN	Anoctamin-2 OS=Homo sapiens GN=ANO2 PE=1 SV=2	40,5
CCPG1_HUMAN	Cell cycle progression protein 1 OS=Homo sapiens GN=CCPG1 PE=1 SV=3	40,0
DYH2_HUMAN	Dynein heavy chain 2, axonemal OS=Homo sapiens GN=DNAH2 PE=1 SV=3	40,0
HRH4_HUMAN	Histamine H4 receptor OS=Homo sapiens GN=HRH4 PE=1 SV=2	39,0
AMGO2_HUMAN	Amphoterin-induced protein 2 OS=Homo sapiens GN=AMIGO2 PE=1 SV=1	38,0
UGGG2_HUMAN	UDP-glucose:glycoprotein glucosyltransferase 2 OS=Homo sapiens GN=UGGT2 PE=1 SV=4	38,0
CQ085_HUMAN	Uncharacterized protein C17orf85 OS=Homo sapiens GN=C17orf85 PE=1 SV=2	37,5
SETD5_HUMAN	SET domain-containing protein 5 OS=Homo sapiens GN=SETD5 PE=1 SV=2	37,5
MYO3A_HUMAN	Myosin-IIIa OS=Homo sapiens GN=MYO3A PE=1 SV=2	37,0
TYK2_HUMAN	Non-receptor tyrosine-protein kinase TYK2 OS=Homo sapiens GN=TYK2 PE=1 SV=3	37,0
RM03_HUMAN	39S ribosomal protein L3, mitochondrial OS=Homo sapiens GN=MRPL3 PE=1 SV=1	36,5
B4GT5_HUMAN	Beta-1,4-galactosyltransferase 5 OS=Homo sapiens GN=B4GALT5 PE=2 SV=1	36,0
CB039_HUMAN	UPF0407 protein C2orf39 OS=Homo sapiens GN=C2orf39 PE=2 SV=2	36,0
DC8L2_HUMAN	DDB1- and CUL4-associated factor 8-like protein 2 OS=Homo sapiens GN=DCAF8L2 PE=2 SV=1	36,0
DOCK5_HUMAN	Dedicator of cytokinesis protein 5 OS=Homo sapiens GN=DOCK5 PE=1 SV=3	36,0
MUC12_HUMAN	Mucin-12 OS=Homo sapiens GN=MUC12 PE=1 SV=2	36,0
ELL_HUMAN	RNA polymerase II elongation factor ELL OS=Homo sapiens GN=ELL PE=1 SV=1	35,0
SEM3G_HUMAN	Semaphorin-3G OS=Homo sapiens GN=SEMA3G PE=1 SV=1	33,5
CAC1E_HUMAN	Voltage-dependent R-type calcium channel subunit alpha-1E OS=Homo sapiens GN=CACNA1E PE=1 SV=3	33,0
CU025_HUMAN	C2 domain-containing protein 2 OS=Homo sapiens GN=C2CD2 PE=1 SV=2	33,0
AP3D1_HUMAN	AP-3 complex subunit delta-1 OS=Homo sapiens GN=AP3D1 PE=1 SV=1	30,5
RELL2_HUMAN	RELT-like protein 2 OS=Homo sapiens GN=RELL2 PE=1 SV=1	30,5
RRP7A_HUMAN	Ribosomal RNA-processing protein 7 homolog A OS=Homo sapiens GN=RRP7A PE=1 SV=2	30,5

Tab. A9 BZLF1\_5693 intersect 5694

prot_acc	BZLF1_5694_intersect_5693_prot_desc_only	highest_mean
HSP7C_HUMAN	Heat shock cognate 71 kDa protein OS=Homo sapiens GN=HSPA8 PE=1 SV=1	981,0
ROA1_HUMAN	Heterogeneous nuclear ribonucleoprotein A1 OS=Homo sapiens GN=HNRNPA1 PE=1 SV=5	698,0
PDIP3_HUMAN	Polymerase delta-interacting protein 3 OS=Homo sapiens GN=POLDIP3 PE=1 SV=2	696,0
ROA2_HUMAN	Heterogeneous nuclear ribonucleoproteins A2/B1 OS=Homo sapiens GN=HNRNPA2B1 PE=1 SV=2	649,5
NUCL_HUMAN	Nucleolin OS=Homo sapiens GN=NCL PE=1 SV=3	635,5
NPM_HUMAN	Nucleophosmin OS=Homo sapiens GN=NPM1 PE=1 SV=2	595,5
EF1A1_HUMAN	Elongation factor 1-alpha 1 OS=Homo sapiens GN=EEF1A1 PE=1 SV=1	584,5
RBM25_HUMAN	RNA-binding protein 25 OS=Homo sapiens GN=RBM25 PE=1 SV=3	547,0
HNRPU_HUMAN	Heterogeneous nuclear ribonucleoprotein U OS=Homo sapiens GN=HNRNPU PE=1 SV=6	488,0
DDX5_HUMAN	Probable ATP-dependent RNA helicase DDX5 OS=Homo sapiens GN=DDX5 PE=1 SV=1	420,5
DDX21_HUMAN	Nucleolar RNA helicase 2 OS=Homo sapiens GN=DDX21 PE=1 SV=5	414,0
ATX2L_HUMAN	Ataxin-2-like protein OS=Homo sapiens GN=ATXN2L PE=1 SV=2	410,0
SFPQ_HUMAN	Splicing factor, proline- and glutamine-rich OS=Homo sapiens GN=SFPQ PE=1 SV=2	406,5
TBB2A_HUMAN	Tubulin beta-2A chain OS=Homo sapiens GN=TUBB2A PE=1 SV=1	405,0
GRP78_HUMAN	78 kDa glucose-regulated protein OS=Homo sapiens GN=HSPA5 PE=1 SV=2	385,0
HNRPM_HUMAN	Heterogeneous nuclear ribonucleoprotein M OS=Homo sapiens GN=HNRNPM PE=1 SV=3	377,0
ACTB_HUMAN	Actin, cytoplasmic 1 OS=Homo sapiens GN=ACTB PE=1 SV=1	363,0
HSP71_HUMAN	Heat shock 70 kDa protein 1A/1B OS=Homo sapiens GN=HSPA1A PE=1 SV=5	358,0
NONO_HUMAN	Non-POU domain-containing octamer-binding protein OS=Homo sapiens GN=NONO PE=1 SV=4	353,5
HNRH1_HUMAN	Heterogeneous nuclear ribonucleoprotein H OS=Homo sapiens GN=HNRNPH1 PE=1 SV=4	333,5
HNRPC_HUMAN	Heterogeneous nuclear ribonucleoproteins C1/C2 OS=Homo sapiens GN=HNRNPC PE=1 SV=4	323,0
NOLC1_HUMAN	Nucleolar and coiled-body phosphoprotein 1 OS=Homo sapiens GN=NOLC1 PE=1 SV=2	323,0
TBB5_HUMAN	Tubulin beta chain OS=Homo sapiens GN=TUBB PE=1 SV=2	321,0
HSP76_HUMAN	Heat shock 70 kDa protein 6 OS=Homo sapiens GN=HSPA6 PE=1 SV=2	308,0
HNRPK_HUMAN	Heterogeneous nuclear ribonucleoprotein K OS=Homo sapiens GN=HNRNPK PE=1 SV=1	307,5
K2C1_HUMAN	Keratin, type II cytoskeletal 1 OS=Homo sapiens GN=KRT1 PE=1 SV=6	300,0
RL4_HUMAN	60S ribosomal protein L4 OS=Homo sapiens GN=RPL4 PE=1 SV=5	296,0
RL23_HUMAN	60S ribosomal protein L23 OS=Homo sapiens GN=RPL23 PE=1 SV=1	286,0
RS3_HUMAN	40S ribosomal protein S3 OS=Homo sapiens GN=RPS3 PE=1 SV=2	285,0
DDX17_HUMAN	Probable ATP-dependent RNA helicase DDX17 OS=Homo sapiens GN=DDX17 PE=1 SV=1	278,0
RS8_HUMAN	40S ribosomal protein S8 OS=Homo sapiens GN=RPS8 PE=1 SV=2	252,0
HNRPL_HUMAN	Heterogeneous nuclear ribonucleoprotein L OS=Homo sapiens GN=HNRNPL PE=1 SV=2	251,5
PARP1_HUMAN	Poly [ADP-ribose] polymerase 1 OS=Homo sapiens GN=PARP1 PE=1 SV=4	249,0
G3P_HUMAN	Glyceraldehyde-3-phosphate dehydrogenase OS=Homo sapiens GN=GAPDH PE=1 SV=3	243,5
H4_HUMAN	Histone H4 OS=Homo sapiens GN=HIST1H4A PE=1 SV=2	242,5
RL7_HUMAN	60S ribosomal protein L7 OS=Homo sapiens GN=RPL7 PE=1 SV=1	235,5
PAIRB_HUMAN	Plasminogen activator inhibitor 1 RNA-binding protein OS=Homo sapiens GN=SERBP1 PE=1 SV=2	216,0

RL13_HUMAN	60S ribosomal protein L13 OS=Homo sapiens GN=RPL13 PE=1 SV=4	206,5
PR40A_HUMAN	Pre-mRNA-processing factor 40 homolog A OS=Homo sapiens GN=PRPF40A PE=1 SV=2	203,5
RL21_HUMAN	60S ribosomal protein L21 OS=Homo sapiens GN=RPL21 PE=1 SV=2	202,5
HNRPD_HUMAN	Heterogeneous nuclear ribonucleoprotein D0 OS=Homo sapiens GN=HNRNPD PE=1 SV=1	201,0
RL15_HUMAN	60S ribosomal protein L15 OS=Homo sapiens GN=RPL15 PE=1 SV=2	199,0
RS25_HUMAN	40S ribosomal protein S25 OS=Homo sapiens GN=RPS25 PE=1 SV=1	191,5
HNRPR_HUMAN	Heterogeneous nuclear ribonucleoprotein R OS=Homo sapiens GN=HNRNPR PE=1 SV=1	186,0
LYAR_HUMAN	Cell growth-regulating nucleolar protein OS=Homo sapiens GN=LYAR PE=1 SV=2	182,0
ACTBL_HUMAN	Beta-actin-like protein 2 OS=Homo sapiens GN=ACTBL2 PE=1 SV=2	181,5
RS19_HUMAN	40S ribosomal protein S19 OS=Homo sapiens GN=RPS19 PE=1 SV=2	179,0
RS15_HUMAN	40S ribosomal protein S15 OS=Homo sapiens GN=RPS15 PE=1 SV=2	175,0
PRP19_HUMAN	Pre-mRNA-processing factor 19 OS=Homo sapiens GN=PRPF19 PE=1 SV=1	173,5
POTEF_HUMAN	POTE ankyrin domain family member F OS=Homo sapiens GN=POTEF PE=1 SV=2	166,0
ENOA_HUMAN	Alpha-enolase OS=Homo sapiens GN=ENO1 PE=1 SV=2	163,5
ENOB_HUMAN	Beta-enolase OS=Homo sapiens GN=ENO3 PE=1 SV=4	163,5
TOP2A_HUMAN	DNA topoisomerase 2-alpha OS=Homo sapiens GN=TOP2A PE=1 SV=3	163,5
RL14_HUMAN	60S ribosomal protein L14 OS=Homo sapiens GN=RPL14 PE=1 SV=4	163,0
RS11_HUMAN	40S ribosomal protein S11 OS=Homo sapiens GN=RPS11 PE=1 SV=3	162,0
RL37A_HUMAN	60S ribosomal protein L37a OS=Homo sapiens GN=RPL37A PE=1 SV=2	161,0
RS5_HUMAN	40S ribosomal protein S5 OS=Homo sapiens GN=RPS5 PE=1 SV=4	160,0
RL23A_HUMAN	60S ribosomal protein L23a OS=Homo sapiens GN=RPL23A PE=1 SV=1	159,0
RL38_HUMAN	60S ribosomal protein L38 OS=Homo sapiens GN=RPL38 PE=1 SV=2	157,0
RS16_HUMAN	40S ribosomal protein S16 OS=Homo sapiens GN=RPS16 PE=1 SV=2	155,5
DAZP1_HUMAN	DAZ-associated protein 1 OS=Homo sapiens GN=DAZAP1 PE=1 SV=1	148,5
FUS_HUMAN	RNA-binding protein FUS OS=Homo sapiens GN=FUS PE=1 SV=1	147,5
SF3B2_HUMAN	Splicing factor 3B subunit 2 OS=Homo sapiens GN=SF3B2 PE=1 SV=2	147,5
RL19_HUMAN	60S ribosomal protein L19 OS=Homo sapiens GN=RPL19 PE=1 SV=1	147,0
ACACA_HUMAN	Acetyl-CoA carboxylase 1 OS=Homo sapiens GN=ACACA PE=1 SV=2	142,5
NOP2_HUMAN	Putative ribosomal RNA methyltransferase NOP2 OS=Homo sapiens GN=NOP2 PE=1 SV=2	141,0
RL27A_HUMAN	60S ribosomal protein L27a OS=Homo sapiens GN=RPL27A PE=1 SV=2	140,0
RL29_HUMAN	60S ribosomal protein L29 OS=Homo sapiens GN=RPL29 PE=1 SV=2	140,0
DHX9_HUMAN	ATP-dependent RNA helicase A OS=Homo sapiens GN=DHX9 PE=1 SV=4	137,5
RL8_HUMAN	60S ribosomal protein L8 OS=Homo sapiens GN=RPL8 PE=1 SV=2	134,5
RS4X_HUMAN	40S ribosomal protein S4, X isoform OS=Homo sapiens GN=RPS4X PE=1 SV=2	134,0
RL24_HUMAN	60S ribosomal protein L24 OS=Homo sapiens GN=RPL24 PE=1 SV=1	133,0
KI67_HUMAN	Antigen KI-67 OS=Homo sapiens GN=MKI67 PE=1 SV=2	131,0
NOP58_HUMAN	Nucleolar protein 58 OS=Homo sapiens GN=NOP58 PE=1 SV=1	129,5
RL3_HUMAN	60S ribosomal protein L3 OS=Homo sapiens GN=RPL3 PE=1 SV=2	129,5
ROA3_HUMAN	Heterogeneous nuclear ribonucleoprotein A3 OS=Homo sapiens GN=HNRNPA3 PE=1 SV=2	127,5
RL18A_HUMAN	60S ribosomal protein L18a OS=Homo sapiens GN=RPL18A PE=1 SV=2	127,0
PABP1_HUMAN	Polyadenylate-binding protein 1 OS=Homo sapiens GN=PABPC1 PE=1 SV=2	124,5
RS2_HUMAN	40S ribosomal protein S2 OS=Homo sapiens GN=RPS2 PE=1 SV=2	124,5
RS3A_HUMAN	40S ribosomal protein S3a OS=Homo sapiens GN=RPS3A PE=1 SV=2	122,5

H15_HUMAN	Histone H1.5 OS=Homo sapiens GN=HIST1H1B PE=1 SV=3	121,5
RS10_HUMAN	40S ribosomal protein S10 OS=Homo sapiens GN=RPS10 PE=1 SV=1	121,5
SMD1_HUMAN	Small nuclear ribonucleoprotein Sm D1 OS=Homo sapiens GN=SNRPD1 PE=1 SV=1	120,5
FBRL_HUMAN	rRNA 2~-O-methyltransferase fibrillarin OS=Homo sapiens GN=FBL PE=1 SV=2	119,0
RS18_HUMAN	40S ribosomal protein S18 OS=Homo sapiens GN=RPS18 PE=1 SV=3	119,0
RS7_HUMAN	40S ribosomal protein S7 OS=Homo sapiens GN=RPS7 PE=1 SV=1	117,0
THOC4_HUMAN	THO complex subunit 4 OS=Homo sapiens GN=THOC4 PE=1 SV=3	116,5
NUFP2_HUMAN	Nuclear fragile X mental retardation-interacting protein 2 OS=Homo sapiens GN=NUFIP2 PE=1 SV=1	115,5
XRCC5_HUMAN	X-ray repair cross-complementing protein 5 OS=Homo sapiens GN=XRCC5 PE=1 SV=3	112,0
IF16_HUMAN	Gamma-interferon-inducible protein 16 OS=Homo sapiens GN=IFI16 PE=1 SV=3	110,5
RL13A_HUMAN	60S ribosomal protein L13a OS=Homo sapiens GN=RPL13A PE=1 SV=2	107,0
RS24_HUMAN	40S ribosomal protein S24 OS=Homo sapiens GN=RPS24 PE=1 SV=1	106,5
RL26_HUMAN	60S ribosomal protein L26 OS=Homo sapiens GN=RPL26 PE=1 SV=1	106,0
RL10_HUMAN	60S ribosomal protein L10 OS=Homo sapiens GN=RPL10 PE=1 SV=4	103,5
KHDR1_HUMAN	KH domain-containing, RNA-binding, signal transduction-associated protein 1 OS=Homo sapiens GN=KHDRBS1 PE=1 SV=1	103,0
RL9_HUMAN	60S ribosomal protein L9 OS=Homo sapiens GN=RPL9 PE=1 SV=1	103,0
RS6_HUMAN	40S ribosomal protein S6 OS=Homo sapiens GN=RPS6 PE=1 SV=1	100,0
ROAA_HUMAN	Heterogeneous nuclear ribonucleoprotein A/B OS=Homo sapiens GN=HNRNPAB PE=1 SV=2	99,5
RS29_HUMAN	40S ribosomal protein S29 OS=Homo sapiens GN=RPS29 PE=1 SV=2	99,5
TOP1_HUMAN	DNA topoisomerase 1 OS=Homo sapiens GN=TOP1 PE=1 SV=2	99,0
PPIA_HUMAN	Peptidyl-prolyl cis-trans isomerase A OS=Homo sapiens GN=PPIA PE=1 SV=2	97,0
ILF3_HUMAN	Interleukin enhancer-binding factor 3 OS=Homo sapiens GN=ILF3 PE=1 SV=3	95,5
RL36A_HUMAN	60S ribosomal protein L36a OS=Homo sapiens GN=RPL36A PE=1 SV=2	94,0
RL6_HUMAN	60S ribosomal protein L6 OS=Homo sapiens GN=RPL6 PE=1 SV=3	92,5
SET_HUMAN	Protein SET OS=Homo sapiens GN=SET PE=1 SV=3	90,0
RL5_HUMAN	60S ribosomal protein L5 OS=Homo sapiens GN=RPL5 PE=1 SV=3	89,5
RL35_HUMAN	60S ribosomal protein L35 OS=Homo sapiens GN=RPL35 PE=1 SV=2	88,5
NAT10_HUMAN	N-acetyltransferase 10 OS=Homo sapiens GN=NAT10 PE=1 SV=2	87,0
SRSF3_HUMAN	Serine/arginine-rich splicing factor 3 OS=Homo sapiens GN=SRSF3 PE=1 SV=1	85,5
SF3B1_HUMAN	Splicing factor 3B subunit 1 OS=Homo sapiens GN=SF3B1 PE=1 SV=3	85,0
RS20_HUMAN	40S ribosomal protein S20 OS=Homo sapiens GN=RPS20 PE=1 SV=1	83,5
RL11_HUMAN	60S ribosomal protein L11 OS=Homo sapiens GN=RPL11 PE=1 SV=2	81,5
RS15A_HUMAN	40S ribosomal protein S15a OS=Homo sapiens GN=RPS15A PE=1 SV=2	81,5
H13_HUMAN	Histone H1.3 OS=Homo sapiens GN=HIST1H1D PE=1 SV=2	79,0
RL10A_HUMAN	60S ribosomal protein L10a OS=Homo sapiens GN=RPL10A PE=1 SV=2	78,5
RL34_HUMAN	60S ribosomal protein L34 OS=Homo sapiens GN=RPL34 PE=1 SV=3	76,5
RL17_HUMAN	60S ribosomal protein L17 OS=Homo sapiens GN=RPL17 PE=1 SV=3	76,0
RS23_HUMAN	40S ribosomal protein S23 OS=Homo sapiens GN=RPS23 PE=1 SV=3	75,0
RBM14_HUMAN	RNA-binding protein 14 OS=Homo sapiens GN=RBM14 PE=1 SV=2	74,0
RS30_HUMAN	40S ribosomal protein S30 OS=Homo sapiens GN=FAU PE=1 SV=1	74,0
GEMI4_HUMAN	Component of gems 4 OS=Homo sapiens GN=GEMIN4 PE=1 SV=2	73,5
RTTN_HUMAN	Rotatin OS=Homo sapiens GN=RTTN PE=1 SV=3	73,5
TRRAP_HUMAN	Transformation/transcription domain-associated protein OS=Homo sapiens GN=TRRAP PE=1 SV=3	73,5

RL7A_HUMAN	60S ribosomal protein L7a OS=Homo sapiens GN=RPL7A PE=1 SV=2	70,5
RL18_HUMAN	60S ribosomal protein L18 OS=Homo sapiens GN=RPL18 PE=1 SV=2	68,5
SF3A1_HUMAN	Splicing factor 3A subunit 1 OS=Homo sapiens GN=SF3A1 PE=1 SV=1	67,5
RS17_HUMAN	40S ribosomal protein S17 OS=Homo sapiens GN=RPS17 PE=1 SV=2	65,5
RL30_HUMAN	60S ribosomal protein L30 OS=Homo sapiens GN=RPL30 PE=1 SV=2	65,0
RS14_HUMAN	40S ribosomal protein S14 OS=Homo sapiens GN=RPS14 PE=1 SV=3	64,0
RAN_HUMAN	GTP-binding nuclear protein Ran OS=Homo sapiens GN=RAN PE=1 SV=3	62,5
RL27_HUMAN	60S ribosomal protein L27 OS=Homo sapiens GN=RPL27 PE=1 SV=2	62,5
XRCC6_HUMAN	X-ray repair cross-complementing protein 6 OS=Homo sapiens GN=XRCC6 PE=1 SV=2	62,5
HS74L_HUMAN	Heat shock 70 kDa protein 4L OS=Homo sapiens GN=HSPA4L PE=1 SV=3	60,5
HMGN2_HUMAN	Non-histone chromosomal protein HMG-17 OS=Homo sapiens GN=HMGN2 PE=1 SV=3	58,5
HMGA1_HUMAN	High mobility group protein HMG-I/HMG-Y OS=Homo sapiens GN=HMGA1 PE=1 SV=3	58,0
BUB3_HUMAN	Mitotic checkpoint protein BUB3 OS=Homo sapiens GN=BUB3 PE=1 SV=1	56,0
DDX6_HUMAN	Probable ATP-dependent RNA helicase DDX6 OS=Homo sapiens GN=DDX6 PE=1 SV=2	56,0
CHD3_HUMAN	Chromodomain-helicase-DNA-binding protein 3 OS=Homo sapiens GN=CHD3 PE=1 SV=3	55,5
HMGB2_HUMAN	High mobility group protein B2 OS=Homo sapiens GN=HMGB2 PE=1 SV=2	54,5
TERT_HUMAN	Telomerase reverse transcriptase OS=Homo sapiens GN=TERT PE=1 SV=1	54,5
HNRPQ_HUMAN	Heterogeneous nuclear ribonucleoprotein Q OS=Homo sapiens GN=SYNCRIP PE=1 SV=2	54,0
MATR3_HUMAN	Matrin-3 OS=Homo sapiens GN=MATR3 PE=1 SV=2	54,0
MBB1A_HUMAN	Myb-binding protein 1A OS=Homo sapiens GN=MYBBP1A PE=1 SV=2	52,5
PSIP1_HUMAN	PC4 and SFRS1-interacting protein OS=Homo sapiens GN=PSIP1 PE=1 SV=1	51,5
EBP2_HUMAN	Probable rRNA-processing protein EBP2 OS=Homo sapiens GN=EBNA1BP2 PE=1 SV=2	49,5
U2AF1_HUMAN	Splicing factor U2AF 35 kDa subunit OS=Homo sapiens GN=U2AF1 PE=1 SV=3	48,0
PRKDC_HUMAN	DNA-dependent protein kinase catalytic subunit OS=Homo sapiens GN=PRKDC PE=1 SV=3	45,0
RL32_HUMAN	60S ribosomal protein L32 OS=Homo sapiens GN=RPL32 PE=1 SV=2	41,0
RB6I2_HUMAN	ELKS/Rab6-interacting/CAST family member 1 OS=Homo sapiens GN=ERC1 PE=1 SV=1	40,0
UCHL1_HUMAN	Ubiquitin carboxyl-terminal hydrolase isozyme L1 OS=Homo sapiens GN=UCHL1 PE=1 SV=2	39,0
DHAK_HUMAN	Bifunctional ATP-dependent dihydroxyacetone kinase/FAD-AMP lyase (cyclizing) OS=Homo sapiens GN=DAK PE=1 SV=2	38,0
FREM3_HUMAN	FRAS1-related extracellular matrix protein 3 OS=Homo sapiens GN=FREM3 PE=2 SV=1	37,0
MPIP1_HUMAN	M-phase inducer phosphatase 1 OS=Homo sapiens GN=CDC25A PE=1 SV=2	33,5
CAC1B_HUMAN	Voltage-dependent N-type calcium channel subunit alpha-1B OS=Homo sapiens GN=CACNA1B PE=1 SV=1	33,0
PDK1_HUMAN	[Pyruvate dehydrogenase [lipoamide]] kinase isozyme 1, mitochondrial OS=Homo sapiens GN=PDK1 PE=1 SV=1	33,0
RADIL_HUMAN	Ras-associating and dilute domain-containing protein OS=Homo sapiens GN=RADIL PE=1 SV=5	33,0
SEC63_HUMAN	Translocation protein SEC63 homolog OS=Homo sapiens GN=SEC63 PE=1 SV=2	33,0

# CURRICULUM VITAE

## Personal Information

Name	Marisa Schöffner
Date of birth	31.12.1985
Place of birth	Tübingen
Nationality	German

## Education

1992-1995	Primary school (“Carl-Joseph-Leiprecht Schule”), Rottenburg am Neckar, Germany
1995-1996	Primary school (“Grundschule Söcking”), Starnberg, Germany
1996-2005	Secondary school (“Gymnasium Starnberg”), Starnberg, Germany Qualification for university: Abitur
2005-2008	Biology (B.Sc.), University of Bayreuth, Bayreuth, Germany
2008	Bachelor thesis at the faculty of biology, chemistry and earth sciences, University Bayreuth, Bayreuth, Germany Department of cell biology Prof. Dr. Benedikt Westermann “Rolle von Mdm36 bei der mitochondrialen Verteilung und Morphologie in <i>S. cerevisiae</i> ”
2008-2010	Biochemistry (M.Sc.), Technical University of Munich, Munich, Germany
2010	Master thesis at the the Helmholtz Center Munich, Munich, Germany Institute of virology Prof. Dr. Christine Leib-Mösch “Regulation der Expressionsaktivität humaner endogener Retroviren (HERVs) im Gehirn”



**PhD work**

2011-2015

PhD thesis at the Helmholtz Center Munich, Munich, Germany

Department of gene vectors

Prof. Dr. Wolfgang Hammerschmidt

“Chromatin remodeling in Epstein-Barr virus after induction of the lytic phase: molecular characterization of the role of BZLF1 and its interactions”

# VIELEN DANK

...an alle Freunde und Kollegen, die mich während meiner Ausbildungs- und Promotionszeit begleitet haben.

Mein besonderer Dank gilt

**Wolfgang:** Vielen Dank für die Bereitstellung meines Themas, deine Hilfe, dein entgegengebrachtes Vertrauen, für dein Interesse und viele spannende Diskussionen.

**Dirk:** Herzlichen Dank nicht nur für die Übernahme der Pflichten als mein offizieller Betreuer an der Universität, sondern auch für dein stetiges Interesse an meiner Arbeit und für viele hilfreiche Anregungen und Ideen im Thesis Committee.

allen, die mir bei meiner Arbeit intellektuell und experimentell geholfen haben: Ganz besonders danke ich den **SFB 1064** Mitgliedern **Philipp Korber**, **Axel Imhof**, **Felix Müller-Planitz**, **Karl-Peter Hopfner** und **Andreas Ladurner** für die gute Kooperation, Bereitstellung vieler Materialien und Hilfe bei der Auswertung meiner Experimente.

meiner Arbeitsgruppe: Ein Dankeschön an **Rosi**, **Christine und Dagi**, den guten Seelen der AGV, für die stetige Hilfsbereitschaft, sowie an **Romana**, **Markus**, **Mika**, **Montse**, **Anne**, **Paulina**, **Alex**, **Manuel** und dem Rest der AGV für die wunderbare Arbeitsatmosphäre.

meiner **Familie** und Personen, die mich während dieser Lebensphase bedingungslos und liebevoll unterstützt haben: Ich danke euch von ganzem Herzen.